From FIC to BID:

Target Identification and Functional Characterization of *Bartonella* Effector Proteins.

Inauguraldissertation

zur

Erlangung der Würde eines Doktors der Philosophie

vorgelegt der

Philosophisch-Naturwissenschaftlichen Fakultät

der Universität Basel

von

Kathrin Pieles

aus Oldenburg, Deutschland

Basel, 2014

Genehmigt von der Philosophisch-Naturwissenschaftlichen Fakultät auf Antrag von

Prof. Dr. Christoph Dehio

Prof. Dr. Sebastian Hiller

Basel, den 29.10.2013

                                        Prof. Dr. Jörg Schibler

                                                Dekan

Statement to my Thesis

This work was carried out in the group of Prof. Christoph Dehio in the Focal Area Infection Biology at the Biozentrum of the University of Basel, Switzerland.

My PhD thesis committee consisted of:

Prof. Christoph Dehio
Prof. Sebastian Hiller
Prof. Tilman Schirmer

My thesis is written as a cumulative dissertation. It consists of an abstract summarizing the major findings of my thesis, a synopsis covering a variety of aspects related to my work and is followed by result sections composed of two scientific publications and unpublished results. Finally, I discuss some facets of this work.

Abstract

Abstract

Pathogens belonging to the genus *Bartonella* employ a unique stealth infection strategy that involves evasion from the host immune system, replication in the endothelium and persistence in erythrocytes. A key factor in colonization of the replicative niche is the manipulation of nucleated cells to the benefit of bacterial uptake, survival, proliferation or spreading. To this end, *Bartonella* spp. translocate a set of bacterial effectors via a VirB/VirD4 type IV secretion system (T4SS) into the host cell. Upon translocation, several *Bartonella* effector proteins (Beps) hijack host cell signaling cascades, thus, subverting host cellular functions to promote pathogenicity, yet their underlying mechanism remains largely elusive.

Although pathogenicity factors evolved independently in radiating lineages of *Bartonellae*, Beps share a common domain architecture. The C-terminal part of all Beps consists of a *Bartonella* intracellular delivery domain (BID) and a positively charged tail region that primarily serve as a bi-partite secretion signal. Apart from translocation, some BID-domains acquired additional functions and interfere with host cell signaling resulting in cytoskeletal rearrangements during pathogen entry. The N-terminal part is less conserved and can harbor phospho-tyrosine motifs, additional BID-domains or share the ancestral domain architecture with a filamentation induced by cAMP (FIC) domain. This domain was recently shown to catalyze the transfer of an AMP-moiety onto target proteins, a process called AMPylation or adenylylation. Although the FIC-domain is widely distributed and can be found in all kingdoms of life, the only identified targets are small GTPases of the Ras superfamily. In this study, we aimed to identify target proteins of different Beps and to gain insights into their molecular function.

In *Research Article I*, we describe that BepA of *B. henselae* elevates intracellular cAMP-levels by activating eukaryotic adenylyl cyclase (AC) synergistically with the α-subunit of stimulating heterotrimeric G-protein (Gα$_s$). Further we could show that BepA is a conditional activator of AC and directly interacts with at least one of the catalytically active cytosolic AC domains.

Furthermore, we established a mass spectrometry based strategy to identify targets of post translational modifications on the example of AMPylation that is presented in *Research Article II*. To this end, we used stable isotope-labeled ATP in *in vitro* AMPylation assays on crude cell lysates which results in the formation of reporter ion clusters in subsequent LC-MS analysis. Applying this strategy on an exemplary Fic protein, Bep2 of *B. rochalimae*, we

identified vimentin as a target protein. As vimentin is not structurally related to small GTPases, we exhibit cytoskeletal components as a new target class of Fic protein-mediated AMPylation.

Taken together, *Bartonella* effector proteins target a plethora of host cell proteins and are thereby manipulating key elements of host cell signaling. Therefore, they developed a high level of versatility in their target proteins and molecular mechanisms ranging from complex formation to posttranslational modifications. We hypothesize that both of these attributes play fundamental roles in the establishment of chronic infections. Furthermore, the understanding of these basic functionalities will be useful in the development of cell biology tools or of innovative therapeutics.

Index

1. Introduction

1.1 Host pathogen interactions

During evolution, mammalian hosts developed the innate and adapted immune system that provides strategies for intervention, control and elimination of pathogens. Yet, pathogens acquired in parallel a variety of weapons to fight or avoid the host immune system and establish acute or chronic infections. These weapons are not only used to fight immune cells but also to manipulate immune signaling and to establish a primary niche for replication and persistence. Central components of bacterial manipulation of the host are secreted proteins that interfere in signaling cascades mostly by altering the activity of host cell proteins.

1.1.1 Bacterial effectors and toxins

In order to establish a replicative niche, bacterial pathogens are actively manipulating host cell functions and processes. In most cases, this is accomplished by either proteins called exotoxins (or toxins) that are secreted into the extracellular matrix (1) or bacterial effector proteins that are targeted directly into the host cell (2, 3).

Upon secretion into the extracellular matrix, cellular entry of toxins is mediated by either surface association and subsequent endocytic internalization (e.g. clathrin dependent-endocytosis of *Shigella* toxin) (4) or by a pore forming activity. In addition to the internalized toxin domains, perturbation of the membrane by pore forming toxins can be lethal as described for CytolysinA of *Escherichia coli* (5). In contrast to toxins, bacterial effectors are transferred directly into the host cell via dedicated machineries, called secretion systems (6-8).

Apart from the translocation process, the most fundamental difference between toxins and bacterial effector proteins is the level of regulation. The activities of bacterial effectors are highly orchestrated resulting in an efficient yet minimalized manipulation of host cell signaling. To achieve the required level of regulation, bacteria adapted a whole battery of regulation systems ranging from conditional expression to counteracting activities whereas stand-alone effectors are rare (e.g. CagA of *Helicobacter pylorii*). Instead, a set of effectors secreted often with opposing activities needing a temporal regulation that is provided by the secretion system or protein degradation. One example is *Salmonella typhimurium* that secretes among others the effector

proteins SopE and SptE. While the early secreted SopE is a RhoA activating proteins and is quickly degraded, SptE is inactivating RhoA and slower degraded than SopE (9).

Alternatively, the opposing activity can be harbored within the same effector as described for the *Legionella pneumophilia* protein DrrA that is on the one hand activating Rab1 (10) but can also deactivate Rab1 through a covalent modification (11) that is reversed by yet another *Legionella* effector SidD (12). In addition, DrrA also represent a strategy for spatial regulation of effectors by its Phosphatidylinositol 4-phosphate-binding motif that directs it to the membrane of *Legionella* containing vacuole (LCV) (13).

In contrast to bacterial effectors, toxins are generally highly effective in generating one single effect that changes a multitude of signaling events in the host cell. However, the specificity and regulation of bacterial effectors may allow co-existence of the host and pathogen and are thus key factors in the persistence of bacterial infection. Distinct secretion machineries are required to direct bacterial effectors to the target cell.

1.1.2 The type IV secretion system is evolutionary related to conjugation machineries

In order to establish initial contact to the host, bacteria are utilizing distinct strategies that are mostly conserved, e.g. adhesions, receptor coupling etc. One of these strategies involves secretion systems that on the one hand establish adherence of pathogens to the host during symbiosis and virulence but are also essential in the manipulation of the host (14).

While some of the known secretion systems are delivering effectors indirectly requiring multiple steps for the effectors to reach their targets within the host cell, others form tunnel like complexes that span the inner and outer bacterial membrane as well as the eukaryotic plasma membrane like the Type III (T3SS) and Type IV (T4SS) secretion systems.

The T3SS is characterized by the injectisome, a multiprotein complex that is ancestrally related to the flagellar export machinery (15, 16). Within the last 10 years, the temporal regulation of T3SS effector secretion could be linked to chaperones as reviewed by J.E. Galán and H. Wolf-Watz (8). These chaperones were shown to regulate effector expression (17, 18) and to bind the partially unfolded effectors and direct them to the secretion machinery (19, 20).

Although the temporal regulation of effector secretion is rather well resolved for T3SS effectors, it is only poorly understood in the context of machinery expression for T4SS.

The T4SS evolved several times in parallel from bacterial conjugation machineries (21). Like the T3SS, it is proposed to form a channel like protein complex with a rod that spans through both bacterial membranes (6). In addition, they harbor docking proteins that recognize substrates which are then passed through the channel into the host cell.

The best understood virulence-associated T4SS is the VirB/VirD4 system of the plant pathogen *Agrobacterium tumefaciens* that is encoded on the tumor-inducing plasmid that is required for virulence (22). The VirB/VirD4 T4SS mediates the conjugation of tumorigenic T-DNA into infected plant cells (23). It is composed of proteins from the *virB* operon (VirB1 to VirB11) and the coupling protein VirD4. While VirB3, VirB4 and VirB6-11 form the rod that spans both bacterial membranes, VirB2 and VirB5 form the pilus (24). VirB4, VirB11 and the coupling protein VirD4 are ATPases that energize machine assembly and substrate translocation (25). VirD4 binds to the relaxase and thereby induces the translocation process (26).

Upon horizontal inter-bacterial gene transfer, conjugation machineries functionally diverged, e.g. from transfer of DNA to proteins. Mammalian pathogens utilize T4SS to dock onto host cells or to transmit virulence factors (26).

One example of this evolutionary adaptation is the taxonomic group of *Bartonellae* that acquired three distinct T4SS, the Vbh-, the VirB/VirD4- and the Trw- T4SS.

1.1.3 The genus *Bartonella*

Bartonella spp. are facultative intracellular pathogens that cause a characteristic infection of erythrocytes. *Bartonella* spp. infect specific mammalian hosts called reservoir host, upon transmission via an arthropod, and several species were found to infect humans either as reservoir or as an incidental host with the most prominent examples of *B. bacilliformis* (*Bb*), *B. quintana* (*Bq*) and *B. henselae* (*Bh*). If not treated with antibiotics, infections with *Bb* cause the biphasic Corrion`s disease with the acute phase (Oroya fever) that is frequently accompanied with haemolytic anemia and the chronic stage (verruga peruana) that is characterized by vascular tumor formation caused by colonization of endothelial cells. The colonization of endothelial cells is also seen for *Bq*, the causative agent of trench fever, and *Bh* that leads to bacilliary

angiomatosis in immune-compromised patients and can be the causative agent of pathologies like bacillary angiomatosis and peliosis that are characterized by tumor-like lesions of the vasculature.

	Reservoir Host	VirB/ D4 T4SS	Vbh T4SS	Trw T4SS	Flagellation	
Bartonella vinsonii vinsonii	Vole	+	–	+	–	Lineage 4
Bartonella vinsonii berkhoffii	Dog	+	–	+	–	
Bartonella vinsonii arupensis	Vole	+	–	+	–	
Bartonella alsatica	Rabbit	+	–	+	–	
Bartonella taylorii	Mouse, Vole	+	–	+	–	
Bartonella grahamii	Mouse, Vole	+	+	+	–	
Bartonella elizabethae	Rat	+	+	+	–	
Bartonella tribocorum	Rat	+	+	+	–	
Bartonella koehlerae	Cat	+	–	+	–	
Bartonella henselae	Cat	+	–	+	–	
Bartonella quintana	Human	+	–	+	–	
Bartonella doshiae	Vole	+	+	+	–	
Bartonella birtlesii	Mouse	+	+	+	–	
Bartonella rochalimae	Dog, Fox	+	–	–	+	Lineage 3
Bartonella sp. 1-1C	Rat	+	–	–	+	
Bartonella sp. AR 15-3	Red Squirrel	+	–	–	+	
Bartonella clarridgeiae	Cat	+	–	–	+	
Bartonella bovis	Cattle	–	+	–	–	Lineage 2
Bartonella chomelii	Cattle	–	+	–	+	
Bartonella capreoli	Roe Deer	–	+	–	+	
Bartonella schoenbuchensis	Roe Deer	–	+	–	+	
Bartonella bacilliformis	Human	–	–	–	+	L1
Brucella abortus						

Figure 1.1.1: Phylogenic tree of the genus *Bartonella*. The phylogeny is based on a maximum-likelihood analysis using an alignment of 478 genes from the core genome of ten sequenced *Bartonella* species (bold and underlined) and *Brucella abortus*. Additional *Bartonella* species have been added using the sequences of four housekeeping genes as described previously (27). The primary mammalian hosts as well as key virulence factors are indicated for each species. The deadly human pathogen *B. bacilliformis* forms a deep-branching ancestral lineage. All modern species harbor a type IV secretion system allowing the exploration of new niches. The Vbh and Trw T4SSs are characteristics of lineage 2 and 4 respectively. Adapted from (28).

While untreated *Bb* infections can lead to a mortality rate of 80%, *Bh* causes comparably mild symptoms indicating a difference in infection strategy.

Phylogenetic analysis allowed the classification of *Bartonella* spp. that differ in the acquisition of the T4SS. As each acquisition coincided with a radiation, the genus *Bartonella* was originally subdivided into four lineages (lineage 1-4) (27, 29) placing the T4SS-free pathogen *Bb* into lineage 1. While lineage 2 species harbor a Vbh (VirB homologous) T4SS, lineage 3 and 4

acquired the VirB/VirD4 system. Lineage 4 species additionally encode for Trw T4SS that is associated with the contact establishment to erythrocytes.

Although all species belonging to the lineage 2 harbor the Vbh T4SS, its role in virulence remains unclear. The Vbh T4SS is encoded on a plasmid and is associated with conjugation. In addition to the genes encoding the secretion machinery and the proteins required for conjugational DNA transfer, the Vbh plasmid also encodes an effector protein (VbhT). Although this protein contains a secretion signal its secretion into and target within the host cell remains to be investigated.
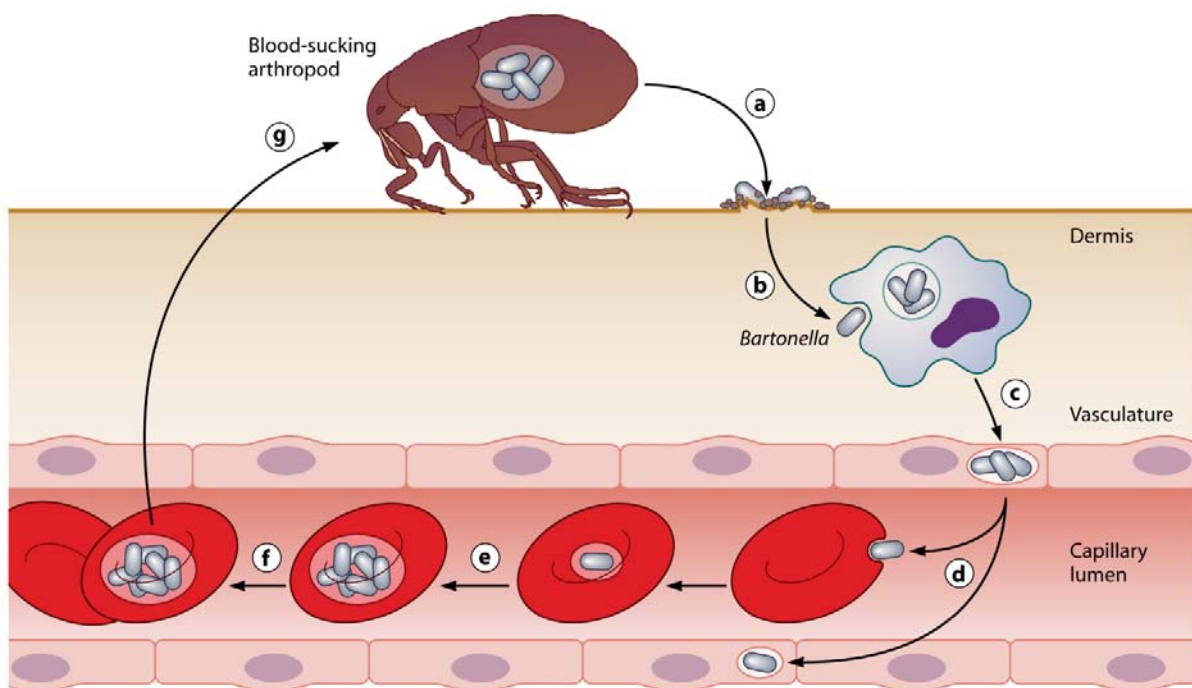
Figure 1.1.2: Infection model of *Bartonella* spp. Depicted is the general multi stepped infection model of arthropod transmitted bartonellae (a) that likely colonize the primary niche utilizing migratory cells (b) for the transport to vascular endothelium (c) where the pathogen persists intracellularly. From the primary niche, the pathogen is seeded into the bloodstream (d) where it invades erythrocytes and re-infects the primary niche. Upon replication in erythrocytes (e), *Bartonella* persists (f) and is competent for retransmission into an arthropod vector (g). Adapted from (28).

Both lineage 3 and lineage 4 harbor the VirB/VirD4 T4SS that is evolutionary related to the AvrB/TraG conjugation machinery of *A. tumefaciens*. It is encoded by an operon comprising 10

genes (*virB2 - virB11*) and a downstream encoded coupling protein VirD4. Upon infection the VirB/VirD4 T4SS of *Bartonella* is translocating effector proteins called Beps (*Bartonella* effector proteins) into the eukaryotic host cell (30) but is also retained the ability to interact with an ectopically expressed relaxase and to mediate conjugational DNA transfer (31). This T4SS was first shown to be essential for colonization of the replicative niche (32) in the lineage 4 species *B. tribocorum* where it is dispensable for subsequent erythrocyte infection. Assuming that endothelial cells are an important component of the primary niche, the VirB/VirD4 T4SS was envisioned to be required during infection of endothelial cells. In fact, the *virB*-operon was found to be induced during *in vitro* infection of endothelial cells (33). Furthermore, our group was able to show that expression of the *virB*-operon is induced at the physiological pH of blood by the two component system BatR/BatS (34). While Beps are encoded within one locus in lineage 4, they are scattered within lineage 3 genome (27) possibly allowing differential expression during infection.

Additionally to the VirB/VirD4 system, species of the lineage 4 also harbor a Trw T4SS that was most likely acquired from the conjugative *Escherichia coli* Trw system that is encoded on the R388-plasmid. Yet, a coupling protein as it can be found in the *E. coli* Trw-system is not encoded within the *Bartonella trw* locus. All genes of the *trw* locus are co-regulated by the heterodimeric repressor system KorA/KorB-complex (21). In previous studies, the Trw T4SS of *B. tribocorum* was found to be essential for erythrocyte infection (21) by mediating adhesion between bacterium and erythrocyte (35).

1.1.4 *Bartonella* effector proteins share a common domain architecture

In the current understanding, the VirB/VirD4 secretion system and its secreted effector proteins play a central role in infection of endothelial cells and colonization of the primary niche (28). *In silico* analysis revealed that *Bartonella* effector proteins (Beps) share a common domain architecture that includes a C-terminal *Bartonella* intracellular delivery (BID) domain followed by a positively charged C-tail. Together, they form a bi-partite secretion signal that results in recognition by the T4SS coupling protein VirD4 and translocation of the Bep into the eukaryotic host cell (30, 36). While the composition of the C-terminus is conserved in all Beps, the N-

termini show a diverse composition that involves additional BID-domains, tyrosine rich regions or filamentation induced by cAMP (FIC) domains (27).

While several Beps of lineage 4 species carry additional BID-domains in their N-terminus, the vast majority of Beps of the lineage 3 species harbor a FIC-domain. Although the FIC-domain was long thought of as the putative effector domain of the Beps, so far most physiological phenotypes were linked to the BID-domains (37-39).

In order to understand evolutionary relations between the Beps of different species of both lineage 4 and lineage 3, phylogenetic analysis were inferred on the primary amino acid sequences. This allowed classification of orthologous Beps into distinct clusters that are named in lineage 3, clade 1-10 and in lineage 4, clade A-I. Due to the conserved architecture and sequence similarities of individual domains, it is hypothesized that Beps derived from an ancestral effector with a FIC-BID architecture and evolved by gene duplication and gene diversification (27).

1.2 The FIC-domain

The name "filamentation induced by cAMP" (FIC) refers to a mutant within the *fic* gene of *E. coli* that impairs cell division and causes a filamenting phenotype when bacteria are grown at elevated temperature (43°C) and high extracellular concentrations of cAMP (1.5 mM) (40, 41). The FIC-domain is evolutionary highly conserved and can be found in all kingdoms of life from bacteria to viruses, archaea and eukaryotes (42).

FIC-domain containing proteins, also referred to as Fic proteins, are classified together with DOC (death on curing) proteins, a toxin-antitoxin module found in *E. coli* phage P1, in the Fic/Doc protein family which was later named fido superfamily (43, 44). Although this family comprises thousands of proteins, only few were successfully investigated on a structural level (e.g. PDB codes 2G03, 2F6S, 3EQX, and 3CUC) (45-47). Based on these observed structures, the FIC-domain is defined by eight α-helices where four of them (α2- α5) form the Fic core as defined by Pfam (44) and four are surrounding the core. The conserved fido motif (HPFx[D/E]GN[G/K]R) lies embedded in the Fic core in between helix α4 and α5. One additional helix that can be found N- or C-terminally (α`-helix) lies, close to the motif and completes the fold.

In addition to the α-helices, a β-hairpin loop that is located between α2 and α3 is a common feature of Fic proteins.
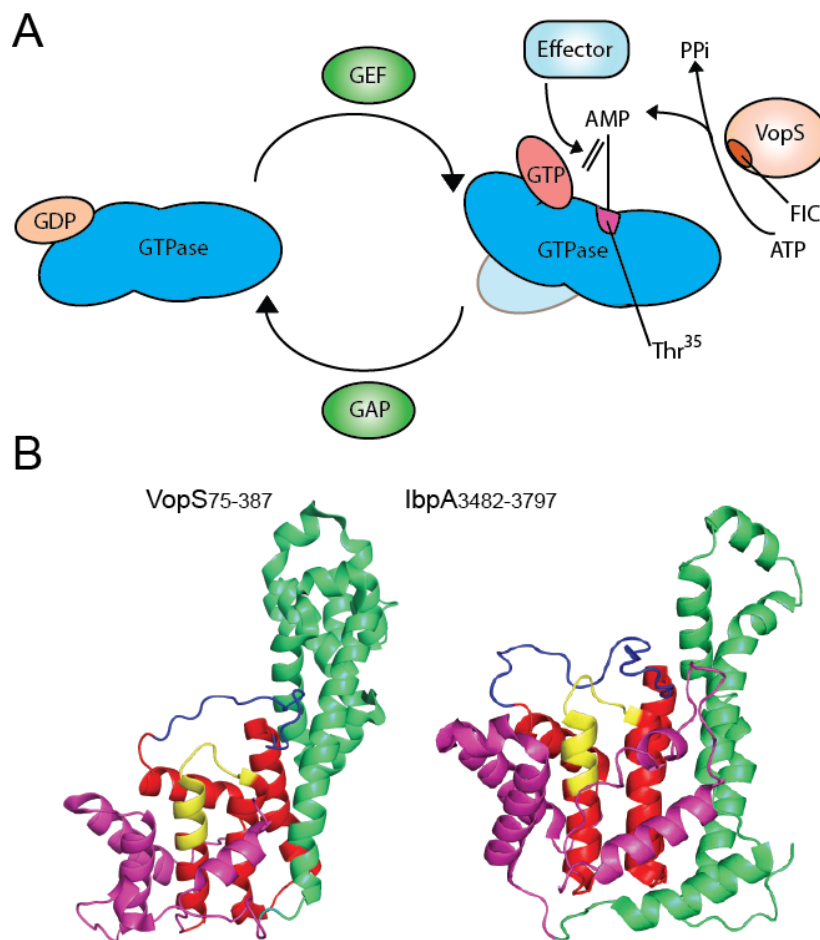
Figure 1.2.1: VopS of *V. parahaemolyticus* AMPylates small GTPases and inhibits downstream signaling. A) GTPases get activated by GEF proteins that induce the exchange of GDP for GTP. While GTP-hydrolysis can be accelerated by GAP, VopS recognizes activated small GTPases and transfers an AMP-moiety onto their switch I region and thus prohibits binding of downstream effector proteins. Adapted from (49). B) Crystal structures of VopS and IbpA reveal that both proteins harbor a FIC-domain (magenta) with the signature motif shown in yellow, the Fic core shown in red and the arm-domain in green. Proteins are shown in ribbon style. PDB codes 3LET (VopS), 4ITR (IbpA).

The family of Fic proteins is divided into three classes that are distinguished by an α-helix, α_{inh}, that is positioned at the Fic core and has been shown to inhibit AMPylation. Structural analysis revealed that a conserved glutamic acid interferes with substrate coordination by interaction with the arginine with the active site (42, 48). While this helix is encoded in a separate protein called

the antitoxin for class I Fic proteins, it is encoded N- or C-terminally in class II or class III Fic proteins, respectively (42).

Although the FIC-domain was long thought of as the putative effector domain of Beps, its role in establishing infections remained elusive.

Only recent studies of Yarbrough *et al.* and Worby *et al.* on T3SS effector proteins provided first insights into the function of Fic proteins showing that VopS of *Vibrio parahaemolyticus* (50) and IbpA of *Histophilus somni* (51) are adenylylating small GTPases of the Rho family.

Upon ingestion, *V. parahaemolyticus* can cause acute infections with severe symptom like gastroenteritis and can even be lethal in immune-compromised patients. *In vitro* infections with *V. parahaemolyticus* leads to an increase of autophagy (52) and collapse of the cytoskeleton in a T3SS-dependent manner. T3SS effector VopS was found to be sufficient to induce cytoskeletal collapse and cell death by targeting small GTPases of the Ras superfamily (47). Using enrichment strategies and subsequent mass spectrometry analysis, VopS was identified to adenylylate a conserved threonine of Rho GTPases that is located in the switch I region (53). This post translational modification (PTM) impairs the interaction of small GTPases with downstream binding proteins and is thus disrupting signaling cascades which ultimately leads to cytoskeletal collapse (50).

VopS consists of an N-terminal T3SS secretion signal within the first 30 aa and a FIC-domain that is characterized by a conserved Fic fold and an active site motif (HxFx[D/E]GNGRxxR). A histidine to alanine mutation within this motif abolishes adenylylation activity and is no longer inducing cell rounding.

In parallel, another T3SS effector protein IbpA, a multidomain protein of *H. somnus*, was also found to target small GTPases of the Ras superfamily and to induce cytoskeletal collapse. Although IbpA is not AMPylating the threonine T35 but the neighboring tyrosine residue Y32 instead it also impairs GTPase signaling leading to cytoskeleton collapse like VopS (51).

Despite the high abundance of Fic proteins, only one other Fic protein, HYPE, was identified to also harbor an AMPylation activity. HYPE is the only Fic protein in humans and is associated with Huntington`s disease as it was found to interact with Huntingtin that when mutated causes the fatal neurodegenerative disease. While *in vitro* experiments with purified protein revealed an adenylylation activity of HYPE towards Rho family GTPases as observed for IbpA and VopS, endogenous AMPylation of the small GTPases could not be monitored. As over expression of

HYPE is not as lethal as described for IbpA or VopS, HYPE might be tightly regulated or target other proteins in its physiological role that are yet unknown (51).

In contrast to VopS and IbpA, the T4SS effector AnkX of *L.a pneumophilia* is not targeting Rho GTPases but Rab1 and Rab35 which is crucial for the maturation of *Legionella* containing vacuoles (LCVs) to an ER-like replicative niche (54). Yet, AnkX is not only target another subclass of the Ras superfamily, but is also performing phosphocholination instead of AMPylation. Rab1 phosphocholination can be reversed by another *Legionella* effector, Lem3, allowing a fine tuned regulation of Rab1 activation state (55).

These recent advances in the understanding of different Fic proteins functions provided valuable indications for a possible role of the FIC-domain in *Bartonella* effector proteins. Yet, the differences between VopS/IbpA to AnkX indicate that Fic proteins have diverged in substrate and target recognition during evolution.

1.2.1 Fic protein-mediated AMPylation of targets

AMPylation, or adenylylation, is already known since the 1960s where it was studied in the context of *E. coli* glutamine synthetase (GS) that catalyzes the condensation of ammonia with glutamate to produce glutamine. This reaction is highly dependent on nitrogen levels and is thus regulated by a bi-functional protein called ATase that contains two nucleotidyl transferase domains in addition to a regulatory domain (56).

If nitrogen levels are high, glutamine binds to ATase leading to an activation of the adenylylation domain resulting in an adenylylation of GS. The AMP-moiety is supposedly blocking the active site of GS thus inhibiting the catalysis. If nitrogen levels are low, the second nucleotidyl transferase domain (adenylyl removase) is activated by α-ketoglutarate leading to a de-adenylylation of GS and is restoring GS-activity (57).

ATase is AMPylating a hydroxyl group of a tyrosine and is thereby introducing a stable phosphodiester (C-O-P-O-C). Yet, other enzymes were reported to catalyze the formation of less stable groups like carboxylate-phosphate anhydrid ((COO)-P-O-C) or phosphoamides (C-N-P-O). Thus, unreactive groups can be activated by AMPylation to form intermediates with more efficient leaving groups like reported for i) loading of tRNA with acetylated amino acid (58), ii)

synthesis of cofactors (59, 60) or iii) activation of phosphorylated sugars during glucagen synthesis (61).

All so far described Fic proteins perform PTMs on hydroxyl groups of tyrosines or threonines of target proteins forming stable phosphodiesters. This PTM results in a change of size and/or charge und is thus interfering with protein-protein interactions of the targets with their interaction partners (50).
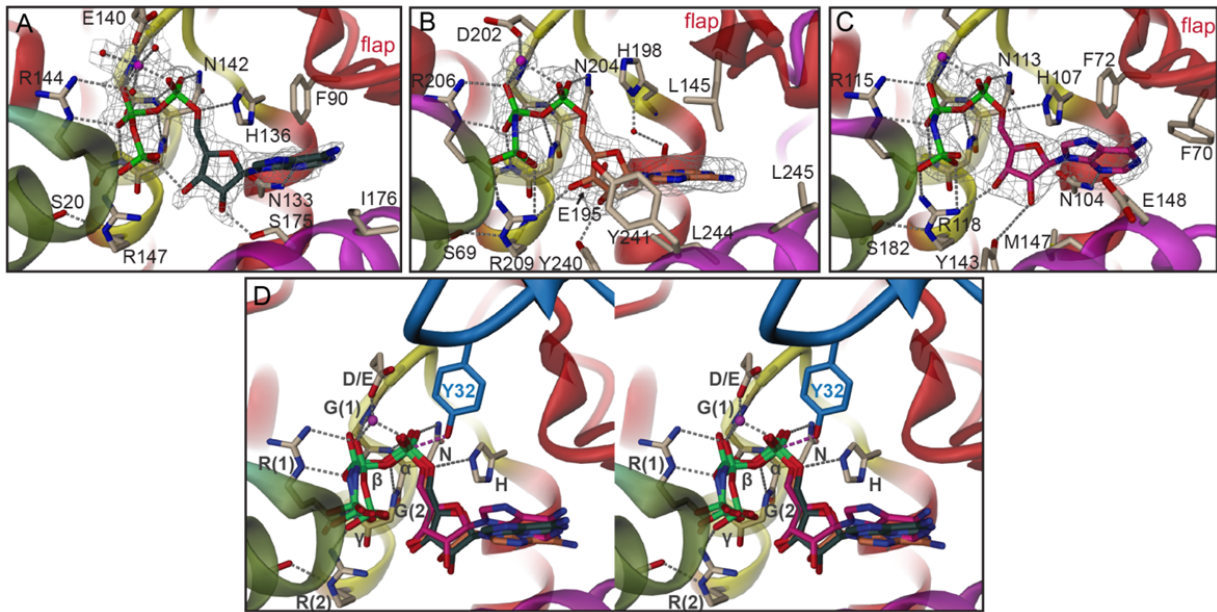
Figure 1.2.2: substrate coordination by Fic proteins favors an in-line attack on the ATP . A) VbhA$_{E24G}$/VbhT(FIC) in complex with ATP/Mg^{2+}; B) SoFic$_{E73G}$, C) NmFic$_{E186G}$, both in complex with AMPPNP/Mg^{2+}. Mg^{2+}-ions are shown as magenta spheres. The 2Fo-Fc simulated annealing omit maps covering the nucleotide/Mg^{2+} ligands are contoured at 1.1 σ. D) Stereo view of the superposition of the ligand structures shown in panels B) and C) onto the VbhA$_{E24G}$/VbhT(FIC) complex (same as in panel A). Note that the nucleotides of the various complexes are distinguished by their carbon color (VbhA$_{E24G}$/VbhT(FIC) ATP in green, SoFic$_{E73G}$ AMPPNP in orange and NmFic$_{E186G}$ AMPPNP in pink). The residues of the HxFx(D/E)GNGRxxR signature motif are labeled with the phenylalanine not shown. Also shown is the modifiable hydroxyl side-chain Y32 of Cdc42 (blue) after superposition of the IbpA(FIC2)/Cdc42 complex (46) onto VbhA$_{E24G}$/VbhT(FIC). For the superposition, only the Fic active site loops were used. The α-phosphate moieties appear well-suited for in-line attack of the target hydroxyl group (broken line in magenta). Taken from (48).

First structural insights into the mechanism of AMPylation were gained by a complex of the *Staphylococcus aureus* Kanamycin resistance adenylyl transferase with Kanamycin and a non-

hydrolysable ATP analoga revealing an in-line nucleophilic attack of the Kanamycin hydroxyl group on the α-Phosphate of ATP (62).

Recent studies on the Fic protein IbpA in complex with its target Cdc42 confirmed a similar mechanism for FIC-domain mediated AMPylation (46). Like seen in the complex of the *S. aureus* adenylyl transferase with Kanamycin, the hydroxyl group of Cdc42 tyrosin (Y32) performs a nucleophilic attack on the α-Phosphate of ATP. The low nucleophilicity of the tyrosine Y32 hydroxyl group of Cdc42 is increased by the histidine residue within the active side motif of IbpA that is inducing the de-protonation of Cdc42 at Y32 by an acid-base reaction.

While several mutations within the active motif with the exception of the first Glycine and first Arginine impaired AMPylation activity of Fic domains (46), not all mutations may abolish catalytic activity but rather lead to an alternative substrate specificity. The first known example of a substrate switch is AnkX of *L. pneumophilia*. The Rab1 phosphocholinating protein carries a mutation within the first Glycine that is exchanged for Alanine (HPFRD<u>A</u>NGR). This recent finding is a first indication that Fic proteins might have further evolved in target and substrate recognition.

To achieve AMPylation instead of phosphorylation, the substrate needs to be coordinated by the nucleotidyl transferase. First insights into substrate coordination were gained by structural investigation of nucleotidyl transferases of the nucleotidyltransferase/α/β-phosphodiesterase superfamily involved in cofactor synthesis like the Nicotinamide/nicotinic acid mononucleotide adenylyltransferase (NMNAT) of NAD+ synthesis (63), Flavin mononucleotide adenylyltransferase (FMNAT) to form FAD (PDB code: 1T6Y, to be published) and Phosphopantetheine adenylyltransferase (PPAT) (64) that is involved in Coenzyme A synthesis . The structures revealed a high conservation between all three enzymes which contain a nucleotide binding Rossmann fold, a defined secondary structure where α-helices are connected by β-sheets. In addition, all three proteins harbor the signature motif (H/T)xGH which a key element of nucleotide binding. Flanking histidines of the transferases are coordinating the substrates phosphates and act as proton donors for the negatively charged phosphates. A Mn^{2+} ion is additionally stabilizing the α- and γ-phosphates in PPAT.

Nucleotides are similarly coordinated in Fic proteins as shown in the complex structure of *Neisseria meningitidis* Fic protein with ATP (NmFic), VbhA/VbhT of *B. schoenbuchensis*, the Fic protein of *Shewanella oneidensis* but also the phosphocholinating protein AnkX of

L. pneumophila (PDB codes of histidine to alanine mutants 3ZEC, 3ZCB, 3ZCN and 4BER) (42, 48, 65).

In NmFic, a Mg^{2+}-ion complexes the α- and β-Phosphate of ATP and the arginines, R115 and R118, stabilize the β- and γ-Phosphates. In AnkX, however, the second arginine is not present und the nucleotide is only coordinated by one arginine R236.

While some Fic proteins seem to have a spacious active pocket and are thus more flexible in binding ATP-analoga (e.g. VopS that can bind to an alkyl ATP analoga), others seem to have a narrower pocket and are therefore restricted in substrate recognition. The substrate recognition is a major restriction in the development of tools to identify new AMPylation targets as most ATP-analoga that are used in enrichment strategies have an increased size or charge.

1.2.2 Target recognition is dependent on main chain-main chain interactions

In addition to Doc, Fic proteins also show structural similarities with the T3SS effector protein AvrB of plant pathogen *Pseudomonaa syringae*. Upon secretion, AvrB up-regulates hormone signaling and increases thereby the plants susceptibility. To this end, AvrB interferes in the signaling cascades of jasmonic acid response by inducing phosphorylation of RIN4, an interaction partner of RPM1 (resistance to *P. maculicula* protein 1). Although in recent studies, AvrB was identified to induce indirectly RIN4 phosphorylation by activation of the MAP-Kinase MPK4, it was long thought of to be directly targeting RIN4 and was even co-crystallized with ADP (the end production after phosphorylation) and a short peptide of RIN4. In this structure, RIN4 and the ADP moiety are facing each other in the presumable active pocket of AvrB. The main chains of the β-hairpin are binding to the target peptide via hydrogen bonds forming an anti-parallel β-strand. Furthermore, mutations in these AvrB-residues impaired *in vivo* the increase of plant susceptibility confirming their role on a functional level (66, 67).

The only Fic protein that was yet crystallized in complex with its target protein is IbpA binding to AMPylated Cdc42. Like seen in AvrB, IbpA is interacting with Cdc42 via its β-hairpin loop forming an anti-parallel β-strand. Target recognition at the active center is thus not mediated by ionic or hydrophobic interactions but by main chain-main chain interactions which is mostly sequence unspecific. The specificity towards one residue with thin target is therefore probably received by the features of the AMPylation region, e.g. position of the targeted site within the

quaternary structure, or by additional interaction sites of the Fic protein, e.g. localizing domains. Additionally, side chains of L3668 and K3670 of IbpA form a clamp that holds the target tyrosine of Cdc42 in a potent conformation.
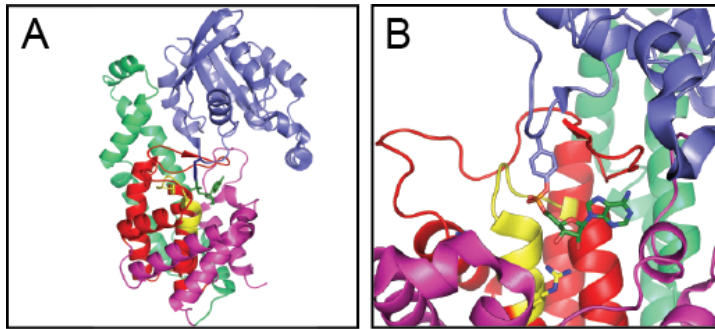
Figure 1.2.3: Target recognition by IbpA is mediated by its β-hairpin loop and an arm domain. IbpAFic2[H3717A]:Cdc42 complex is shown in ribbon style. A) Structural analysis of a complex of tyrosine Y32-AMPylated (dark blue, sticks) Cdc42 (blue) with IbpAFic2 reveals target recognition is mediated by an arm domain (green) of IbpA that interacts with the switch II region of Cdc42 (46). The HPFAEGNGRMAR motif of IbpA is colored in yellow, the Fic-domain is shown in magenta with the Fic core in red. The two arginines (R3725 and R3728) within the motif as well as the AMPylated tyrosine Y32 are shown as sticks. B) Zoom-in on the active site motif within the IbpAFic2[H3717A]:Cdc42 complex. The β-hairpin loop if IbpA forms an antiparallel β-sheet with the target switch I region of Cdc42 (PDB code 4ITR).

As target recognition is mediated by main chain-main chain interactions and therefore not restricted to any sequence properties, the range of potential targets is unlimited. Yet, IbpA and VopS were only shown to target small GTPases but not any other unrelated protein class indicating that in addition to the β-hairpin loop another part of the protein is required for target recognition. Consistently, both IbpA and VopS harbor a region that interacts with the switch II region of small GTPases.

Apart from the FIC-domain, several Fic proteins harbor additional domains, like DNA-binding domains, that might mediate Fic protein localization but might also play a role in target recognition.

1.3 The BID-domain

As stated above, the BID-domain of Beps forms together with the positively charged C-tail a bi-partite secretion signal that allows recognition of the Beps by the coupling protein VirD4. As the bipartite C-terminus can also be found in conjugal relaxases, its evolutionary origin is most likely found within conjugation systems.

Yet, several Bep proteins of the lineage 4 *Bartonellae* harbor more than one BID domain indicating that it may have adapted additional functions. Consistent with this hypothesis, most Bep-induced cellular phenotypes were linked to the BID-domain (37-39) ranging from small GTPase function to activation with adenylyl cyclases.

The first described Bep with functional BID-domains was BepG of *B. henselae* that was shown to be sufficient to inhibit endocytic uptake of bacteria and to induce invasome formation in endothelial cells. BepG harbors four BID-domains that show homology to previous described proteins. Although the first BID-domain of BepG harbors the signature motif WxxxE that is typically for Guanine nucleotide exchange factors (GEF) proteins, mutation of this motif did not impair BepG-mediated invasome formation (39) indicating that BepG is not a GEF. Consistently, BepG acts independently of cofilin1, a downstream effector of small GTPases.

In addition to BepG, also the combined action of BepF and BepC was shown to induce invasome formation (68). BepF consists of three BID domains in addition to the positively charged C-tail and a tyrosine-rich N-terminus while BepC harbours a FIC domain and the bipartite secretion signal. In contrast to BepG, the first two BID-domains of BepF are activating the small GTPase Cdc42 which is a critical step in actin nucleation (68). As BepF is activating small GTPases, yet, over-expression of Cdc42 and Rac1 were shown to decrease invasome formation, it is speculate that BepC might counteract BepF for optimal regulation of Cdc42 and Rac1. Yet, the target as well as the function of BepC remains elusive at this point.

Effector translocation and thus effector influence on the cytoskeleton that lead to invasome formation can result in sever damages for migrating cells. Recently, our group was able to show that these unwanted side effects can be overcome by an additional effector protein, BepE. BepE consists of two BID-domains in addition to the C-tail and a tyrosine-rich N-terminus. Again, the BID-domains alone acting synergistically are sufficient to reduce migration defects. Furthermore, the data indicate that BepE activates RhoA and is thereby inducing rear end retraction (69).

In contrast to the Beps that target F-actin regulating components, BepA was shown to inhibit host cell apoptosis by increasing intracellular cAMP-levels via its BID-domain (70).

1.3.1 BID$_{BepA}$ of *B. henselae* increases intracellular cAMP levels

A prominent phenotype upon *in vitro* infection with *B. henselae* is the inhibition of endothelial cell apoptosis which is believed to contribute to the unique vasculotumorigenic activity of *B. henselae (70)*.

BepA is one of seven T4SS effector proteins in *B. henselae* that get translocated into host cell upon infection. It consists of an N-terminal FIC-domain and a C-terminal BID-domain (BID$_{BepA}$). BID$_{BepA}$ localizes to the plasma membrane of host cells where it is sufficient to inhibit apoptosis (37, 70) .

Furthermore, BepA was shown to reduce activation of apoptosis associated protease Caspase-3 and to increase expression of cAMP response genes *pde4B* and *crem*. Utilizing cAMP-ELISA assays, BepA-dependent increase of intracellular cAMP-levels were confirmed (70).

BepA shares a common domain architecture with its paralogs BepB and BepC. While BepC plays a role in bacterial uptake into the host cell, the cellular function of BepB remains unknown. Although both ectopically expressed proteins, BepB and BepC, localize to the plasma membrane neither BepB nor BepC inhibited apoptosis in endothelial cells (70).

1.4 Targets of *Bartonella* effector proteins

In previous studies, a variety of targets for bacterial effector proteins were identified like the Rho GTPase that are covalently modified by the Fic proteins IbpA and VopS. Similarly, the predominant target class of proteins of *Bartonella* effector proteins seemed to be small GTPases as found for BepF of *B. henselae* and Bep1 of *B. rochalimae*. In this study, we furthermore present adenylylate cyclases (ACs) as a target of BepA of *B. henselae* and tubulin and vimentin as targets of Bep2 of *B. rochalimae*.

1.4.1 The role of small GTPases in pathogenicity

In humans, there are 18 members of Rho GTPases that belong to the Ras superfamily with the best investigated members being Rho, Rac and Cdc42. They function as a molecular switch in signal transduction and can be converted from an inactive GDP-bound form into an active GTP-bound form. An intrinsic GTPase activity catalyzes the hydrolysis of GTP to GDP and is thereby reversing the activation (71). The switch in activity can be promoted by guanine nucleotide exchange factors (GEFs) that induces the GDP to GTP-exchange or by GTPase activating proteins (GAPs) that increase the intrinsic GTPase activity and are therefore de-activating (72). Within the human genome, 67 GAP proteins for Rho GTPases, 71 GEFs with a Dbl homology (DH) domain and another 11 GEFs of the DOCK family that are specifically targeting Rac and Cdc42 (73) were identified. In addition to GEFs and GAPs, G-protein activity is regulated by guanine nucleotide dissociating inhibitors (GDIs) that are impairing the dissociation of GDP from the GTPase and are thereby locking the GTPase in its inactive form (74). In the human genome, three GDIs were identified. The high abundance of G-protein regulators implicates a complex network of regulation (75).

Although the extend of the regulatory network is still not completely resolved, many interaction partners of Rho GTPases were identified within the last 30 years and their function was linked to most major pathways of eukaryotic signaling. Among the targets of Rho GTPases are approximately 30 kinases and a huge variety of scaffolding and adaptor-like proteins but also crosstalk between GTPases themselves has been described.

Hence, it is not surprising that several pathogens were found to influence G-protein activities either indirectly or directly by an intrinsic GEF activity or covalent modification to hijack host cell pathways and influence them in favor of bacterial internalization and colonization of the pathogens replicative niche.

1.4.2 Pathogen internalization is dependent on small GTPase signaling

Internalization of pathogens into a host cell can be solely host-dependent or pathogen-driven. In the first case, specialized phagocytic cells internalize the pathogen without its active contribution. In order to invade host cells which are not professional phagocytes, pathogens have developed an

arsenal of fine-tuned tools to manipulate host cell functions. Pathogen internalization is described by either a "zipper" or "trigger" mechanism (76).

Salmonella typhimurium and S. *enterica* utilize a trigger mechanism to induce their internalization. To this end, effector proteins are secreted via a type III secretion system into the host cell insertion of the translocon proteins SipB/SipC into the plasma membrane. SipC harbors to functional cytoplasmic domains where the N-terminal domain binds actin while the other is inducing actin nucleation (77). In a following step, SopE1 and SopE2 are secreted into the cell and activate the small GTPases Cdc42 and Rac1 that further induce actin nucleation (78). Next, a phosphatidylinositol phosphatase, SopB stimulates actin rearrangements while SipA stabilizes existing actin fibers (79, 80). Last, SptP is secreted that regulates MAPK (mitogen-activated protein kinase) through a tyrosine phosphatase activity and deactivates Cdc42 via a GAP activity thus leading to cup closure, actin depolymerization and pathogen internalization (81).

Another example of a pathogen utilizing a trigger mechanism is *Listeria* that cross the blood-brain and blood-placenta barriers by infecting non-phagocytic cells like epithelial cells via two adhesins InlA and InlB that interact with E-cadherin (82) and Met (83), respectively . InlA binds to E-cadherin that binds intracellularly via catenin to actin and induces *de novo* actin nucleation by the Arp2/3 complex (84-87). InlB binds to the Met receptor and induces its autophosphorylation that in turn activates Rac1/WAVE/Arp2/3 complex and cofilin activation (88).

Apart from adhesions that dock pathogens onto the host cells, a variety of pathogens like *Yersinia enterocolitica* and *Y. pseudotuberculosis* but also *B. henselae* have been shown to bind to β-integrins (89, 90). Our group demonstrated that interaction of *B. henselae* with integrin-β1 is required for invasome formation as integrin-β1 signaling leads to activation of Rac1 by recruitment and autophosphorylation of the focal adhesion kinase FAK (90).

Auto-phosphorylation of FAK creates a binding site for Scr-kinase that in return increases phosphorylation of FAK (92). The complex of integrin-β1/FAK/Scr also binds the scaffolding protein p180Cas (93) that binds the unconventional Rac1-GEFs, Dock180 and ELMO1 (94), through the adaptor protein Crk. In addition, β-integrin1/FAK/Scr complex also interacts with paxillin which subsequently recruits β-PIX, a GEF for Cdc42 and Rac1 (95). Rac1 in turn binds to a number of interaction partners that directly influence actin polymerization, e.g. by activating the Arp2/3 complex.

Next to the activation of the Arp2/3 complex and subsequent rearrangements of the cytoskeleton, Rho GTPases also influence cell responses in respect to cell migration inflammation signaling that play crucial roles in pathogenicity.
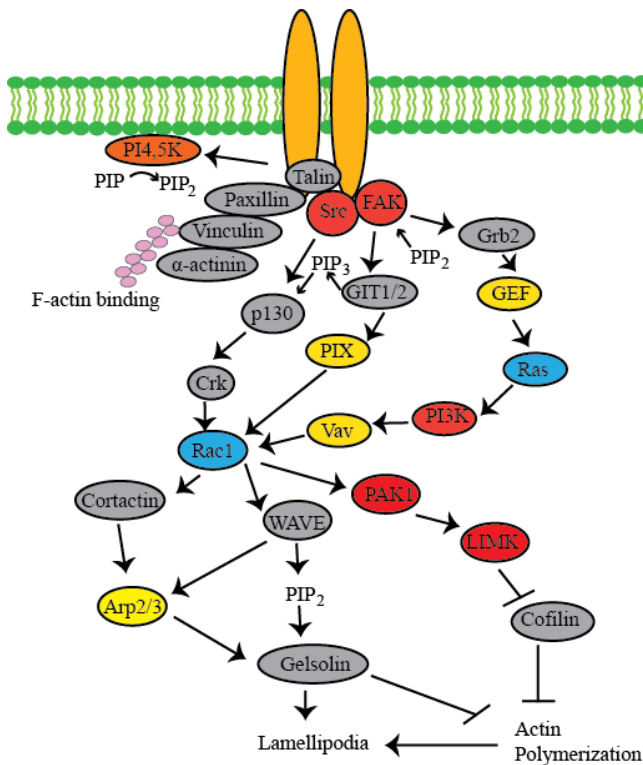
Figure 1.4.1: Integrin signaling engages Rho GTPases to control actin polymerization. Upon stimulus binding to integrin, a signaling complex involving several kinases and adaptor proteins is formed at the cytoplasmic site of integrin. Phosphorylation events then lead to the activation of small GTPases that interact with a variety of actin polymerization regulators. The complexity of the signaling network indicates a fine tuned system that allows distinct F-actin formation locally or globally. Adapted from (91).

1.4.3 Rac1 activation in immune response

A central factor in pathogen defense strategies of host cells is the NF-κB complex that translocates one out of five subunits, p65, into the cell nucleus and induces the transcription of cytokine precursors (96). Once translated, precursors are processed by activated caspase-1 and secreted into the tissue where they promote inflammation (97). The protein levels of pro-inflammatory signals are orchestrated by a variety of signaling processes including TOLL-like

receptors (TLRs) and NOD-like receptors (NLRs). While TLRs as well as NLR1 and NLR2 are regulating NF-κB and thereby transcription of pro-inflammatory genes, other NLRs like NLR3 are involved in the processing of precursors via the inflammasome. The inflammasome protein complex is formed upon NLR-stimulation by PAMPs (pathogen-associated molecular patterns) and induces the activation of caspase-1 (97).

Interestingly, the small GTPases Cdc42 and mainly Rac1 are associated with the regulation of both TLRs and NLRs.

Upon stimulation of TLR2, Rac1 and PI3K (Phosphoinositol-3 kinase) make part of an active protein complex located at TLR2 (98). In this complex, Rac1 binds to the regulatory subunit of PI3K that in turn binds to phosphorylated tyrosines of TLR2. Rac1 induces PI3K activation and the phosphorylated lipid products generated by PI3K induce autophosphorylation of Akt that promotes the localization of p65 subunit into the nucleus (98).

Recently, activation of Rac1 was shown to up-regulate inflammasome formation and caspase-1 activation. Although the mechanism behind Rac1-mediated inflammasome formation is not resolved, effectors of both *S. typhimurium* and *Chlamydia pneumoniae* were shown to induce caspase-1 activation in a Rac1-dependent manner thus influencing the immune response of the host (99, 100).

1.4.4 Synthesis of cAMP: one key for many locks

A common strategy in pathogenicity is elevation of cAMP that has a broad influence on the host cell signaling including phagocytosis, apoptosis and cytokine expression. cAMP is produced by adenylyl cyclases (also known as adenylate cyclase, AC). Most eukaryotic ACs are transmembrane proteins with the exception of one cytosolic AC.

Once activated, AC produces cAMP that in turn activates a variety of different proteins. Apart from calcium and potassium ion channels, PKA (protein kinase A), Epac-1 and Epac-2 (Exchange proteins directly activated by cAMP) are the best studied downstream effectors. All of these proteins, PKA and Epacs, consist of a regulatory and a catalytic subunit that are interacting with each other in an inactive state of the protein (101).

Upon binding of cAMP to the regulatory subunit, the catalytic subunit is released and activates downstream effectors either through phosphorylation or GEF activity. The catalytic subunit of

Epac exhibits a GEF activity in particular towards the small GTPases Rab1 and Rab2 and thus influences cell attachment, calcium fluxes and exocytosis (102), PKA instead phosphorylates a variety of proteins including ERK and the CREB (cAMP response element binding protein) ultimately leading to a change on the transcription level of target genes (103).
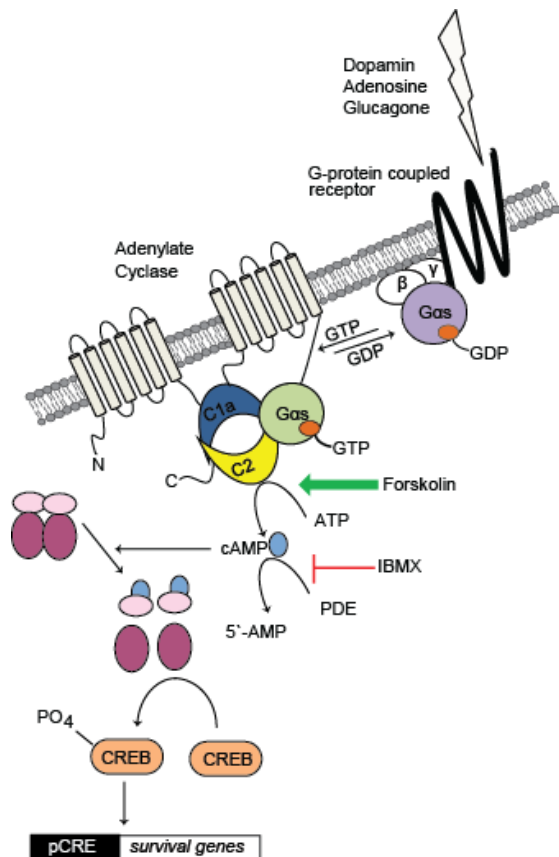
Figure 1.4.2: cAMP synthesis induces transcription of genes under the CRE-promoter. Receptor activation induces the exchange of GDP for GTP within the alpha subunit of stimulating heterotrimeric G-protein (Gαs) and its release from the receptor complex. The GTP-bound Gαs binds to both cytosolic domains of adenylyl cyclase (AC) and induces cAMP production which can be increased by the plant diterpene Forskolin. cAMP then can be degraded by phosphodiesterase (PDE) that can be inhibited by IBMX or it can bind to the regulatory subunit of protein kinase A (PKA). Upon binding of cAMP, the complex of regulatory and catalytic subunits of PKA dissociate and the catalytic subunits phosphorylate cAMP response element binding protein (CREB). Phosphorylated CREB translocates into the nucleus and induces transcription of genes under the CRE-promoter which inhibit Caspase-3 activity.

The tremendous number of downstream effectors allows a multifaceted response to the elevation of cAMP levels and requires a tight and often cell type specific regulation. One level of regulation is provided by spatial restriction that is mediated by lipid rafts or AKAPs (A-kinase anchoring proteins). AKAPs form multiprotein complexes and thus lock PKA to distinct upstream and downstream effectors. This compartmentalization leads to an increased efficiency of the cAMP-response. They were originally identified in 1982 by Theurkauf *et al.* (104) and are highly diverse with the exception of a PKA docking motif (105). To date, more than 50 AKAPs are identified with different subcellular localization. Another important aspect of AKAPs is the intrinsic feedback loop that allows temporal control of the cAMP response (106). As AKAPs are expressed in a cell type-dependent manner, cAMP responses are also cell type dependent and often opposing effects are described. Similarly to AKAPs, also cAMP-producing ACs are subject to cell type specificity and spatial regulation.

All nine isoforms of transmembrane AC can be inhibited by adenosine analogs named P-site inhibitors (107, 108) and (with exception of AC9) are activated by the α-subunit of stimulating heterotrimeric G-protein (Gα_s) (109). Apart from these shared features and the common domain architecture comprising two membrane spanning and two cytosolic domains, the nine isoforms mostly differ in respect to their regulation patterns (110). While AC1 and AC8 are inhibited by the βγ-subunit of heterotrimeric G-proteins, βγ-subunit was found to be a conditional activator of AC5 and AC6 (111) and while AC3 is inhibited by Ca^{2+}, AC1 and AC8 are stimulated upon Ca^{2+}-influx (112).

The complex network of AC regulators comprises several cytosolic or receptor-coupled G-proteins, Calmodulin signaling, RGS (regulators of G-protein signaling) and phosphoinositol-signaling. The most generic and thus best understood activator is Gα_s that is coupled by the βγ-subunit of heterotrimeric G-proteins to receptors e.g. to the β-adrenergic receptor (βAR). Upon hormone stimulation, the receptor binds the C-terminus of Gα_s which leads to a reorganization of β6-α5 region that is engaged in GDP-coordination via its purine moiety. Additionally, the receptor interacts with the N-terminus of Gα_s which abolishes the stabilization of the diphosphate of GDP. This leads to the release of the co-factor and leaves the Gα_s in an opened conformation. This opened form can either bind GDP and return to its inactive form or GTP inducing the release of Gα_s from the receptor (113).

Once dissociated from the receptor, $G\alpha_s$ can interact with both cytosolic domains (C1- and C2-domain) of AC thereby holding both domains together in an active conformation (114-116). At the interface between the C1 and C2, the active pocket is formed where ATP is converted to cAMP. A pocket similar to the active site is also positioned in the interface between C1 and C2. In this latter pocket, the plant diterpene Forskolin can bind and, similarly to $G\alpha_s$, increase the interaction between C1 and C2 (117). Together, Forskolin and $G\alpha_s$ can synergistically active ACs (118, 119).
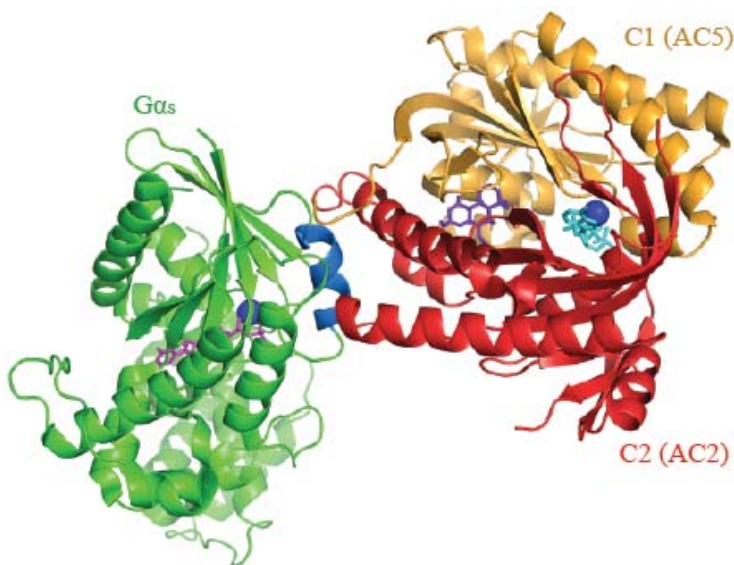
Figure 1.4.3: $G\alpha_S$ interacts with C1 and C2 cytosolic domains of adenylyl cyclases. The crystal structure of a complex of $G\alpha_s$ (green), the C1-domain of AC5 (orange), and the C2-domain of AC2 (red) shows that $G\alpha_s$ interacts via its switch II region (marine) with both AC domains. Chains are represented as cartoons; cofactors are shown as sticks with GDP in magenta, Forskolin in purple, and 2'-deoxy-adenosine 3'-monophosphate together with pyrophosphate in cyan. Coordinating Mg^{2+}-ions are shown as blue spheres. PDB code 1CUL.

In contrast to $G\alpha_s$, $G\alpha_i$ inhibits the formation of the C1/C2 dimer and the formation of an active pocket thus dampening cAMP production (120). Yet, $G\alpha_i$ like $G\alpha_s$ binds to and acts on the C1 domain of ACs (121).

Apart from the cytosolic domains C1 and C2, also the cytosolic N-terminus of ACs, in particular the one of AC5, was reported to play a key role in regulation of AC activity by interacting with and thus directing regulatory proteins to the AC. Ric8a (122), a GEF for the inactivating G-

protein Gα$_i$, AKAPs (123), Gβγ (124), phosphatases (125) or calmodulin were shown to influence AC activity by binding to the AC N-terminus (126).

Due to the huge variety of downstream effectors, cAMP is a very generic component of cellular signaling and is in fact found to be often misregulated in diseases like microbial infection. Several pathogens have been described to alter inflammatory responses by increasing cAMP-levels by either directly synthesizing cAMP either intracellularly (*Bordetella pertussis, Pseudomonas aeruginosa*) or extracellularly (*Mycobacterium tuberculosis*), by stimulating receptor proteins (*Bacillus thuringiensis*) or by altering the activity state of host cell proteins. The latter is well understood for *Vibrio cholerae* toxin that ADP-ribosylates an arginine residue within Gα$_s$ which converts the G-protein into a constitutively active form (127). In contrast, *Pasteurella multocida* toxin activates Gα$_i$ by deamidation thus disabling the intrinsic GTPase activity and thereby keeps Gα$_i$ in a constitutively active form (128).

1.4.4 cAMP-signaling in apoptosis

There are two pathways that lead to cell death by apoptosis that are distinguished by the initiating signal into the extrinsic and the intrinsic pathway. While extrinsic apoptosis is induced by an external signal that stimulates death receptors, the intrinsic pathway starts with mitochondria and leads to release of cytochrome c.

One family of death receptors is the family of TNF-receptors (tumor necrosis factor) that has cysteine rich extracellular domains that trimerize upon an incoming signal (129). In turn, the intracellular death domains (DD) sequester DD-containing adaptor proteins like FADD or TRADD thereby forming the DISC (Death inducing signaling complex) as reviewed by Ashkenazi (130, 131). In addition to DD, FADD also contains a DED (death effector domain) that recruits DED-containing procaspase-8 through homotypic DED-DED interaction leading to autocleavage of procaspare-8 to active caspase-8. In typeI cells, this starts a signaling cascade of caspase activation eventually resulting in cell death (132). Yet, in type II cells, the caspase signaling is not sufficient to results in apoptosis. Instead, the pathway of intrinsic apoptosis is activated through Bid, a member of the Bcl-2 family that is cleaved by caspase-8 and translocates into mitochondria (133).

Apart from Bcl-2 proteins, the intrinsic pathway of apoptosis can be induced e.g. by DNA damage, oxidative stress or starvation (135). This leads to a disruption of mitochondrial inner transmembrane potential (Dy) and permeability transition (PT) inducing an influx of water and subsequently to a swelling of mitochondria and the release of proapoptotic proteins like cytochrome c. Cytosolic cytochrome c is binding to monomeric Apaf-1 which in an dATP-dependent manner forms wheel like oligomers with a 7-fold symmetry called apoptosome that triggers the activation of caspase-9. Caspase-9, like caspase-8, starts a signaling cascade of caspase activation (136).
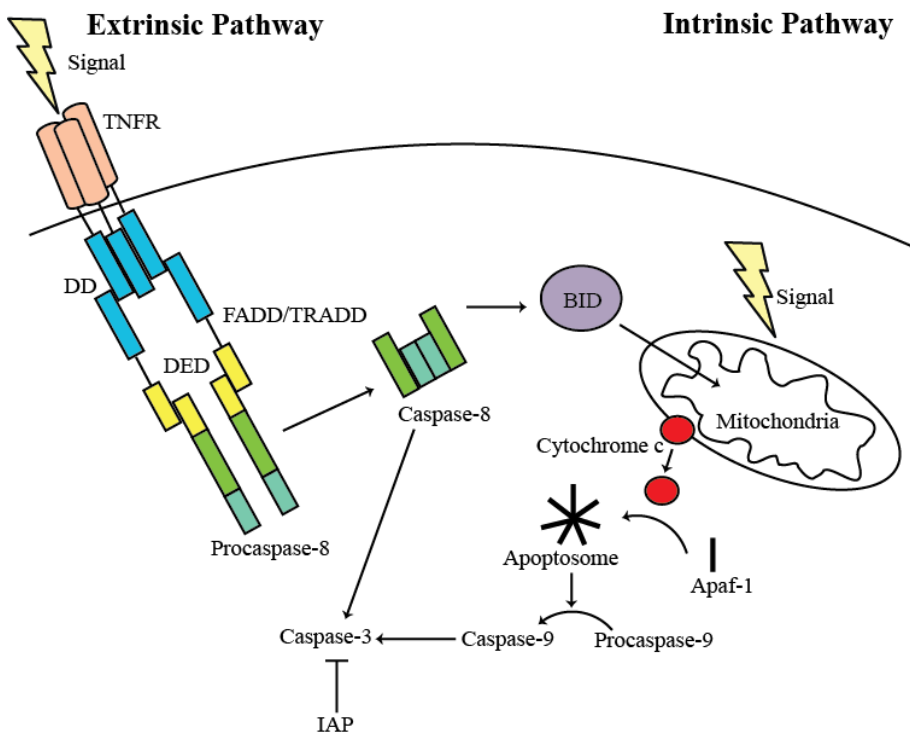
Figure 1.4.4: The extrinsic and intrinsic pathways of apoptosis. Schematic overview of extrinsic or intrinsic induced apoptosis. Death receptor signaling activates caspase-8 via the adaptor proteins TRADD and FADD consisting of DD (death domain) and DED (death effector domain) forming the DISC complex (death inducing signaling complex). Active Caspase-8 either activates Caspase-3 and directly induces apoptosis or additionally induces the intrinsic pathway through activation of the Bcl2-family member BID. Cleaved BID translocates into mitochondria and induces the release of Cytochrome C that binds to Apaf-1 in the cytosol. Cytochrome C bound Apaf-1 forms the apoptosome with a 7-fold symmetry and activates Caspase-9. Caspase-9 in turn can activate Caspase-3 leading to apoptosis. Adapted from (134).

Ultimately, both pathways lead to the activation of caspase-3 that induces cell death (136). Yet, caspase-3 but also other caspases can be inhibited by IAPs (inhibitors of apoptosis proteins) that interact with and inhibit caspases through a BIR-domain (baculovirus IAP repeat) (137). Additionally, some IAPs harbor a RING-domain that has an E3 ubiquitin ligase activity through which IAPs ubiquitinate themselves and induce protein degradation of themselves but possibly also of their interactors (138).

While cAMP is not prohibiting the autocleavage of procaspase-3 leading to activate caspase-3, it was shown to elevate expression of IAPs and thereby to inhibit caspase-3 activity resulting in and anti-apoptotic effect (139).

1.4.5 Microtubules and intermediate filaments

Microtubules (MTs) are an essential component of the eukaryotic cell and were found to play key roles in most cellular processes like cell division, migration or trafficking. They are filamentous structures formed by polymerization of heterodimers of α- and β-tubulin (αβ-tubulin). The polymer network stabilizes the cell shape and protrusions like lamellipodia. MTs are associated with a variety of scaffolding proteins that are spatially directed by but also dependent in their activity on MT dynamics. Hence, MTs are regulated by but also regulate and influence themselves a broad signaling network as reported for migration, endosomal maturation (140) or autophagy (141).

Both, α- and β-tubulin, are P-loop GTPases that bind GDP in their curved, heterodimeric form. Upon nucleotide exchange for GTP, αβ-dimers can assemble to form polar polymers with a slow growing minus-end exposing α-tubulin and a fast growing plus-end exposing β-subunits. In mammalian cells, the minus-end is often anchored to cellular structures, e.g. the Golgi, while the plus end is elongating. During polymerization, the αβ-tubulin is changing its conformation so that the curved heterodimer completely straightened within the polymer (MT lattice). Along with the switch in conformation, GTP is hydrolyzed by the intrinsic GTPase activity of tubulin leaving the vast majority of the MT lattice intact, but in a GDP bound form (142).

For the maintenance of MT organization, a high level of regulation is required that is provided in part by MT plus-end tracking proteins (+TIPs). +TIPs are a structurally and functionally diverse group of proteins that can be distinguished by their accumulation on MTs. They are classified by protein components that mediate MT accumulation and polymerization (144). The first described
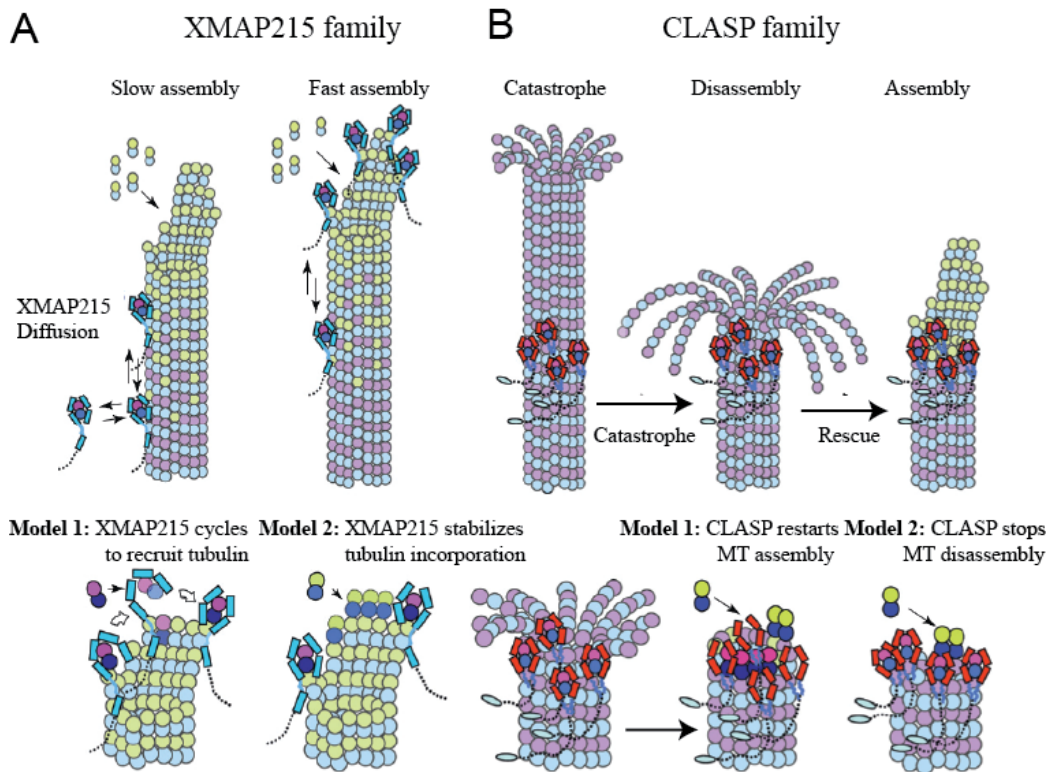
Figure 1.4.5. Models for the regulation of MT dynamics by TOG-domain containing proteins. **A)** XMAP215 binds tubulin dimers via its TOG-domains and the MT lattice via its SK domain. XMAP215-tubulin complexes accumulate at the MT plus end, which accelerates MT assembly. Model 1: XMAP215 cycles to load its TOG-domain bound tubulin dimer at growing MT ends that induces the release of the tubulin dimer. Model 2: XMAP215 stabilizes the assembly conformation of a microtubule by binding and stabilizing polymerized-tubulin conformation (yellow) with its TOG domains. B) CLASP family proteins promote MT rescues and inhibit MT catastrophes. CLASP binds tubulin dimer via its TOG domains and binds MT lattices with high affinity via its SR-rich domain similar to XMAP215. The high affinity of CLASP leads to sites of high concentration along MTs. When a dynamic MT undergoes catastrophe, MT disassembly occurs until the plus end reaches a site of high CLASP concentration (lower middle). There, CLASP locally promotes rescue in which MT depolymerization halts and MT assembly reinitiates. Model 1: CLASP molecules release their loaded tubulin dimer into the MT plus end and reinitiate polymerization. Model 2: CLASP molecules utilize their loaded tubulin to prevent MT disassembly and restore MT to the assembly phase. Adapted from (143).

+TIP was the cytosolic linker protein with a molecular weight of 170 kDa (CLIP-170, officially known as CLIP1) (145).

While some +TIPs were found to recognize the growing end of MTs autonomously, others require adaptors or motor proteins like kinesin to hitchhike to the plus-end. Examples of adaptor

proteins are provided by the EB (end-binding) protein family that can interact with most +TIPs by interaction of their EBH-domain and an SxIP-motif on the +TIP. EB proteins can bind through their C-terminal EEY/F motif together with the same C-terminal motif on α-tubulin to CAP-Gly proteins like CLIP-170 (146).

Such motif based interactions can be interrupted by post translational modifications like the serine-phosphorylation in the proximity of SxIP or the de-tyrosination of the α-tubulin EEY/F motif.

In recent studies, the autonomous +TIP class of XMAP215/Dis1 and CLASP protein families were found to catalyze polymerization or rescue after spontaneous depolymerization (catastrophe) through their TOG-domains that on the one hand can bind to plus-end or lattice of MT but also to free αβ-dimers. Furthermore, all proteins of the XMAP215/Dis1 and CLASP families harbor SK- or SR-rich sequences that are thought to mediate attachment to the MT-lattice (147, 148) in addition to the TOG-mediated association to curved or straightened tubulin. Through their C-tail region, many members of both families were reported to bind to different +TIPs thereby mediating directionality of MT assembly.

Structural investigation of the TOG-domain of yeast Stu2 protein belonging to the XMAP215/Dis1 family, revealed that this domain is interacting simultaneously with both the α- and β-tubulin subunits. The TOG1-domain of Stu2 is interacting via its Loop5 region with α-tubulin and via its Loop1 region with Y106 β-tubulin. The interaction between TOG and tubulin was found to be partly mediated by salt bridges between the hydroxyl group of β-tubulin Y106 and R116 of Stu2 (149).

Further, both TOG1 and TOG2 were found to preferably bind to the curved form of αβ-tubulin independent of the nucleotide bound to tubulin. This indicates that the nucleotide itself does not suffice to induce straightening of the heterodimer (149).

As both TOG domains bind to curved tubulin, it is envision that the TOG2 binds to the plus-end thereby localizing the protein while the TOG1-domain captures free αβ-dimers. In this model, Stu2 would recruit free tubulin and to the growing MT-filament. Polymerization would then induce straightening of the captured αβ-dimers leading to the dissociation of the TOG1-tubulin complex (149).

However, structural studies of CLASP proteins revealed the opposite behavior: This family shows a binding preference for straightened αβ-dimers offering a first hypothesis on how the

different functionalities of TOG-domain containing proteins evolved (150). It remains unclear, id CLASP proteins rescue MTs upon an MT-catastrophe by merely stabilizing the polymer via TOG-tubulin interactions or by actively inducing the re-polymerization (150).

In comparison to microtubules, little is known about the function of vimentin intermediate filaments. Only within the last 10 years, vimentin was found to be engaged in several cellular processes ranging from lymphocyte migration to autophagy regulation. Vimentin can be found from the cell nucleus to the extracellular matrix making it difficult to assess and study distinct functionalities. The expression of vimentin is cell type dependent which could imply an expression regulation and thus an importance of vimentin and vimentin knockout mice can develop without any prominent abnormalities (151).
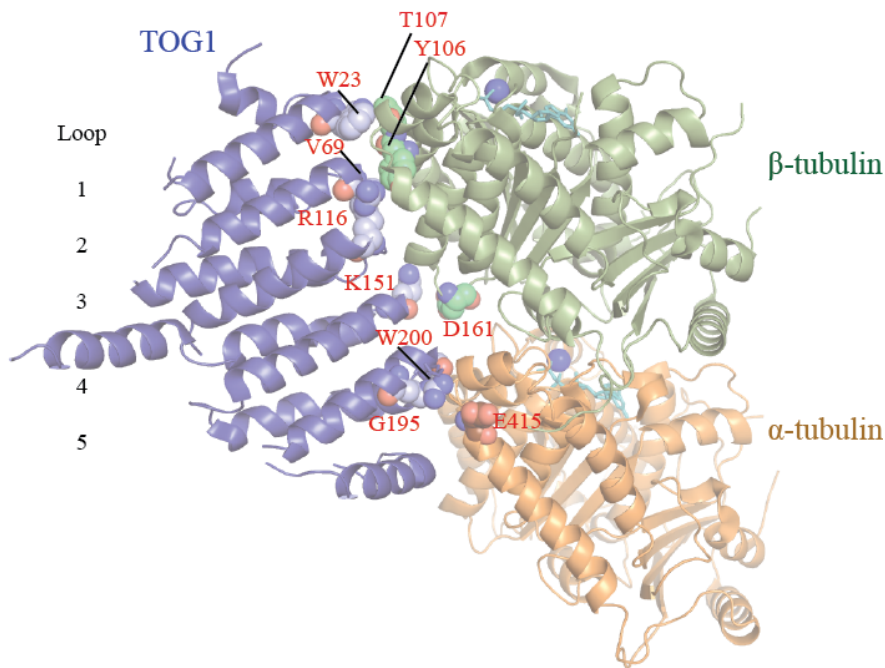
Figure 1.4.6: TOG1-domain of Stu2 interacts with α- and β-tubulin. Crystal structure of the complex with α-(orange) and β-tubulin (green) with TOG1-domain (purple) of Stu2 from *S. cerevisiae*, a member of the XMAP215 family. Chains are shown as cartoons and the residues contributing to complex formation are depicted as spheres. Tubulin-bound GTP molecules are shown as stick in cyan, coordinating Mg^{2+}-ions are shown as blue spheres. PDB code 4FFB (149)

Vimentin consists of an N-terminal head domain, an α-helical rod and a C-terminal tail. Its polymerization as well as its secretion by monocytes is dependent on the serine phosphorylation

in the N-terminal head domain. One kinase that catalyzes vimentin phosphorylation is PKC. Consistently, the anti-inflammatory cytokine IL-10 that inhibits PKC is also decreasing vimentin secretion while the pro-inflammatory cytokine TNF-α increases secretion. As phagocytic monocytes are producing reactive oxygen species (ROS) upon stimulation with 12-*O*-tetradecanoylphorbol-13-acetate or particulate agents, vimentin was tested for its ability to influence ROS levels and in fact extracellular vimentin was found to increase ROS levels and microbicidal activity of *E. coli* challenged macrophages through an unknown signaling pathway (152).

In addition to PKC, other kinases like PKA or p35^{cdc2} were reported to phosphorylate the N-terminal head domain of vimentin on S38, S55, S56 and S72 which induces the disassembly of vimentin filaments (153, 154). As the polymer binds to a variety of scaffolding proteins, the dynamics of filamentation are a regulating factor of other cellular processes. The interrelation between vimentin and autophagy was recently described to be mediated by the scaffolding protein 14-3-3 that binds to vimentin intermediate filaments but also to phosphorylated Beclin1where the association of Beclin1 with vimentin is inhibiting Beclin1-induced autophagy (155).

Furthermore, vimentin was identified to stabilize focal adhesion sites thereby increasing attachment of the cells. To this end, plectin that is hitchhiking via kinesin on MTs to integrin-β3 recruits intermediate filaments to focal adhesion sites (156).

Despite these recent advances in understanding the cellular function of vimentin, its active contribution to pathogenicity remains to be investigated.

1.5 References

1. Henkel JS, Baldwin MR, & Barbieri JT (2010) Toxins from bacteria. *Exs* 100:1-29.
2. Galan JE (2009) Common Themes in the Design and Function of Bacterial Effectors. *Cell Host Microbe* 5(6):571-579.
3. Freche B, Reig N, & van der Goot FG (2007) The role of the inflammasome in cellular responses to toxins and bacterial effectors. *Semin Immunopathol* 29(3):249-260.
4. Lord JM & Roberts LM (1998) Toxin entry: retrograde transport through the secretory pathway. *J Cell Biol* 140(4):733-736.
5. Ludwig A, Bauer S, Benz R, Bergmann B, & Goebel W (1999) Analysis of the SlyA-controlled expression, subcellular localization and pore-forming activity of a 34 kDa haemolysin (ClyA) from Escherichia coli K-12. *Mol Microbiol* 31(2):557-567.
6. Christie PJ, Atmakuri K, Krishnamoorthy V, Jakubowski S, & Cascales E (2005) Biogenesis, architecture, and function of bacterial type IV secretion systems. *Annu Rev Microbiol* 59:451-485.
7. Filloux A, Hachani A, & Bleves S (2008) The bacterial type VI secretion machine: yet another player for protein transport across membranes. *Microbiol-Sgm* 154:1570-1583.
8. Galan JE & Wolf-Watz H (2006) Protein delivery into eukaryotic cells by type III secretion machines. *Nature* 444(7119):567-573.
9. Kubori T & Galan JE (2003) Temporal regulation of salmonella virulence effector function by proteasome-dependent protein degradation. *Cell* 115(3):333-342.
10. Murata T, *et al.* (2006) The Legionella pneumophila effector protein DrrA is a Rab1 guanine nucleotide-exchange factor. *Nat Cell Biol* 8(9):971-U976.
11. Muller MP, *et al.* (2010) The Legionella Effector Protein DrrA AMPylates the Membrane Traffic Regulator Rab1b. *Science* 329(5994):946-949.
12. Tan YH & Luo ZQ (2011) Legionella pneumophila SidD is a deAMPylase that modifies Rab1. *Nature* 475(7357):506-U102.
13. Brombacher E, *et al.* (2009) Rab1 guanine nucleotide exchange factor SidM is a major phosphatidylinositol 4-phosphate-binding effector protein of Legionella pneumophila. *J Biol Chem* 284(8):4846-4856.
14. Buttner D (2012) Protein export according to schedule: architecture, assembly, and regulation of type III secretion systems from plant- and animal-pathogenic bacteria. *Microbiol Mol Biol Rev* 76(2):262-310.
15. Kudryashev M, *et al.* (2013) In situ structural analysis of the Yersinia enterocolitica injectisome. *Elife* 2:e00792.
16. Mueller CA, Broz P, & Cornelis GR (2008) The type III secretion system tip complex and translocon. *Mol Microbiol* 68(5):1085-1095.
17. Ramamurthi KS & Schneewind O (2003) Substrate recognition by the Yersinia type III protein secretion machinery. *Mol Microbiol* 50(4):1095-1102.
18. Ramamurthi KS & Schneewind O (2003) Yersinia yopQ mRNA encodes a bipartite type III secretion signal in the first 15 codons. *Mol Microbiol* 50(4):1189-1198.
19. Stebbins CE & Galan JE (2001) Maintenance of an unfolded polypeptide by a cognate chaperone in bacterial type III secretion. *Nature* 414(6859):77-81.

20. Francis MS, Wolf-Watz H, & Forsberg A (2002) Regulation of type III secretion systems. *Curr Opin Microbiol* 5(2):166-172.
21. Seubert A, Hiestand R, de la Cruz F, & Dehio C (2003) A bacterial conjugation machinery recruited for pathogenesis. *Mol Microbiol* 49(5):1253-1266.
22. Watson B, Currier TC, Gordon MP, Chilton MD, & Nester EW (1975) Plasmid required for virulence of Agrobacterium tumefaciens. *J Bacteriol* 123(1):255-264.
23. Binns AN & Thomashow MF (1988) Cell Biology of Agrobacterium Infection and Transformation of Plants. *Annu Rev Microbiol* 42:575-606.
24. Chen I, Christie PJ, & Dubnau D (2005) The ins and outs of DNA transfer in bacteria. *Science* 310(5753):1456-1460.
25. Wallden K, Rivera-Calzada A, & Waksman G (2010) Type IV secretion systems: versatility and diversity in function. *Cell Microbiol* 12(9):1203-1212.
26. Cascales E & Christie PJ (2004) Definition of a bacterial type IV secretion pathway for a DNA substrate. *Science* 304(5674):1170-1173.
27. Engel P, *et al.* (2011) Parallel evolution of a type IV secretion system in radiating lineages of the host-restricted bacterial pathogen Bartonella. *PLoS Genet* 7(2):e1001296.
28. Harms A & Dehio C (2012) Intruders below the radar: molecular pathogenesis of Bartonella spp. *Clin Microbiol Rev* 25(1):42-78.
29. Guy L, *et al.* (2013) A gene transfer agent and a dynamic repertoire of secretion systems hold the keys to the explosive radiation of the emerging pathogen Bartonella. *PLoS Genet* 9(3):e1003393.
30. Schulein R, *et al.* (2005) A bipartite signal mediates the transfer of type IV secretion substrates of Bartonella henselae into human cells. *Proc Natl Acad Sci U S A* 102(3):856-861.
31. Schroder G, Schuelein R, Quebatte M, & Dehio C (2011) Conjugative DNA transfer into human cells by the VirB/VirD4 type IV secretion system of the bacterial pathogen Bartonella henselae. *Proc Natl Acad Sci U S A* 108(35):14643-14648.
32. Schulein R & Dehio C (2002) The VirB/VirD4 type IV secretion system of Bartonella is essential for establishing intraerythrocytic infection. *Mol Microbiol* 46(4):1053-1067.
33. Schmiederer M, Arcenas R, Widen R, Valkov N, & Anderson B (2001) Intracellular induction of the Bartonella henselae virB operon by human endothelial cells. *Infect Immun* 69(10):6495-6502.
34. Quebatte M, *et al.* (2010) The BatR/BatS Two-Component Regulatory System Controls the Adaptive Response of Bartonella henselae during Human Endothelial Cell Infection. *J Bacteriol* 192(13):3352-3367.
35. Vayssier-Taussat M, *et al.* (2010) The Trw type IV secretion system of Bartonella mediates host-specific adhesion to erythrocytes. *PLoS Pathog* 6(6):e1000946.
36. Dehio C (2008) Infection-associated type IV secretion systems of Bartonella and their diverse roles in host cell interaction. *Cell Microbiol* 10(8):1591-1598.
37. Pulliainen AT, *et al.* (2012) Bacterial effector binds host cell adenylyl cyclase to potentiate Galphas-dependent cAMP production. *Proc Natl Acad Sci U S A* 109(24):9581-9586.
38. Truttmann MC, Guye P, & Dehio C (2011) BID-F1 and BID-F2 domains of Bartonella henselae effector protein BepF trigger together with BepC the formation of invasome structures. *PLoS One* 6(10):e25106.

39. Rhomberg TA, Truttmann MC, Guye P, Ellner Y, & Dehio C (2009) A translocated protein of Bartonella henselae interferes with endocytic uptake of individual bacteria and triggers uptake of large bacterial aggregates via the invasome. *Cell Microbiol* 11(6):927-945.

40. Utsumi R, Nakamoto Y, Kawamukai M, Himeno M, & Komano T (1982) Involvement of cyclic AMP and its receptor protein in filamentation of an Escherichia coli fic mutant. *J Bacteriol* 151(2):807-812.

41. Utsumi R, Noda M, Kawamukai M, & Komano T (1989) Control mechanism of the Escherichia coli K-12 cell cycle is triggered by the cyclic AMP-cyclic AMP receptor protein complex. *J Bacteriol* 171(5):2909-2912.

42. Engel P, *et al.* (2012) Adenylylation control by intra- or intermolecular active-site obstruction in Fic proteins. *Nature* 482(7383):107-110.

43. Kinch LN, Yarbrough ML, Orth K, & Grishin NV (2009) Fido, a novel AMPylation domain common to fic, doc, and AvrB. *PLoS One* 4(6):e5818.

44. Punta M, *et al.* (2012) The Pfam protein families database. *Nucleic Acids Res* 40(Database issue):D290-301.

45. Das D, *et al.* (2009) Crystal structure of the Fic (Filamentation induced by cAMP) family protein SO4266 (gi|24375750) from Shewanella oneidensis MR-1 at 1.6 A resolution. *Proteins* 75(1):264-271.

46. Xiao J, Worby CA, Mattoo S, Sankaran B, & Dixon JE (2010) Structural basis of Fic-mediated adenylylation. *Nat Struct Mol Biol* 17(8):1004-1010.

47. Luong P, *et al.* (2010) Kinetic and structural insights into the mechanism of AMPylation by VopS Fic domain. *J Biol Chem* 285(26):20155-20163.

48. Goepfert A, Stanger FV, Dehio C, & Schirmer T (2013) Conserved inhibitory mechanism and competent ATP binding mode for adenylyltransferases with fic fold. *PLoS One* 8(5):e64901.

49. Roy CR & Mukherjee S (2009) Bacterial FIC Proteins AMP Up Infection. *Sci Signal* 2(62):pe14.

50. Yarbrough ML, *et al.* (2009) AMPylation of Rho GTPases by Vibrio VopS disrupts effector binding and downstream signaling. *Science* 323(5911):269-272.

51. Worby CA, *et al.* (2009) The fic domain: regulation of cell signaling by adenylylation. *Mol Cell* 34(1):93-103.

52. Sreelatha A, *et al.* (2013) Vibrio effector protein, VopQ, forms a lysosomal gated channel that disrupts host ion homeostasis and autophagic flux. *Proc Natl Acad Sci U S A* 110(28):11559-11564.

53. Biou V & Cherfils J (2004) Structural principles for the multispecificity of small GTP-binding proteins. *Biochemistry* 43(22):6833-6840.

54. Ragaz C, *et al.* (2008) The Legionella pneumophila phosphatidylinositol-4 phosphate-binding type IV substrate SidC recruits endoplasmic reticulum vesicles to a replication-permissive vacuole. *Cell Microbiol* 10(12):2416-2433.

55. Tan Y, Arnold RJ, & Luo ZQ (2011) Legionella pneumophila regulates the small GTPase Rab1 activity by reversible phosphorylcholination. *Proc Natl Acad Sci U S A* 108(52):21212-21217.

56. Xu Y, Carr PD, Vasudevan SG, & Ollis DL (2010) Structure of the adenylylation domain of E. coli glutamine synthetase adenylyl transferase: evidence for gene duplication and evolution of a new active site. *J Mol Biol* 396(3):773-784.

57. Jaggi R, van Heeswijk WC, Westerhoff HV, Ollis DL, & Vasudevan SG (1997) The two opposing activities of adenylyl transferase reside in distinct homologous domains, with intramolecular signal transduction. *Embo J* 16(18):5562-5571.
58. Delarue M (1995) Aminoacyl-tRNA synthetases. *Curr Opin Struct Biol* 5(1):48-55.
59. Huerta C, Borek D, Machius M, Grishin NV, & Zhang H (2009) Structure and mechanism of a eukaryotic FMN adenylyltransferase. *J Mol Biol* 389(2):388-400.
60. Bowers-Komro DM, Yamada Y, & McCormick DB (1989) Substrate specificity and variables affecting efficiency of mammalian flavin adenine dinucleotide synthetase. *Biochemistry* 28(21):8439-8446.
61. Preiss J & Romeo T (1994) Molecular biology and regulatory aspects of glycogen biosynthesis in bacteria. *Prog Nucleic Acid Res Mol Biol* 47:299-329.
62. Pedersen LC, Benning MM, & Holden HM (1995) Structural investigation of the antibiotic and ATP-binding sites in kanamycin nucleotidyltransferase. *Biochemistry* 34(41):13305-13311.
63. D'Angelo I, *et al.* (2000) Structure of nicotinamide mononucleotide adenylyltransferase: a key enzyme in NAD(+) biosynthesis. *Structure* 8(9):993-1004.
64. Izard T (2002) The crystal structures of phosphopantetheine adenylyltransferase with bound substrates reveal the enzyme's catalytic mechanism. *J Mol Biol* 315(4):487-495.
65. Campanacci V, Mukherjee S, Roy CR, & Cherfils J (2013) Structure of the Legionella effector AnkX reveals the mechanism of phosphocholine transfer by the FIC domain. *Embo J* 32(10):1469-1477.
66. Cui HT, *et al.* (2010) Pseudomonas syringae Effector Protein AvrB Perturbs Arabidopsis Hormone Signaling by Activating MAP Kinase 4. *Cell Host Microbe* 7(2):164-175.
67. Desveaux D, *et al.* (2007) Type III effector activation via nucleotide binding, phosphorylation, and host target interaction. *PLoS Pathog* 3(3).
68. Truttmann MC, Rhomberg TA, & Dehio C (2011) Combined action of the type IV secretion effector proteins BepC and BepF promotes invasome formation of Bartonella henselae on endothelial and epithelial cells. *Cell Microbiol* 13(2):284-299.
69. Okujava RG, P.; Lu, Y.Y.; Mistl, C.; Polus, F.; Vayssier-Taussat, M.; Halin, C.; Rolink, A.; Dehio, C. (2013) A translocated effector BepE of *Bartonella* is required for bacterial dissemination from derma to blood and safeguards migratory host cells from injury by co-translocated effectors. in *in preparation* (Biozentrum Basel).
70. Schmid MC, *et al.* (2006) A translocated bacterial protein protects vascular endothelial cells from apoptosis. *PLoS Pathog* 2(11):e115.
71. Vetter IR & Wittinghofer A (2001) Signal transduction - The guanine nucleotide-binding switch in three dimensions. *Science* 294(5545):1299-1304.
72. Bos JL, Rehmann H, & Wittinghofer A (2007) GEFs and GAPs: Critical elements in the control of small G proteins (vol 129, pg 865, 2007). *Cell* 130(2):385-385.
73. Kulkarni K, Yang J, Zhang ZG, & Barford D (2011) Multiple Factors Confer Specific Cdc42 and Rac Protein Activation by Dedicator of Cytokinesis (DOCK) Nucleotide Exchange Factors. *Journal of Biological Chemistry* 286(28):25341-25351.
74. Olofsson B (1999) Rho guanine dissociation inhibitors: Pivotal molecules in cellular signalling. *Cell Signal* 11(8):545-554.
75. Hall A (2012) Rho family GTPases. *Biochem Soc T* 40:1378-1382.
76. Cossart P & Sansonetti PJ (2004) Bacterial invasion: The paradigms of enteroinvasive pathogens. *Science* 304(5668):242-248.

77. Hayward RD & Koronakis V (1999) Direct nucleation and bundling of actin by the SipC protein of invasive Salmonella. *Embo Journal* 18(18):4926-4934.

78. Hapfelmeier S*, et al.* (2004) Role of the Salmonella pathogenicity island 1 effector proteins SipA, SopB, SopE, and SopE2 in Salmonella enterica subspecies 1 serovar Typhimurium colitis in streptomycin-pretreated mice. *Infect Immun* 72(2):795-809.

79. Zhou D, Mooseker MS, & Galan JE (1999) Role of the S-typhimurium actin-binding protein SipA in bacterial internalization. *Science* 283(5410):2092-2095.

80. Norris FA, Wilson MP, Wallis TS, Galyov EE, & Majerus PW (1998) SopB, a protein required for virulence of Salmonella dublin, is an inositol phosphate phosphatase. *Proc Natl Acad Sci U S A* 95(24):14057-14059.

81. Stebbins CE & Galan JE (2000) Modulation of host signaling by a bacterial mimic: structure of the Salmonella effector SptP bound to Rac1. *Mol Cell* 6(6):1449-1460.

82. Schubert WD*, et al.* (2002) Structure of internalin, a major invasion protein of Listeria monocytogenes, in complex with its human receptor E-cadherin. *Cell* 111(6):825-836.

83. Veiga E & Cossart P (2007) Listeria InIB takes a different route to met. *Cell* 130(2):218-219.

84. Condeelis J (2001) How is actin polymerization nucleated in vivo? *Trends Cell Biol* 11(7):288-293.

85. Bailly M*, et al.* (2001) The F-actin side binding activity of the Arp2/3 complex is essential for actin nucleation and lamellipod extension. *Current Biology* 11(8):620-625.

86. Ichetovkin I, Bailly M, Zebda N, Chan A, & Condeelis J (2001) Cofilin and Arp2/3 synergize in the generation of barbed ends in stimulated actin polymerization. *Mol Biol Cell* 12:290a-290a.

87. Sousa S*, et al.* (2007) Src, cortactin and Arp2/3 complex are required for E-cadherin-mediated internalization of Listeria into cells. *Cell Microbiol* 9(11):2629-2643.

88. Bierne H*, et al.* (2001) A role for cofilin and LIM kinase in Listeria-induced phagocytosis. *Journal of Cell Biology* 155(1):101-112.

89. Van Nhieu GT, Krukonis ES, Reszka AA, Horwitz AF, & Isberg RR (1996) Mutations in the cytoplasmic domain of the integrin beta1 chain indicate a role for endocytosis factors in bacterial internalization. *J Biol Chem* 271(13):7665-7672.

90. Truttmann MC*, et al.* (2011) Bartonella henselae engages inside-out and outside-in signaling by integrin beta1 and talin1 during invasome-mediated bacterial uptake. *J Cell Sci* 124(Pt 21):3591-3602.

91. Cell Signaling Technology I (2008) Regulation of actin dynamics.

92. Mitra SK & Schlaepfer DD (2006) Integrin-regulated FAK-Src signaling in normal and cancer cells. *Curr Opin Cell Biol* 18(5):516-523.

93. Chodniewicz D & Klemke RL (2004) Regulation of integrin-mediated cellular responses through assembly of a CAS/Crk scaffold. *Biochim Biophys Acta* 1692(2-3):63-76.

94. Brugnera E*, et al.* (2002) Unconventional Rac-GEF activity is mediated through the Dock180-ELMO complex. *Nat Cell Biol* 4(8):574-582.

95. ten Klooster JP, Jaffer ZM, Chernoff J, & Hordijk PL (2006) Targeting and activation of Rac1 are mediated by the exchange factor beta-Pix. *J Cell Biol* 172(5):759-769.

96. Rothwarf DM & Karin M (1999) The NF-kappa B activation pathway: a paradigm in information transfer from membrane to nucleus. *Sci STKE* 1999(5):RE1.

97. Broz P & Monack DM (2011) Molecular mechanisms of inflammasome activation during microbial infections. *Immunol Rev* 243(1):174-190.

98. Arbibe L*, et al.* (2000) Toll-like receptor 2-mediated NF-kappa B activation requires a Rac1-dependent pathway. *Nat Immunol* 1(6):533-540.

99. Eitel J*, et al.* (2012) Rac1 regulates the NLRP3 inflammasome which mediates IL-1beta production in Chlamydophila pneumoniae infected human mononuclear cells. *PLoS One* 7(1):e30379.

100. Muller AJ*, et al.* (2009) The S. Typhimurium effector SopE induces caspase-1 activation in stromal cells to initiate gut inflammation. *Cell Host Microbe* 6(2):125-136.

101. Rehmann H, Das J, Knipscheer P, Wittinghofer A, & Bos JL (2006) Structure of the cyclic-AMP-responsive exchange factor Epac2 in its auto-inhibited state. *Nature* 439(7076):625-628.

102. Branham MT*, et al.* (2009) Epac Activates the Small G Proteins Rap1 and Rab3A to Achieve Exocytosis. *Journal of Biological Chemistry* 284(37):24825-24839.

103. Sands WA & Palmer TM (2008) Regulating gene transcription in response to cyclic AMP elevation. *Cell Signal* 20(3):460-466.

104. Theurkauf WE & Vallee RB (1982) Molecular Characterization of the Camp-Dependent Protein-Kinase Bound to Microtubule-Associated Protein-2. *Journal of Biological Chemistry* 257(6):3284-3290.

105. Wong W & Scott JD (2004) AKAP signalling complexes: Focal points in space and time. *Nat Rev Mol Cell Bio* 5(12):959-970.

106. Smith FD, Langeberg LK, & Scott JD (2006) The where's and when's of kinase anchoring. *Trends Biochem Sci* 31(6):316-323.

107. Dessauer CW, Tesmer JJG, Sprang SR, & Gilman AG (1999) The interactions of adenylate cyclases with P-site inhibitors. *Trends Pharmacol Sci* 20(5):205-210.

108. Tesmer JJG*, et al.* (2000) Molecular basis for P-site inhibition of adenylyl cyclase. *Biochemistry* 39(47):14464-14471.

109. Bundey RA & Insel PA (2006) Adenylyl cyclase 6 overexpression decreases the permeability of endothelial monolayers via preferential enhancement of prostacyclin receptor function. *Mol Pharmacol* 70(5):1700-1707.

110. Sadana R & Dessauer CW (2009) Physiological roles for G protein-regulated adenylyl cyclase isoforms: insights from knockout and overexpression studies. *Neurosignals* 17(1):5-22.

111. Gao XL, Sadana R, Dessauer CW, & Patel TB (2007) Conditional stimulation of type V and VI adenylyl cyclases by g protein beta gamma y subunits. *Faseb J* 21(5):A430-A431.

112. Dessauer CW (2009) Adenylyl Cyclase-A-kinase Anchoring Protein Complexes: The Next Dimension in cAMP Signaling. *Mol Pharmacol* 76(5):935-941.

113. Chung KY*, et al.* (2011) Conformational changes in the G protein Gs induced by the beta(2) adrenergic receptor. *Nature* 477(7366):611-U143.

114. Tesmer JJG, Sunahara RK, Gilman AG, & Sprang SR (1997) Crystal structure of the catalytic domains of adenylyl cyclase in a complex with G(s alpha).GTP gamma S. *Science* 278(5345):1907-1916.

115. Dessauer CW & Gilman AG (1997) The catalytic mechanism of mammalian adenylyl cyclase - Equilibrium binding and kinetic analysis of P-site inhibition. *Journal of Biological Chemistry* 272(44):27787-27795.

116. Dessauer CW, Scully TT, & Gilman AG (1997) Interactions of forskolin and ATP with the cytosolic domains of mammalian adenylyl cyclase. *Journal of Biological Chemistry* 272(35):22272-22277.

117. Seamon K, Padgett W, & Daly JW (1981) Forskolin - a Unique Diterpene Activator of Adenylate-Cyclase Which Potentiates Calcium-Calmodulin and Hormone Responses. *Fed Proc* 40(6):1728-1728.
118. Whisnant RE, Gilman AG, & Dessauer CW (1996) Interaction of the two cytosolic domains of mammalian adenylyl cyclase. *Proc Natl Acad Sci U S A* 93(13):6621-6625.
119. Yan SZ, Hahn D, Huang ZH, & Tang WJ (1996) Two cytoplasmic domains of mammalian adenylyl cyclase form a G(s alpha)- and forskolin-activated enzyme in vitro. *Journal of Biological Chemistry* 271(18):10941-10945.
120. Dessauer CW, Chen-Goodspeed M, & Chen J (2002) Mechanism of G alpha(i)-mediated inhibition of type V adenylyl cyclase. *Journal of Biological Chemistry* 277(32):28823-28829.
121. Dessauer CW, Tesmer JJ, Sprang SR, & Gilman AG (1998) Identification of a Gialpha binding site on type V adenylyl cyclase. *J Biol Chem* 273(40):25831-25839.
122. Wang SC*, et al.* (2007) Regulation of type V adenylate cyclase by Ric8a, a guanine nucleotide exchange factor. *Biochem J* 406:383-388.
123. Kapiloff MS*, et al.* (2009) An Adenylyl Cyclase-mAKAP beta Signaling Complex Regulates cAMP Levels in Cardiac Myocytes. *Journal of Biological Chemistry* 284(35):23540-23546.
124. Sadana R, Dascal N, & Dessauer CW (2009) N Terminus of Type 5 Adenylyl Cyclase Scaffolds G(s) Heterotrimer. *Mol Pharmacol* 76(6):1256-1264.
125. Crossthwaite AJ, Ciruela A, Rayner TF, & Cooper DMF (2006) A direct interaction between the N terminus of adenylyl cyclase AC8 and the catalytic subunit of protein phosphatase 2A. *Mol Pharmacol* 69(2):608-617.
126. Simpson RE, Ciruela A, & Cooper DMF (2006) The role of calmodulin recruitment in Ca2+ stimulation of adenylyl cyclase type 8. *Journal of Biological Chemistry* 281(25):17379-17389.
127. Cassel D & Pfeuffer T (1978) Mechanism of Cholera Toxin Action - Covalent Modification of Guanyl Nucleotide-Binding Protein of Adenylate-Cyclase System. *Proc Natl Acad Sci U S A* 75(6):2669-2673.
128. Orth JHC*, et al.* (2009) Pasteurella multocida toxin activation of heterotrimeric G proteins by deamidation. *Proc Natl Acad Sci U S A* 106(17):7179-7184.
129. Naismith JH & Sprang SR (1998) Modularity in the TNF-receptor family. *Trends Biochem Sci* 23(2):74-79.
130. Ashkenazi A (2002) Targeting death and decoy receptors of the tumour-necrosis factor superfamily. *Nat Rev Cancer* 2(6):420-430.
131. Kischkel FC*, et al.* (1995) Cytotoxicity-Dependent Apo-1 (Fas/Cd95)-Associated Proteins Form a Death-Inducing Signaling Complex (Disc) with the Receptor. *Embo Journal* 14(22):5579-5588.
132. Scaffidi C*, et al.* (1998) Two CD95 (APO-1/Fas) signaling pathways. *Embo J* 17(6):1675-1687.
133. Li H, Zhu H, Xu CJ, & Yuan J (1998) Cleavage of BID by caspase 8 mediates the mitochondrial damage in the Fas pathway of apoptosis. *Cell* 94(4):491-501.
134. Ashe PC & Berry MD (2003) Apoptotic signaling cascades. *Prog Neuropsychopharmacol Biol Psychiatry* 27(2):199-214.
135. Wang X (2001) The expanding role of mitochondria in apoptosis. *Gene Dev* 15(22):2922-2933.

136. Li P*, et al.* (1997) Cytochrome c and dATP-dependent formation of Apaf-1/caspase-9 complex initiates an apoptotic protease cascade. *Cell* 91(4):479-489.
137. Salvesen GS & Duckett CS (2002) IAP proteins: blocking the road to death's door. *Nat Rev Mol Cell Biol* 3(6):401-410.
138. Yang Y, Fang S, Jensen JP, Weissman AM, & Ashwell JD (2000) Ubiquitin protein ligase activity of IAPs and their degradation in proteasomes in response to apoptotic stimuli. *Science* 288(5467):874-877.
139. Nishihara H, Kizaka-Kondoh S, Insel PA, & Eckmann L (2003) Inhibition of apoptosis in normal and transformed intestinal epithelial cells by cAMP through induction of inhibitor of apoptosis protein (IAP)-2. *Proc Natl Acad Sci U S A* 100(15):8921-8926.
140. Huotari J & Helenius A (2011) Endosome maturation. *Embo Journal* 30(17):3481-3500.
141. Mackeh R, Perdiz D, Lorin S, Codogno P, & Pous C (2013) Autophagy and microtubules - new story, old players. *J Cell Sci* 126(5):1071-1080.
142. Nogales E & Wang HW (2006) Structural intermediates in microtubule assembly and disassembly: how and why? *Curr Opin Cell Biol* 18(2):179-184.
143. Al-Bassam J & Chang F (2011) Regulation of microtubule dynamics by TOG-domain proteins XMAP215/Dis1 and CLASP. *Trends Cell Biol* 21(10):604-614.
144. Akhmanova A & Steinmetz MO (2010) Microtubule plus TIPs at a glance. *J Cell Sci* 123(20):3415-3419.
145. Perez F, Diamantopoulos GS, Stalder R, & Kreis TE (1999) CLIP-170 highlights growing microtubule ends in vivo. *Cell* 96(4):517-527.
146. Honnappa S, John CM, Kostrewa D, Winkler FK, & Steinmetz MO (2005) Structural insights into the EB1-APC interaction (vol 24, pg 261, 2005). *Embo Journal* 24(4):872-872.
147. Brouhard GJ*, et al.* (2008) XMAP215 is a processive microtubule polymerase. *Cell* 132(1):79-88.
148. Al-Bassam J*, et al.* (2010) CLASP Promotes Microtubule Rescue by Recruiting Tubulin Dimers to the Microtubule. *Dev Cell* 19(2):245-258.
149. Ayaz P, Ye X, Huddleston P, Brautigam CA, & Rice LM (2012) A TOG:alphabeta-tubulin complex structure reveals conformation-based mechanisms for a microtubule polymerase. *Science* 337(6096):857-860.
150. Leano JB, Rogers SL, & Slep KC (2013) A cryptic TOG domain with a distinct architecture underlies CLASP-dependent bipolar spindle formation. *Structure* 21(6):939-950.
151. Colucci-Guyon E*, et al.* (1994) Mice lacking vimentin develop and reproduce without an obvious phenotype. *Cell* 79(4):679-694.
152. Mor-Vaknin N, Punturieri A, Sitwala K, & Markovitz DM (2003) Vimentin is secreted by activated macrophages. *Nat Cell Biol* 5(1):59-63.
153. Eriksson JE*, et al.* (2004) Specific in vivo phosphorylation sites determine the assembly dynamics of vimentin intermediate filaments. *J Cell Sci* 117(Pt 6):919-932.
154. Chou YH, Bischoff JR, Beach D, & Goldman RD (1990) Intermediate Filament Reorganization during Mitosis Is Mediated by P34cdc2 Phosphorylation of Vimentin. *Cell* 62(6):1063-1071.
155. Wang RC*, et al.* (2012) Akt-mediated regulation of autophagy and tumorigenesis through Beclin 1 phosphorylation. *Science* 338(6109):956-959.

156.   Bhattacharya R, *et al.* (2009) Recruitment of vimentin to the cell surface by beta3 integrin and plectin mediates adhesion strength. *J Cell Sci* 122(Pt 9):1390-1400.

2. Aim of Thesis

Aim of thesis

The primary aim of my thesis, starting in February 2010, was to investigate how *Bartonella* effector proteins manipulate host cell signaling to promote bacterial uptake or survival including the identification of effector targets and the analysis of the molecular mechanism of effector functions.

I validated adenylyl cyclases (AC) and the α-subunit of the stimulatory G-protein (Gα$_s$) as targetproteins of BepA from *B. henselae*. To this end, I established a biochemical assays to monitor *in vitro* AC activity and applied biochemical techniques to further investigate protein-protein interactions.

Furthermore, I established an experimental strategy to identify targets of posttranslational modifications on the example of AMPylation performed by FIC-domain containing effectors. I could identify vimntin and tubulin as target proteins of Bep2 of B. rochalimae. I then focused on elucidating the influence of AMPylation on tubulin polymerization by studying the interaction of AMPylated tubulin with the polymerization catalysor Stu2.

Additionally, I aimed to reveal the role of Fic protein regulators in the context of bacterial infection.

3. Results

3.1 Research Article I (*published*)

A bacterial effector binds host cell adenylyl cyclase to potentiate Gαs-dependent cAMP production

Arto T. Pulliainen*, Kathrin Pieles*, Barbara Hauert, Alex Böhm, Maxime Quebatte, Alexander Wepf, Matthias Gstaiger, Cameron S. Brand, Ruedi Aebersold, Carmen W. Dessauer, and Christoph Dehio

* These authors contributed equally to this work

Statement of my own contribution

I contributed to this publication by expressing and purifying MBP-BepA$_{305-544}$, MBP-BepB$_{303-542}$, MBP-BepC$_{292-532}$, His-Gα$_s$ and His-C2 of AC2. I also performed *in vitro* AC-activity assays with and analyzed protein-protein interactions using SPR. I furthermore reproduced the bi-molecular fluorescent cytometry and MacConkey experiments that were initially established by A.T. Pulliainen with the help of A. Boehm and B. Hauert.
The manuscript was written by me, A.T. Pulliainen, and C. Dehio.

Bacterial effector binds host cell adenylyl cyclase to potentiate Gαs-dependent cAMP production

Arto T. Pulliainen [a,1,2], Kathrin Pieles [a,2], Cameron S. Brand [b], Barbara Hauert [a], Alex Böhm [a,3], Maxime Quebatte [a], Alexander Wepf [c], Matthias Gstaiger [c], Ruedi Aebersold [c], Carmen W. Dessauer [b], and Christoph Dehio [a,4]

[a]Biozentrum, University of Basel, CH-4056 Basel, Switzerland; [b]Department of Integrative Biology and Pharmacology, University of Texas Health Science Center at Houston, Houston, TX 77030; and [c]Institute of Molecular Systems Biology, Eidgenössische Technische Hochschule, CH-8093 Zurich, Switzerland

Subversion of host organism cAMP signaling is an efficient and widespread mechanism of microbial pathogenesis. Bartonella effector protein A (BepA) of vasculotumorigenic Bartonella henselae protects the infected human endothelial cells against apoptotic stimuli by elevation of cellular cAMP levels by an as yet unknown mechanism. Here, adenylyl cyclase (AC) and the α-subunit of the AC-stimulating G protein (Gαs) were identified as potential cellular target proteins for BepA by gel-free proteomics. Results of the proteomics screen were evaluated for physical and functional interaction by: (i) a heterologous in vivo coexpression system, where human AC activity was reconstituted under the regulation of Gαs and BepA in Escherichia coli; (ii) in vitro AC assays with membrane-anchored full-length human AC and recombinant BepA and Gαs; (iii) surface plasmon resonance experiments; and (iv) an in vivo fluorescence bimolecular complementation-analysis. The data demonstrate that BepA directly binds host cell AC to potentiate the Gαs-dependent cAMP production. As opposed to the known microbial mechanisms, such as ADP ribosylation of G protein α-subunits by cholera and pertussis toxins, the fundamentally different BepA-mediated elevation of host cell cAMP concentration appears subtle and is dependent on the stimulus of a G protein-coupled receptor-released Gαs. We propose that this mechanism contributes to the persistence of Bartonella henselae in the chronically infected vascular endothelium.

bacterial infection | apoptosis | tumorigenesis | type IV secretion

Bacterial pathogens use a plethora of molecular mechanisms to interfere with the host cell signaling to promote their replication, propagation, and escape from the immune system. Pathogens often act via posttranslational protein modifications (phosphorylation, ubiquitylation, sumoylation, AMPylation, ADP ribosylation, and deamidation) to alter activities, subcellular localization, and half-lives of the host proteins (1, 2). Many pathogens also elevate cellular cAMP concentrations using at least five distinct mechanisms. (i) Some bacteria, such as *Bordetella pertussis* and *Pseudomonas aeruginosa*, increase cAMP concentration in the target cell by secreting toxins that possess the adenylyl cyclase (AC) activity (3). (ii) Bacteria, such as *Vibrio cholerae* and *B. pertussis*, increase cAMP concentration in the target cell by secreting toxins that possess ADP ribosylation activity toward heterotrimeric G proteins (4, 5). In the case of *V. cholerae*, cholera toxin-catalyzed ADP ribosylation of a specific arginine residue of the α-subunit of the AC-stimulating G protein (Gαs) converts the α-subunit into a constitutively active form (4). In the case of *B. pertussis*, pertussis toxin-catalyzed ADP ribosylation of a specific cysteine residue of Gαi prevents the coupling of α-subunit to G protein-coupled receptor (GPCR), thus abolishing the GPCR-mediated AC inhibition (5). (iii) *Bacillus subtilis* has been reported to produce an acylpeptide, which inhibits the activity of cAMP-degrading phosphodiesterases (PDEs) in vitro, and increases the cytosolic cAMP concentration in vivo (6). (iv) Recently, *Mycobacterium tuberculosis* was proposed to deliver cAMP from its own cytosol into the cytosol of a macrophage (7). (v) Cry1Ab toxin of *Bacillus thuringiensis* has been reported to elevate cellular cAMP concentration by binding to BT-R1, a single-pass cadherin-like plasma-membrane receptor present in the host insect cell (8). In

the present study, we have identfied and characterized a previously undescribed type of molecular mechanism by which bacterial pathogens increase host cell cAMP concentration.

Bartonella spp. are arthropod-borne facultative intracellular bacteria that typically cause a long-lasting hemotrophic bacteremia in their mammalian hosts, including humans (9). Endothelial cells (ECs) are efficiently colonized by these bacteria and it has been reported that *Bartonella henselae* (Bh) and *Bartonella quintana* inhibit actinomycin D-induced apoptosis of human dermal microvascular ECs and human umbilical vein ECs (HUVECs) (10). Most likely, pathogen-triggered blockage of host cell death facilitates a slow microbial replication process and enables chronic persistence. Recently, it was shown that the capacity of Bh to inhibit apoptosis of HUVECs, induced either by actinomycin D or by cytotoxic T lymphocytes, is dependent on the VirB/VirD4-type IV secretion system (T4SS) and its *Bartonella* effector protein A (BepA) (11, 12). Translocation of BepA into ECs during infection coincides with an increase in cellular cAMP concentration (12). Pharmacological elevation of cAMP by combined action of the AC activator forskolin and the PDE inhibitor isobutylmethylxanthine (IBMX) or by addition of the nonhydrolyzable cAMP analog dibutyryl-cAMP similarly protected ECs from apoptosis (12). This direct phenocopy-effect indicates that the BepA-induced cAMP elevation is the molecular basis of BepA-mediated antiapoptosis. However, the molecular mechanism of how BepA induces the cAMP elevation has remained elusive. Here, we provide evidence that BepA of Bh directly binds the host cell AC to potentiate Gαs-dependent cAMP production.

Results

Gel-Free Proteomics Identify AC and Gαs as Potential Cellular Target Proteins for BepA. We hypothesized that after T4SS-mediated translocation, BepA binds a host cell protein to increase cellular cAMP concentrations. To initiate gel-free proteomics screens for the identification of cellular target proteins of BepA, we first cloned stable Bep-expressing cell lines. The homologous T4SS effectors BepA, BepB, and BepC of Bh share ≈30% amino acid identity and contain in their C terminus the ≈140 amino acid large Bep intracellular delivery domain and a short positively charged tail sequence (Fig. 1 A), which together compose a bipartite signal for T4SS-dependent protein translocation from the bacterium into the host cell (13). Previous transient transfection studies with

Fig. 1. Endothelial hybridoma-based cell line that stably expresses HA-EGFP-tagged BepA displays constitutively activated cAMP signaling. (A) Schematic representation of constructs that were used to select Bep-expressing cell lines. (B) Flow cytometry-pro files of the selected cell lines. (C) Proteolytic stability of HA-EGFP-fusion proteins in the cell lines were ana-lyzed by Western blotting and immunodetection with polyclonal anti-EGFP antibodies (antiactin Western blotting shown as the loading control). Sam-ple numbering 1 –5 is based on B. (D) Expression of the cAMP-responsive genes pde4B (phosphodiesterase isoform 4b) and crem (cAMP responsive element modulator) was determined by qRT-PCR, as previously described (12). The mean values ± SDs (SD) from a representative experiment are shown for samples analyzed in triplicate. Sample numbering 1 –5 is based on B. (E) Quanti fication of cellular cAMP concentration in con fluent monolayers of the stable cell lines. Sample numbering 1 –5 is based on B.

truncated forms of BepA demonstrated that the Bep intracellular delivery-domain (E305-S446) is suf ficient for the antiapoptotic activity of BepA (12). In the present study, a C-terminal fragment of BepA (E305-S544), and the corresponding fragments of the not antiapoptotic homologs BepB and BepC, were N-terminally tag-ged with HA-EGFP (Fig. 1 A). These constructs localized primarily to the plasma membrane in transiently transfected HEK293T cells, as judged by confocal microscopic imaging (Fig. S1 A). To clone cell lines expressing these constructs for the gel-free proteomics (Fig. S2A), expression plasmids were transfected into Ea.hy926 cells. Ea. hy926 cells were chosen for this study as they are readily trans-fectable and Bh infection induced activation of the canonical cAMP/PKA/CREB (cAMP response element-binding) pathway in a BepA-dependent manner (Fig. S1 B and C). Flow cytometry was used to verify clonality of the cell lines and to analyze the expres-sion levels of the fusion proteins (Fig. 1 B). Proteolytic stability of the expressed fusion proteins was verified by anti-EGFP Western blotting (Fig. 1 C). Quantitative RT-PCR (qRT-PCR) of crem and pde4B expression was used to demonstrate that the BepA-expressing cell line displays a constitutively activated cAMP sig-naling (Fig. 1 D). Moreover, the concentration of cAMP was sig-nificantly elevated in the clone that stably expresses HA-GFP-BepA, but not in any other analyzed cell line (Fig. 1 E). Therefore,

the cloned cell lines were regarded as useful tools to identify the possible cellular protein targets for BepA by gel-free proteomics.

Because BepA, BepB, and BepC appear to associate with the plasma membrane (see Fig. 4B and Fig. S1 A) it was reasoned that the putative BepA –cellular protein interaction leading to the elevation of cAMP concentration might be dependent on the lipophilic membrane environment. Therefore, Triton X-100 lysates of the stable cell lines were prepared in the presence of a lipophilic primary amine cross-linker. Anti-HA immunopreci-pitated material was eluted from the beads with low pH and the whole trypsin-treated eluate was subjected to LC-electrospray ionization (ESI)-MS/MS analysis. This nonbiased gel-free pro-teomics approach is schematically represented in Fig. S2 A. Anti-EGFP Western blotting was routinely used to control each step of the sample preparation (Fig. S1D). Given that BepA induces an elevation of cellular cAMP concentration in Ea.hy926 cells (Fig. 1 E) and activates the canonical cAMP/PKA/CREB path-way (Fig. 1D and Fig. S1 B and C), it was of nterest to identify AC isoform 7 and the G αs as possible cellular target proteins for BepA (Fig. S2 B). The data indicate that to induce elevation of cAMP concentration in the host cell, BepA might bind and alter activities of the core components of host cell cAMP generation system, the actual enzyme or its stimulatory G-protein α-subunit.

BepA Is a Conditional G αs-Dependent Activator of Host Cell AC. To substantiate the proteomics findings (Fig. S2), possible stimula-tory effect of BepA on human AC activity was first analyzed in vivo in a heterologous Escherichia coli background. The main reason for this approach was the ability to study possible Gαs-dependent regulation of human AC without the interference of other cellular regulators of G-protein signaling. To this end, the catalytic C1a and C2 subunits of human AC7 (Fig. 2 A) were expressed alone or in combination in an E. coli mutant strain, ΔcyaΔcpdA, which lacks the E. coli AC and the cAMP-speci fic PDE. To activate AC7 in E. coli , G αs was coexpressed in the ΔcyaΔcpdA strain by another plasmid, either in its native form or as a constitutively active GTPase-de ficient Q213L-mutant. As an in vivo read-out for functionality of human AC7 activity under regulation of G αs in E. coli , growth of bacteria on MacConkey maltose plates was used (14). On these plates, wild-type E. coli colonies are brightly red pigmented because they use maltose as a carbon source through a catabolic activity, which is dependent on cAMP. In contrast, ΔcyaΔcpdA colonies do not get pig-mented on the MacConkey maltose plates (Fig. 2 B). As shown in Fig. 2B, the ΔcyaΔcpdA strain expressing Gαs-Q213L together with C2-AC7 and C1a-AC7 turned red. This result indicates that the reconstitution of human AC7 activity under the regulation of G αs in E. coli was successful. Next, the effect of BepA on the G αs-regulated AC7 activity was studied by introducing bepA into the system in a third plasmid. The smallest antiapoptotic frag-ment of BepA (E305-S446) (12), and the corresponding frag-ments of the homologous but not antiapoptotic BepB and BepC, were N-terminally tagged with maltose-binding protein (MBP). Of note, N-terminal tagging of a BepA subfragment with MBP was necessary to acquire a stable form of BepA (see stability of the full-length nontagged BepA in Fig. S3 C). As shown in Fig. 2C, expression of BepA $_{E305-S446}$ (referred hereafter as MBP-BepA) alone in the ΔcyaΔcpdA strain did not reverse the cata-bolic defect. Moreover, cAMP production was not signi ficant when BepA was coexpressed with the catalytic subunits of AC7. However, when BepA was coexpressed with both of the catalytic subunits of AC7 and G αs, a clear reversal of the catabolic defect was detected. Importantly, this phenotype was not detected with the control proteins MBP, MBP-BepB $_{E303-S444}$ (referred here-after as MBP-BepB), or MBP-BepC $_{D293-G434}$ (referred hereafter as MBP-BepC). The main findings were recapitulated with an alternative coexpression set-up where BepA was expressed as a full-length form with or without G αs and the catalytic subunits of AC7. Despite extensive instability of the full-length BepA, the protein still activated the AC in a G αs-dependent manner (Fig. S3A). In conclusion, data from the E. coli reconstitution system

Fig. 2. In vivo reconstitution of BepA-regulated host cell adenylyl cyclase activity in E. coli . (A) Topology model of mammalian AC (17). Arrows indicate amino acid positions, the first and the last amino acid, of the expressed recombinant C1a and C2 subunits of human AC7 (23). (B) Dots of E. coli grown on a MacConkey maltose indicator plate with or without IPTG. AB472 (λDE3) turns red because it can use maltose as a carbon source through a catabolic activity, which is strictly dependent on cAMP. AB472(λDE3)Δ cyaΔcpdA double knockout strain cannot use maltose as a carbon source. However, AB472(λDE3)ΔcyaΔcpdA expressing G αs-Q213L by one plasmid together with HIS-C2-AC7 and C1a-AC7-S-tag by another plasmid turns red on the MacConkey plate as an indication of cAMP production. (C) AB472 (λDE3)ΔcyaΔcpdA strain expressing MBP-BepA by one plasmid and G αs by another plasmid together with HIS-C2-AC7 and C1a-AC7-S-tag by a third plasmid turns red on the MacConkey plate as an indication of cAMP production. See also Fig. S3 A.

indicate that BepA binds the catalytic subunits of the AC and G αs to induce cAMP synthesis in a G αs-dependent manner.

To substantiate the findings of the E. coli reconstitution system, we used a highly sensitive in vitro AC assay (15) with membrane preparations of Sf9 insect cells that ectopically overexpress full-length human AC2 (16). AC2 is in the same family and shares many regulatory properties with AC7 (17). The stimulatory effect of G αs on the membrane-bound AC2, with or without Beps, was studied by using a highly pure recombinant and N-terminally HIS-tagged form (Fig. S4). In the E. coli reconstitution system, this form activated AC7 together with MBP-BepA in a similar fashion to the nontagged form of Gαs (Fig. S3 D). The effect of Beps on the AC2 activity was studied using purified recombinant and N-terminally MBP-tagged forms (Fig. S4). As shown in Fig. 3 A, the basal activity of AC2 could significantly be increased by Gαs-GDP/ γS-GTP. With this designation of G αs we refer to a condition

where we add recombinant Gαs, purified from E. coli in its GDP-loaded form, together with a nonhydrolyzable GTP analog (γS-GTP) into the AC assay. During the AC assay, G αs-GDP gets activated by spontaneous exchange of GDP with γS-GTP. The effect of BepA on the AC2 activity was analyzed by addition of MBP-BepA in an equimolar ratio to G αs-GDP/ γS-GTP. As shown in Fig. 3 A, the specific activity of AC2 was significantly higher in the presence of MBP-BepA and G αs-GDP/ γS-GTP compared with the presence of Gαs-GDP/ γS-GTP alone. In fact, exclusion of G αs-GDP/ γS-GTP completely abolished the BepA-mediated activation of AC2. Next, the AC stimulatory potential of a pre-activated G αs; that is, G αs-GDP that is preincubated with a saturating amount of γS-GTP and subsequently puri fied from unbound nucleotide (referred hereafter as G αs-γS-GTP) was determined. As shown in Fig. 3 B, G αs-γS-GTP was more potent than G αs-GDP/ γS-GTP to activate AC, as expected. However, this canonically high AC-stimulatory potential of G αs could significantly be increased by inclusion of MBP-BepA into the reaction mixture in an equimolar ratio to G αs-GDP/ γS-GTP. MBP-BepA could also increase the AC stimulatory potential of G αs-GDP, which can activate AC, albeit less potently than active G αs (18). MBP-BepA also increased the AC stimulatory potential of G αs in the presence of GTP.

To verify BepA-speci ficity, MBP-BepB, MBP-BepC, and MBP were analyzed in parallel in the presence and absence of Gαs-GDP/ γS-GTP. Only BepA increases the speci fic activity of AC2 (Fig. 3 D). To verify the G αs-dependency, Gαs dose–response analysis of AC2 activation was performed in the presence and absence of a fixed concentration of MBP-BepA. If BepA were stimulating AC activity in a G αs-independent manner, we would expect the Gαs dose–response curve to shift to consistently higher values across all G αs-concentrations. Alternatively, if BepA were stimulating AC2 activity in a G αs-dependent manner, we would expect a right-end shift in the Gαs dose–response curve. The data of the experiment (Fig. 3 E) strongly indicate that the latter model applies for BepA. We also performed forskolin dose –response analysis of AC2 activation in the presence and absence of a fixed concentration of MBP-BepA. Forskolin activates the AC by interchalating the C1 and C2 subunits into a catalytically active form (19). As shown in Fig. 3 F, MBP-BepA signi ficantly potentiates the stimulation of AC by forskolin. Taken together, the data indicate that BepA is a conditional G αs-dependent activator of AC, and that BepA is able to use the AC stimulatory potential of G αs or forskolin and may directly bind AC.

BepA Directly Binds the C2 Catalytic Subunit of the Host Cell AC. To examine protein–protein interactions of the BepA-G αs-AC triad, single-cycle surface plasmon resonance (SPR) analyses with pu-rified recombinant components were conducted. To this end, a highly pure recombinant C2 catalytic subunit of AC2 (Fig. S4) was immobilized via amine coupling on a CM5 sensorchip flow chamber, followed by binding measurements of MBP-BepA, MBP-BepC, and MBP that were injected on the C2-coated surface in flow pulses of increasing concentrations. As shown in Fig. 4A, the increase in SPR signal was signi ficantly higher during the flow pulses with MBP-BepA than with MBP or MBP-BepC. It is concluded that BepA directly binds the C2 catalytic subunit of the host cell AC.

BepA Is in Close Proximity to G αs in Living Cells. BepA (E305-S544) and the corresponding fragments of the homologous but not antiapoptotic BepB and BepC (Fig. 1 A) were N-terminally tagged with HA-YFP2, whereas G αs was C-terminally tagged with YFP1. Folding of the nonfluorescent YFP1 and YFP2 fragments into a functional YFP upon YFP1- and YFP2-fusion partner inter-actions (20) were quantified by flow cytometry. Importantly, none of the single or double transfections were deleterious for the cell viability (Table S1). As shown in Fig. 4 B and Fig. S5 , cotransfection of HA-YFP2-BepA and G αs-YFP1 resulted in YFP signal from a significant portion of the cell population (43 ± 2%). In contrast, the number of YFP [+] cells from expression of HA-YFP2-BepB and

Fig. 3. In vitro reconstitution of BepA-regulated host cell AC activity. Activity assays of membrane bound human AC in the presence and absence of purified recombinant His-tagged Gαs and MBP-tagged Beps. Specific activity of AC was determined radiometrically by quantification of produced cAMP as described in Materials and Methods. (A) AC was preincubated before the substrate (α-[^{32}P]ATP) addition with either buffer, GDP-bound Gαs (100 nM), or with a combination of GDP-bound Gαs and equal molar amounts of MBP-BepA. γS-GTP was added to the reaction (100 μM) to activate GDP-bound Gαs during the assay (referred as Gαs-GDP/γS-GTP). (B) AC was preincubated before the substrate (α-[^{32}P]ATP) addition with either buffer, GDP-bound Gαs, or preactivated γS-GTP-bound Gαs (Gαs-γS-GTP) in the presence or absence of equal molar amounts of MBP-BepA (100 nM). γS-GTP and GTP were added to the reactions (100 μM) as indicated to activate GDP-bound Gαs during the assay (referred as Gαs-GDP/γS-GTP and Gαs-GTP, respectively). Gαs-GDP refers to an experimental condition where no external guanine nucleotide was added to the reaction mixture. (C) AC was preincubated either with buffer, MBP-BepA, MBP-BepB, MBP-BepC, or MBP in the presence of Gαs-GDP/γS-GTP (100 nM). (D) AC was preincubated either with buffer, MBP-BepA, MBP-BepB, MBP-BepC, or MBP in the absence of Gαs-GDP/γS-GTP. As a positive control, MBP-BepA was analyzed in the presence of equal molar amount of Gαs-GDP/γS-GTP (100 nM). (E) Concentration-dependent activation of AC by Gαs in the presence and absence of a constant amount of MBP-BepA. (F) Concentration-dependent activation of AC by forskolin in the presence and absence of a constant amount of MBP-BepA. Statistics based on Student t test with two sample equal variance (homoscedastic): n.s., non-significant; * $P < 0.05$, ** $P < 0.01$, and *** $P < 0.005$.

HA-YFP2-BepC together with Gαs-YFP1 was not significantly different from control HA-YFP2 (16 ± 1%, 17 ± 1%, and 15 ± 1%, respectively). For HA-YFP2-BepC, this result is particularly significant, because the subcellular fractionation data (Fig. 4B) indicate that HA-YFP2-BepC is even more abundant membrane-associated protein than HA-YFP2-BepA. Furthermore, when the HA-YFP2 was forced to interact with the plasma membrane by the means of a C-terminal fusion to the K-ras plasma-membrane trafficking domain (HA-YFP2-CAAX), the size of the YFP+ population was significantly lower (23 ± 2%) than with HA-YFP2-BepA and Gαs-YFP1 cotransfections (43 ± 2%). In conclusion, the bimolecular fluorescence complementation (BiFC) data indicate that BepA might directly interact with Gαs. However, the BiFC data could also indicate an indirect BepA-Gαs interaction; that is, BepA binds a cellular protein that is in very close proximity to Gαs at some stage of its activity cycle, such as the AC (Fig. 4A). The latter possibility is supported by the fact that the C2 catalytic subunit of the AC is also the primary binding domain for Gαs (19).

Discussion

Bacillary angiomatosis (BA) and bacillary peliosis (BP) are clinical manifestations of chronic Bh infection in immunocompromised individuals, such as AIDS patients (9). The tumor-like lesions of BA and BP are composed of proliferated and misshapen ECs, a mixed leukocytic infiltrate and bacteria that are associated with the proliferated ECs (9). One of the bacteria-derived factors, which may influence the disease progression, is the antiapoptotic VirB/VirD4 T4SS effector BepA. Translocation of BepA into primary human ECs coincides with an increase in cellular cAMP concen-

tration and pharmacological elevation of cAMP similarly protects the primary human ECs from apoptosis (12). In the present study, we identified and characterized the most proximal signaling event of BepA-mediated inhibition of EC apoptosis, namely how this protein elevates the host cell cAMP concentration.

cAMP is a ubiquitous second messenger. In mammals, nine multipass plasma membrane-bound isoforms of cAMP-producing AC, as well as one soluble AC isoform, have been identified (17). Regulation of the membrane-bound ACs is primarily mediated by the activation of GPCR, release of the GPCR-associated α-subunit of a heterotrimeric G protein (αβγ), and subsequent binding of the Gα with the C1 and C2 catalytic domains of the ACs. Depending on the nature of the α-subunit, ACs can either be inhibited (αi) or activated (αs) (17). Regulators of G-protein signaling proteins act as GTPase activating proteins for α-subunits, thereby reducing the amplitude and duration of signaling (21). The AC activity is also regulated by protein phosphorylation (17). The intracellular concentration of cAMP is further controlled by PDEs, which degrade cAMP to the inactive 5′AMP (22).

In the present study, we hypothesized that after the T4SS-mediated translocation into the host cell, BepA binds and alters the activity of a protein that influences cellular cAMP concentration. Gel-free proteomics identified AC but also Gαs as potential cellular target proteins of BepA. To study the putative activation of host cell AC by BepA in vivo, human AC activity was first reconstituted under the regulation of Gαs in an E. coli mutant strain that is devoid of the AC and the cAMP-specific PDE. The main reason for this approach was the ability to study Gαs-dependent regulation of human AC without the regulatory

Fig. 4. In vitro and in vivo studies of the protein –protein interactions of BepA-AC-Gαs triad. (A) Sensorgrams of the binding of MBP (black), MBP-BepC (red), and MBP-BepA (green) on immobilized catalytic domain 2 (C2) of AC2. Interactions were monitored with a Biacore T100 system using five different concentrations of the analytes (1.0, 3.0, 5.0, 7.5, and 10.0 μM). The nonspecific binding of each concentration was determined and subtracted using an untreated control flow chamber. Displayed are representative differential binding curves of the sensor surface carrying immobilized C2 domain. (B) Protein –protein interaction analysis by BiFC in HEK293T cells. Folding of the inherently non fluorescent YFP1 and YFP2 fragments into a functional YFP upon putative YFP1- and YFP2-fusion partner interactions was analyzed and quanti fied by flow cytometry. The quantitation is based on triplicate samples (means ± SD) and it refers to the fractions of the cell populations displaying YFP signal over the threshold set by nontransfected HEK293T cells. Western analysis of membrane localization of YFP1- and YFP2-tagged proteins by Western blotting and immunodetection with polyclonal anti-Gαs, and subsequently after membrane stripping with monoclonal anti-HA antibodies. Membrane-enriched cellular fractions were prepared by differential centrifugation after hypotonic cell lysis.

interference of receptors, G proteins, or other regulatory proteins that are present in the cell, such as the regulators of G-protein signaling proteins. The catabolic defect of ΔcyaAΔcpdA E. coli strain was complemented by coexpression of BepA with the C1a and C2 catalytic subunits of AC7, but only when Gαs was also expressed in the system. Therefore, BepA appeared to act as a Gαs-dependent activator of AC. In principle, BepA could have acted in analogy to ADP ribosylating bacterial toxins and covalently modify Gαs into a constitutively active form. To study this possibility, we took advantage of a highly sensitive in vitro AC assay (15) with membrane preparations of Sf9 cells overexpressing full-length human AC2 (16) and recombinant BepA and Gαs. BepA activated AC in a Gαs-dependent manner, even in the absence of NAD$^+$, a necessary substrate for ADP ribosylation. Most importantly, the in vitro AC activity assays recapitulated the main finding of the heterologous expression system, (i.e., BepA-mediated activation of AC is dependent on Gαs).

In its inactive GPCR-coupled heterotrimeric βγ-bound conformation, the α-subunit of the G protein binds GDP. Agonist stimulation of GPCR promotes the release of GDP from the α-subunit and subsequent binding of GTP, which is accompanied by extensive conformational changes. The GTP-bound active α-subunit dissociates from the βγ-dimer and activates the AC by scaffolding the C1 and C2 catalytic domains. The cycle ends by GTP hydrolysis and the α-subunit returns into a conformation that favors sequestration to the βγ-dimer and GPCR (17). It was of interest to detect under in vitro conditions that BepA-mediated Gαs-dependent stimulation of AC was not dependent on the nature of the Gαs-bound guanine nucleotide. BepA could increase the AC stimulatory potential of inactive Gαs-GDP, but also of Gαs-γS-GTP, which is a preactivated form because of an exchange of GDP with a nonhydrolyzable GTP analog γS-GTP. With respect to Gαs-GDP, the result is not completely unexpected, because Gαs-GDP has been reported to be only 10-fold less potent than Gαs-γS-GTP to activate AC in vitro (18). The authors proposed that the full inactivation of Gαs requires sequestration of the Gαs-GDP with the βγ-complex and GPCR. However, the fact that BepA could increase the stimulatory potential of a canonically 100% active Gαs, Gαs-γS-GTP, was a surprise. Three possibilities were envisioned: (i) BepA binds Gαs and acts as a guanine nucleotide independent activator of Gαs; (ii) BepA binds Gαs and AC and thereby scaffolds the AC/Gαs-complex into an active cAMP producing conformation; or (iii) BepA binds AC and potentiates the Gαs-mediated activation of the AC. We experimentally addressed these possibilities by performing protein–protein interaction studies based on SPR. A direct interaction was detected between recombinant BepA and the C2 catalytic subunit of the AC. Although we could not detect direct interaction between BepA and Gαs by SPR, BepA still appeared to be in very close proximity to Gαs in the cell, as indicated by the data of our BiFC-analyses.

Forskolin binds at the interface of the C1 and C2 domains of AC, in the pocket structurally related to the AC active site, and converts the AC into a catalytically active form (20). It was therefore of interest to detect that BepA potentiates the stimulation of AC activity not only by Gαs but also by forskolin. We thus propose that BepA acts allosterically on AC to favor C1 and C2 subunit association, and via this mechanism is able to increase the efficacy of AC activation by Gαs and forskolin. At the cellular level, we propose that BepA directly binds the AC to increase the efficacy of AC activation by Gαs-GTP that has been released from the GPCR/G protein βγ-complex upon endogenous agonist stimulation of GPCRs, but might also additionally decrease the dissociation rate of Gαs-GDP from the AC (Fig. 5). BepA is a bacterial protein that directly binds host cell adenylyl cyclase to potentiate cAMP production.

Physiologically, the direct BepA-AC interaction is interesting because BepA-mediated elevation of host cell cAMP concentration appears to rely on endogenous GPCR signaling (i.e., on agonist stimulation of GPCRs and subsequent release of the stimulatory α-subunit). This mechanism appears to corroborate well with the lifestyle of Bartonella spp. These bacteria typically cause chronic and relapsing infections, which are pronounced in their reservoir hosts, but also evident in the case of vascular tumor formation by B. henseale in immune-compromised individuals, such as AIDS patients (9). The majority of bacterial mechanisms increasing the cellular cAMP concentration, such as the ADP ribosylation of Gαs by cholera toxin (4), cause acute and severe symptoms, including death of the host organism. The BepA-mediated activation of host cell AC is subtle and therefore more suitable for the typical persistence of B. henselae in the infected vascular endothelium.

Materials and Methods

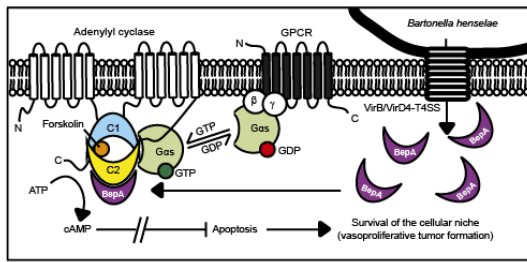Pulliainen et al.　　　　　　　　　　　PNAS | June 12, 2012 | vol. 109 | no. 24 | 9585

Page | 49

Fig. 5. The molecular basis of BepA-mediated elevation of host cell cAMP concentration. Canonically, in its inactive GPCR-coupled heterotrimeric βγ-bound conformation, the α-subunit of the stimulatory G protein binds GDP. Agonist stimulation of GPCR promotes the release of GDP from the α-subunit and subsequent binding of GTP, which is accompanied by extensive conformational changes. The GTP-bound active α-subunit conformation dissociates from the βγ-dimer and activates the AC. The cycle ends by GTP hydrolysis and the α-subunit returns into a conformation that favors sequestration to the βγ-dimer and GPCR. BepA is translocated by VirB/VirD4-T4SS into the host cell. BepA directly binds the C2 catalytic subunit of AC to increase the efficacy of AC activation by Gαs. BepA also potentiates the efficacy of AC activation by forskolin, a plant (*Coleus forskohlii*)-derived compound that activates the AC by interchalating the C1 and C2 subunits into a catalytically active form (19). We propose that BepA acts allosterically to favor C1 and C2 subunit association and via this mechanism is able to increase the rate of AC activation by both Gαs and forskolin. Physiologically, the BepA-mediated elevation of host cell cAMP concentration that leads into host cell survival relies on endogenous GPCR signaling (i.e., on agonist stimulation of GPCRs and subsequent release of the stimulatory α-subunit). This apparently subtle mechanism corroborates well with the lifestyle of *Bartonella* spp. because these bacteria typically cause chronic and relapsing infections (9).

Reconstitution of BepA-Regulated AC Activity in *E. coli*. To reconstitute the BepA-regulated human AC activity in *E. coli*, plasmids encoding for catalytic subunits of AC7, bovine Gαs, and Beps were introduced into the AC and cAMP-specific PDE-deficient *E. coli* strain APE304 by the polyethylene glycol-method. Colonies from freshly transformed plates were subcultured overnight in Luria Bertani (LB) medium with appropriate antibiotics at 37 °C in a 96-well format. The following day, the strains were dotted (3 μL/dot) on MacConkey agar (MacConkey Agar Base; BD Biosciences, 281810) plates supplemented with appropriate antibiotics, 1% (wt/vol) maltose and 5 μM

isopropyl- β-D-thiogalactopyranoside (IPTG) when indicated. The plates were incubated at 30 °C.

In Vitro AC Assays. Activity of a membrane-bound full-length AC2 was monitored in the presence and absence of highly pure recombinant Gαs and Beps using an assay described by Salomon et al. (15). AC2-containing membranes (15 μg) (16) and various amounts of Gαs or forskolin were incubated for 2 min on ice with indicated concentrations of recombinant MBP, MBP-BepA, MBP-BepB, or MBP-BepC in a final volume of 25 μL. In parallel, reaction mixture containing 0.2 mM ATP, 100 mM MgCl$_2$, 1 mM ETDA, and 10^6 counts per tube [α-^{32}P]adenosine 5′triphosphate (Hartmann Analytic; SRP-207, 3000 Ci/mmol) was heated at 30 °C. To initiate the reaction, 25 μL of the preheated reaction mix was added into the AC2-containing samples and the samples were incubated at 30 °C. After 10 min, reactions were stopped by the addition of 800 μL of stopping solution [0.25% (wt/vol) SDS, 5 mM ATP, 0.175 mM cAMP] and spiked with 10^4 counts per tube [2,8-3H]-cAMP (Hartmann Analytic; MT616, 15 –20 mCi/mmol). cAMP was then purified via a two-column system and quantified by liquid scintillation analysis as described by Salomon et al. (15).

Protein Interaction Analysis by SPR. To immobilize C2 domain of AC2 on a CM5 sensorchip flow chamber (GE Healthcare), the surface was first activated with a mixture of 77 μL of N-hydroxysuccinimide and 77 μL of N-ethyl-N′(dimethylaminopropyl)-carbodiimide at 25 °C. After activation, the flow chamber was washed for 4,000 s with 10 μM C2 domain solution at a flow rate of 5 μL/min. Saturation of unreacted carboxymethyl sites was achieved using 1 M ethanolamine solution (pH 8.0). An untreated flow chamber was used as reference during the experiment. MBP-BepA, MBP-BepC, and MBP were diluted in running buffer [100 mM Tris-HCl; pH 8.0, 200 mM NaCl, 5 mM β-mercaptoethanol, 0.05% (wt/vol) N-dodecyl- β-D-maltoside] to a final concentration of 1.0 μM, 3.0 μM, 5.0 μM, 7.5 μM, and 10.0 μM, and injected over the different surfaces with a flow rate of 10 μL/min for 10 min. Samples were kept at 8 °C, experiments were performed at 30 °C. Binding was monitored with Biacore T100 system (GE Healthcare) and surfaces were regenerated in-between samples by washing for 1 min with running buffer. The blank bulk refraction curves from the control flow chamber of every sample [Biacore T100 Evaluation Software (2.0.3.)] as well as buffer response of every channel (OriginPro8) were subtracted.

1. Ribet D, Cossart P (2010) Pathogen-mediated posttranslational modifications: A re-emerging field. Cell 143:694 –702.
2. Orth JH, et al. (2009) Pasteurella multocida toxin activation of heterotrimeric G proteins by deamidation. Proc Natl Acad Sci USA 106:7179 –7184.
3. Ahuja N, Kumar P, Bhatnagar R (2004) The adenylate cyclase toxins. Crit Rev Microbiol 30:187 –196.
4. Cassel D, Pfeuffer T (1978) Mechanism of cholera toxin action: Covalent modification of the guanyl nucleotide-binding protein of the adenylate cyclase system. Proc Natl Acad Sci USA 75:2669 –2673.
5. Katada T, Ui M (1982) Direct modification of the membrane adenylate cyclase system by islet-activating protein due to ADP-ribosylation of a membrane protein. Proc Natl Acad Sci USA 79:3129 –3133.
6. Hosono K, Suzuki H (1985) Morphological transformation of Chinese hamster cells by acylpeptides, inhibitors of cAMP phosphodiesterase, produced by Bacillus subtilis. J Biol Chem 260:11252 –11255.
7. Agarwal N, Lamichhane G, Gupta R, Nolan S, Bishai WR (2009) Cyclic AMP intoxication of macrophages by a Mycobacterium tuberculosis adenylate cyclase. Nature 460:98 –102.
8. Zhang X, Candas M, Griko NB, Taussig R, Bulla LA, Jr. (2006) A mechanism of cell death involving an adenylyl cyclase/PKA signaling pathway is induced by the Cry1Ab toxin of Bacillus thuringiensis. Proc Natl Acad Sci USA 103:9897 –9902.
9. Pulliainen AT, Dehio C (2012) Persistence of Bartonella spp. stealth pathogens: From subclinical infections to vasoproliferative tumor formation. FEMS Microbiol Rev 36:563 –599.
10. Kirby JE, Nekorchuk DM (2002) Bartonella-associated endothelial proliferation depends on inhibition of apoptosis. Proc Natl Acad Sci USA 99:4656 –4661.
11. Schmid MC, et al. (2004) The VirB type IV secretion system of Bartonella henselae mediates invasion, proinflammatory activation and antiapoptotic protection of endothelial cells. Mol Microbiol 52:81 –92.
12. Schmid MC, et al. (2006) A translocated bacterial protein protects vascular endothelial cells from apoptosis. PLoS Pathog 2:e115.
13. Schulein R, et al. (2005) A bipartite signal mediates the transfer of type IV secretion substrates of Bartonella henselae into human cells. Proc Natl Acad Sci USA 102:856 –861.
14. Tang WJ, Gilman AG (1995) Construction of a soluble adenylyl cyclase activated by Gs alpha and forskolin. Science 268:1769 –1772.
15. Salomon Y, Londos C, Rodbell M (1974) A highly sensitive adenylate cyclase assay. Anal Biochem 58:541 –548.
16. Dessauer CW, Chen-Goodspeed M, Chen J (2002) Mechanism of Galpha i-mediated inhibition of type V adenylyl cyclase. J Biol Chem 277:28823 –28829.
17. Sadana R, Dessauer CW (2009) Physiological roles for G protein-regulated adenylyl cyclase isoforms: Insights from knockout and overexpression studies. Neurosignals 17:5 –22.
18. Sunahara RK, Dessauer CW, Whisnant RE, Kleuss C, Gilman AG (1997) Interaction of Gsalpha with the cytosolic domains of mammalian adenylyl cyclase. J Biol Chem 272:22265 –22271.
19. Tesmer JJ, Sunahara RK, Gilman AG, Sprang SR (1997) Crystal structure of the catalytic domains of adenylyl cyclase in a complex with Gsalpha.GTPgammaS. Science 278:1907 –1916.
20. Kerppola TK (2006) Visualization of molecular interactions by fluorescence complementation. Nat Rev Mol Cell Biol 7:449 –456.
21. Sjögren B, Blazer LL, Neubig RR (2010) Regulators of G protein signaling proteins as targets for drug discovery. Prog Mol Biol Transl Sci 91:81 –119.
22. Francis SH, Houslay MD, Conti M (2011) Phosphodiesterase inhibitors: Factors that influence potency, selectivity, and action. Handb Exp Pharmacol 204:47 –84.
23. Yan SZ, Tang WJ (2002) Construction of soluble adenylyl cyclase from human membrane-bound type 7 adenylyl cyclase. Methods Enzymol 345:231 –241.

Supporting Information

SI Materials and Methods

Bacterial Strains and Growth Conditions. The bacterial strains are described in Table S1. *Bartonella henselae* was grown on Columbia agar plates containing 5% (vol/vol) defibrinated sheep blood in a humidified atmosphere at 37 °C and 5% CO_2 for 2–3 d. Unless otherwise indicated, *Escherichia coli* was cultured in Luria-Bertani (LB) medium with vigorous aeration at 37 °C. When needed, the medium was solidified by 1.5% (wt/vol) agar. Antibiotics and other supplements were used at the following concentrations unless other indicated: (*i*) *B. henselae*: 50 μg/mL of kanamycin, 50 μg/mL of spectinomycin, and 500 μM isopropyl β-D-thiogalactosidase (IPTG); (*ii*) *E. coli*: 50 μg/mL of kanamycin, 100 μg/mL of ampicillin and 35 μg/mL of chloramphenicol.

Generation of the CyaA- and CpdA-Deficient E. coli Strain. To reconstitute human adenylyl cyclase (AC) activity under the regulation of the α-subunit of the AC-stimulating G protein (G αs) in *E. coli*, a strain (APE304) that is devoid of AC, cAMP-specific phoshodiesterase (PDE), and capable of expressing genes cloned under a T7 polymerase-dependent promoter (e.g., genes in a pET-series vector) was engineered. To this end, the prophage λDE3 from the widely used expression strain BL21(λDE3) (1) was transferred into *E. coli* K-12 MG1655 (2) and subsequently the genes *cyaA* and *cpdA*, coding for the AC- and the cAMP-specific PDE, were deleted. First, the *galKMTE* operon, adjacent to λDE3 in BL21(λDE3), was replaced with a kanamycin cassette as previously described (3). This cassette was used as a selectable marker to P1-transduce λDE into K-12 MG1655 following standard procedures. The kanamycin marker was removed with the help of FLP-mediated site directed recombination to obtain strain AB472 (λDE3) (3). Subsequently, P1 transduction was used to introduce a Δcya::kan construct from an *E. coli* mutant JW3778 (4) into this strain. The kanamycin marker present in Δcya was removed as above. The resulting strain APE216 is λDE3 (T7pol⁺) ΔgalKMTE Δcya. Subsequently, P1 transduction was used to introduce a ΔcpdA::kan construct from an *E. coli* mutant JW3000 (4) into this strain. The kanamycin marker present in ΔcpdA was removed as above. The resulting strain APE304 is λDE3 (T7pol⁺) ΔgalKMTE ΔcyaΔcpdA.

DNA Manipulations. Oligonucleotide primers are described in Table S2. Plasmids are described in Table S3.

Mammalian expression vector of HA/EGFP-Bartonella effector protein A. A subfragment of Bartonella effector protein A (BepA) (encoding for amino acids 305–544, UniProtKB accession code Q6G2A9) was PCR-amplified with oligos prAP015 and prAP016. This PCR fragment was used as a template for PCR with primers prAP014 and prAP016 to generate 5′extension encoding for single HA-tag (N-MAYPYDVPDYAAA-BepA 305–544). The extension PCR product was digested with XhoI and BamHI and ligated into XhoI- and BamHI-digested pcDNA3.1/Hygro(-) (Invitrogen) to acquire pAP001. pAP013 was acquired by digesting pAP001 with NotI and after SAP treatment ligating with egfp that was acquired with NotI digestion of a PCR product amplified with oligos prAP022 and prAP023 using pWay21 [Molecular Motion Lab (http://momotion.cns.montana.edu)] as the template.

Mammalian expression vector of HA/EGFP-BepB. A subfragment of BepB (encoding for amino acids 303–542, UniProtKB accession code Q6G2A7) was PCR-amplified with oligos prAP017 and prAP018. This PCR fragment was used as a template for PCR with primers prAP014 and prAP018 to generate 5′extension encoding for single HA-tag (N-MAYPYDVPDYAAA-BepB 303–542). The

extension PCR product was digested with XhoI and BamHI and ligated into XhoI- and BamHI-digested pcDNA3.1/Hygro(-) (Invitrogen) to acquire pAP002. pAP014 was acquired by digesting pAP002 with NotI and after SAP treatment ligating with egfp that was acquired with NotI digestion of pAP013.

Mammalian expression vector of HA/EGFP-BepC. A subfragment of BepC (encoding for amino acids 292–532, UniProtKB accession code Q6G2A6) was PCR amplified with oligos pBH001f and pBH001r and ligated into NotI- and BamHI-digested pAP001 to acquire pBH002. pBH004 was acquired by digesting pBH002 with NotI and after SAP treatment ligating with egfp that was acquired with NotI digestion of pAP013.

Mammalian expression vector of HA/EGFP. pAP015 was acquired by digesting pAP001 with NotI and BamHI and ligating with egfp that was acquired with NotI and BamHI digestion of a PCR product amplified with oligos prAP022 and prAP025 using pWay21 as the template.

Mammalian expression vectors of human AC isoform 7 (AC7). The full-length human AC isoform 7 (GenBank accession no. D25538) in pCMV-SK (pCMV-ACVII) was a kind gift of Boris Tabakoff (Department of Pharmacology, University of Colorado School of Medicine, Aurora, CO) (5). Upon receipt, the insert was sequenced and was found to contain one synonymous substitution (Leu88: CTC to CTT) compared with D25538 (GenBank accession no.). To acquire a vector to express an N-terminally HA-tagged AC7, a full-length AC7 was PCR amplified from pCMV-ACVII with oligos prAP058 and prAP053 and ligated into NotI- and BamHI-digested pAP001 to acquire pAP023. pAP023 was used as the template for all of the subsequent subclonings of AC7.

Mammalian expression vectors of bovine Gαs. The short splice form Gnas-2 of bovine G αs (UniprotKB accession code P04896-2), which lacks E71-S84 of Gnas-1 (UniprotKB accession code P04896-1), in pQE60 *E. coli* overexpression plasmid (pQE60-G αs) was a kind gift of Stephen Sprang (Center for Biomolecular Structure and Dynamics, University of Montana, Missoula, MT). Upon receipt, the insert was sequenced and was found to contain nonsynonymous substitutions that result in Ala18 to Gly and Gly86 to Ser amino acid differences compared with the canonical sequence of bovine Gnas (UniprotKB accession codes P04896). Ala18 to Gly substitution in bovine G αs has been previously reported (6). No documented evidence was found for Gly86 to Ser variation in bovine G αs. However, by analyzing the highly conserved Gαs proteins of other mammals, Gly86 to Ser was found to be part of natural variation (e.g., in mouse G αs) (UniprotKB accession code P63094). To acquire a vector to express a nontagged bovine Gαs, the G αs was PCR-amplified from pQE60-G αs with oligos prAP055 and prAP083 and ligated into Xhol- and HindIII-digested pcDNA3.1/Hygro(-) (Invitrogen) to acquire pAP024. To acquire a vector to express a nontagged GTP-locked and constitutively active bovine G αs [Gln213 replaced by Leu, where amino acid numbering refers to the Gnas-2 sequence (UniprotKB accession code P04896-2)], pAP024 was linearized by PCR using the mutagenic oligos prAP085 and prAP086. The purified PCR products were treated with T4 polynucleotide kinase (Promega), digested with DpnI (Promega) to reduce the number of parental molecules, gel-isolated, and religated to acquire pAP039. pAP024 and pAP039 served as templates for all of the subsequent clonings of bovine G αs.

Mammalian expression vectors for bimolecular fluorescence complementation analysis. G αs was PCR amplified from pAP024 with oligos prAP162 and prAP163 and ligated into KpnI- and ClaI-digested

MCFD2-cYFP1 (7, 8) to acquire pAP078. The cloned plasmid allows expression of Gαs that is C-terminally tagged with a linker sequence (IDGGGGSGGGGSSG) followed by a subfragment (amino acids V2-Q158) of YFP. A subfragment of YFP encoding for amino acids K159-Y238 (YFP2) together with a linker sequence (QIDGGGGSGGGGSARV) following the YFP2 fragment was PCR-amplified from ssYFP2-ERGIC53 (7, 8) with oligos prAP157 and prAP158 and ligated to NotI-digested pAP013, pAP014 and pBH004 to acquire pAP082, pAP076, and pAP075, respectively. The cloned plasmids allow expression of N-terminally HA-YFP2-LINKER-tagged BepA305-544, BepB303-542 and BepC292-532. A subfragment of YFP encoding for amino acids K159-Y238 (YFP2) together with a linker sequence (QID-GGGGSGGGGSARV) following the YFP2-fragment was PCR-amplified from ssYFP2-ERGIC53 (7, 8) with oligos prAP157 and prAP159, and ligated to NotI- and BamHI-digested pAP015 to acquire pAP074. The cloned plasmid allows expression of N-terminally HA-tagged YFP2. A subfragment of YFP encoding for amino acids K159-Y238 (YFP2) together with a linker sequence (QIDGGGGSGGGGSARV) following the YFP2 fragment and HA-tag preceding the YFP2 fragment was PCR-amplified from pAP074 with oligos prAP167 and prAP186 and ligated to NcoI- and BamHI-digested pTriEx-GFP-CAAX (a kind gift of Olivier Pertz, Department of Biomedicine, University of Basel, Basel, Switzerland) to acquire pAP085. The cloned plasmid allows expression of HA-tagged YFP2, which is C-terminally fused to a sequence cassette GSDKMSKEGKKKKKKSK-TKCVIM containing a lipid modifiable (farnesyl-moiety) plasma membrane targeting signal of K-Ras (9).

E. coli expression vectors of maltose-binding protein (MBP)-BepA. A subfragment of BepA (encoding for amino acids 305–446) was PCR-amplified with oligos prAP004 and prAP006 and ligated into EcoRI- and PstI-digested pMal-c2X (New England Biolabs) to acquire pAP004.

E. coli expression vectors of MBP-BepB. A subfragment of BepB (encoding for amino acids 303–444) was PCR-amplified with oligos prAP034 and prAP036 and ligated into EcoRI- and PstI-digested pMal-c2X (New England Biolabs) to acquire pAP067.

E. coli expression vectors of MBP-BepC. A subfragment of BepC (encoding for amino acids 293–434) was PCR-amplified with oligos prAP113 and prAP114 and ligated into EcoRI- and PstI-digested pMal-c2X (New England Biolabs) to acquire pAP052. All these above clonings introduced an additional thrombin cleavage site (underlined) into the linker region between MBP and Beps that already contains a Factor Xa cleavage site (double underlined) (NLG IEGRISEF LVPRGS-Beps). The naive pMal-c2X overexpress an extended version of MBP (MBP-EXT) (NLG IEGRISEFGSSRVDLQASLALAVVLQRRDWENPGV-TQLNRLAAHPPFASWRNSEEARTDRPSQQLRSLNGEWQ-LGCFGG).

E. coli expression vector of MBP. To acquire an E. coli expression vector to express MBP without the C-terminal extension (MBP) that is present in MBP-EXT, MBP was PCR-amplified from pAP004 using the oligos prKP012 and prKP013. The PCR product was digested with NdeI and BamHI and ligated into NdeI- and BamHI-digested pAP004 to acquire pKP03.

E. coli expression vectors of the catalytic subunits of human AC7. pAP023 was used as the template for all of the subclonings of AC7 catalytic C1a and C2 subunits. Construct junctions were designed based on ref. 10. A subfragment of AC7 (encoding for C1a catalytic subunit amino acids P263-L476) was PCR-amplified with oligos prAP064 and prAP065 and ligated into BamHI- and HindIII-digested pACYCDuet-1 (Novagen) to acquire pAP033 (N-terminal HIS-tag). The same subfragment was also PCR-amplified with oligos prAP070 and prAP071 and ligated into NdeI- and XhoI-digested pACYCDuet-1 (Novagen) to acquire pAP034 (C-terminal S-tag). A subfragment of AC7 (encoding for C2 catalytic subunit amino acids D864-N1080) was PCR-amplified with oligos prAP068 and

prAP069 and ligated into BamHI- and HindIII-digested pA-CYCDuet-1 (Novagen) to acquire pAP035 (N-terminal HIS-tag). The same subfragment was also PCR-amplified with oligos prAP066 and prAP067 and ligated into NdeI- and XhoI-digested pACYCDuet-1 (Novagen) to acquire pAP036 (C-terminal S-tag). To acquire pACYCDuet-1 derivatives encoding simultaneously for both of the C1a and C2 subunits, C2 subfragment was digested offfrom pAP036 with NdeI and XhoI and ligated into pAP033 that was digested with NdeI and XhoI to acquire pAP037 (C1a with N-terminal HIS-tag and C2 with C-terminal S-tag). In addition, C1a subfragment was digested offfrom pAP034 with NdeI and XhoI and ligated into pAP035 that was digested with NdeI and XhoI to acquire pAP038 (C2 with N-terminal HIS-tag and C1a with C-terminal S-tag).

E. coli expression vectors of bovine Gαs. To acquire a vector to express a nontagged bovine Gαs, the Gαs was PCR-amplified from pAP024 with oligos prAP063 and prAP083 and ligated into NcoI- and HindIII-digested pRSFDuet-1 (Novagen) to acquire pAP025. To acquire a vector to express an N-terminally HIS-tagged bovine Gαs, the Gαs was PCR-amplified from pAP024 with oligos prAP060 and prAP083 and ligated into SacI- and HindIII-digested pRSFDuet-1 (Novagen) to acquire pAP027. To acquire a vector to express a C-terminally S-tagged bovine Gαs, the Gαs was PCR-amplified from pAP024 with oligos prAP061 and prAP084 and ligated into NdeI- and XhoI-digested pRSFDuet-1 (Novagen) to acquire pAP026. To acquire a similar vector set to express a nontagged, N-terminally HIS-tagged or C-terminally S-tagged GTP-locked and constitutively active bovine Gαs-Q213L, the same PCR conditions as above were used on pAP039 template to acquire pAP030, pAP031, and pAP032, respectively.

E. coli expression vectors of nontagged full-length BepA with and without Gαs. To acquire pAP055 vector to express a nontagged full-length BepA together with the nontagged bovine Gαs, the BepA was digested out from pPG101 (11) with NdeI and was ligated into NdeI-digested pAP025. To acquire pAP061 vector to express a nontagged full-length BepA without the nontagged bovine Gαs, the BepA was digested out from pPG101 (11) with NdeI and was ligated into NdeI-digested pRSFDuet-1.

Cloning and Characterization of Stable Bep-Expressing Cell Lines. Validation of Ea.hy926 as the hybridoma background for the generation of BepA-expressing stable cell lines.

qRT-PCR for crem (cAMP responsive element modulator).Ea.hy926 cells were seeded into six-well plates (120,000 cells per well) in DMEM/10% (vol/vol) FCS. The next day, fresh M199/10% (vol/vol) FCS medium supplemented with 500 μM IPTG (Promega) was added. The cells were infected in triplicate with different B. henselaestrains (Table 4) at a multiplicity of infection (MOI) of 300 (as calculated for the initial cell seeding density) and incubated for 30 h at 37 °C. In parallel, some cells were left uninfected or were treated with the phosphodiesterase inhibitory drug 3-isobutyl-1-methylxanthine (IBMX) (Sigma) as 100 μM together with the AC activatory drug forskolin (Sigma) as 10 μM. Isolation of total cellular RNA, RNA manipulation, and qRT-PCR for crem has been described previously (11).

pCRE-d2EGFP reporter studies. Ea.hy926 cells were seeded into 12-well plates (25,000 cells per well) in DMEM/10% (vol/vol) FCS. The next day, the cells were transfected for 6 h using Effectene (Qiagen) in fresh DMEM/10% (vol/vol) FCS with 300 ng/well of pCRE-d2EGFP reporter plasmid (Clontech). In this reporter plasmid, the expression of EGFP is under the control of a TATA-like promoter fused to three copies a cAMP response element (CRE)-binding sequence that mainly responds to CREB (cAMP response element-binding) protein activatory stimulus, and it has been used to monitor the activity of cellular cAMP signaling (12). To control transfection efficiency, some of the cells were also transfected with pWay19 [Molecular Motion Lab

Page | 52

(http://momotion.cns.montana.edu)]. Fresh M199/10% (vol/vol) FCS medium supplemented with 500 μM IPTG (Promega) was added 6 h posttransfection. The cells were infected in triplicate with different B. henselae strains (Table 4) at a MOI of 200 (as calculated for the initial cell-seeding density) and incubated for 24 h at 37 °C. In parallel, some cells were left uninfected or were treated with the phosphodiesterase inhibitory drug IBMX (Sigma) as 100 μM together with the AC activatory drug forskolin (Sigma) as 10 μM. Cells were trypsinized 24 h postinfection, recovered in medium, and analyzed by a FACSCalibur flow cytometer (Becton Dickinson) for EGFP expression. Nontransfected Ea.hy926 cells were used to set the threshold for EGFP expression. The data were visualized by the FlowJo7 software (Tree Star).

Confocal imaging of HA-EGFP-Bep fusions. HEK293T cells were seeded into gelatin-coated [0.2% (wt/vol)] glass covers-lips in 24-wells in DMEM/10% (vol/vol) FCS. The next day, the cells were transfected for 6–8 h using Effectene (Qiagen) in fresh DMEM/10% (vol/vol) FCS with 200 ng/well of plasmid DNA. The next day, the cells were fixed with 3.7% (wt/vol) paraformaldehyde, washed three times for 10 min in PBS, stained for 10 min in PBS containing 5 μg/mL of Wheat Germ Agglutinin (WGA) Alexa Fluor647-conjugate (Invitrogen/Molecular Probes), washed three times for 10 min in PBS, and finally mounted with Mowiol (polyvinyl alcohol 4–88) (Fluka) mounting medium. The specimens were analyzed for EGFP and WGA-Alexa Fluor647 signal using a Leica SP5 laser-scanning confocal microscope.

Cloning and Validation of Ea.hy926-Based Cell Lines That Stably Express BepA, BepB, and BepC. Cloning. Ea.hy926 cells were seeded into 96-well plates (4,000 cells per well) in DMEM/10% (vol/vol) FCS. The next day, 50 μL off resh DMEM/10% (vol/vol) FCS was added and the cells were transfected with of pAP013, pAP014, pBH004 or pAP015 using Effectene (Qiagen) by adding 50 μL the following transfection mixture into each well (mixture is enough for one 96-well plate): 1.45 mL of EC-buffer containing 5.6 μg of plasmid DNA, 39 μL of enhancer, 24 μL of Effectene, and 4.8 mL of DMEM/10% (vol/vol) FCS. The amount of Effectene transfection reagent was titrated down from the recommendations of the manufacturer to obtain a low amount of clones (zero to three clones per well) under Hygromycin B selection. The following day, 100 μL off resh DMEM/10% (vol/vol) FCS was added and the cells were incubated for 3 d. Next, 100 μL off resh DMEM/10% (vol/vol) FCS supplemented with 75 μM Hygromycin B (Sigma) was added. The cells were incubated for a period of 2–4 wk under constant Hygromycin B selection, changing fresh medium at 3-d intervals. The survived clones were trypsinized from the 96-well plates and were further expanded under constant Hygromycin B selection in DMEM/10% (vol/vol) FCS.

Validation. qRT-PCR. Isolation of total cellular RNA, RNA manipulation and qRT-PCR for crem and pde4b have been described previously (11).

FACS. Cells were trypsinized, recovered in medium, and analyzed (50,000 cells per sample) by a FACSCalibur flow cytometer (Becton Dickinson) for EGFP expression. Nontransfected Ea.hy926 cells were used to set the threshold for EGFP expression. The data were visualized by the FlowJo7 software (Tree Star).

Western blotting. Cells of confluent monolayers in 25 cm^2 cell-culture bottles were harvested by trypsinization, washed once with ice-cold PBS, and were stored at –80 °C. The cell pellets were lysed in 750 μL of ice-cold modified RIPA buffer [50 mM Hepes (pH 7.5), 250 mM NaCl, 1 mM EDTA, 0.3% (wt/vol) of SDS, 1% (vol/vol) Triton X-100 supplemented with Complete EDTA-free Protease Inhibitor Mixture (Roche)] [40 μL/mL of stock solution (one tablet/2 mL H$_2$O)]. The lysate was incubated at 4 °C for 1 h in a rotatory shaker followed by centrifugation (21,000 × g, 4 °C, 15 min). Protein concentrations of the cleared lysates were quantified with Nanodrop-1000 (Nanodrop Tech-

nologies) based on absorbance at 280 nm. Then, 10 μg of the cleared lysates were separated via SDS/PAGE using 10% (wt/vol) SDS-gel and transferred onto a Hypond-C Extra nitro-cellulose membrane (Amersham Biosciences). The membrane was examined for EGFP using primary rabbit polyclonal anti-EGFP antibody (1:5,000; Invitrogen, A11122), for HA-epitope using primary mouse monoclonal anti-HA antibody (1:5,000; Sigma, clone HA-7, H9658) and as the loading control for actin using primary mouse monoclonal antiactin antibody (1:7,500; Millipore, clone C4, MAB1501). For stripping of the different antibodies, the membrane was incubated for 15 min at 50 °C in 50 mL in stripping buffer [62.5 mM Tris-HCl (pH 6.8), 2% (wt/vol) SDS, 0.7% (vol/vol) β-mercaptoethanol]. After five washing steps in 20 mL PBS, the membrane was examined with a different antibody. Proteins were visualized using the ECL System (GE Healthcare) for the HRP-conjugated ECL donkey anti-rabbit IgG (1:5,000; GE Healthcare, NA934V) or HRP-conjugated ECL sheep anti-mouse IgG (1:5,000; GE Healthcare, NA931V).

Gel-Free Proteomics. Sample preparation for gel-less proteomics. Immunoprecipitation. Stable cell lines (HA-EGFP-BepA clone B12, HA-EGFP-BepB clone E10, HA-EGFP-BepC clone BH3 and HA-EGFP clone A9) were cultured in DMEM/10% FCS in 150-cm^2 cell culture flasks. Cells of confluent monolayers were harvested by trypsinization, washed once with ice-cold PBS, and stored at –80 °C until the MS-sample preparation. Before freezing, the cell numbers were adjusted to 1×10^7 cells per MS-sample. However, with BepA expressing cell line 1×10^8 cells per MS-sample were used because of lower recovery of the fusion protein into the Triton X-100 lysates (Fig. 2). The frozen pellets were supplied with 5 mL of ice-cold MS-lysis buffer [50 mM Hepes (pH 7.5), 250 mM NaCl, 1 mM EDTA, 1 μM of pepstatin, 1 μM of leupeptin and 1% (vol/vol) of Triton X-100]. Just before use, the MS-lysis buffer was supplemented with 1.5 mM dithiobis [succinimidylpropionate] (DSP) (Pierce; 22585) to serve as a lipophilic membrane permeable and primary amine targeting cross-linker. The lysates were incubated on ice for 30 min after which the DSP cross-linker was quenched by adding 1.25 mL of 1 M Tris-HCl (pH 7.5) followed by incubation on ice for 20 min. The lysates were drawn six times through a 22-gauge needles and were further incubated at 4 °C for 1 h in a rotatory shaker followed by centrifugation (21,000 × g, 4 °C, 15 min). The cleared lysates were mixed with 100 μL of monoclonal anti-HA agarose conjugate (Sigma; clone HA-7, A2095) settled with the MS-lysis buffer and were incubated at 4 °C for 2 h in a rotatory shaker. The samples were loaded on Bio Spin Disposable Chromatography columns (BioRad; 732 –6008) and by gravity flow the nonimmunoprecipitated part was separated from the beads. The beads were washed in the columns by gravity flow 10 times with 1 mL of MS-lysis buffer and 10 times with 1 mL of wash buffer [50 mM Hepes (pH 7.5), 250 mM NaCl, 1 mM EDTA]. To obtain the best elution efficiency of the bait fusion proteins and the copurified proteins from anti-HA beads, the beads were removed from the columns into microcentrifuge tubes with 1 mL of wash buffer. Subsequently, the beads were pelleted by centrifugation (3,000 × g, 1 min, 4 °C). Low pH elution of the bait and the copurified proteins from anti-HA beads was done five times by adding 200 μL elution buffer [0.2 M glycine (pH 2.5)] followed by centrifugation (3,000 × g, 1 min, 4 °C). Each eluate was neutralized for the pH by addition of 100 μL of neutralization buffer [1 M NH$_4$HCO$_3$ (pH 8.8)]. The eluates were pooled and to eliminate residual anti-HA beads still present in the eluates, the eluates were transferred three times to a new microcentrifuge tube after a short centrifugation step (3,000 × g, 1 min, 4 °C). The quality of the eluted material (in total 1.5 mL) was analyzed by (i) rabbit polyclonal anti-EGFP Western analysis and (ii) silver staining of SDS/PAGE gels that contained TCA-precipitated proteins from 200 μL of the eluates. To fulfill the

criteria for a sample taken into the next trypsinization step, the eluates had to contain clearly detectable levels of HA/EGFP-tagged proteins in anti-EGFP Western analysis as well as to show clear protein patterns and preferably differences in the protein patterns in silver-stained gels.

Preparation peptides. TCEP (Sigma; 93284) was added to the eluates as 5 mM to reduce disulfide bonds to free thiol groups and the eluates were incubated at 37 °C for 30 min. Then, iodoacetamide (Sigma; 57670) was added to the eluates as 10 mM to stabilize the free thiol groups and the eluates were incubated for 30 min at room temperature in the dark. One microgram of trypsin (Sequencing Grade Modified Trypsin; Promega, V5113) was added to each sample followed by incubation at 37 °C overnight. Completeness of the trypsin digestion was controlled by rabbit polyclonal anti-EGFP Western analysis and no detectable signal was allowed for samples that were taken into the next peptide purification step.

Purification of peptides. Reverse-phase chromatography with Macro Spin Column (Harvard Apparatus; 74 –4101) having silica octadecyl carbon chain (C18) matrix was used to purify the peptides. Reverse-phase columns were hydrated for 15 min with 500 μL of water. Then the columns were centrifuged for 4 min at 3,100 rpm (Heraeus Biofuge Fresco with rotor #3328) at room temperature. The hydration step with water was repeated. The resins were subsequently washed twice with 1% (vol/vol) acetonitrile (ACN) (Sigma; 92679) by centrifugation (3 min, 3,100 rpm, Heraeus Biofuge Fresco with rotor #3328) and equilibrated three times with 0.1% (vol/vol) formic acid (FA) (Sigma; 94318) by the same centrifugation steps as before. Peptide samples were acidified by adding FA to a final concentration of 0.1% (vol/vol). The final pH between 2 and 3 was checked with a pH indicator paper. In 150- μL portions the samples were loaded into the columns and spun down (3,100 rpm, 4 min, room temperature, Heraeus Biofuge Fresco with rotor #3328) the flow-through was added to a second column. This procedure was continued until each sample had passed through two columns. Then the columns were washed three times with 0.1% (vol/vol) FA, 1% (vol/vol) ACN (Sigma, 92679) (centrifuged at 3,100 rpm, 3 min, Heraeus Biofuge Fresco with rotor #3328). The elution of the peptides was achieved by adding twice 0.1% (vol/vol) FA, 50% (vol/vol) ACN (centrifuged at 3,100 rpm, 3 min, Heraeus Biofuge Fresco with rotor #3328). The two peptide eluates per sample were pooled together. The solvent was evaporated on a spin vacuum pump. Based on the sample criteria outlined above the final set of samples coming from four independent immunoprecipitations that were finally subjected for LC-MS/MS analysis included: MS-data I: BepA, BepB and EGFP; MS-data II: BepA and BepC; MS-data III: BepA, BepB and BepC; and MS-data IV: BepA, BepB, BepC and EGFP.

LC-ESI-MS/MS analysis. LC-ESI-MS/MS analysis was performed using an Agilent 1100 series pump (Agilent Technologies) and a LTQ mass spectrometer (Thermo Electron). The setup of the μRPLC system and the capillary column has been described previously (13). The electrospray voltage was set to 1.8 kV. The samples were loaded from the Agilent auto sampler onto the precolumn at a flow rate of 4 μL/min in 5 min. Mobile phase A was 0.1% (vol/vol) FA and mobile phase B was 100% (vol/vol) acetonitrile (Sigma). For analysis, a separating gradient from 5 – 45% (vol/vol) mobile phase B over 40 min at 0.2 μL/min was applied. The three most abundant precursor ions in each MS scan were selected for collision-induced dissociation if the intensity of the precursor ion exceeded 20,000 ion counts. The dynamic exclusion window was set to 2 min. To prevent cross-contamination between the different samples, the LC system was washed with a pulse of 8 μL trifluoroethanol (Fluka) after every sample. A peptide standard containing 200 fmol of [Glu1]-Fibrinopeptide B human (Sigma) was analyzed by LC-MS/MS to constantly monitor the performance of the LC-MS/MS system.

Acquired MS2 scans were searched against the human International Protein Index protein database (v.3.26) complemented with the amino acid sequences of BepA, BepB, and BepC using the XTandem search algorithm (14) with k-score plug-in (15). In silico trypsin digestion was performed after lysine and arginine (unless followed by proline) into fully tryptic peptides. Allowed monoisotopic mass error for the precursor ions was 3 Da. A fixed residue modification parameter was set for carboxyamidomethylation (57.02 Da) of cysteine residues. Oxidation of methionine (15.99 Da) was set as variable residue modification parameter. Model refinement parameters were set to allow phosphorylation (79.96 Da) of serine, threonine, and tyrosine residues as variable modifications. Furthermore semi tryptic peptides were allowed for refinement searches. For scoring, a maximum of two missed cleavages were considered. Search results were evaluated on the Trans Proteomic Pipeline (TPP v3.2) using PeptideProphet (16) and ProteinProphet (17, 18). In the end a protein identification probability cutoff of 0.9 was applied to get the list of proteins present in any given immunoprecipitation.

Data filtering. Because of the quality criteria of the sample preparation (see above), some of the samples were discarded before the LC-ESI-MS/MS. To identify BepA interacting proteins based on the raw proteomics data of the four independent immunoprecipitations, each experiment was first filtered individually (i.e., proteins identified in non-BepA samples were removed from the list of proteins identified in the BepA samples). To this end, proteins identified in EGFP-BepB and EGFP samples were removed from the list of proteins identified in the BepA sample (MS-data I); proteins identified in EGFP-BepC sample were removed from the list of proteins identified in the BepA sample (MS-data II); proteins identified in EGFP-BepB and EGFP-BepC samples were removed from the list of proteins identified in the BepA sample (MS-data III); and finally, in the full comparative analysis proteins identified in EGFP-BepB, EGFP-BepC, and EGFP samples were removed from the list of proteins identified in the BepA sample (MS-data IV). Then, an arbitrary cutoff was applied where protein had to be identified at least in two different experiments as a BepA-specific to be regarded as BepA-binding cellular protein.

Expression and Purification of Recombinant Proteins. HIS-tagged Gαs. For recombinant expression of N-terminally HIS-tagged G αs, Ca-competent E. coli BL21(λDE3)Rosetta were transformed with pAP027 and cultured at room temperature in LB media containing 50 μg/mL of kanamycin and chloramphenicol. At an OD $_{600}$ of 0.5, the expression was induced with 30 μM IPTG. After 18 h of culturing at room temperature, cultures were harvested and stored at −20 °C. Frozen bacteria were thawed and lysed by French press in lysis buffer [100 mM Tris pH = 8.0, 200 mM NaCl, 10 mM MgCl $_2$, 2.5 mM βME, 10 μM GDP (Sigma)] supplemented with 2 mg of DNaseI from bovine pancrease (Roche) and Complete EDTA-free Protease Inhibitor Mixture (Roche) [40 μL/mL of stock solution (one tablet/2 mL H $_2$O]. HIS-tagged G αs was purified using Ni-NTA columns (GE Healthcare) coupled to an ÄKTApurifier 10 (GE Healthcare) and elution with 100 mM imidazole. Peak fractions were pooled and loaded on a Superdex 200 16/60 column (GE Healthcare) for size-exclusion chromatography coupled to an ÄKTApurifier 10 (GE Healthcare). To analyze the purification by size-exclusion chromatography, 10 μL of the peak fractions were separated via SDS/PAGE using 12% (wt/vol) SDS-gel and either stained with Coomassie staining solution or transferred on a Hybond-C Extra nitrocellulose membrane for Western blotting. The membrane was examined for Gαs using primary rabbit polyclonal anti-G αs antibody (1:1,000; Santa Cruz Biotechnology, sc-383). Proteins were visualized using HRP-conjugated ECL donkey anti-rabbit IgG (1:5,000; GE Healthcare, NA934V) and the ECL System (GE Healthcare). Fractions containing pure G αs were pooled

and the concentration was measured via absorbance at 280 nm with Nanodrop-1000 (Nanodrop Technologies). Next, 300 μL aliquots were stored at −80 °C.

HIS-tagged C2-AC2. For recombinant expression of C2-domain of AC2 (IIC2), Ca-competent E. coli BL21(λDE3) were transformed with IIC2H6-pQE60 and cultured at room temperature in LB media containing 200 μg/mL of ampicillin. At an OD_{600} of 0.5, expression was induced with 30 μM IPTG. After 18 h of culturing at room temperature, cultures were harvested and stored at −20 °C. Frozen bacteria were thawed and lysed by French press in lysis buffer (50 mM Hepes pH = 7.5, 200 mM NaCl, 10 mM $MgCl_2$, 2.5 mM βME) supplemented with 2 mg DNaseI from bovine pancrease (Roche) and Complete EDTA-free Protease Inhibitor Mixture (Roche) [40 μL/mL of stock solution (one tablet/2 mL H_2O)]. IIC2 was puri fied using metal affinity using Ni-NTA columns (GE Healthcare) coupled to an ÄKTApuri fier 10 (GE Healthcare) and elution with 150 mM imidazole. Peak fractions were pooled and loaded on a Superdex 200 30010 column (GE Healthcare) coupled to an ÄKTApuri fier 10 (GE Healthcare) for size-exclusion chromatography. To analyze the purification by size exclusion chromatography, 10 μL of the peak fractions were separated via SDS/PAGE using 12% (wt/vol) SDS-gel and stained with Coomassie staining solution. Fractions containing IIC2 were pooled and the concentration was measured via absorbance at 280 nm with Nanodrop-1000 (Nanodrop Technologies) and stored at 4 °C.

MBP-Beps and MBP. For expression of $BepA_{305-446}$, $BepB_{303-444}$, $BepC_{293-434}$ as C-terminal fusion proteins of MBP, E. coli BL21 (λDE3) were transformed with pAP004, pAP067, and pAP052, respectively. To additionally express and purify the MBP not carrying any fusion protein (MBP), E. coli BL21(λDE3) were transformed with pKP03. Single colonies were picked to inoculate 50-mL overnight cultures. The next day, 2 L of Terri fic Broth media were inoculated with 20 mL of the overnight cultures and gently shaken for 24 h at room temperature. After removal of culture media, bacterial pellets were stored at −20 °C. Frozen bacteria were thawed in 20 mL oflysis buffer [100 mM Tris pH = 8.0, 200 mM NaCl, 5 mM β-mercaptoethanol, 0.5% (wt/vol) DDM (n-Dodecyl-β-D-Maltopyranoside; Sol-Grade, Affymetrix Anatrace)], 2 mg DNaseI from bovine pancrease (Roche), Complete EDTA-free Protease Inhibitor Mixture (Roche) [40 μL/mL of stock solution (one tablet/2 mL H_2O)], lysed, and the filtered high-speed supernatant was incubated with 1 mL of amylose resin (New England Biolabs; #E8021S) for 1 h at 4 °C on a rotary shaker. The amylose resin was washed three times with 5 mL buffer [100 mM Tris pH 8.0, 200 mM NaCl, 5 mM βME and 0.05% (wt/vol) DDM] before proteins were eluted with 20 mM D-(+)-maltose. For further purification, a Superdex 200 16/60 column coupled to an ÄKTApuri fier 10 (GE Healthcare) was used. To analyze the purification by size-exclusion chromatography, 10 μL of the peak fractions were used for SDS/PAGE and Western blot analysis. After transfer, Hybond-C-Extra nitrocellulose membranes were examined for MBP fusion proteins using HRP-conjugate of mouse polyclonal anti-MBP antibodies (1:50,000; New England Biolabs, #E8038S). Proteins were visualized using ECL System. Fractions containing MBP fusion proteins were pooled and the concentration was measured via absorbance at 280 nm with Nanodrop-1000. Fifty-microliter aliquots were stored at −80 °C.

Activation of G αs. When indicated, HIS-G αs was not used in its GDP-bound form (G αs-GDP) but in its activated state bound to GTP (G αs-γS-GTP). To exchange nucleotides and thereby activating purified HIS-G αs, 500 μL of 10 μM HIS-G αs was incubated for 30 min with 0.1 mM γS-GTP (Sigma) at 30 °C. To remove excessive nucleotides, PD10 columns (GE Healthcare) were used for desalting the sample. Elution buffer: 100 mM Tris pH = 8.0, 200 mM NaCl, 10 mM $MgCl_2$, 2.5 mM βME.

Subcellular Fractionation of the Bimolecular Fluorescence Complementation Analysis. To analyze for the membrane localization of different YFP1- and YFP2-tagged proteins, cells from three independent transfections were pooled after the FACS-analysis and washed once with ice-cold PBS. The cells were resuspended into 1 mL of hypotonic lysis buffer [20 mM Hepes; pH 7.5, 2.5 mM $MgCl_2$, 1 mM EDTA, and 1 mM DTT supplemented with Complete EDTA-free Protease Inhibitor Mixture (Roche)] [40 μL/mL of stock solution (one tablet/2 mL H_2O)] and 25 U/mL of benzonase (Novagen). The cells were incubated at 4 °C for 1 h in a rotatory shaker to allow them to swell and partially lyse. The partial lysates were drawn 20 times through 27-gauge needles and centrifuged with low speed [2,500 rpm, 4 °C, 10 min (Heraeus Biofuge Fresco, rotor #3328)] to pellet the nuclei and insoluble cell debris. The low-speed supernatant was subjected to high-speed centrifugation [20,000 rpm, 4 °C, 30 min (Heraeus Biofuge Stratos, rotor #3331)] to pellet the membranes. The membranes were resolubilized into 50 μL of 50 mM Hepes; pH 7.5, 200 mM NaCl, 1 mM EDTA and 10 mM DTT, 0.3% (wt/vol) SDS and 2% (vol/vol) Triton X-100 supplemented with protease inhibitors, as described above. Next, 25 μL of 3× Laemmli loading dye (19) was added and 15μL of the boiled samples (95 °C, 10 min) were separated via SDS/PAGE using 12% (wt/vol) SDS-gel and transferred onto a Hypond-C Extra nitrocellulose membrane (Amersham Biosciences). The membrane was examined for HA-epitope using primary mouse monoclonal anti-HA antibody (1:5,000; Sigma, clone HA-7, H9658) and for endogenous Gαs (serving as a loading control) as well as for the C-terminally YFP1-tagged G αs using primary rabbit polyclonal anti-G αs/olf antibody (1:1,000; Santa Cruz Biotechnology, sc-383). Proteins were visualized using the ECL System (GE Healthcare) for th e HRP-conjugated ECL donkey anti-rabbit IgG (1:5,000; GE Healthcare, NA934V) or HRP-conjugated ECL sheep an ti-mouse IgG (1:5,000; GE Healthcare, NA931V).

Preparation of Polyclonal Antibodies Speci fic for BepA. Expression and purification of recombinant N-terminally HIS-tagged FIC-domain of BepA has been described previously (20). Rabbits were immunized subcutaneously with 1.0 mL of a mixture of the recombinant FIC-BepA and Freund 's complete adjuvant (1:1, vol/vol) at Laboratoire d 'Hormonologie, Marloie, Belgium. For the first injection, 0.2 mg of FIC-BepA was used. Booster injections with 0.1 mg of FIC-BepA were given at 14, 28, and 56 d. Sera collected 10 d after the last booster were used for subsequent work.

Determination of Cellular cAMP-Levels. To analyze effects of BepA on intracellular cAMP-levels, Ea.hy926 cells and Ea.hy296 cells that stably express HA-EGFP- or HA-EGFP-tagged Beps were seeded into white-bottom 96-well plates (10,000 cells per well) and in parallel into transparent 96-well plates. After incubation for 24 h at 37 °C, cells in the transparent 96-well plates were analyzed under the microscope to visualize equal confluency of the seeded cells. Cells in the white-bottom 96-well plates were washed twice with 50μL PBS. In addition to the samples, eight cAMP-standard ranging from 712 nmol/L to 0 nmol/L were used on each plate. To lyse the cells and to detect cAMP, 25 μL of cAMP-d2 working solution of cAMP dynamic2 kit (Cisbio) as well as 25 μL of Ab-cryptate working solution (Cisbio) were added to each well and plates were incubated for 1 h at room temperature in the dark. Using an In finite F500 plate reader (TECAN) samples were excited at 340 nm and emission at 620 nm as well as at 665 nm was measured. cAMP concentrations were calculated based on the ratios of the both emissions. Protein concentrations of the cell lysates were determined after the fluorescence emission measurements using the Bradford dye binding procedure (21).
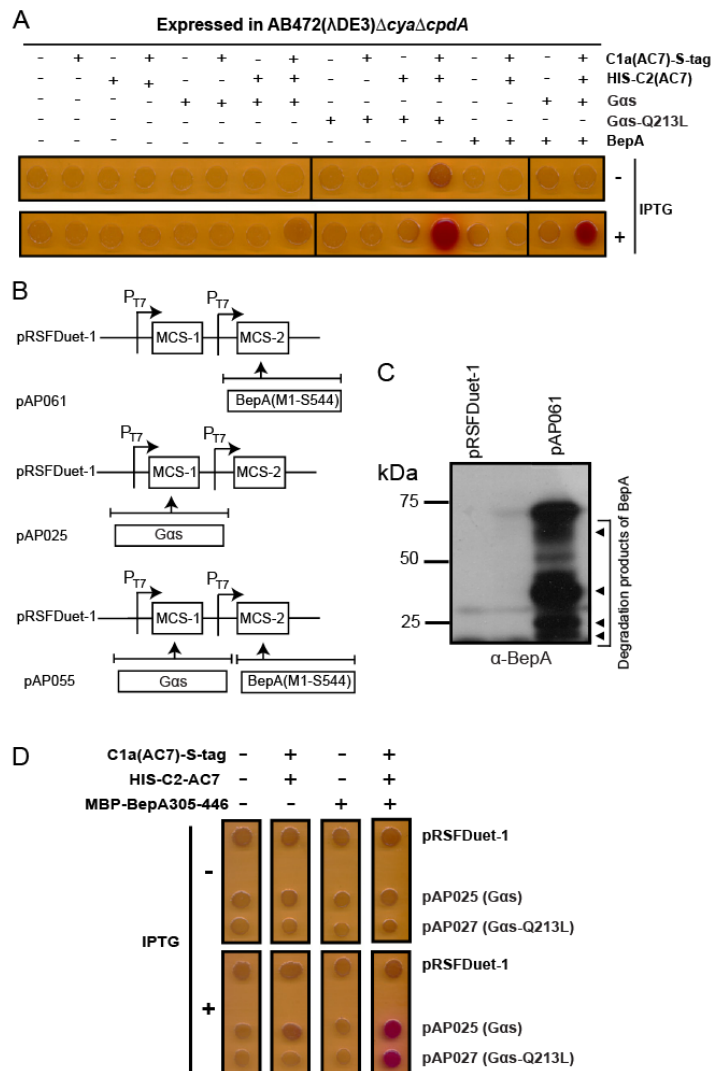
1. Studier FW, Rosenberg AH, Dunn JJ, DubendorffJW (1990) Use of T7 RNA polymerase to direct expression of cloned genes. Methods Enzymol 185:60 –89.
2. Blattner FR, et al. (1997) The complete genome sequence of Escherichia coli K-12. Science 277:1453 –1462.
3. Datsenko KA, Wanner BL (2 000) One-step inactivatio n of chromosomal genes in Escherichia coli K-12 using PCR products. Proc Natl Acad Sci USA 97:6640 –6645.
4. Baba T, et al. (2006) Construction of Escherichia coli K-12 in-frame, single-gene knockout mutants: The Keio collection. Mol Syst Biol 2: 2006.0008.
5. Hellevuo K, et al. (1995) The characterization of a novel human adenylyl cyclase which is present in brain and other tissues. J Biol Chem 270:11581 –11589.
6. Robishaw JD, Russell DW, Harris BA, Smigel MD, Gilman AG (1986) Deduced primary structure of the alpha subunit of the GTP-binding stimulatory protein of adenylate cyclase. Proc Natl Acad Sci USA 83:1251 –1255.
7. Nyfeler B, Michnick SW, Hauri HP (2005) Capturing protein interactions in the secretory pathway ofl iving cells. Proc Natl Acad Sci USA 102:6350 –6355.
8. Nyfeler B, et al. (2008) Identi fi cation of ERGIC-53 as an intracellular transport receptor of alpha1-antitrypsin. J Cell Biol 180:705 –712.
9. Hancock JF (2003) Ras proteins: Different signals from different locations. Nat Rev Mol Cell Biol 4:373 –384.
10. Yan SZ, Tang WJ (2002) Construction of soluble adenylyl cyclase from human membrane-bound type 7 adenylyl cyclase. Methods Enzymol 345:231 –241.
11. Schmid MC, et al. (2006) A translocated bacterial protein protects vascular endothelial cells from apoptosis. PLoS Pathog 2:e115.
12. Tian L, et al. (2007) Screening for novel human genes associated with CRE pathway activation with cell microarray. Genomics 90:28 –34.
13. Yi EC, Lee H, Aebersold R, Goodlett DR (2003) A microcapillary trap cartridge-microcapillary high-performance liquid chromatography electrospray ionization emitter device capable of peptide tandem mass spectrometry at the attomole level on an ion trap mass spectrometer with automated routine operation. Rapid Commun Mass Spectrom 17:2093 –2098.
14. Craig R, Beavis RC (2004) TANDEM: Matching proteins with tandem mass spectra. Bioinformatics 20:1466 –1467.
15. MacLean B, Eng JK, Beavis RC, McIntosh M (2006) General framework for developing and evaluating database scoring algorithms using the TANDEM search engine. Bioinformatics 22:2830 –2832.
16. Keller A, Nesvizhskii AI, Kolker E, Aebersold R (2002) Empirical statistical model to estimate the accuracy of peptide identi fi cations made by MS/MS and database search. Anal Chem 74:5383 –5392.
17. Keller A, Eng J, Zhang N, Li XJ, Aebersold R (2005) A uniform proteomics MS/MS analysis platform utilizing open XML file formats. Mol Syst Biol 1: 2005.0017.
18. Nesvizhskii AI, Keller A, Kolker E, Aebersold R (2003) A statistical model for identifying proteins by tandem mass spectrometry. Anal Chem 75:4646 –4658.
19. Laemmli UK (1970) Cleavage of structural proteins during the assembly of the head of bacteriophage T4. Nature 227:680 –685.
20. Palanivelu DV, et al. (2011) Fic domain-catalyzed adenylylation: Insight provided by the structural analysis of the type IV secretion system effector BepA. Protein Sci 20: 492 –499.
21. Bradford MM (1976) A rapid and sensitive method for the quantitation of microgram quantities of protein utilizing the principle of protein-dye binding. Anal Biochem 72: 248 –254.

Fig. S1. (A) Subcellular localization of N-terminally HA-EGFP-tagged Beps (see Fig. 1 A) in HEK293T cells. The cells were transiently transfected for 24 h. Subsequently, the cells were surface-labeled by staining with Alexa Fluor 647-conjugated WGA. Confocal images were taken for EGFP (green channel) and WGA (red channel) in the x-y plane (lower image is an overlay of both channels). Width of the merged images: HA-EGFP-BepA305-544, 22.5 µm; HA-EGFP-BepB303-542, 24.0 µm; HA-EGFP-BepC292-532, 22.5 µm; HA-EGFP, 22.5 µm. (B and C) Validation of Ea.hy926 cells as the hybridoma background to clone the Bep-expressing cell lines. (B) qRT-PCR analysis of *crem* expression. Expression of the cAMP-responsive gene *crem* was determined by qRT-PCR after infection of Ea.hy926 for 30 h with a MOI of 300. The mean values ± SDs from a representative experiment are shown for samples measured in triplicate. (C) pCRE-d2EGFP reporter studies. In pCRE-d2EGFP, the expression of destabilized form of EGFP (faster turnover) is under the control of a TATA-like promoter fused to three copies of cAMP CRE-binding sequence that mainly respond to the activatory stimulus of CREB. pCRE-d2EGFP-transfected cells were infected at an MOI of 200 for 24 h and the EGFP expression was quantified by flow cytometry. In the figure, percentages of EGFP-positive cells refer to cells in the population that show EGFP signal above the threshold set by mock-transfected cells. In B and C, the assays have been positively controlled with 100 µM pan-phosphodiesterase inhibitor IBMX together with 10 µM AC activator forskolin. (D) Quality analysis of the sample preparation in gel-free proteomics. Samples were retrieved at different points of the sample preparation as indicated in Fig. S2 A, and were processed for anti-EGFP Western analysis.

A

B

Protein[1]	Length[2]	ID[3]	Peptides[4]	Coverage-%[5]
Bartonella effector protein A (Q6G2A9)	240	4	ALGVSPLLQK (3) ELTSLLQK (3) LRQEVPMPSQSLQDLLSLPK (2) TPYSVHSLAGFDLICFK (2) NIIEIIKNPSK (2) HVALLSCAVANFTHAVK (1) GQQLATQIER (1) TLAMAS (1)	41.3
Galectin 3-binding protein (Q08380)	585	3	ELSEALGQIFDSQR (2) YSSDYFQAPSDYR (2) EGWKAAIPSALDTNSSK (1) STSSFPCPAGHFNGFR (1) AVDTWSWGER (1) RIDITLSSVK (1)	14.5
72 kDa type IV collagenase (P08253)	660	3	AFQVWSDVTPLR (2) CGNPDVANYNFFPR (1) FQGTSYDSCTTEGR (1) VDAAFNWSK (1)	7.4
Adenylyl cyclase type 7 (P51828)	1080	2	ILGDCYYCVSGLPVSLPTHAR (2) YFLNEGEEGPDQDALYEK (1) TYLVIDPR (1)	4.3
Guanine nucleotide-binding protein stimulatory alpha subunit (P63092)	394	2	QADYVPSDQDLLR (2) LLLLGAGESGK (1) VLTSGIFETK (1)	8.6
60S ribosomal protein L13 (P26373)	211	2	GFSLEELR (2) TIGISVDPR (1)	8.1
Serum albumin (P02768)	609	2	KVPQVSTPTLVEVSR (2) SHCIAEVENDEMPADLPSLAADFVESK (1) QEPERNECFLQHKDDNPNLPR (1) NECFLQHKDDNPNLPR (1) RPCFSALEVDETYVPK (1) VPQVSTPTLVEVSR (1) AVMDDFAAFVEK (1) QNCELFEQLGEYK (1) YICENQDSISSK (1) QTALVELVK (1) FQNALLVR (1)	21.8

[1]UniProtKB accession codes in parentheses.
[2]Length of the longest known isoform in amino acids.
[3]Number of identifications for a given protein in 4 independent analyses in parentheses.
[4]Number of identifications for a given peptide in 4 independent analyses in parentheses.
[5]Peptide coverage-% to the longest known isoform or with BepA to the used subfragment (E305-S544).

Fig. S2. (A) Schematic representation of the gel-free proteomics approach. The bait protein and possible interaction partners are eluted from the beads with low pH and the eluate is processed for trypsin digestion (16). See also Fig. S1 D. (B) Results of the gel-free proteomics screens. The table is a list of proteins that were detected specifically in BepA samples at least twice in four independent analyses.

Page | 58

Fig. S3. In vivo reconstitution of BepA-regulated mammalian AC activity in E. coli . (A) Dots of λDE3-lysogenic E. coli AB472(λDE3)ΔcyaΔcpdA grown on a MacConkey maltose indicator plate with or without IPTG. (B) Description of plasmid constructs that were used to express the full-length nontagged BepA (M1-S544) with or without Gαs in E. coli AB472(λDE3)ΔcyaΔcpdA strain. (C) Anti-BepA Western analysis of BepA expression in E. coli AB472(λDE3)ΔcyaΔcpdA strain to illustrate the extensive instability of the full-length and nontagged BepA. This instability was the prime motivation to N-terminally tag subfragments of Beps with MBP. (D) Dots of λDE3-lysogenic E. coli AB472(λDE3)ΔcyaΔcpdA grown on a MacConkey maltose indicator plate with or without IPTG. This experiment illustrates that the N-terminally HIS-tagged form of Gαs (used in Fig. 3 in vitro experiments) acts in a similar fashion to nontagged form of Gαs in the process of BepA-mediated activation of host cell AC.
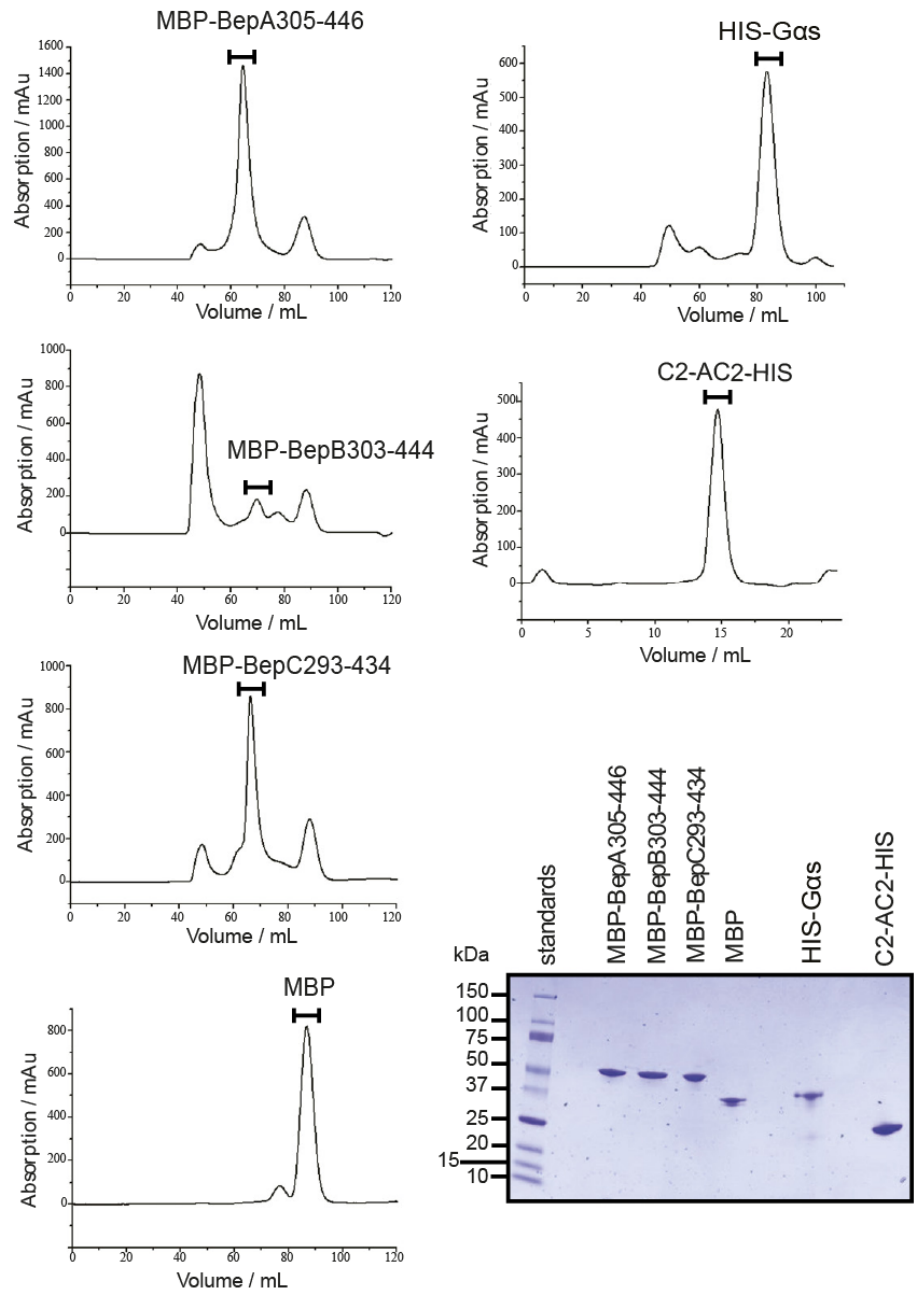
Fig. S4. Purification of the recombinant proteins used in the in vitro AC assays and surface plasmon resonance (SPR) analyses. Gel- filtration chromatography after primary puri fication of the HIS-tagged C2 and HIS-tagged G αs with Ni-NTA resin and MBP-tagged Beps with amylose-resin. Peak fractions as indicated by black bars were pooled to obtain the highly pure preparations. Coomassie-stained SDS/PAGE gel of the gel filtration peak fractions.

Page | 60

Fig. S5.   Protein –protein interaction analysis in living HEK293T cells by bimolecular   fluorescence complementation (BiFC)-FACS. Representative FACS pro   files [FCS/FL-1(YFP)] of single samples of the BiFC-FACS analysis, which is quanti   fied with triplicate samples in Fig. 4   B.

Table S1.   Quantitation of the amount of dead cells in the BiFC-FACS analysis

	pcDNA3.1-Hygro(-)	Gαs-YFP1
pcDNA3.1-Hygro(-)	1.68 ± 0.4	3.79 ± 2.03
HA-YFP2-BepA	2.95 ± 0.86	5.30 ± 1.57
HA-YFP2-BepB	2.18 ± 0.52	4.79 ± 2.50
HA-YFP2-BepC	2.26 ± 1.01	5.01 ± 2.90
HA-YFP2	3.30 ± 0.99	4.98 ± 3.49
HA-YFP2-CAAX	3.53 ± 1.46	5.20 ± 3.93

The dead cells (Annexin V $^+$, PI$^+$) were gated out from the analysis for the YFP signal that is presented in Fig. 4   C and Fig. S4. Numbers mean the percent (%) ± SD of dead cells in three independent experiments.

Table S2.   Bacterial strains used in this study

Strain	Designation	Relevant characteristics	Reference or source
B. henselae	RSE247	Spontaneous streptomycin resistant strain of ATCC 49882^T	(1)
	MSE150	ΔbepA-G mutant of RSE247	(2)
	MSE218	MSE150 containing pMS100-A that encodes for FLAG:: Bh BepA (E305-S544)	(3)
	MSE226	MSE150 containing pMS100-B that encodes for FLAG:: Bh BepB (E303-S542)	(3)
	MSE228	MSE150 containing pMS100-C that encodes for FLAG:: Bh BepC (D292-N532)	(3)
	MSE269	MSE150 containing pMS106 that encodes for FLAG:: Bq BepA2	(3)
E. coli	DH5α		Laboratory stock (C.D.)
	BL21(λDE3)	λDE3 (T7pol $^+$)	Novagen
	K-12 MG1655		(4)
	AB472(λDE3)	Derivative of K-12 MG1655 with λDE3 (T7pol $^+$) P1-transduced from BL21(λDE3). ΔgalMKTE	Present study
	JW3778	ΔcyaA ::kan	(5)
	APE216	Derivative of AB472(λDE3) with ΔcyaA P1-transduced from JW3778.	Present study
	JW3000	ΔcpdA ::kan	(5)
	APE304	Derivative of APE216 with ΔcpdA P1-transduced from JW3000.	Present study

1. Schmid MC, et al. (2004) The VirB type IV secretion system of   Bartonella henselae   mediates invasion, proin flammatory activation and antiapoptotic protection of endothelial cells.   Mol Microbiol 52:81 –92.
2. Schulein R, et al. (2005) A bipartite signal mediates the transfer of type IV secretion substrates of   Bartonella henselae   into human cells. Proc Natl Acad Sci USA   102:856 –861.
3. Schmid MC, et al. (2006) A translocated bacterial protein protects vascular endothelial cells from apoptosis.   PLoS Pathog 2:e115.
4. Blattner FR, et al. (1997) The complete genome sequence of   Escherichia coli K-12. Science 277:1453 –1462.
5. Baba T, et al. (2006) Construction of   Escherichia coli K-12 in-frame, single-gene knockout mutants: The Keio collection.   Mol Syst Biol 2:2006.0008.

Table S3. Oligonucleotide primers used in this study

Primer	Sequence (5′ → 3′) with restriction sites underlined (restriction enzyme)
pBH001f	ATAAGAAT GCGGCCGCGCTCGATCTGAAAGAAATAT (NotI)
pBH002r	CGCGGATCCTTAGTTGGTAAGAGCCCTTGC (BamHI)
prAP015	GATGTTCCAGATTACGCGGCCGCGGAATTAAAAAAAACACTCATCCCA (none)
prAP016	TTTTTT GGATCCTTAGCTAGCCATGGCAAGCGTTTTTGA (BamHI)
prAP014	TTTTTT CTCGAGACCATGGCCTACCCATACGATGTTCCAGATTACGCGGCCGCG (XhoI)
prAP022	TTTTTT GCGGCCGCGATGGTGAGCAAGGGCGAG (NotI)
prAP023	TTTTTT GCGGCCGCCCCGGGCCCGCCACCCTT (NotI)
prAP025	TTTTTT GGATCCTTACCCGGGCCCGCCACCCTT (BamHI)
prAP017	GATGTTCCAGATTACGCGGCCGCGGAGCTTGAAAACACGCTCATTCCA (none)
prAP018	TTTTTT GGATCCTTAGCTGGCAATAGCAAGCGTATTTGA (BamHI)
prAP004	TTTTTT GAATTCCTGGTTCCGCGTGGATCCGAATTAAAAAAAAACACTCATCCCAAAAG (EcoRI)
prAP006	TTTTTT CTGCAGTTAACTTGGCATAGGGACCTCTTGTCT (PstI)
prAP034	TTTTTT GAATTCCTGGTTCCGCGTGGATCCGAGCTTGAAAACACGCTCATTCCA (EcoRI)
prAP036	TTTTTT CTGCAGTTAACTGGGCTTTTCTACTGTTTTACC (PstI)
prAP113	TTTTTT GAATTCCTGGTTCCGCGTGGATCCGATCTGAAAGAAATATTGATTCCAAAAGAG (EcoRI)
prAP114	TTTTTT CTGCAGTTATCCTGGTTTTTCCACAGAGTGTGC (PstI)
prAP058	TTTTTT GCGGCCGCGATGCCAGCCAAGGGGCGCTACTTC (NotI)
prAP053	TTTTTT GGATCCTCAGTTCAGCCCCAGCCCCTGAAACTTGGC (BamHI)
prAP064	TTTTTT GGATCCGCCTGACAACAACTTCCACAGC (BamHI)
prAP065	TTTTTT AAGCTTTCACAGGGCCGCGTCCCCCTTGGG (HindIII)
prAP070	TTTTTT CATATGCCTGACAACAACTTCCACAGC (NdeI)
prAP071	TTTTTT CTCGAGCAGGGCCGCGTCCCCCTTGGG (XhoI)
prAP068	TTTTTT GGATCCGGACAAGTTAAACGAGGACTGG (BamHI)
prAP069	TTTTTT AAGCTTTCAGTTCAGCCCCAGCCCCTG (HindIII)
prAP066	TTTTTT CATATGGACAAGTTAAACGAGGACTGG (NdeI)
prAP067	TTTTTT CTCGAGGTTCAGCCCCAGCCCCTG (XhoI)
prAP055	TTTTTT CTCGAGACCATGGGCTGTCTGGGAAACAGC (XhoI)
prAP083	TTTTTT AAGCTTTCAAAGCAGCTCATACTGACGGAG (HindIII)
prAP085	GGCGGCCTGCGCGATGAACGC (none)
prAP086	CACGTCAAACATGTGGAAGTT (none)
prAP063	TTTTTT CCATGGGCTGTCTGGGAAACAGC (NcoI)
prAP060	TTTTTT GAGCTCGATGGGCTGTCTGGGAAACAGC (SacI)
prAP061	TTTTTT CATATGGGCTGTCTGGGAAACAGC (NdeI)
prAP084	TTTTTT CTCGAGAAGCAGCTCATACTGACGGAG (XhoI)
prAP162	TTTTTT GGTACCATGGGCTGTCTGGGAAACAGC (KpnI)
prAP163	TTTTTT ATCGATAAGCAGCTCATACTGACGGAGGTG (ClaI)
prAP157	TTTTTT GCGGCCGCGAAGAACGGCATCAAGGTGAACTTC (NotI)
prAP158	TTTTTT GCGGCCGCAACTCGAGCGGACCCACCACCTCC (NotI)
prAP159	TTTTTT GGATCCTTAAACTCGAGCGGACCCACCACCTCC (BamHI)
prAP167	TTTTTT CCATGGCCTACCCATACGATGTTCCAG (NcoI)
prAP186	TTTTTT GGATCCAACTCGAGCGGACCCACCACCTCC (BamHI)
prKP012	GAAAA CATATGAAAATCGAAGAAGGTAAACTGGTAATC (NdeI)
prKP013	GAAAAGGATCCGAATTCTGAAATCCTTCACTCGATCCCGA (BamHI)

Table S4.   Plasmids used in this study

Plasmid	Relevant characteristics	Reference or source
pcDNA3.1-Hygro(-)	Mammalian expression vector (CMV-promoter).	Invitrogen
pAP001	Derivative of pcDNA3.1-Hygro(-) encoding N-terminally HA-tagged BepA (E305-S544).	Present work
pAP002	Derivative of pcDNA3.1-Hygro(-) encoding N-terminally HA-tagged BepB (E303-S542).	Present work
pBH002	Derivative of pAP001 encoding N-terminally HA-tagged BepC (D292-N532).	Present work
pAP013	Derivative of pAP001 encoding N-terminally HA-EGFP-tagged BepA (E305-S544).	Present work
pAP014	Derivative of pAP002 encoding N-terminally HA-EGFP-tagged BepB (E303-S542).	Present work
pBH004	Derivative of pBH002 encoding N-terminally HA-EGFP-tagged BepC (D292-N532).	Present work
pAP015	Derivative of pAP001 encoding HA-EGFP.	Present work
pWay21	Mammalian expression vector (CMV-promoter) for C-terminal EGFP-fusions.	Molecular Motion Laboratory*
pMal-c2X	E. coli expression plasmid for N-terminal MBP-fusions or MBP-EXT in its empty form.	New England BioLabs
pAP004	Derivative of pMal-c2X encoding N-terminally MBP-tagged BepA (E305-S446).	Present work
pAP067	Derivative of pMal-c2X encoding N-terminally MBP-tagged BepB (E303-S444).	Present work
pAP052	Derivative of pMal-c2X encoding N-terminally MBP-tagged BepC (L293-G434).	Present work
pCMV-ACVII	Derivative of pCMV-SK encoding full length nontagged human AC7.	(1)
pAP023	Derivative of pAP001 encoding N-terminally HA-tagged full length human AC7.	Present work
pWay19	Mammalian expression vector encoding EGFP.	Molecular Motion Laboratory*
pACYCDuet-1	E. coli expression vector.	Novagen
pAP033	Derivative of pACYCDuet-1 encoding N-terminally HIS-tagged C1a (P263-L476) of AC7.	Present work
pAP034	Derivative of pACYCDuet-1 encoding C-terminally S-tagged C1a (P263-L476) of AC7.	Present work
pAP035	Derivative of pACYCDuet-1 encoding N-terminally HIS-tagged C2 (D864-N1080) of AC7.	Present work
pAP036	Derivative of pACYCDuet-1 encoding C-terminally S-tagged C2 (D864-N1080) of AC7.	Present work
pAP037	Derivative of pAP033 and pAP036 encoding N-terminally HIS-tagged C1a (P263-L476) and C-terminally S-tagged C2 (D864-N1080) of AC7.	Present work
pAP038	Derivative of pAP034 and pAP035 encoding C-terminally S-tagged C1a (P263-L476) and N-terminally HIS-tagged C2 (D864-N1080) of AC7.	Present work
pQE60-Gs	Derivative of pQE60 encoding the short splice form of bovine G αs with C-terminal HIS-tag.	Stephen Sprang**
IIC2H6-pQE60	Derivative of pQE60 encoding C2 of AC2 with C-terminal HIS-tag.	C.W.D.
pAP024	Derivative of pcDNA3.1-Hygro(-) encoding the short splice form of bovine G αs.	Present work
pAP039	Derivative of pAP024 encoding GTP-locked and constitutively active form of the short splice form of bovine G αs (Gln213 ⬚ Leu).	Present work
pRSFDuet-1	E. coli over-expression vector.	Novagen
pAP025	Derivative of pRSFDuet-1 encoding the short splice form of bovine G αs.	Present work
pAP027	Derivative of pRSFDuet-1 encoding N-terminally HIS-tagged short splice form of bovine G αs.	Present work
pAP026	Derivative of pRSFDuet-1 encoding C-terminally S-tagged short splice form of bovine G αs.	Present work
pAP030	Derivative of pRSFDuet-1 encoding GTP-locked and constitutively active form of the short splice form of bovine G αs (Gln213 ⬚ Leu).	Present work
pAP031	Derivative of pRSFDuet-1 encoding N-terminally HIS-tagged GTP-locked and constitutively active form of the short splice form of bovine G αs (Gln213 ⬚ Leu).	Present work
pAP032	Derivative of pRSFDuet-1 encoding C-terminally S-tagged GTP-locked and constitutively active form of the short splice form of bovine G αs (Gln213 ⬚ Leu).	Present work
MCFD2-cYFP1	For expression of C-terminally YFP1(V2-Q158)-tagged MCFD2 (multiple coagulation factor de ficiency 2).	Hans-Peter Hauri***
pAP078	Derivative of MCFD2-cYFP1 encoding for C-terminally YFP1(V2-Q158)-tagged short splice form of bovine G αs.	Present work
ssYFP2-ERGIC53	For expression of N-terminally YFP2 (K159-Y238)-tagged endoplasmic reticulum-Golgi intermediate compartment (ERGIC) protein ERGIC53.	Hans-Peter Hauri***
pAP082	Derivative of pAP013 encoding N-terminally HA-YFP2-tagged BepA (E305-S544).	Present work
pAP076	Derivative of pAP014 encoding N-terminally HA-YFP2-tagged BepB (E303-S542).	Present work
pAP075	Derivative of pBH004 encoding N-terminally HA-YFP2-tagged BepC (D292-N532).	Present work
pAP074	Derivative of pAP015 encoding HA-YFP2.	Present work
pTrieX-GFP-CAAX	Dual mammalian and E. coli expression vector encoding His-Myc-EGFP with C-terminal CAAX-domain of K-Ras.	Olivier Pertz****
pAP085	Derivative of pTriex-GFP-CAAX having EGFP replaced with HA-YFP2.	This work
pPG101	E. coli-Bartonella shuttle plasmid encoding N-terminally FLAG-tagged BepA of B. henselae.	(2)
pAP055	Derivative of pAP025 encoding nontagged BepA of B. henselae from pPG101.	Present work
pAP061	Derivative of pRSFDuet-1 encoding nontagged BepA of B. henselae from pPG101.	Present work
pKP03	Derivative of pMal-c2x encoding maltose binding protein (MBP).	Present work

*Molecular Motion Laboratory (http://momotion.cns.montana.edu).
**Center for Biomolecular Structure and Dynamics, University of Montana, Missoula, MT.
***Biozentrum, University of Basel, Basel, Switzerland.
****Department of Biomedicine, University Hospital Basel, Basel, Switzerland.

1. Hellevuo K, et al. (1995) The characterization of a novel human adenylyl cyclase which is present in brain and other tissues. J Biol Chem 270:11581 –11589.
2. Schmid MC, et al. (2006) A translocated bacterial protein protects vascular endothelial cells from apoptosis. PLoS Pathog 2:e115.

3.2 Research Article II (*submitted*)

An experimental strategy for the identification of AMPylation targets from complex protein samples

Kathrin Pieles*, Timo Glatter*, Alexander Schmidt, Christoph Dehio

* These authors contributed equally to this work

Statement of my own contribution

I contributed to this publication by expressing and purifying of Bep2 and $Bep2_{1-360}$ in complex with BiaAE61G. I also performed the presented *in vitro* AMPylation assays and in-gel digestions of the analyzed samples.

The manuscript was written by me, T. Glatter A. Schmidt and C. Dehio.

3.2.1 Summary

AMPylation is a posttranslational modification (PTM) that has recently caught much attention in the context of bacterial infections as pathogens were shown to secrete Fic proteins that AMPylate Rho GTPases and thus interfere with host cell signaling processes. Although Fic proteins are widespread and found in all kingdoms of life, only a small number of AMPylation targets is known to date. A major obstacle to target identification is the limited availability of generic strategies allowing sensitive and robust identification of AMPylation events. Here, we present an unbiased mass spectrometry (MS) based approach utilizing stable isotope-labeled ATP. The ATP isotopes are transferred onto target proteins in crude cell lysates by *in vitro* AMPylation introducing specific reporter ion clusters that allow detection of AMPylated peptides in complex biological samples by MS-analysis. Applying this strategy on the secreted Fic protein Bep2 of *Bartonella rochalimae*, we identified the filamenting protein vimentin as an AMPylation target which was confirmed by independent assays. Vimentin represents a new class of target proteins and its identification emphasizes our method as a valuable tool to systematically uncover AMPylation targets. Furthermore, the approach can be generically adapted to study targets of other PTMs that allow incorporation of isotopically labeled substrates.

3.2.2 MAIN TEXT

Protein AMPylation (also known as adenylylation) is a post-translational modification (PTM) in which an AMP moiety is transferred onto threonine or tyrosine residue of a target protein. AMPylation was discovered in the 1960s in the context of regulation of glutamine synthetase activity in *E. coli* (1). Recently, proteins belonging to the Fic family (Filamentation induced by cAMP) were also shown to catalyze protein AMPylation. Fic proteins are found in all kingdoms of life and are conserved from bacteria to human (2-4). Although this protein family comprises thousands of proteins, for only two Fic proteins physiological roles have emerged. Yarbrough and co-workers were first to demonstrate that a translocated bacterial Fic protein subverts host cell defense mechanisms within bacterial infection processes (5). In particular, a type III secretion system (T3SS) effector from *Vibrio parahemolyticus*, VopS, is secreted into the host cell where it AMPylates a conserved threonine (T35) of Rho family GTPases. AMPylation impairs binding of GTPase interaction partners and thereby interferes with the host cell signaling machinery leading to cytoskeleton collapse and cell death (6). Similarly, the surface antigen IbpA of *Histophilus somni* was shown by Worby and co-workers to target Rho GTPases. Though IbpA does not modify T35 but the neighboring tyrosine (Y32), it also impairs GTPase signaling leading to cytoskeleton collapse (7, 8). Moreover, the human Fic protein HYPE was identified to target Rho GTPases *in vitro*, yet, its physiological role and potential *in vivo* targets remain elusive (7).

Despite this recent progress, comprehensive functional details into Fic protein-mediated AMPylation and its impact on cellular signaling events are still in its infancy. This is underlined by the fact that among the large number of existing Fic proteins only a handful are characterized as AMPylators (4) with small GTPases representing the only identified target class. The main reason for the limited insights into the biological role of Fic proteins and Fic-mediated target AMPylation is the limited availability of selective enrichment strategies specifically targeting the AMPylated moiety. This hampers the systematic analysis of AMPylation events and renders target identification a challenging task. Though target enrichment advanced with the introduction of an antibody raised against AMPylated threonine (9), tyrosine modified peptides and proteins would escape purification. Another promising step forward was recently presented by a strategy utilizing a functionalized ATP analogue which can be trapped by an azide alkyne cycloaddition

(also known as CLICK chemistry approach) to enrich for modified proteins (10, 11). Yet, the modification of ATP goes along with changes in size and electron density of the substrate, which might impair binding to the substrate binding site of Fic proteins (10). Therefore, experimental strategies enabling unbiased and specific identification of AMPylated proteins are required to further elucidate the biological mechanism underlying protein AMPylation and its effect on cellular signaling. Here, we present an unbiased method to identify AMPylated targets from cell lysates building on *in vitro* activity assays using stable isotope-labeled ATP substrates. The *in vitro* reaction generates AMPylated peptide isotopes that can be detected as reporter ion clusters with defined mass shifts in mass spectrometry (MS) analysis.

In the first step, an *in vitro* reaction of lysates of *E. coli* expressing an AMPylator and a eukaryotic cell extract is performed in the presence of α^{32}P-ATP to screen for possible AMPylation events (Figure 1A). As AMPylation includes the transfer of the radioactive α-phosphate of the ATP, potential AMPylation targets and their apparent molecular weight can be visualized by autoradiography. Once an AMPylation event is detected, an *in vitro* reaction is performed in which a 3-plexed labeled ATP mix is used as a substrate. The substrate mix contains unlabeled ATP ($^{15}N_0{}^{13}C_0$-ATP), medium-labeled ATP ($^{15}N_5{}^{13}C_0$-ATP) and heavy-labeled ATP ($^{15}N_5{}^{13}C_{10}$-ATP), which after AMP transfer will result in predictable mass shifts of the AMPylated peptides that are detectable by MS-analysis and serve as a reporter cluster specific for an AMPylation event. The AMPylated targets and modified residues are identified after an in-gel digest performed on excised gel bands corresponding to the known molecular weight of the target proteins by LC-MS analysis (Figure 1A). Building on recently introduced experimental strategies that used a mix of isotope-labeled crosslinker in post lysis reactions to ultimately increase specificity in crosslinked peptide identification (12, 13), we used a mixture of unlabeled and stable isotope-labeled forms of ATP to increase the specificity and reliability in detecting an AMPylation event on target proteins. In our strategy, next to the MS-based sequencing information, the AMP-peptide isotopes are used as a reporter cluster displaying an additional level of information for AMPylation detection. Thus, the detection of these isotopic peptide ion triplets of AMP-peptides may also serve as an indication of an AMPylation if MS-sequencing identification scores are close to or below a given significance threshold. This improves target detectability and reliability even for low abundant target proteins. Subsequently, the fragment spectra of these triplets can be subjected to manual interpretation or the sample can

be re-analyzed using optimized MS-parameters or different fragmentation techniques in combination with directed LC-MS analysis to increase the number of unambiguous identifications (14).

In order to evaluate our experimental strategy, we recapitulated the experiments done by Yarbrough *et al.* and incubated VopS with the purified small GTPase RhoA in the presence of 3-plexed ATP. Following protein digestion by AspN and MS analysis, we identified the peptide DQFPVYVPTVFENYVA with increment masses matching to the three incorporated isotopically labeled substrates (+329, +334, +344) indicating an AMPylation event (Supporting Information Figure 1). Closer inspection of the fragment spectra then indicated an AMPylation of RhoA on T35 by VopS as previously described by Yarbrough *et al.* (5). This finding emphasizes the applicability of our experimental workflow in detecting AMPylation events.

In contrast to pathogens like *V. parahaemolyticus* that secrete only one Fic protein, pathogens belonging to the genus <u>B</u>artonella translocate a variety of FIC-domain containing <u>e</u>ffector <u>p</u>roteins (Beps) into the host cell (15). Yet, *Bartonella* infections are typically benign despite high pathogen load both on the cellular and organismic level (16). This implies that *Bartonella* effectors likely target a variety of different host proteins for subtle alterations of host cell functioning. In order to gain first insights into the target specificity of Beps, we applied our strategy on the effector Bep2 of *Bartonella rochalimae*.

To screen for a possible AMPylation activity of Bep2 we performed *in vitro* AMPylation assays with *E. coli* cells expressing Bep2 and crude cell lysates derived from J774 mouse macrophages in the presence of α^{32}P-ATP. Following SDS-PAGE a protein band with an apparent molecular weight of 50 kDa was detected on the autoradiogram indicating that Bep2 indeed AMPylates a target protein in J774 mouse macrophages (Figure 1B). The molecular size estimation already indicates that the potential target is unlikely to fall in the class of small GTPases, which is the only known class of AMPylation targets and are represented by lower molecular weight (4).

In order to identify this protein we performed in-gel digestion and LC-MS analysis of a parallel processed sample that underwent *in-vitro* AMPylation reaction using the 3-plexed ATP mix. Upon LC-MS analysis and database search including the phospho-adenosine modification in all isotopic versions as a variable modification, we obtained a positive hit identifying a potential AMPylation on the peptide SLYSSSPGGAYVTR matching to the intermediate filament protein vimentin (Supporting Information Figure 2). We found further evidence confirming the

AMPylation event on this peptide when examining its isotopic distribution. As three isotopically labeled ATPs (unlabeled ATP, $^{15}N_5$-ATP, $^{15}N_5^{13}C_{10}$-ATP) were used for AMP transfer reaction we observed an peptide ion reporter cluster with three distinct peaks matching the expected mass shifts introduced by the different labels (Figure 1C). Closer examination of the three AMP-peptide peaks showed that equal amounts of modified peptides were generated in the *in vitro* reaction emphasizing that no detectable background AMPylation by potential endogenous AMPylating proteins occurred.

In order to show that the observed AMPylation event is based on the activity of the FIC-domain, we generated a catalytically inactive Bep2 mutant (Bep2°) by replacing the histidine within the conserved Fic motif with an alanine (H161A). As the histidine is considered to act as general base to increase nucleophilicity of the AMPylation acceptor amino acid of the target, the replacement with alanine inhibits AMPylation as previously demonstrated for VopS and IbpA (5, 7). Then wild-type and mutant Bep2 were separately incubated with J774 mouse macrophage lysates to perform *in vitro* AMPylation reaction using $^{15}N_5^{13}C_0$-ATP for wild-type and $^{15}N_5^{13}C_{10}$-ATP for mutant Bep2. Samples were pooled and proteins were separated by SDS-gelelectrophoresis. Upon in-gel digestion and LC-MS analysis, we obtained SLYSSSPGGAYVTR to be AMPylated only with $^{15}N_5$-ATP but not with $^{15}N_5^{13}C_{10}$-ATP. This indicates that *in vitro* reaction with wild-type Bep2, but not with the catalytically inactive Bep2-mutant protein, leads to AMPylation of SLYSSSPGGAYVTR, confirming that the reaction is specifically catalyzed by the active FIC-domain of Bep2 (Figure 2 A and B).

In order to confirm vimentin as a target protein of Bep2, we performed *in vitro* AMPylation assays with $\alpha^{32}P$-ATP and purified proteins. To increase Bep2 solubility, we deleted the C-terminal BID domain of Bep2 that serves as a signal for translocation into the host cell via a type IV secretion system but apparently does not contribute to the AMPylation activity (17). Solubility was further increased by co-expression of BiaA(E34G), a mutant of the Bep2-interacting antitoxin BiaA of *B. rochalimae* that binds Bep2 without impairing AMPylation activity (Figure 2C). Following purification by metal affinity and size exclusion chromatography, purified Bep2$_{1-360}$ complexed with BiaA(E34G) was used in AMPylation assays with $\alpha^{32}P$-ATP and purified vimentin or BSA that was used as negative control. While there was no apparent AMPylation band in addition to the auto-AMPylation of Bep2 in the negative control, a clear AMPylation signal at the size of 50 kDa was detected in samples containing the Bep2-construct and vimentin

confirming that vimentin is indeed a target protein of Bep2-mediated AMPylation (Figure 2C). Furthermore, as vimentin is a component of the cytoskeleton and shows no homology to small GTPases, it represents a new class of target proteins of Fic protein-mediated AMPylation.

In our study, we presented an experimental strategy for the identification of protein AMPylation events in complex biological samples. We use stable isotope-labeled ATP in activity-based assays to introduce an AMP-reporter cluster to increase specificity of AMPylation target detection by mass spectrometry. The relative intensity of peptide isotopes additionally allows us to distinguish between background signal of intrinsic AMPylation and specific target AMPylation of the introduced Fic protein. Certainly, peptides generated from proteolytic digests have to be within MS compatible size range. Therefore it may be important to incorporate alternative digestion schemes in case *in vitro* AMPylation assays indicate a protein modification, but MS results did not reveal any significant hits. In addition we anticipate that our strategy will improve the detection of AMPylation events on low abundant proteins as the use of reporter clusters is largely independent of the known under-sampling effect in MS/MS based identification (18). Although we established the procedure to specifically identify AMPylation targets, it is generally applicable to any protein modification for which isotope-labeled analogs are available and the modified peptides result in MS detectable reporter ion clusters.

References

1.   Brown MS, Segal A, & Stadtman ER (1971) Modulation of Glutamine Synthetase Adenylylation and Deadenylylation Is Mediated by Metabolic Transformation of Pii-Regulatory Protein. *Proc Natl Acad Sci U S A* 68(12):2949-&.
2.   Kinch LN, Yarbrough ML, Orth K, & Grishin NV (2009) Fido, a novel AMPylation domain common to fic, doc, and AvrB. *PLoS One* 4(6):e5818.
3.   Engel P*, et al.* (2012) Adenylylation control by intra- or intermolecular active-site obstruction in Fic proteins. *Nature* 482(7383):107-110.
4.   Roy CR & Mukherjee S (2009) Bacterial FIC Proteins AMP Up Infection. *Sci Signal* 2(62):pe14.
5.   Yarbrough ML*, et al.* (2009) AMPylation of Rho GTPases by Vibrio VopS disrupts effector binding and downstream signaling. *Science* 323(5911):269-272.
6.   Higa N*, et al.* (2013) Vibrio parahaemolyticus effector proteins suppress inflammasome activation by interfering with host autophagy signaling. *PLoS Pathog* 9(1):e1003142.
7.   Worby CA*, et al.* (2009) The fic domain: regulation of cell signaling by adenylylation. *Mol Cell* 34(1):93-103.
8.   Mattoo S*, et al.* (2011) Comparative analysis of Histophilus somni immunoglobulin-binding protein A (IbpA) with other fic domain-containing enzymes reveals differences in substrate and nucleotide specificities. *J Biol Chem* 286(37):32834-32842.
9.   Hao YH*, et al.* (2011) Characterization of a rabbit polyclonal antibody against threonine-AMPylation. *J Biotechnol* 151(3):251-254.
10.   Grammel M, Luong P, Orth K, & Hang HC (2011) A chemical reporter for protein AMPylation. *J Am Chem Soc* 133(43):17103-17105.
11.   Broncel M, Serwa RA, & Tate EW (2012) A New Chemical Handle for Protein AMPylation at the Host-Pathogen Interface. *Chembiochem* 13(2):183-185.
12.   Pimenova T*, et al.* (2008) Epitope mapping on bovine prion protein using chemical cross-linking and mass spectrometry. *J Mass Spectrom* 43(2):185-195.
13.   Rinner O*, et al.* (2008) Identification of cross-linked peptides from large sequence databases (vol 5, pg 315, 2008). *Nat Methods* 5(8):748-748.
14.   Frese CK*, et al.* (2011) Improved peptide identification by targeted fragmentation using CID, HCD and ETD on an LTQ-Orbitrap Velos. *J Proteome Res* 10(5):2377-2388.
15.   Engel P*, et al.* (2011) Parallel evolution of a type IV secretion system in radiating lineages of the host-restricted bacterial pathogen Bartonella. *PLoS Genet* 7(2):e1001296.
16.   Harms A & Dehio C (2012) Intruders below the radar: molecular pathogenesis of Bartonella spp. *Clin Microbiol Rev* 25(1):42-78.
17.   Schulein R*, et al.* (2005) A bipartite signal mediates the transfer of type IV secretion substrates of Bartonella henselae into human cells. *Proc Natl Acad Sci U S A* 102(3):856-861.
18.   Nilsson T*, et al.* (2010) Mass spectrometry in high-throughput proteomics: ready for the big time. *Nat Methods* 7(9):681-685.
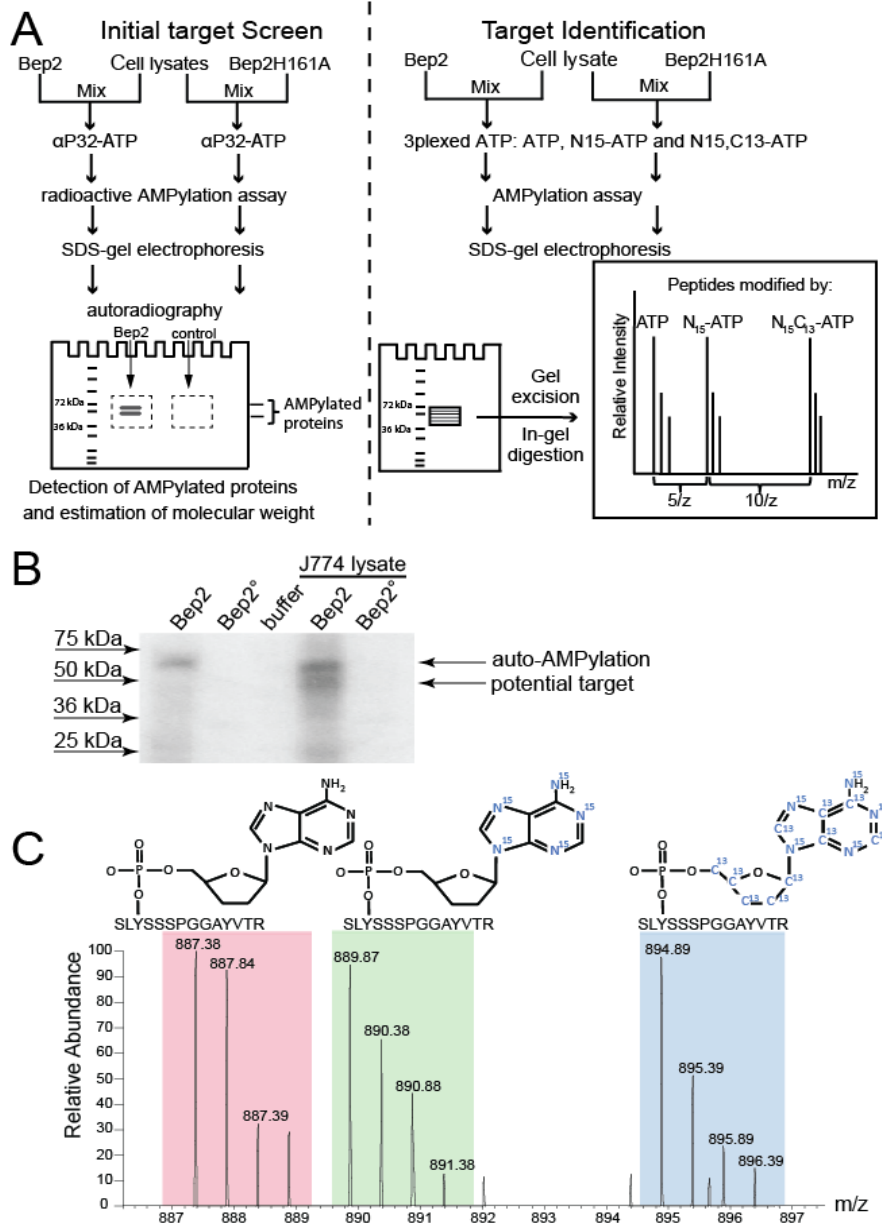
Figure 1: Workflow overview and target identification of *Bartonella rochalimae* effector protein Bep2. A) Overview on the experimental workflow. Depicted is the workflow for identification of potential AMPylation targets on the example of Bep2. AMPylation assays are performed with radioactively labeled α^{32}P-ATP to estimate size of potential targets (left). In parallel, assays are performed with 3-plexed ATP ($^{15}N_0$ $^{13}C_0$-ATP, $^{15}N_5$-ATP and $^{15}N_5$ $^{13}C_{10}$-ATP), and the gel area at the running height of expected targets is excised and used for in-gel digestion and mass spectrometry analysis (right). AMPylated peptides are identified by the AMP-reporter cluster characterized by specific mass shifts between the AMPylated peptide isotopes introduced by the 3-plexed ATP substrate mix. B) Initial target screen by autoradiography. Representative autoradiogram of an *in vitro* AMPylation assay with active and inactive Bep2 is depicted. *In vitro* AMPyation assays were performed on wild-type and the inactive mutant of

Bep2 and mouse macrophage lysates in the presence of α^{32}P-ATP . After SDS-gel electrophoresis, AMPylated proteins were visualized via autoradiography. C) Target identification by AMPylation specific reporter ion clusters. Samples derived from *in vitro* AMPylation assays with Bep2 using 3-plexed ATP were analyzed by in-gel digest and LC-MS/MS. The mass spectrum shows the m/z of the 3-plexed AMPylated peptide SLYSSSPGGAYVTR matching to the protein vimentin. The reporter ion cluster specifically encoding for an AMPylation modification by the characteristic mass shift between peptide isotopes are highlighted by color shading.
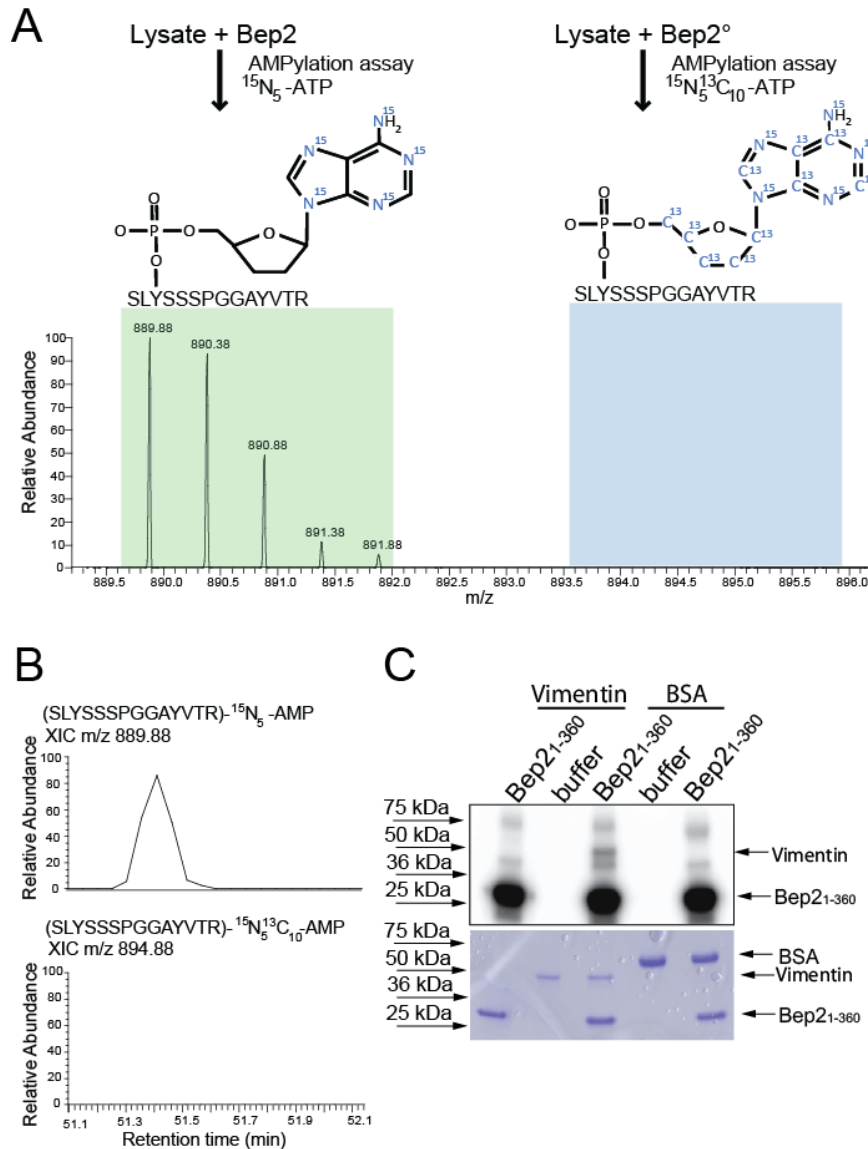
Figure 2: Validation of vimentin as an AMPylation target of Bep2. A) Mass spectrum of AMP-reporter ions in the presence and absence of active Bep2. Samples derived from AMPylation assays with either Bep2 and $^{15}N_5^{13}C_0$-ATP or the inactive mutant of Bep2 (Bep2°) and $^{15}N_5^{13}C_{10}$-ATP were pooled and analyzed by LC-MS/MS. Depicted is a mass spectrum zoomed on the m/z range of the reporter clusters. B) Extracted-ion chromatogram (XIC) of samples derived from *in vitro* AMPylation assays. Assays were performed on wild type Bep2 incubated with $^{15}N_5$-ATP and Bep2° incubated with $^{15}N_5^{13}C_{10}$-ATP. Samples were pooled and analyzed by LC-MS/MS. The XIC of AMPylated SLYSSSPGGAYVTR is shown for $^{15}N_5$-AMP reporter channel for Bep2 (top) and $^{15}N_5^{13}C_{10}$-AMP for Bep2° (bottom). C) Validation experiments on vimentin as an AMPylation target of Bep2. *In vitro* AMPylation assays were performed with purified Bep2$_{1-360}$ in complex with BiaA(E34G) and either buffer, vimentin or BSA in the presence of $\alpha^{32}P$-ATP. AMPylated proteins were visualized by autoradiography (top). The SDS-gel used for autoradiography was then stained with Coomassie to visualize all proteins (bottom).

3.2.3 Supporting Information

Material and Methods

DNA manipulations

E. coli Expression Constructs - Bep2 of *B. rochalimae* was amplified with the primers prAH072 (CCGCTCGAGATGAAGAAAGTGAAATGATGATA) and prAH073 (CCGCTCGA GTTAACAAACCATAGCTGTCGC) from genomic DNA of *B. rochalimae* and cloned via XhoI into pET15b to achieve pAH019. Using primers prAH110 (CAATTATATTGCACCTTTTAGGGAAGGTAATGGACG) and prAH111 (CCTAAAAGGTGCAATATAATTGATAGAGCCAAATATTTTTG) in site-directed mutagenesis (2), pAH051 encoding for the inactive site mutant of Bep2 was achieved. BiaA of *B. rochalimae* that is homologous to VbhA which is a small protein inhibiting the Fic protein VbhT of *B. schoenbuchensis* (3), was amplified using prAG0013 (GCCCATGGTGAAAAAAACAACTGATCATTCTAC) and prAG0014 (GCGGATCCTTA TAGTGTTGCATTGTCCATAAGAG) from genomic DNA of *B. rochalimae* and cloned via NcoI and BamHI restriction into pRSFDUET-1 to achieve pAG0056. The FIC-domain of Bep2 was amplified using prAG029 (GGGAATTCCATATGGATATTAACATC CCTTCTCC) and prAG035 (CGACCTCGAGTTAGTGATGGTGATGGTGATGTTCA CTCAAAGCAGCTAA TTTTTC) and introduced via NdeI and XhoI into pAG0056 to achieve pAG0061. In a next step, *biaA* was then mutated via site directed mutagenesis PCR to abolish its inhibitory activity using prAG047 (GCAATTGGAG GAATCACTCTTCATTCTAAAACG) and prAG048 (GAGTGATTCCTCCAATTG CATGTGTACTAATAG) to achieve pKP090.

RhoA was amplified using prAH179 (GAAACTGGTGATTGTTGGTGATGGAGCCTGTG GAAAGACATGC) and prAH180 (CCACAGGCTCCATCACCAACAATCACCA GTTTCTTCCGGATGGC) from pRK5myc-RhoA (4) and cloned via BamHI and XhoI into pGEX-6p-1 to achieve pAH049.

Constructs for *E. coli* expression of GST-VopS$_{30-387}$ and GST-VopSH348A$_{30-387}$ were a kind gift of K. Orth (1).

Preparation of cell lysates

J774 mouse macrophages were cultured in DMEM supplemented with 10% FCS up to a confluence of 90%. Cells were trypsinized, resuspended extensively in 10mL DMEM supplemented with 10% FCS, pellet at 3000 rpm and resuspended in 400uL Lysis buffer (10mM Tris, pH=8.0, 150mM NaCl, 10mM MgCl2, 5mM βME). Cells were lysed by 3x 10 pulses of sonication and centrifuged for 15min at 4°C and 4500rpm. Supernatants were stored in aliquots at -80°C.

Expression and purification of recombinant proteins

For recombinant expression of Bep2 or its inactive mutant (Bep2°) of *B. rochalimae*, Ca-competent *E. coli* were transformed with pAH019 or pAH051 and cultured at RT in Terrific Broth media containing 200 mg/L Ampicillin. At an OD_{600}=0.5 expression was induced with 100 μM IPTG (Promega). After 18 h, cultures were harvested, aliquoted and stored at -20°C. Frozen bacteria were thawed and lysed in AMPylation buffer (10 mM Tris pH=8.0, 150 mM NaCl, 10 mM $MgCl_2$, 2.5 mM βME) supplemented with 2 mg DNaseI from bovine pancreas (Roche) and Complete EDTA-free Protease Inhibitor Cocktail (Roche) [40 μl/ml of stock solution (1 tablet / 2 ml H_2O]. For AMPylation assays with full lysates, bacteria were lysed with 3x 15pulses of sonication, centrifuged for 5 min at 13000 rpm and supernatents utilized for AMPylation assays.

In order to purify Bep2$_{1-360}$, Ca-competent *E. coli* were transformed with pKP090 and cultured at RT in 6 L Terrific Broth media containing 50 mg/L Kanamycin. At an OD_{600}=0.5, expression was induced with 100 μM IPTG (Promega). After 18 h, cultures were harvested, and stored at -20°C. Frozen pellets of bacteria were thawed and lysed using French Press and cell debris was removed by high speed centrifugation (1 h, 100 g, 4°C). Bep2$_{1-360}$ was purified using metal affinity utilizing Ni-NTA columns and elution with 200 mM imidazole. Peak fractions were pooled and loaded onto a Superdex 200 10/300 column (GE Healthacre) for size exclusion chromatography. 10 μL of the peak fractions were separated via SDS-PAGE using 12% SDS-gel and stained with Coomassie staining solution. Fractions containing Bep2$_{1-360}$ were pooled and the concentration was measured via absorbance at 280 nm with Nanodrop-1000 (Nanodrop Technologies, Wilmington, USA). Protein was stored at 4°C.

For recombinant expression of GST-fusion proteins, Ca-competent *E. coli* were transformed with pVopS or pVopSH348A (1) or pAH049 and cultured at RT in Terrific Broth media containing 200 mg/L Ampicillin. At an OD_{600}=0.5 expression was induced with 50 μM IPTG (Promega). After 8 h, cultures were harvested and stored at -20°C. Frozen bacteria were thawed and lysed in PBS buffer supplemented with 5mM βME, 2 mg DNaseI from bovine pancrease (Roche) and Complete EDTA-free Protease Inhibitor Cocktail (Roche) [40 μl/ml of stock solution (1 tablet / 2 ml H_2O]. For AMPylation assays with full lysates, bacteria were lysed with 3x 15 pulses of sonication, centrifuged for 5 min at 13000 rpm and supernatents were used in AMPylation assays.

In order to purify GST-fusion proteins, cells were lysed using French Press and cell debris was removed by high speed centrifugation (1 h, 100 g, 4°C). GST-VopS, GST-VopSH348A or GST-RhoA were purified using affinity chromatography utilizing GST-Trap columns (GE Healthcare) and elution with 10 mM Glutathion (Sigma) in AMPylation buffer (10 mM Tris pH=8.0, 150 mM NaCl, 10 mM $MgCl_2$, 2.5 mM βME). Peak fractions were pooled and 10μL of the peak fractions were separated via SDS-PAGE using 12% SDS-gel and stained with Coomassie staining solution. The concentration of fractions containing VopS was measured via absorbance at 280 nm with Nanodrop-1000 (Nanodrop Technologies, Wilmington, USA). Protein was stored at 4°C.

AMPylation assays

In order to determine the size of potential target proteins, *in vitro* AMPylation assays with radioactive labeled $α^{32}$P-ATP were performed using full cell lysates as described in previous studies (3). To this end, aliquots of eukaryotic cell lysates were thawed on ice and bacterial lysates were freshly prepared. Then, 25 uL of eukaryotic cell lysates mixed with 1.5 μL of 7.5 mg/mL RNAseI (Roche), 25 μL freshly prepared *E. coli* lysates and 1 μL of $α^{32}$P-ATP (Hartmann Analytics, SRP-207). Alternatively, 250 pmol of purified $Bep2_{1-360}$ were mixed with 1.5 uL of 7.5 mg/mL RNAseI, 1 uL of $α^{32}$P-ATP and either AMPylation buffer, 200 pmol vimentin or 250 pmol of BSA. Samples were then incubated for 1 h at 30°C, reactions were stopped by the addition of 25 uL SDS-loading buffer and incubated for 5 min at 95°C. Samples were loaded onto pre-cast gradient SDS-gels (Bio-Rad). Electrophoresis was performed 150 V for 52 min. Proteins were fixed for 1 h in Fixation buffer (50% water, 40% MeOH, 10% glacial

acid), gels were sealed in plastic bags and exposed on autoradio-screens overnight. Screens were developed using a Typhoon FLA 7000 system (GE Healthcare)

Target identification by mass spectrometry

After target size determination via radioactive AMPylation assays, AMPylation assays were repeated using heavy isotope labeled ATP (3-plexed), gel area from approximately 35 kDa to 70 kDa proteins was excised and divided into 5 pieces. In-gel digestion was adopted from Shevchenko *et al*. (5).

Prior to mass spectrometry analysis the peptides were purified using C18 Microspin columns (Harvard Apparatus) according to the manufactures instruction.

LC-MS/MS analysis was performed on a dual pressure LTQ-Orbitrap mass spectrometer (Thermo Electron), which was connected to an electrospray ion source (Proxeon Biosystems). Peptide separation was carried out using an easy nano-LC systems (Proxeon Biosystems) equipped with an RP-HPLC column packed with C18 resin (Magic C18 AQ 3 μm; Michrom BioResources). A 0.2 μl/min linear gradient from 96% solvent A (0.15% formic acid, 2% acetonitrile) and 4% solvent B (98% acetonitrile, 0.15% formic acid) to 40% solvent B over 60 min was applied. The data acquisition mode was set to obtain one high-resolution MS scan in the FT part of the mass spectrometer at a resolution of 60,000 FWHM followed by MS/MS scans in the linear ion trap of the 20 most intense ions. For peak detection and extraction of peptide intensities Progenesis (Nonlinear Dynamics) was used in default settings.

Peptide identification was carried out using the Mascot and SEQUEST search tool and the mouse swissprot protein database containing forward and reversed-decoy protein sequences and containing target protein sequences. The search criteria were set as follows: full tryptic specificity was required (cleavage after lysine or arginine residues); 2 missed cleavages were allowed; carbamidomethylation (C) was set as fixed modification; oxidation (M) and AMPylation (Phospoadenosine, T, Y) as variable modifications. For AMP-modifications, masses of the $^{15}N_0$ $^{13}C_0$-, $^{15}N_5$- and $^{15}N_5 {}^{13}C_{10}$-AMP labeled moieties were included in the search.

The mass tolerance was set to 10 ppm for precursor ions and 0.6 Da for fragment ions.

References

1.   Yarbrough ML*, et al.* (2009) AMPylation of Rho GTPases by Vibrio VopS disrupts effector binding and downstream signaling. *Science* 323(5911):269-272.
2.   Zheng L, Baumann U, & Reymond JL (2004) An efficient one-step site-directed and site-saturation mutagenesis protocol. *Nucleic Acids Res* 32(14).
3.   Engel P*, et al.* (2012) Adenylylation control by intra- or intermolecular active-site obstruction in Fic proteins. *Nature* 482(7383):107-110.
4.   Besson A, Gurian-West M, Schmidt A, Hall A, & Roberts JM (2004) p27(Kip1) modulates cell migration through the regulation of RhoA activation. *Gene Dev* 18(8):862-876.
5.   Shevchenko A, Tomas H, Havlis J, Olsen JV, & Mann M (2006) In-gel digestion for mass spectrometric characterization of proteins and proteomes. *Nat Protoc* 1(6):2856-2860.
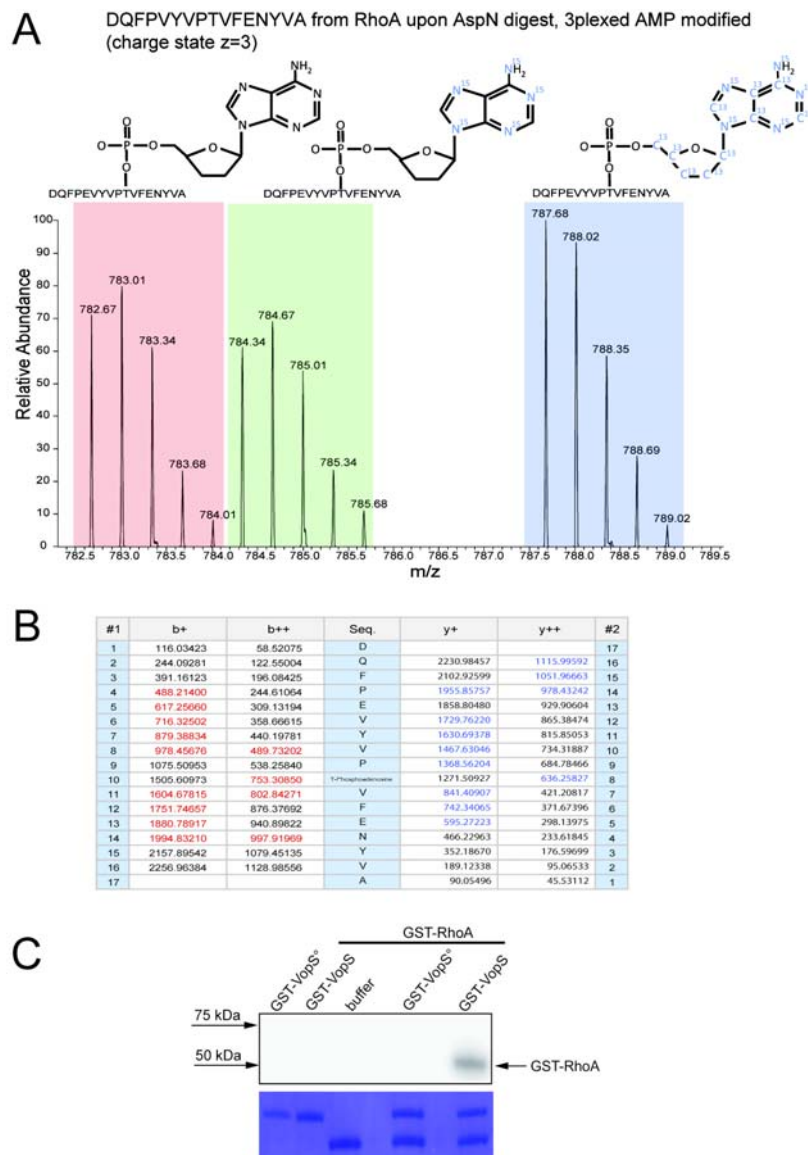
Figure S1: Workflow validation by confirming RhoA as AMPylation target of VopS. A) Target identification by AMPylation specific reporter ion clusters. *In vitro* AMPylation assay was performed on purified RhoA and VopS in the presence of 3plexed ATP. The sample was then analyzed by in-gel digest and LC-MS/MS. The mass spectrum shows the m/z of the 3plexed AMPylated peptide DQFPVYVPTVFENYVA confirming RhoA as an AMPylation target of VopS as reported previously (1). More details are shown in the Material and Method section provided as Supporting Information. B) Ion series of the AMPylated peptide of RhoA. The ion series are shown and b/y-ions covering the AMPylated residue are indicated. C) VopS-mediated AMPylation of RhoA. *In vitro* AMPylation assays were performed with purified GST-VopS or the inactive mutant GST-VopS° and purified GST-RhoA in the presence of α[32]P-ATP. AMPylated proteins were visualized by autoradiography (top). The SDS-gel used for autoradiography was then stained with Coomassie to visualize all proteins (bottom).

A

#1	b+	b++	Seq.	y+	y++	#2
1	88.03931	44.52329	S			14
2	201.12338	101.06533	L	1686.72721	843.86724	13
3	693.23922	347.12325	Y-Phosphoadenosine	1573.64314	787.32521	12
4	780.27125	390.63926	S	1081.52730	541.26729	11
5	867.30328	434.15528	S	994.49527	497.75127	10
6	954.33531	477.67129	S	907.46324	454.23526	9
7	1051.38808	526.19768	P	820.43121	410.71924	8
8	1108.40955	554.70841	G	723.37844	362.19286	7
9	1165.43102	583.21915	G	666.35697	333.68212	6
10	1236.46814	618.73771	A	609.33550	305.17139	5
11	1399.53146	700.26937	Y	538.29838	269.65283	4
12	1498.59988	749.80358	V	375.23506	188.12117	3
13	1599.64756	800.32742	T	276.16664	138.58696	2
14			R	175.11896	88.06312	1

B
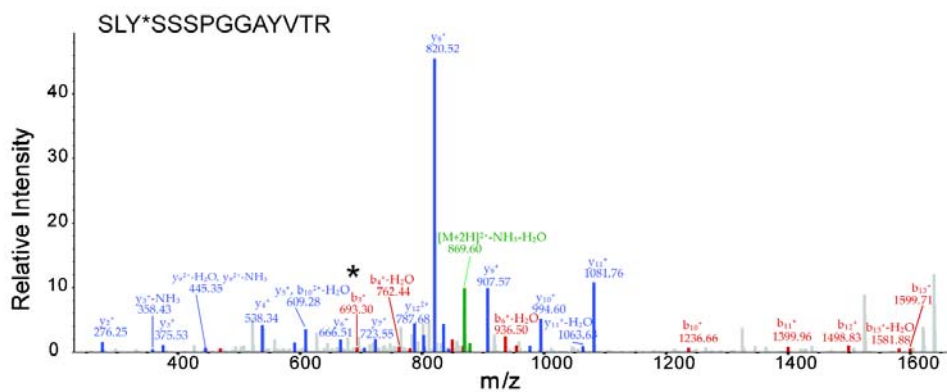
Figure S2: Ion series and MS/MS spectrum of AMPylated vimentin peptide SLYSSSPGGGAYVTR. A) Ion series of detected fragment ions derived from SLY(AMP)SSSPGGGAYVTR. Samples derived from *in vitro* AMPylation assays with Bep2 using 3plexed ATP were analyzed after in-gel digestion by LC-MS/MS. B) MS/MS spectrum of SLY(AMP)SSSPGGGAYVTR. From mapped ion series and fragment spectra tyrosine 3 in the peptide sequence is the most likely residue carrying the AMPylation PTM.

Table S1: Peptides detected by in-gel digest and LC-MS analysis. List of all peptides detected by in-gel digest and LC-MS analysis over the linear gradient (0-60min) upon activity based assays using 3-plexed ATP in the presence of Bep2 and J774 mouse macrophage lysates. Peptide FDR was adjusted to 1% using the reverse decoy strategy.

(Extract shown here)

Protein ID	Protein description	modification
sp|P20152|VIME_MOUSE	Vimentin OS=Mus musculus GN=Vim PE=1 SV=3	
sp|P20152|VIME_MOUSE	Vimentin OS=Mus musculus GN=Vim PE=1 SV=3	
sp|P20152|VIME_MOUSE	Vimentin OS=Mus musculus GN=Vim PE=1 SV=3	
sp|P20152|VIME_MOUSE	Vimentin OS=Mus musculus GN=Vim PE=1 SV=3	
sp|P20152|VIME_MOUSE	Vimentin OS=Mus musculus GN=Vim PE=1 SV=3	
sp|P20152|VIME_MOUSE	Vimentin OS=Mus musculus GN=Vim PE=1 SV=3	Oxidation (M)
sp|P20152|VIME_MOUSE	Vimentin OS=Mus musculus GN=Vim PE=1 SV=3	
sp|P20152|VIME_MOUSE	Vimentin OS=Mus musculus GN=Vim PE=1 SV=3	Oxidation (M)
sp|P20152|VIME_MOUSE	Vimentin OS=Mus musculus GN=Vim PE=1 SV=3	
sp|P20152|VIME_MOUSE	Vimentin OS=Mus musculus GN=Vim PE=1 SV=3	
sp|P20152|VIME_MOUSE	Vimentin OS=Mus musculus GN=Vim PE=1 SV=3	
sp|P20152|VIME_MOUSE	Vimentin OS=Mus musculus GN=Vim PE=1 SV=3	
sp|P20152|VIME_MOUSE	Vimentin OS=Mus musculus GN=Vim PE=1 SV=3	
sp|P20152|VIME_MOUSE	Vimentin OS=Mus musculus GN=Vim PE=1 SV=3	
sp|P20152|VIME_MOUSE	Vimentin OS=Mus musculus GN=Vim PE=1 SV=3	
sp|P20152|VIME_MOUSE	Vimentin OS=Mus musculus GN=Vim PE=1 SV=3	
sp|P20152|VIME_MOUSE	Vimentin OS=Mus musculus GN=Vim PE=1 SV=3	
sp|P20152|VIME_MOUSE	Vimentin OS=Mus musculus GN=Vim PE=1 SV=3	
sp|P20152|VIME_MOUSE	Vimentin OS=Mus musculus GN=Vim PE=1 SV=3	
sp|P20152|VIME_MOUSE	Vimentin OS=Mus musculus GN=Vim PE=1 SV=3	
sp|P20152|VIME_MOUSE	Vimentin OS=Mus musculus GN=Vim PE=1 SV=3	Oxidation (M)
sp|P20152|VIME_MOUSE	Vimentin OS=Mus musculus GN=Vim PE=1 SV=3	Oxidation (M)
sp|P20152|VIME_MOUSE	Vimentin OS=Mus musculus GN=Vim PE=1 SV=3	Oxidation (M)
sp|P20152|VIME_MOUSE	Vimentin OS=Mus musculus GN=Vim PE=1 SV=3	Oxidation (M)
sp|P20152|VIME_MOUSE	Vimentin OS=Mus musculus GN=Vim PE=1 SV=3	
sp|P20152|VIME_MOUSE	Vimentin OS=Mus musculus GN=Vim PE=1 SV=3	Oxidation (M)
sp|P20152|VIME_MOUSE	Vimentin OS=Mus musculus GN=Vim PE=1 SV=3	Oxidation (M)
sp|P20152|VIME_MOUSE	Vimentin OS=Mus musculus GN=Vim PE=1 SV=3	Oxidation (M)
sp|P20152|VIME_MOUSE	Vimentin OS=Mus musculus GN=Vim PE=1 SV=3	
sp|P20152|VIME_MOUSE	Vimentin OS=Mus musculus GN=Vim PE=1 SV=3	
sp|P20152|VIME_MOUSE	Vimentin OS=Mus musculus GN=Vim PE=1 SV=3	Oxidation (M)

sp|P20152|VIME_MOUSE	Vimentin OS=Mus musculus GN=Vim PE=1 SV=3	Oxidation (M)
sp|P20152|VIME_MOUSE	Vimentin OS=Mus musculus GN=Vim PE=1 SV=3	Oxidation (M)
sp|P20152|VIME_MOUSE	Vimentin OS=Mus musculus GN=Vim PE=1 SV=3	
sp|P20152|VIME_MOUSE	Vimentin OS=Mus musculus GN=Vim PE=1 SV=3	Oxidation (M)
sp|P20152|VIME_MOUSE	Vimentin OS=Mus musculus GN=Vim PE=1 SV=3	Oxidation (M)
sp|P20152|VIME_MOUSE	Vimentin OS=Mus musculus GN=Vim PE=1 SV=3	Oxidation (M)
sp|P20152|VIME_MOUSE	Vimentin OS=Mus musculus GN=Vim PE=1 SV=3	
sp|P20152|VIME_MOUSE	Vimentin OS=Mus musculus GN=Vim PE=1 SV=3	
sp|P20152|VIME_MOUSE	Vimentin OS=Mus musculus GN=Vim PE=1 SV=3	
sp|P20152|VIME_MOUSE	Vimentin OS=Mus musculus GN=Vim PE=1 SV=3	
sp|P20152|VIME_MOUSE	Vimentin OS=Mus musculus GN=Vim PE=1 SV=3	
sp|P20152|VIME_MOUSE	Vimentin OS=Mus musculus GN=Vim PE=1 SV=3	
sp|P20152|VIME_MOUSE	Vimentin OS=Mus musculus GN=Vim PE=1 SV=3	Phosphoadenosine (Y)
sp|P20152|VIME_MOUSE	Vimentin OS=Mus musculus GN=Vim PE=1 SV=3	Phosphoadenosine_5_N15(Y) (Y)
sp|P20152|VIME_MOUSE	Vimentin OS=Mus musculus GN=Vim PE=1 SV=3	Phosphoadenosine_5_N15_10_C13(Y) (Y)
sp|P20152|VIME_MOUSE	Vimentin OS=Mus musculus GN=Vim PE=1 SV=3	
sp|P20152|VIME_MOUSE	Vimentin OS=Mus musculus GN=Vim PE=1 SV=3	
sp|P20152|VIME_MOUSE	Vimentin OS=Mus musculus GN=Vim PE=1 SV=3	
sp|P20152|VIME_MOUSE	Vimentin OS=Mus musculus GN=Vim PE=1 SV=3	
sp|P20152|VIME_MOUSE	Vimentin OS=Mus musculus GN=Vim PE=1 SV=3	

3.3 Bep2 AMPylates β-tubulin

3.3.1 Introduction

Upon bacterial infection, intracellular pathogens hijack the eukaryotic host cell networks in order to facilitate their uptake, survival and replication. To this end, bacteria secrete a set of effector proteins that manipulate host cell signaling by either allosteric or covalent modifications of distinct proteins (1). The best understood covalent modifications are phosphorylation, glycosylation, acetylation and ADP-ribosylation. Recently, another modification, called AMPylation, came back into the focus of research (2). AMPylation, also known as adenylylation, describes the transfer of an AMP-moiety onto the hydroxyl group of tyrosine or threonines and is well understood in the context of glutamine synthetase regulation by so called AMPylators (3, 4). In recent studies, proteins belonging to the family of Fic-proteins (filamentation induced by cAMP) were found to perform AMPylation (2). Although this protein family consists of thousands of proteins that are found in all kingdoms of life, their physiological role remains largely elusive with the exception of a few bacterial effectors that get secreted into host cells (5). The first Fic-proteins that were identified to perform AMPylation on target proteins are the type III secretion (T3S) effectors VopS of *Vibrio parahaemolyticus* and IbpA of *Histophilus somni* (2, 6). While VopS is AMPylating a conserved threonine (T35) within the switch I region of Rho family GTPases, IbpA is targeting the same GTPases but modifies a neighboring tyrosine (Y32) instead of threonine T35. Both of the modifications impair the binding of downstream signaling partners of the small GTPases and are thereby interrupting GTPase signaling leading to a collapse of the cytoskeleton and a cell rounding phenotype (7). Apart from these secreted proteins, only the human homolog HYPE was identified to perform AMPylation. HYPE is the only Fic protein in eukaryotes and was found to target Rho GTPases in *in vitro* studies. Yet, its physiological role is not understood and further potential targets remain unknown (7).

Zoonotic gram negative pathogens belonging to the genus *Bartonella* cause chronic infections of their natural host that often persist symptom-free (8). Upon infection, *Bartonella* translocates a set of effector proteins called Beps (*Bartonella* effector protein) into the eukaryotic host cell via a type IV secretion system (T4SS) (1, 8, 9).

Once translocated, Beps interfere in several intracellular processes leading to an inhibition of host cell apoptosis (10), cytoskeleton rearrangements (11), activation of Nfκb-response and promotion of β-integrin-dependent bacterial uptake (12). The majority of Beps consists of a canonic domain architecture with a C-terminal BID-domain (*Bartonella* intracellular delivery) that serves as a translocation signal and is required for the secretion of Beps into the host cell via a T4SS, and an N-terminal FIC-domain that is thought to be the putative effector domain (13, 14). In contrast to *V. parahaemolyticus* that is only secreting one FIC-domain containing effector, *Bartonellae* are secreting several Fic proteins into the host, yet, translocation of Beps is generally not cytotoxic (15). This indicates that Beps differ from previously described Fic proteins like VopS or IbpA either in their activity or in their target specificity.

We recently introduced a mass spectrometry based method to identify AMPylation targets by utilization of stable isotope labeled ATP and identified the filamenting protein vimentin as one target protein of Bep2, an effector protein of *B. rochalimae*. Bep2 is therefore the first described Fic-protein that does not target small GTPases but a component of the cytoskeleton (see Research Article II).

Here, we present the identification of β-tubulin as a second AMPylation target of the same protein, Bep2 of *B. rochalimae*. β-tubulin is found in heterodimers together with α-tubulin that can polymerize to form microtubules (MTs) that are key elements in intracellular organization and chromosomal segmentation. Upon polymerization, the αβ-tubulin heterodimer exchanges its bound GDP for GTP. The formation and stabilization of the dynamic MT-polymers is mainly mediated by TOG-domain containing proteins belonging to the Stu2/XMAP215 and CLASP families (16-18).

We further show preliminary results indicating that AMPylation of β-tubulin influences the interaction between tubulin and TOG-domain containing proteins which catalyze tubulin polymerization to microtubules (MTs) and stabilize the formed structures (18-20).

3.3.2 Materials and Methods

DNA manipulations

E. coli expression constructs - Bep2 of *B. rochalimae* was amplified with primer prAH072 (CCGCTCGAGATGAAGAAAAGTGAAATGATGATA) and prAH073 (CCGCTCGA GTTAACAAACCATAGCTGTCGC) from genomic DNA of *B. rochalimae* and cloned via XhoI into pET15b to achieve pAH019. Using prAH110 (CAATTATATTGCACCTTTTAGGGAAGGTAATGGACG) and prAH111 (CCTAAAAGGTGCAATATAATTGATAGAGCCAAATATTTTTG) in site directed mutagenesis, pAH051 was produced. BiaA was amplified from genomic DNA of *B. rochalimae* using prAG0013 (GCCCATGGTGAAAAAAACAACTGATCATTCTAC) and prAG0014 (GCGGATCCTTA TAGTGTTGCATTGTCCATAAGAG) and was cloned via NcoI and BamHI restriction into pRSFDUET-1 resulting in pAG0056. The FIC-domain of Bep2 was amplified using prAG029 (GGGAATTCCATATGGATATTAACATCCCTTCTCC) and prAG035 (CGACCTCGAGTTAGTGATGGTGATGGTGATGTTCACTCAAAGCAGCTAA TTTTTC) and introduced via NdeI and XhoI into pAG0056 giving pAG0061 which was then mutated using prAG047 (GCAATTGGAGGAATCACTCTTCATTCTAAAACG) and prAG048 (GAGTGATTCCTCCAATTGCATGTGTACTAATAG) to obtain pKP090.

Constructs for Eukaryotic Expression – mCherry was amplified with prKP199 (AGTAGCAACAGGAGGATCACCCTTGTACAGCTCGTCCATGCCGCCGGTG) and prKP200 (CACCCTTGTACAGCTCGTCCATGCCGCCGGTGGGATCCGCCCTCGAGTAA GAATTCGTCGACAATC) and introduced into pMDK124CM via restriction with EcoRI and BamHI and in-fusion ligation to achieve pKP071. The sequence of Bep2 was codon optimized for eukaryotic expression (Invitrogen) and then amplified with prKP201 (ACACCGACTCTAGAGGATCCGCCACCATGGGAAGCTCTCAC) and prKP214 (GGAGGATCACCCTCGAGCTCGCTCAGGGCGGCCAGCTTTTCCTCGGG) and cloned into pKP071 to get pKP100. The Fic motif was then mutated using prKP212 (CAACTACATCGCACCCTTCCGCGAGGGCAAC) and prKP213 (CGCGGAAGGGTG CGATGTAGTTGATGGAGCCG) to achieve pKP102.

Expression and purification of recombinant proteins

Expression and purification of Bep2 from B. rochalimae. Bep2 was expressed and purified as previously described (Research article II). In brief, Bep2 was expressed in *E. coli* (DE3) BL21 for 24 h at 25 °C upon induction with 100 μM IPTG (Promega). After lysis in AMPylation buffer (10 mM Tris pH=8.0, 150 mM NaCl, 10 mM $MgCl_2$, 2.5 mM βME) supplemented with 2 mg DNaseI from bovine pancrease (Roche) and Complete EDTA-free Protease Inhibitor Cocktail (Roche) [40 μl/ml of stock solution (1 tablet / 2 ml H_2O)], Bep2 was purified using metal affinity and size exclusion chromatography. Purified protein was stored at 4 °C.

Expression and purification of TOG-domain of Stu2 from S. cerevisiae. The N-terminal domain of Stu2 was purified as described by Widlund *et al* (21). For recombinant expression of the TOG of Stu2 from *S. cerevisiae*, Ca-competent *E.coli* were transformed with $pStu2_{1-306}$ (addgene, Plasmid 38315: pGEX-6P-1 Stu2 1-306) and cultured at RT in Terrific Broth medium containing 200 mg/L Ampicillin. At an $OD_{600}=0.5$ expression was induced with 200 μM IPTG (Promega). After 18 h of expression at RT, cultures were harvested by centrifugation and stored at -20 °C. Frozen bacteria were thawed and lysed in 2xPBS buffer supplemented with 5mM βME, 2 mg DNaseI from bovine pancrease (Roche) and Complete EDTA-free Protease Inhibitor Cocktail (Roche) [40 μl/ml of stock solution (1 tablet / 2 ml H_2O]. Bacteria were lysed using French Press and cell debris were removed by high speed centrifugation (1 h, 100 xg, 4 °C). $Stu2_{1-306}$ was purified by affinity chromatography using GST-Trap columns. The protein was eluted with 10 mM Glutathion (Sigma) in AMPylation buffer (10 mM Tris pH=8.0, 150 mM NaCl, 10 mM $MgCl_2$, 2.5 mM βME). Peak fractions were pooled and 10 μL of the peak fractions were separated by SDS-PAGE on a 12% SDS-gel which was subsequently stained with Coomassie staining solution. Glutathion was removed from pooled peak fractions utilizing PD10 desalting columns (GE Healthcare) with AMPylation buffer. The concentration of desalted Stu2 was measured with Nanodrop-1000 (Nanodrop Technologies, Wilmington, USA) via absorbance at 280 nm. Purified protein was stored at 4°C.

TOG-tubulin interaction assays

In order to analyze the impact of tubulin AMPylation on the interaction of tubulin with the TOG-domain of Stu2, the FIC-domain of Bep2 and the TOG-domain of Stu2 were purified as

described above. 50 µL of Protein A/G UltraLink resin (Thermo Scientific, 53132) were washed 2x with 1 mL water and 3x with 1 mL PBS. To couple the TOG-domain to beads, 0.4 mg purified TOG-domain was incubated with the washed resin and 50 µL of primary mouse polyclonal anti-GST antibody (Abcam, ab9085) overnight at 4 °C on a rolling shaker. On the next day, resin was washed 3x with 300 µL PBS and used for tubulin pull-down.

1 nmol of purified tubulin (Cytoskeleton, T240-A) were incubated for 5 h at 30 °C with 1 µL of 100 mM N15C13-labeled ATP in the presence (sample) or absence (reference) of 1 nmol purified FIC-domain of Bep2 in a final volume of 50 µL in AMPylation buffer (10 mM Tris pH=8.0, 150 mM NaCl, 10 mM $MgCl_2$, 2.5 mM βME). 5 µL of the reaction mixtures were directly used for mass spectrometry, 40 µL of each mixture were incubated separately with 25 µL of TOG-coupled resin for 1 h at RT. Supernatants were kept for analysis and the resin was washed 4x with 300 µL PIPES buffer. Proteins were eluted with 2% DOC in PBS at 60 °C for 20 min. Reaction and elution samples were reduced with TCEP at 37 °C, saturated with Iodacetamid at RT in the dark and quenched with N-acetyl cysteine prior to tryptic digest. Peptides were then C18-purified and used for subsequent mass spectrometry. Peak intensities of AMPylated tubulin peptide were compared between samples of reactions and elution with respect to tubulin levels.

AMPylation quantification

Bep2-mediated AMPylation of tubulin was quantified by mass spectrometry. To this end, 250 pmol of tubulin (cytoskeleton, T240-A) were incubated for 1h or 5h with 1uL of 100 mM N15C13-ATP (CIL) in the presence (sample) or absence (reference) of 250 pmol of purified $Bep2_{1-314}$. Protein samples were reduced with TCEP at 37 °C, saturated with Iodacetamid at RT in the dark and quenched with N-acetyl cysteine prior to tryptic digest. Peptides were C18-purified and analyzed by mass spectrometry. Peak intensities were normalized between sample and reference and the percentage of AMPylated tubulin was deduced by label-free quantification using the Progenesis software (nonlinear Dynamics).

Cell lines and cell culture

HEK293T, J774 mouse macrophages, COS-7 and HeLa cells stably expressing GFP-α-tubulin (22) were cultured in DMEM (Sigma) supplemented with 10% FCS (Gibco).

In order to test protein expression and protein stability, 2×10^6 cells were seeded into a 10 cm cell culture dish (Falcon) and incubated over night at 37 °C, 5% CO_2. The next day, cells were transfected using Fugene HD (Promega). Therefore, 5 µg DNA in 600 µL DMEM were gently mixed with 25 µL Fugene HD in 600 µL of DMEM, incubated for 15 min at RT and added dropwise to the cells in culture. After incubation for 8 h at 37 °C with 5% CO_2, medium was exchanged and cells were incubated for 24-36 h at 37 °C with 5% CO_2 until fluorescent marker was visible under microscope. Cells were washed 2x with 7 mL of PBS, scraped in 1 mL of ice cold PBS, pelleted and resuspended in 200 µL of lysis buffer (10 mM Tris pH=8.0, 150 mM NaCl, 10 mM $MgCl_2$, 2.5 mM βME, 0.5% NP40, EDTA-free protease inhibior). Cells were lysed by sonication (3x 10 pulses) and cell debris were removed by centrifugation (21.000 x g, 4 °C, 30 min). 20 µL of the cleared lysates were separated in 12% SDS-PAGE and transferred onto a Hypond-C Extra nitrocellulose membrane (Amersham Biosciences). The membranes were examined for mCherry fusion proteins using primary mouse monoclonal anti-mCherry antibody (1:5000, Sigma). Proteins were visualized using the ECL System (GE Healthcare) with HRP-conjugated ECL[TM] rabbit anti-mouse IgG (1:5000, GE Healthcare, NA934V).

Co-localization and microtubule dynamics

10 000 HeLa ATCC cells stably expressing GFP-α-tubulin or 2000 COS-7 cells were seeded into each well of 6 well slide (ibidi) and incubated over night at 37 °C with 5% CO_2. On the next day, cells were transfected using Fugene HD (Promega). Therefore, 5 µg of DNA in 600 µL of DMEM were gently mixed with 25 µL of Fugene HD in 600 µL of DMEM, incubated for 15 min at RT and mixed with 10 mL of DMEM supplemented with 10% FCS. The medium in the wells was exchanged twice for transfection mix. After incubation for 8 h at 37 °C with 5% CO_2, the transfection medium was exchanged for DMEM supplemented with 10% FCS and cells were incubated for 24-36 h at 37 °C with 5% CO_2 until the fluorescence marker of the ectopically expressed construct was visible under microscope.

Slides with HeLa cells stably expressing GFP-α-tubulin and transiently expressing $Bep2_{1-360}$ or $Bep2H161A_{1-360}$ were analyzed with confocal microscopy.

Immunofluorescent labeling

Indirect immunoflurecent-labeling was performed as previously described (Dehio, 1997). In brief, cells were permeabilized with 0.1% TritonX for 10 min and microtubules were labeled using mouse monoclonal anti-β-tubulin antibody (1:100, Thermo Scientific) and Goat anti-mouse IgG (H+L) Alexa Fluor 488 (1:300, Molecular Probes). DNA was stained with DAPI (Roche, final concentration 1 μg/mL).

3.3.3 Results

Bep2 harbors an AMPylation activity

Bep2 is a 55 kDa effector protein of *B. rochalimae* that is secreted via a T4SS into the eukaryotic host cell upon infection. *In silico* analysis revealed that Bep2 harbors an N-terminal FIC-domain that was identified by its predicted secondary structure and its active site motif. Although it only shares a low sequence identity with other Fic-proteins like BepA of *Bartonella henselae* (47%) or the T3SS effector protein VopS of *V. parahaemolyticus* (12% sequence identity), homology modeling showed that the Fic-fold and the flap region for target docking are conserved (Swiss Model, Figure S2) (23-25). In addition to its FIC-domain, Bep2 harbors an OB (oligonucleotide/oligosaccharide)-fold with a yet unknown role in effector functionality and a C-terminal BID-domain that serves as a secretion signal.

In order to investigate if Bep2 shows AMPylation activity as described for other Fic proteins, we performed *in vitro* AMPylation assays. To this end, lysates of *E. coli* expressing Bep2 were incubated with radioactively labeled α^{32}P-ATP in the presence and absence of eukaryotic cell lysates. AMPylation targets were visualized via autoradiography. In the absence of eukaryotic lysates, only one AMPylation spot at the height of 55 kDa was oberserved. This signal was not detected using the catalytically inactive histidine mutant (Bep2°) which does not allow substrate coordination and thereby abolishes AMPylation. This indicates that Bep2 indeed harbors an AMPylation activity and exhibits auto-AMPylation as described for other Fic proteins. In the presence of eukaryotic cell lysate, a second AMPylation target at approximately 50 kDa was detected. In contrast to all previously described Fic-proteins, Bep2 is not AMPylating small GTPases with an expected size of 20 kDa but a yet unknown target of significantly higher molecular weight (Figure1A).

In order to identify the target protein of Bep2, *in vitro* AMPylation assays were performed in parallel using light and heavy isotope labeled ATP. Subsequent *in gel* digestion and LC-MS analysis were utilized as recently described (see Research Article 2). In short, 3-plexed AMPylated peptides were identified by their specific isotopic shift that could only be detected in samples of wild-type but not of mutated Bep2. We identified AMPylation on the peptide GHYTEGAELVDAVLDVVR which corresponds to the β-chain of tubulin (Figure 1B). Using

the inactive mutant Bep2H161A, the peptide was found not to be modified, indicating that AMPylation of tubulin is Bep2-mediated (Figure 2A).

As a further line of evidence, we aimed at confirming the AMPylation of tubulin by Bep2 utilizing an *in-vitro* AMPylation assay with purified protein. As full length Bep2 could not be purified actively, we expressed Bep2 in *E. coli* and used this bacterial lysate in AMPylation assays with α^{32}P-ATP in the presence and absence of purified tubulin. As shown in Figure 2B, tubulin was AMPylated by Bep2 confirming tubulin as an AMPylation target of Bep2.

To investigate if the target switch from small GTPases to tubulin is dependent on the FIC-domain alone or is mediated by the BID-domain, the C-terminus of Bep2 was deleted and Bep2$_{1-360}$ was purified from *E. coli* and tested for AMPylation of tubulin. Again, auto-AMPylation as well as target AMPylation of tubulin could be detected (Figure 2C). The FIC-core alone (Bep2$_{14-180}$) could not be stably expressed, indicating that the OB-fold is required for protein stability.

Taken together, Bep2 is an AMPylating protein and its N-terminus consisting of the FIC-domain and an OB-fold is sufficient to catalyze the transfer of an AMP-moiety onto β-tubulin. Bep2 is therefore the first described Fic-protein that is not targeting small GTPases but tubulin as a component of the cytoskeleton.

Bep2 is co-localizing with microtubules

Based on our MS-results, our data suggest that upon translocation into the host Bep2 interacts with tubulin and covalently modifies it. In order to investigate the relative spatial distribution of Bep2 and tubulin, we transiently expressed Bep2 in HeLa cells stably expressing GFP-α-tubulin and investigated its subcellular localization by confocal microscopy.

Therefore, constructs for eukaryotic expression of Bep2$_{1-360}$ C-terminally fused to mCherry were cloned for wild-type Bep2$_{1-360}$ as well as for the inactive mutant Bep2°$_{1-360}$. Expression and stability of the fusion proteins were analyzed by Western blotting using an anti-mCherry antibody.

As shown in Figure 3, the mCherry-signal is partially cytosolic but also found in distinct fibrous structures. Essentially, the mCherry signal from both wild type and inactive mutant of Bep2$_{1-360}$ was similar to the signal of endogenous tubulin stained with anti-α-tubulin antibody indicating

that Bep2 is co-localizing with microtubules but was also found in strong fluorescent spots, indicating that Bep2$_{1\text{-}360}$-mCherry is aggregating.

AMPylation of tubulin affects TOG-tubulin interaction

The best understood example of a TOG protein is yeast Stu2 that contains two TOG domains, TOG1 and TOG2 (26). Both TOG-domains are binding αβ-tubulin (19). While TOG1 preferentially binds to the curved GDP-bound form, TOG2 binds the straight GTP-bound form, which is predominantly found at the plus end of MTs. It is therefore hypothesized, that TOG2 and the C-tail of Stu2 direct the protein to the plus end of MTs where unpolymerized αβ-tubulin heterodimer is captured by TOG1 and directed to MTs. Polymerization of the captured αβ-tubulin then induces straightening of the heterodimer decreasing the interaction between TOG1 and αβ-tubulin which leads to the dissociation of TOG1 from the polymerized tubulin (19).

Recently, the group of L. Rice was able to co-crystallize the complex of TOG1 and αβ-tubulin revealing that TOG1 is interacting via its Loop5 region with α-tubulin and via its Loop1 region with β-tubulin. The interaction between TOG and tubulin was found to be mediated by salt bridges between the hydroxyl group of β-tubulin Y106 and arginine R116 of the TOG-domain. Furthermore, mutations in TOG1 (W23A) as well as in β-tubulin (T107E, Y106A) or α-tubulin (E415A) abolished the interaction (19).

To test whether AMPylation of tubulin influences the interaction between the purified TOG1-domain and tubulin, we performed *in vitro* AMPylation assays followed by co-precipitation assays of tubulin with TOG1 of yeast Stu2 and analyzed the amount of the AMPylated tubulin by mass spectrometry.

In the first step, the percentage of modified tubulin upon AMPylation by Bep2 was quantified utilizing mass spectrometry and label free quantification. To this end, we followed the MS1 trace of the unmodified peptide of β-tubulin in the presence and absence of Bep2 and deduced the percentage of AMPylated tubulin. We thereby observed the Bep2-mediated AMPylation is not quantitative but that only 20% of β-tubulin was AMPylated. In these *in vitro* AMPylation assays we also the AMPylation of a peptide belonging to the α-chain of tubulin (AYHEQLSVAEITNACFEPANQMVK). Label free quantification of the unmodified peptide

revealed an equally strong AMPylation as seen for the β-tubulin peptide. Yet, the intensity of the AMPylated peptide was 100 times lower than intensities of the unmodified peptide. Within the quaternary structure, this peptide is located on a flexible exposed loop at the opposite side of the αβ-tubulin heterodimer compared to the Y106/T107 AMPylation site on β-tubulin.

Next, we investigated if the interaction between the TOG-domain and tubulin differs between modified and unmodified tubulin. Therefore, we used TOG1-coated Sepharose beads and captured tubulin before and after Bep2-mediated AMPylation. Subsequent mass spectrometry was utilized to estimate if AMPylated tubulin was enriched on TOG1-coated beads. To this end, we used peak intensities of the AMPylated-peptide normalized to the total tubulin levels and compared between samples of the AMPylation reaction (R-samples) to samples of the elution after the pull down (E-samples). In all assays, the normalized peak intensity of the AMPylated peptide was higher in elution samples indicating that AMPylated tubulin was enriched by pull down assays with TOG1.

To further gain insight into the consequences of AMPylation, we used the previously described structure of the TOG1-tubulin complex (Ayaz *et al.* (19), PDB code 4FFB) and modeled an AMP moiety onto the Y106 lying in the interface between β-tubulin and TOG. In order to model the AMP-moiety onto the hydroxyl group Y106, we used the conformation found in the crystal structure of the published co-complex of IbpA with its AMPylated target protein Cdc42 (PDB code 4ITR).

As shown in Figure 4, the AMPylated tyrosine on the α-chain of tubulin is not located at the interface between TOG and tubulin, but lies on a disorganized loop that is exposed at the opposite side of the αβ-tubulin heterodimer. Therefore, it most likely does not contribute to the TOG-tubulin interaction. In contrast, the AMPylated site on β-tubulin is exactly at the interface of TOG1 and tubulin and located near the salt bridges that stabilize complex formation. Both AMPylation sites are not located at GTP-binding pockets of tubulin.

In this model, the AMP-moiety lies within a groove between both proteins. Although the initial hydrogen bond between the hydroxyl group of Y106 of β-tubulin and the amine group of R116 of TOG1 is disturbed, a salt bridge could be formed between the same amine group of R116 of TOG1 and the phosphate group of the AMP moiety. Moreover, the ribose group could be stabilized via an interaction with T118 of TOG1 and the adenine moiety could be oriented via E410 of β-tubulin. Both of these interactions would further stabilize complex formation between

AMPylated tubulin and the TOG-domain. In this model, the AMP-moiety would therefore not abolish the interaction between TOG1 and tubulin as previously described for the AMPylation of small GTPases.

Overall, we could show that Bep2 is not modifying tubulin quantitatively. However, AMPylation of tubulin is affecting the interaction between tubulin and TOG1 of Stu2 domains that are involved in polymerization control of MTs.

3.3.4 Discussion and Outlook

In this study, we addressed target AMPylation by a secreted Fic protein, Bep2, of the pathogen *B. rochalimae*. While we previously identified vimentin as a target protein of Bep2 using a mass spectrometry based approach utilizing a stable isotope-labeled substrate (see Research Article II), we now also present tubulin as an additional target protein. Bep2-mediated AMPylation of tubulin was verified by *in vitro* AMPylation assays with purified proteins. MS analysis of *in vitro* AMPylated heterodimeric tubulin further revealed that a tyrosine residue of α-tubulin and either tyrosine Y106 or threonine T107 of β-tubulin are modified by Bep2. Structural analysis of Fic proteins revealed that their active grove accommodates the substrate ATP and positions it in favor of an AMPylation activity towards an incoming target residue (27). Yet, target recognition is mediated by a β-hairpin loop via main chain-main chain interaction and is thus sequence independent (27, 28). Therefore, target recognition is restricted by accessibility of the region and the positioning of the targeted residue and its proximity to ATP after complex formation with the Fic protein. This is believed to increase specificity for threonine or tyrosine modification. Hence, the modification of a tyrosine residue in α-tubulin might indicate specificity of Bep2 towards tyrosine-modification which implies that actually Y106 instead of T107 is modified. In ongoing studies, tubulin mutants of Y106 and T107 are utilized to confirm this initial hypothesis.

We next aimed to quantify Bep2-mediated tubulin AMPylation by performance of *in vitro* AMPylation assays with purified proteins and label free quantification via MS analysis. Using equimolar ratios of proteins, we found approximately 20% of β-tubulin and similar amounts of α-tubulin to be AMPylated, although α-tubulin was not identified in the initial target screen. The modified tyrosine of α-tubulin is located on an unstructured loop on the opposing site of the TOG-tubulin interface. It is exposed in the heterodimeric form but is not accessible in the polymer (PDB code 4I4T). Comparing quantities of β-tubulin AMPylation with α-tubulin AMPylations therefore allows insights into a Bep2-preference towards polymerized or heterodimeric tubulin form.

In order to gain insights into Bep2-association with MTs, we investigated if Bep2 localizes at MT sites using transient expression in HeLa cells stably expressing GFP-α-tubulin. Indeed, we found a partial co-localization of Bep2 with tubulin. As wild-type but also a catalytically inactive

mutant of Bep2 (Bep2°) are both co-localizing with MTs, Bep2-localization is independent of AMPylation.

Decoration of MTs with Bep2 might have an additional impact on MT dynamics apart from AMPylation activity and could e.g. disturb movements of motor proteins (29).

Tyrosin Y106 of β-tubulin lies on a small loop of four amino acids in-between two α-helices. In previous studies by Ayaz *et al*., this region was identified to be essential for the interaction of tubulin with the TOG1-domain of Stu2 of *Saccharomyces cerevisiae*. Furthermore, mutation of both residues, Y106 and T107, abolished complex formation (19). We therefore hypothesize that AMPylation of β-tubulin might influence its interaction with TOG-domains.

To address this hypothesis, we performed pull down assays of AMPylated tubulin with immobilized TOG1-domain of Stu2 of *S. cerevisiae*. As an increased interaction leads to a lower dissociation rate from the TOG-domain resulting in an enrichment of the tubulin form with stronger interaction, MS-based quantification of the AMPylated peptide before and after pull down experiments allows an estimation of an increase or decrease in TOG-tubulin interaction upon AMPylation. In fact, the AMPylated peptide was enriched compared to the unmodified peptide indicating an increased affinity towards the TOG-domain. Using the crystal structure solved by Ayaz *et al.* of the TOG-tubulin complex, we next modeled the AMP-moiety onto the tyrosine Y106 of β-tubulin. As the complex is stabilized by a hydrogen bond between Y106 of unmodified β-tubulin and arginine R116 of the TOG-domain, the introduced, negative charge by the phosphate group of the AMP-moiety is not interrupting the interaction. Instead, it might be potent to form a hydrogen bond itself to the arginine R116 of the TOG-domain and stabilize the complex while the adenosine moiety lies within a grove between both proteins.

An increase in complex stability would inhibit dissociation of the TOG-domain from tubulin which is an essential step in TOG protein-mediated MT polymerization (19). AMPylation of β-tubulin would thus decrease levels of active TOG protein resulting in an inhibition of MT polymerization and/or stability. We are currently investigating the role AMPylation in MT dynamics by treatment of Bep2-expressing COS7 cells with Nocodazol and subsequent wash out experiments. However, reliable analysis the AMPylation impact on MTs remains challenging due to aggregation of constructs.

The influence of PTMs on MT dynamics has long been in the focus of research and although most PTMs are believed to regulate MT stability or assembly, their molecular function often remains unclear. The best understood PTMs of tubulin are acetylation, phosphorylation and tyrosination. While tyrosination is only seen on last amino acid of the α-tubulin C-terminal tail of free, heterodimeric tubulin and is required for the binding of +TIPs (30, 31), phosphorylation is performed on heterodimeric and polymerized forms and reduces MT stability (32). Additionally, phosphorylation of serine S173 of β-tubulin that is positioned close to the GTP-binding site, is believed to inhibit the exchange of GDP for GTP and thus to inhibit polymerization (33). In contrast, acetylation is only seen on stable MTs (34). Additionally, acetylation influences dynamics of kinesin motor KIF5 (35) and is, like phosphorylation and tyrosination, a reversible modification (34, 36). Interestingly, uropathogenic *E. coli* (UPEC) was recently shown to activate the de-acetylase HDAC6 which decreases MT-stability and thereby increases pathogen entry (37).

In summary, we presented with tubulin the cytoskeletal components as a new target class of Fic protein-mediated AMPylation. In contrast to all other studied AMPylators that inhibit the interaction of their targets to other proteins, Bep2-mediated AMPylation of tubulin seems to increase its affinity towards TOG-domain containing proteins and is therefore the first example of a gain of function by AMPylation.
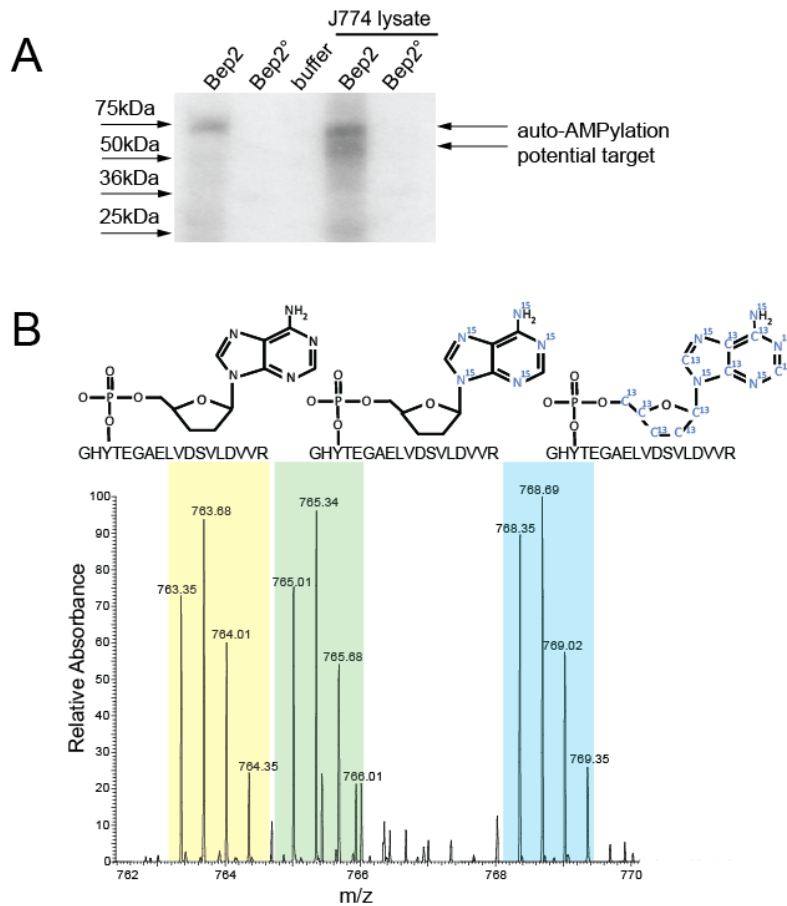
Figure 1: Target identification of *Bartonella rochalimae* effector protein Bep2. A) Initial target screen by autoradiography. A representative autoradiogram of an *in vitro* AMPylation assay with active and inactive Bep2 is depicted. *In vitro* AMPyation assays were performed on wild-type and the inactive mutant of Bep2 and mouse macrophage (J774) lysates in the presence of α^{32}P-ATP. After SDS-gel electrophoresis, AMPylated proteins were visualized by autoradiography. B) Target identification by AMPylation-specific reporter ions. Samples derived from *in vitro* AMPylation assays with Bep2 using 3-plexed ATP were analyzed by in-gel digest and LC-MS/MS. The mass spectrum shows the m/z of the 3-plexed AMPylated peptide GHYTEGAELVDSVLDVVR originating from β-tubulin. The reporter ions specifically encoding an AMPylation modification with characteristic mass shifts are highlighted by different colors.
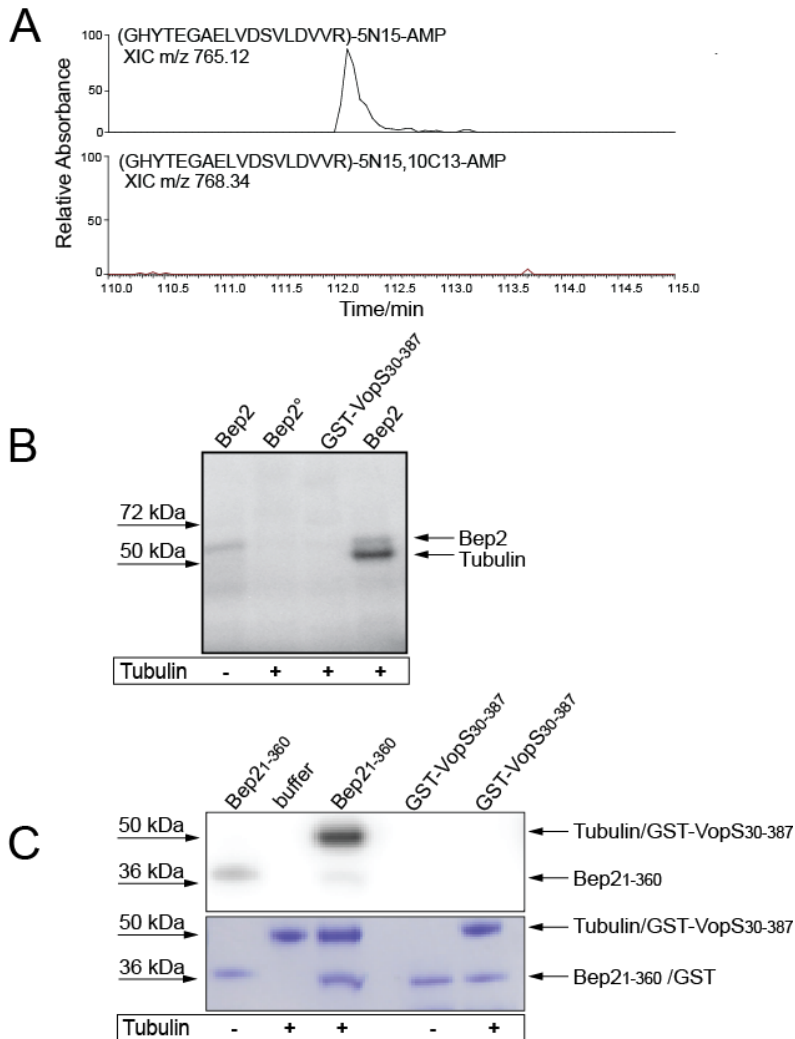
Figure 2: Validation of β-tubulin as an AMPylation target of Bep2. A) Extracted-ion chromatogram (XIC) of samples derived from *in vitro* AMPylation assays. Assays were performed on wild type Bep2 incubated with $^{15}N_5$-ATP and Bep2° incubated with $^{15}N_5^{13}C_{10}$-ATP. Samples were pooled and analyzed by LC-MS/MS. The XIC of AMPylated GHYTEGAELVDSVLDVVR is shown for $^{15}N_5$-AMP reporter channel for Bep2 (top) and $^{15}N_5^{13}C_{10}$-AMP for Bep2° (bottom). B) Validation experiments on tubulin αβ-heterodimer as an AMPylation target of Bep2. *In vitro* AMPylation assays were performed with an *E. coli* lysates Bep2, catalytically inactive mutant of Bep2 (Bep2°) and GST-VopS$_{30-387}$ and purified, heterodimeric tubulin in the presence of α^{32}P-ATP. AMPylated proteins were visualized by autoradiography. C) Validation experiments on Bep2 target recognition. *In vitro* AMPylation assays on tubulin were performed with purified Bep2$_{1-360}$ and α^{32}P-ATP in addition to either buffer or purified GST-VopS$_{30-387}$. AMPylated proteins were visualized by autoradiography (top). The SDS-gel used for autoradiography was then stained with Coomassie to visualize all proteins (bottom).

Peptide	Peptide Intensity after AMPylation assay	Peptide Intensity in Elution-Sample
Sum of all unmodified peptides	$1.46 \cdot 10^9$	$8.76 \cdot 10^9$
AMP- GHYTEGAELVDAVLDVVR (AMPylated peptide)	$2.31 \cdot 10^7$	$2.76 \cdot 10^9$
AMPylated peptide/ Sum of all unmodified peptides	$5.02 \cdot 10^{-2}$	0.31

Tabel 1: Label-free quantification of AMPylated β-tubulin peptide enriched via TOG-domain. For the AMPylation assay in the presence and absence of purified Bep2$_{1-360}$, tubulin was enriched using TOG-domain coated Sepharose beads. Samples from the initial AMPylation assays and from the bead eluate via DOC were trypsin digested and analyzed by mass spectrometry. Shown are the peak intensities of AMPylated peptides and the sum of all unmodified tubulin-peptides representing protein levels of one experiment.
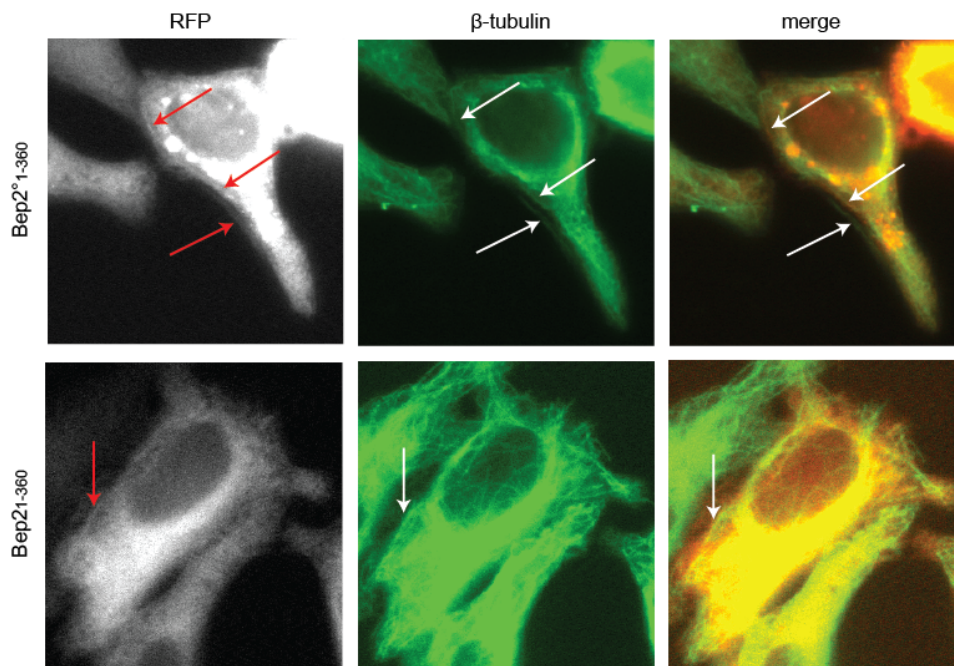
Figure 3: Colocalization of Bep2₁₋₃₆₀-mCherry with microtubules. Shown are selected example images of HeLa cells stably expressing GFP-α-tubulin and transiently expressing Bep2₁₋₃₆₀-mCherry (top) or Bep2°₁₋₃₆₀-mCherry (bottom). MCherry-fusion proteins are depicted in red, endogenous microtubules were immunofluorescently labeled and are shown in green. Arrows indicate distinct structures that are found in both labels.
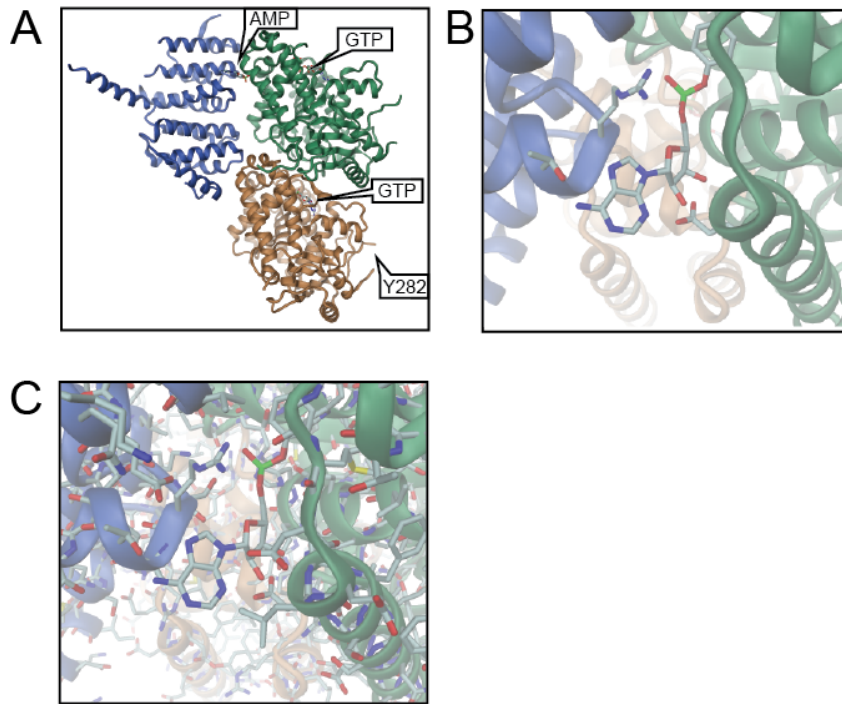
Figure 4: Structural model of AMPylated β-tubulin in complex with the TOG-domain of Stu2. The AMP-moiety was modeled onto Y106 of β-tubulin using the crystal structure of the TOG/tubulin complex (PDB code 4FFB). The conformation of the AMP-moiety was modeled based on the co-crystal of AMPylated Cdc42 and IbpA (PDB code 4ITR). Protein chains are shown in ribbon style. TOG-domain is colored in blue, β-tubulin in green and α-tubulin in orange. A) Overview of the complex with the AMP-moiety within the interface of TOG-domain and β-tubulin. GTP-binding pocket and AMPylated residues are positioned on opposing protein sides. Position of the unstructured loop on α-tubulin that was found to be AMPylated on tyrosine Y282 by MS analysis is indicated. B) Zoom in on the AMPylated residue lying in the interface of TOG-domain and β-tubulin. Modified tyrosine as well as potentially coordinating residues are labeled and shown in full. C) Depicted is the same extract as in B) but with all side chains shown in full to exhibit the absence of steric hindrance in complex formation.
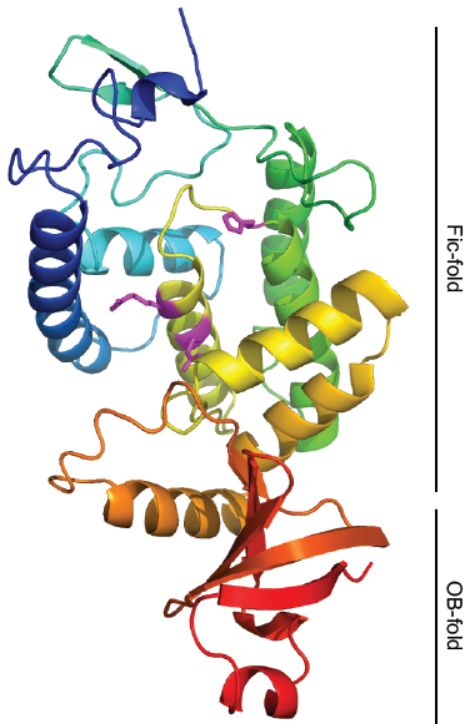
Figure S1: Structure prediction of Bep2$_{1-360}$ of B. rochalimae. The secondary structure of the N-terminal part of Bep2 was predicted using SWISS MODEL. Crystal structure of BepA$_{10-303}$ of B. henselae was used as temple. Bep2 shows a conserved α-helical Fic-fold followed by an OB-fold as described for BepA (38).

CLUSTAL 2.1 multiple sequence alignment

```
Bep2    MKKSEMMIKLEDINIPSPKNYVYPDSRVLKNKYGIMELQKFEERMTHDALKETVKVLEEP 60
BepA    --MPKAKAKTKNTEIISPHHYVYPNTTTLKNKYGIKNLNAFLEKCSHDTAKAMINLREES 58
VbhT    ------MRKYEGSNDP----YTDPETGVMYNLLGIKDQARLERVESAFAYIRSFELGRTS 50
VopS    ------MISFG--------NVSALQAAMPQARNEILNEGKLSIGGKEYTINAATQEFTRA 46
                .             ::        * :    :       .   :      :    .

Bep2    APERFDSSYLKYLHKRLFQHALEWAGCTRDVPFTFLDGTRAVMPSMAKCDSDFGFAFGSE 120
BepA    LPEYFDTAYLCHIHQQLFKNTFEWAGYLRHIPFTFADGTTAAMPEMKRTGWKNAFAIGDE 118
VbhT    ISGKFDLDHMKKIHKKLFGDVYEWAGKTRLVDIVKDNSK---------------FAHYTQ 95
VopS    NPTSGAVARFFEATGKLFREGSTQSVAKAITKAVFDNEQ--------------------- 85
             .          :      :**  .    :         :    .

Bep2    IKEGLDFIDQKLSEKNYLRGLSREEFVHNAAKIFGSINYIHPFREGNGRVQRLFFVKLAR 180
BepA    IQEGLQRLDQTLAEKNNLQGLTREEFNSEAIELFNSLNQLHPFREGNGRTQRLFFENLAK 178
VbhT    IESYAPQITQQLAREQHLRGLDANEFSQRAGYYMGELNALHPFREGNGRTLREFIWQLAR 155
VopS    ---------GQAQRLQTSSSVEHGQMLFKDANLKTPSDVLNAFAKLDSKMVKSHAAELS- 135
                 . :   .:    ::  .       : ::.*  :  :.:  :  .  :*:

Bep2    SVGYKLDFSATTTKRMTYVSVEVTKNAYMKPLQHLFEDISNPEKVGILKQFISNAKEYNI 240
BepA    AAGHQLNFSLITKERMMVASVAVAENGDLEPMQHLFEDISNPEKIRLLKEFMHTMKNTGR 238
VbhT    EAGYHIDWDRVERQEMTRASIESYYGN---------SDLMSALIRRNLTEFTVNRRVDVS 206
VopS    ---------QLAERAMTEVMLETDSGK-------------------NLKALIG------- 160
                 . *  . :     .              *. :

Bep2    FDSNEKLITVAREGETYKGIGKFLASDFIVIEAGDTCILSNKDSLTPEQLRTFKLGSDFI 300
BepA    N-VNDRPVMVAKEGETYTGTYRGAGLEGFALNVKGAYIIGNIDHLPPEQLKILKPGDKIT 297
VbhT    QGINERVLSHIDIDKEWPQKGFNIAIQ-TTQQAPYLSSYTDTSNLEEKAQNALRNEQSYV 265
VopS    --DDAVKSLAVRVVKDYGG-------GVAAAQKNPEVRINQMQAVFDMEVMHLKAAQRHI 211
                  :          : :          . :        : . :       ::  .

Bep2    FTALDTKDLKEIFIPEEKLAALSEDEMIEKILEYSSVREQRDKIQHCARFIYGHSDQLNE 360
BepA    FTAPKAEELKKTLIPKETLVPLTKLEIAEMVAEDAFVHTCRDQICSLSKIVYGSQGVLNK 357
VbhT    DTFKELNDHLKTIYKDPQAAALK--------IEQTILAGKGDKLPDILAKAPNKVGELRG 317
VopS    EGLASTDLNQGVYAEGLPEDAFN---------KAGVTNNVERAAAWIINASNSKGNDAEN 262
                 .  .        .:.        :        . .       .  . .

Bep2    IINMIDMDPNLGEVFSEQIMACCDNKK-----YFISKKTKATN---QSFCKLSNEIKNYA 412
BepA    NIIEIIKNPSKGQQLATQIERTPYSVHSLAGFDLICFKTGARVRAEKHVALLSCAVANFT 417
VbhT    SDRLIDKLKSAGKERKAALYNVPLAIS------------------------TIRRLQ 350
VopS    ITSLLKEYATNGKDLLN--------------------------------MDNLK 284
             :    . *:                                      : .

Bep2    NIVEDSRNQILKEYKERQKRCGQVVKMPSKEVQCILDMPEDMWEKALKSWSLSFLNKSIS 472
BepA    HAVKHARQEITKEHQAEQNRLRQEVPMPSQSLQDLLSLPKEFQQKALG--VSPLLQKELT 475
VbhT    SFYKNSYEKHMDKLTREREQLKVEVPSLSQEAVAYMKNVEVGRNNYSK--IPENINKEFV 408
VopS    ELHARLVPNVERDYRGPNISGGTLPSSIGGEGMLKQHIEGFLKENPVA-------DKDLG 337
              :    .    .         . .          ::           :*.:

Bep2    DFIIKVNHRLSPCECKAINDKNYEELAKSISISESKAKAIIKTIGKVKEIQKKIQVLRAN 532
BepA    SLLQKVNSRLSSSEQRALRENNHETLAKNLGVSEQKAKEITKTVMKAREVQQKSQTRIVS 535
VbhT    QLESALNRRFG----KDVIYKRNFNLSKEIASKQTYDKKLVNELQTAIKFLQQRHIQKQN 464
VopS    KHLFAG---------VIGYHGFTDGNGRMGRMLYAIAELRNDSFNPLAMNAENSLHGIK 387
             .        : :      ::.      : :   .   . :     .

Bep2    ALKATAMVC--- 541
BepA    HSKTLAMAS--- 544
VbhT    NLAITRTPSKGI 476
VopS    ------------
```

Figure S2: Sequence alignment of Bep2$_{1-360}$ with BepA and VopS. The primary amino acid sequence of Bep2 was aligned against BepA of *B. henselae* and VopS of *Vibrio parahaemolyticus* using ClustalW. The alignment reveals low sequence identity comparing all three Fic proteins.
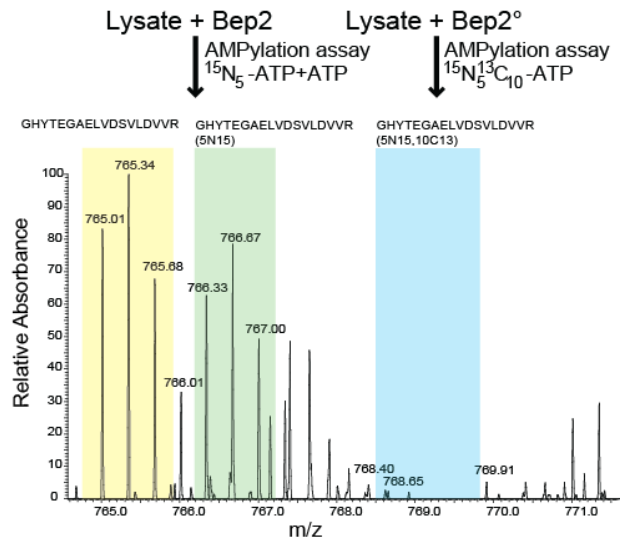
Figure S3: Validation of β-tubulin as an AMPylation target of Bep2. Depicted is the mass spectrum of AMP-reporter ions in the presence and absence of active Bep2. Samples derived from AMPylation assays with either Bep2 and an ATP/$^{15}N_5$-ATP mix or with the inactive mutant of Bep2 (Bep2°) and $^{15}N_5$ $^{13}C_{10}$-ATP were pooled and analyzed by LC-MS/MS. Depicted is a mass spectrum zoomed in on the m/z range of the reporter ions.

3.4 Role of antitoxin in pathogenicity

3.4.1 Introduction

Fic proteins belong to the Fic/Doc family that comprises thousands of members (39, 40). They are found in all kingdoms of life and share a conserved fold and motif from humans to bacteria (5). Fic proteins were recently shown to transfer an AMP-moiety onto target proteins thereby modify the activity of their targets (2, 7, 39). The best understood Fic proteins are the type III secretion effector VopS of *Vibrio parahaemolyticus* and the surface antigen IbpA of *Histophilus somni*. Both proteins were shown to modify small GTPases of the host cell in the switch I region leading to the inhibition of GTPase signaling and ultimately to cytoskeleton collapse and cell death (2, 28). Yet, the majority of Fic proteins is not secreted but associated with endogenous signaling as the eukaryotic Fic protein, HYPE. Although the human homolog of HYPE was found to AMPylate the same GTPases as VopS and IbpA *in vitro*, overexpression in eukaryotes is not toxic indicating a high regulation of AMPylation activity (7).

The Fic-fold is defined by a Fic-core that comprises four helices that are typically surrounded by another four helices. Target recognition is mediated by a β-hairpin flap that interacts with the target by formation of an antiparallel β-sheet between the main chains of the flap region and the targeted loop (27, 28). The conserved histidine within the signature motif (HxFx[D/E]GNGRxxR) acts as a general base and deprotonates the targeted residue thereby increasing nucleophilicity (28). In order to achieve AMPylation, the substrate needs to be coordinated allowing an in-line attack on the α-phosphate (27).

First insights to the mechanism of Fic protein regulation were gained by structure-function analysis of several bacterial Fic proteins that inhibit growth when expressed in *E. coli* thus indicating a bacterial target instead of eukaryotic Rho GTPases as described for the secreted effectors VopS and IbpA (5). In fact, the AMPylation activity of these Fic proteins could be inhibited by the expression of an additional helix, called α_{inh}. This helix is provided by a separate protein called antitoxin for class I Fic proteins, or N- or C-terminally of the Fic-protein itself in class II or class III, respectively (5). A conserved glutamate residue within the α_{inh} competes with the γ-phosphate of ATP to interact with the second arginine within the signature motif and is thus disrupting substrate coordination (27). Thereby, the antitoxin allows activity regulation of Fic

proteins with endogenous targets to avoid constant intoxication as shown for VbhA/VbhT of *Bartonella schoenbuchensis* (5). Yet, several pathogens that secrete Fic proteins with host cellular targets also encode antitoxins but their role in pathogenicity remains elusive.

Bartonella spp. are gram negative, intracellular facultative pathogens that can cause chronic infections by colonization of endothelial cells (8). Upon infection, *Bartonella* secretes a set of effector proteins (Beps) via a VirB/VirD4 type IV secretion system that manipulate host cell functions to the benefit of bacterial uptake and survival (9). To this end, the Beps of *B. henselae*, the causative agent of the cat scratch disease, were found to inhibit host cell apoptosis, activate the pro-inflammatory response and the bacterial uptake into the cell. BepG or the combined action of BepC and BepF were shown to orchestrate the invasion of huge bacterial aggregates into endothelial or epithelial cells, a process called invasome formation (11).

Bh harbors three FIC-domain containing effector proteins (BepA, BepB nd BepC) and one antitoxin (biaA) that is encoded upstream of BepA (41). While the physiological role of the FIC-domain of BepA and BepB are unclear, BepC is required for invasome formation. Here, we aim to gain first insights into the role of BiaA in the context of *Bartonella* infections.

3.4.2 Material & Methods

DNA Manipulations

E. coli Expression Constructs – BiaA of *B. rochalimae* (*Br*) was amplified using prAG0013 (GCCCATGGTGAAAAAAACAACTGATCATTCTAC) and prAG0014 (GCGGATCCTTA TAGTGTTGCATTGTCCATAAGAG) from genomic DNA of *Br* and cloned via NcoI and BamHI restriction into pRSFDUET-1 to achieve pAG0056. The N-terminus of Bep2 of *Br* (Bep2$_{1-360}$) was amplified using prAG029 (GGGAATTCCATATGGATATTAAC ATCCCTTCTCC) and prAG035 (CGACCTCGAGTTAGTGATGGTGATGGTGATGTTC ACTCAAAGCAGCTAA TTTTTC) and introduced via NdeI and XhoI into pAG0056 to achieve pAG0061.

BiaA of *B. henselae* was amplified using prAG007 () and prAG008 () from genomic DNA and cloned via NcoI and BamHI restriction into pRSFDUET-1 to achieve pAG0055. BepA$_{10-303}$ was digested from pAG0001 (38) using NdeI and XhoI and cloned into pAG0055 to achieve pAG0052.

Clean deletion mutants of *Bh* depleted of *biaA* (*Bh* Δ*biaA*) or *biaA* and *bepG* (*Bh* Δ*biaA* Δ*bepG*) were kindly provided by P. Engel.

Protein Purification

Expression and purification of Bep2 from B. rochalimae. Bep2 was co-expressed with BiaA of *B. rochalimae* and purified as previously described (Research article II); In brief, Bep2 was expressed in *E. coli* (DE3) BL21 for 24h at 25°C upon induction with 100uM IPTG (Promega). After lysis in AMPylation buffer (10 mM Tris pH=8.0, 150 mM NaCl, 10 mM MgCl$_2$, 2.5 mM βME) supplemented with 2 mg DNaseI from bovine pancrease (Roche) and Complete EDTA-free Protease Inhibitor Cocktail (Roche) [40 μl/ml of stock solution (1 tablet / 2 ml H$_2$O], Bep2 was purified using metal affinity and size exclusion chromatography. Purified protein was stored at 4°C.

BepA was co-expressed with BiaA of *Bh* and purified via affinity chromatography and size exclusion as described for Bep2 of *Br*.

Immunoblot Analysis

Immunoblot analysis was performed as previously described (42). To detect the BepA expression, total bacterial lysates of *Bh* cultured in M199/10% FCS were separated by SDS-PAGE and transferred onto nitrocellulose membranes (Hybond, Amersham Biosciences). The membranes were thereafter probed with anti-BepA (1:10 000, Laboratory d'Hormonologie, Belgium), primary antibodies and secondary anti-rabbit IgG-HRP antibodies (1:5000).

Infection Assay and Indirect Immunofluorescent Labeling

HeLa ccl2 cells were seeded into 96 well plate with 2000 cells/well and HUVECs cells were seeded in 6 well plate with 200.000 cells/well. Next day, cells were washed once with 100 µL M199 with Earls Salts (M199, Gibco) supplemented with 10% FCS and infected with indicated strains using a multiplicity of infection (MOI) of 100, 300 and 500 bacteria/cell in M199, 10 % FCS. HeLa ccl2 cells were fixated for 8min with 3.7% paraformaldehyde (PFA) after 24 or 48h post induction. Extracellular bacteria, DNA and F-actin were stained and cells were automatically imaged in three different wavelengths (Truttmann, 2010). Indirect immunofluorescent-labeling was performed as previously described (Dehio, 1997). In brief, cells were permeabilized with 0.1% TritonX and microtubules were labeled using mouse monoclonal anti-β-tubulin antibody (Thermo Scientific, 1:100) and Goat anti-mouse IgG (H+L) Alexa Fluor 488 (Molecular Probes, 1:300). DNA was stained with DAPI (Roche, final concentration 1ug mL).

HUVECs were trypsinized 48 h post infections and used for qPCR to quantify *crem* relative expression as previously described (15).

3.4.3 Results

BepA stably interacts with BiaA of *B. henselae*

In previous studies by A. Harms (43), BiaA of *B. rochalimae* (*Br*) was shown to bind to a downstream encoded effector protein Bep1. As *Br* cannot be modified genetically and is not established in *in vitro* infections assays, we chose *B. henselae* (*Bh*) as a model organism to address the function of BiaA. In order to investigate if a complex between BiaA and the downstream encoded Fic protein, BepA, in *Bh* is formed, both proteins were co-expressed and BepA was purified from *E. coli*. BepA consists of an N-terminal FIC-domain followed by an OB-fold (oligo nucleotide/saccharide binding) and a C-terminal BID domain (*Bartonella* intracellular delivery) that serves as translocation signal. Previously, the N-terminal FIC-domain together with the OB-fold was shown to be sufficient for target AMPylation though potential targets remain unidentified (38). To increase solubility of the protein, the C-terminal BID was deleted and a truncated construct of BepA (BepA$_{10-303}$) was co-expressed with BiaA. Next, BepA was purified via a C-terminal His-tag using affinity chromatography and size exclusion. SDS-gelelectrophoresis and Coomassie-staining revealed the enrichment of another protein with the approximate size of the antitoxin (Figure 1).

In order to investigate the specificity of antitoxins of *Bartonella spp.* towards its interacting Fic protein, we tested if a given antitoxin is also forming a complex with a Fic protein that is not encoded within the same gene locus. To this end, we chose the antitoxin of *Br* that was shown to form a stable complex with Bep1 and tested its competence to interact with Bep2 of the same *Bartonella* species. Therefore, a truncated construct of Bep2 that is depleted in its BID-domain was co-expressed with BiaA and purified via affinity chromatography and size exclusion. Again, SDS-gelelectrophoresis and Coomassie staining revealed the specific enrichment of a small protein in the approximate size of the antitoxin.

BiaA does not influence BepA expression of *B. henselae*

While the antitoxin of *B. schoenbuchensis* (VbhA) was previously described to prevent toxicity of the expressed Fic protein when expressed in bacteria (5), we next tested if BiaA is also required for bacterial growth of *Bh*. To this end, *biaA* was deleted and the viability of a clean

deletion mutant was tested. As no growth defect was apparent, we investigated if protein levels of BepA as an example for an antitoxin binding Fic protein were altered in the deletion mutant.

Hence, *Bh* was cultured in M199-medium containing FCS to induce the expression of pathogenicity associated factors like BepA. Western blot analysis indicated no major difference of BepA protein levels in the presence or absence of the antitoxin.

In order to test if the antitoxin is required for expression of other Beps, we aimed to test Bep1 and Bep2 expression of *Br*. As *Br* is not genetically modifiable, we intended to complement a *Bh* effector free mutant (*Bh ΔbepA-bepG*) with Bep2 of *Br*. Yet, conjugation with a plasmid encoding *bep2* did not result in *Bh ΔbepA-bepG* expressing Bep2 indicating a toxic effect of Bep2 in *Bh*.

BiaA is not essential for Fic protein translocation

As BiaA of *B. henselae* had no influence on BepA expression, we aimed to assess if it is required for effector functionality during infection. We therefore tested if BepA-dependent cAMP-elevation is affected by the absence of BiaA. To this end, we infected HUVECs cells with wild-type, *Bh ΔbepA-bepG* or *Bh ΔbiaA* and indirectly assessed cAMP-elevation by quantification of *crem* expression levels (15). As relative crem levels after infection were independent of the presence of BiaA, it seems not essential for effector translocation (Figure 3).

Apart from BepA, *Bh* translocates another two Fic proteins into the eukaryotic host cell, BepB and BepC. While the role of the FIC-domains of BepA and BepB remain unknown, BepC in combination with BepF was shown to induce the uptake of large bacterial aggregates, a process known as invasome formation.

To investigate a potential role of BiaA in effector functionality and translocation, we performed infection assays with *biaA* deleted strain (*Bh ΔbiaA ΔbepG*). This strain also carried a deletion of *bepG*, which pevents invasome formation by an alternative pathway. Hence, invasome formation of this mutant is fully dependent on BepC and BepF (11) and can thus be used as a direct read-out for BepC functionality.

While infection with the effector free mutant (*Bh ΔbepA-bepG*) did not lead to invasome formation, infections with both strains, *Bh ΔbepG* and *Bh ΔbiaA ΔbepG*, induced bacterial aggregation and actin rearrangements (Figure 4).

3.4.4 Discussion and Outlook

In this study, we addressed the role of the antitoxin in the context of *Bartonella* infection. To this end, we investigated if the antitoxin, BiaA, is essential for Bep expression and translocation in *in vitro* infection assays.

We started by validating BiaA binding to *Bartonella henselae* virulence factors by co-expression of BepA of *B. henselae* with the upstream encoded BiaA and subsequent purification. In fact, purification of BepA yielded in co-enrichment of a protein of the approximate size of the antitoxin indicating that BepA forms a stable complex with BiaA.

As *Bartonella spp.* encode for less antitoxins than Fic proteins, we next investigated the specificity of BiaA. Thus, we chose the example of *B. rochalimae* and its *biaA* homolog that was previously shown to bind to Bep1 and tested its affinity towards the FIC-domain containing protein, Bep2. In fact, we could show for the first time that BiaA is not specific for one Fic protein but can bind to several Fic proteins. This indicates that the antitoxin is playing a more global role instead of being confined to the regulation of the activity of one effector. In ongoing studies, we will further test if this lack of specificity is a generic feature of all antitoxins or unique to the one of *B. rochalimae*.

For type III secretion (T3S) effectors, chaperones were identified that keep the effectors partially unfolded to allow secretion but also are involved in regulation of effector levels and temporal control of secretion. An example for this regulation is SopE of *S. typhimurium* and its chaperon SicA that is also involved in the transcriptional regulation of SopE (44, 45).

In order to investigate if the antitoxin is acting similarly as T3S chaperones, we next tested BiaAs influence on effector expression and translocation using deletion mutant of *Bh*. Compared to wild-type, expression of BepA, BepA-mediated elevation of cAMP-levels and invasome formation were not significantly inhibited in the *biaA* mutant. This indicats that the role of BiaA is confined the control of activity. Yet, it should be noted that *in vitro* infections with *Bartonella* were performed in nutrient rich media and therefore under unselective conditions which might mask subtle growth defects of the antitoxin mutant.

Interestingly, expression of Bep2 of *Br* that was shown to AMPylated tubulin and vimentin was toxic when expressed in an effector free mutant of *Bh*. As tubulin and vimentin are not structurally related, Bep2 activity seems to have low target specificity. It is thus tempting to

speculate, that Bep2 also AMPylates tubulin-homologs within bacteria like FtsZ which leads to its toxic effect. We therefore hypothesize that the antitoxins role might be the inhibition of effector activity within the pathogen thus the reduction of toxicity due to unspecific target AMPylation which is further investigated in ongoing studies.
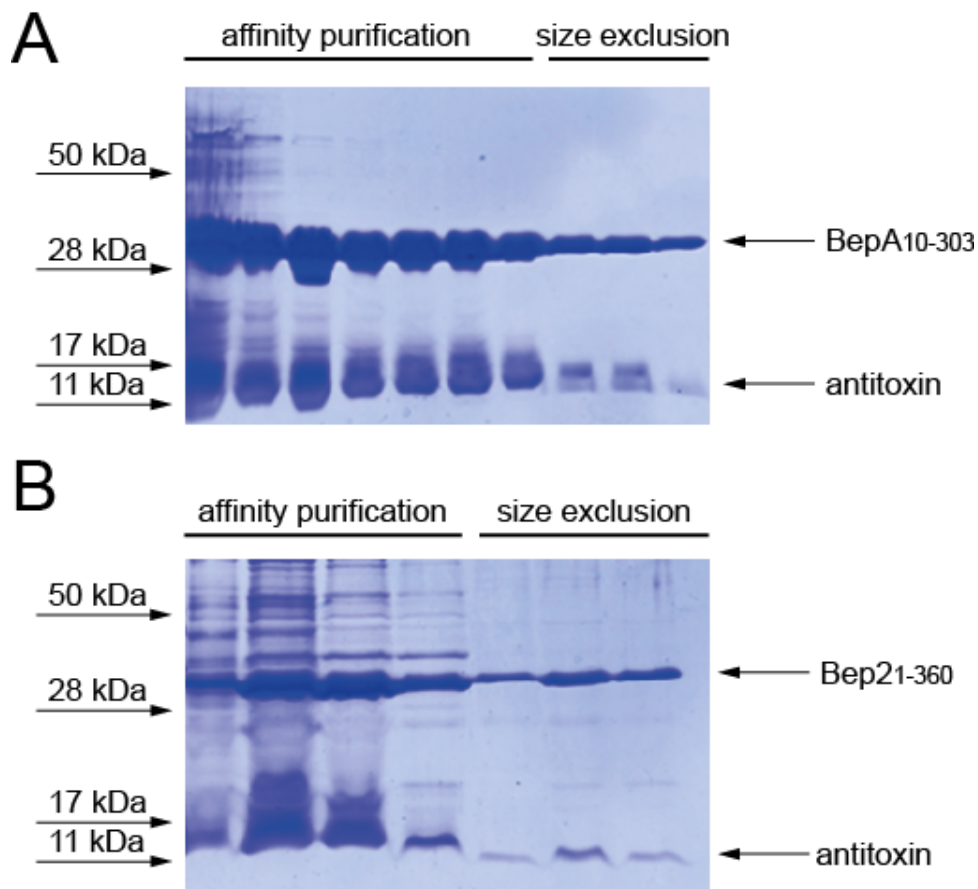
Figure 1.: BiaA of *Bh* binds BepA and BiaA of *Br* binds Bep2. Coomassie-stained SDS-PAGE gel of peak fractions after affinity chromatography using Ni-NTA and after gel filtration. A) Purification of BepA after co-expression together with BiaA of *Bh* in *E. coli*. B) Purification of Bep2 of *Br* upon co-expression with the antitoxin in *E. coli*. For both, BepA of *Bh* and Bep2 of *Br*, co-purification of a small protein with the approximate size of the antitoxin was detected.
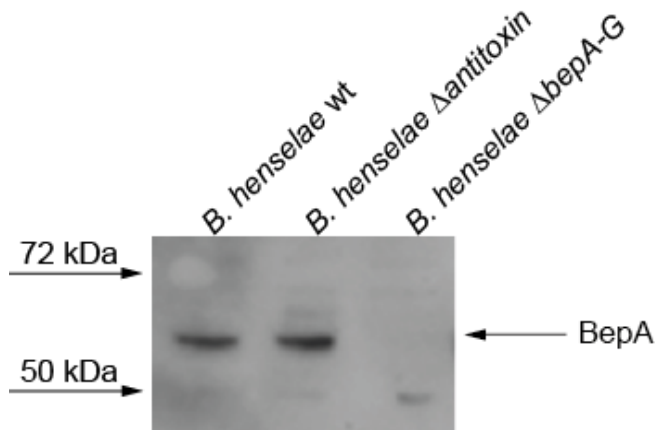
Figure 2.: Endogenous levels of BepA of *B. henselae* in the presence and absence of the antitoxin. Immunoblot analysis of total bacterial lysates of the indicated *B. henselae* strains was performed with an antibodies directed against BepA. Depletion of the antitoxin had no detectable influence on BepA expression.
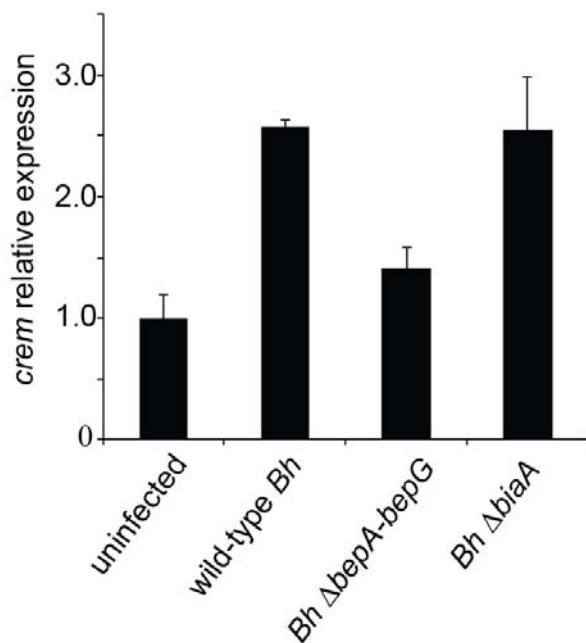
Figure 3.: BepA-mediated elevation of cAMP-levels is independent of BiaA. HUVECs were infected with indicated strains for 48 h and crem expression levels were quantified using qPCR (15). *Crem* expression levels were normalized to level of uninfected conditions.
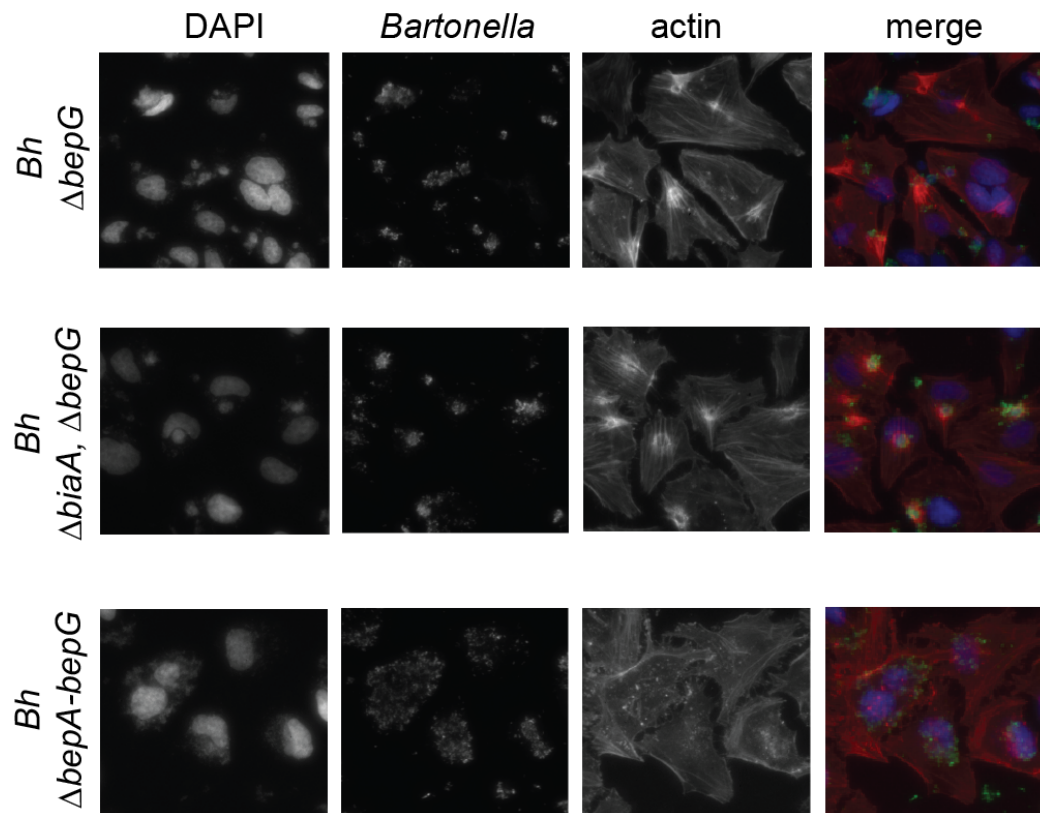
Figure 4.: Invasome formation is independent of BiaA. HeLa ccl2 cells infected with the indicated *B. henselae* strains at MOI of 100 for 48h were fixed, stained with TRITC-labelled phalloidin, DAPI and an antibody directed against Bartonella followed by fluorescent microscopy. In contrast to *Bh ΔbepA-bepG*, both strains, *Bh ΔbepG* and *Bh ΔbiaA ΔbepG*, lead to invasome formation.

3.5 BepC induces actin polymerization and bacterial aggregation

3.5.1 Introduction

The Gram-negative bacterium *Bartonella henselae* (*Bh*) is a worldwide distributed zoonotic pathogen that causes intraerythrocytic bacteremia in its feline reservoir host (cats). Upon transmission into humans, *Bh* can cause cat-scratch disease in immune competent patients but also pathologies like bacillary angiomatosis and peliosis that are characterized by tumor-like lesions of the vasculature in immune-compromised patients.

Once transmitted to a new host, *Bh* translocates seven effector proteins (BepA-G) into the eukaryotic host cell via a VirB/VirD4 type IV secretion system. Beps are then hijacking the host cell system thereby promoting a variety of distinct phenotypes like inhibition of host cell apoptosis (10), activation of the pro-inflammatory response (46), sprout formation of endothelial cells (47) and invasion of huge bacterial aggregates into endothelial or epithelial cells, a process called invasome formation (11). Furthermore, *Bh* was shown to engage integrin-mediated outside-in and inside-out signaling in a Bep-dependent manner which on the one hand induces engulfment of the pathogen by actin rearrangements but also mediates pathogen attachment to the cell and clusters at the site of entry.

In previous studies, BepG alone as well as the combination of BepC and BepF were shown to be sufficient for invasome formation by interference of the Rac1/Scr/WAVE/Arp2/3 and Cdc42/WASP/Arp2/3 pathways which induced F-actin polymerization (11). Although BepG suffices for bacterial engulfment, BepC was shown to drastically increase invasome formation.

While BepF was identified to induce nucleotide exchange of Cdc42 (GEF activity) thereby directly regulating the activity of small GTPases, the molecular function of BepC remains unknown (48). In addition to a C-terminal BID-domain, BepC harbors an N-terminal FIC-domain. Recently, secreted FIC-domain containing proteins of *Vibrio parahaemolyticus*, VopS, and *Histophilus somni*, IbpA, were shown to perform AMPylation on Rho family GTPases thereby impairing the binding of downstream effectors and thus inhibiting GTPase signaling. Yet, BepC did not show target AMPylation and only weak auto-AMPylation in *in vitro* studies (43). The molecular detail of BepC-mediated bacterial entry thus remained elusive.

Here, we present that BepC is sufficient to induce F-actin polymerization locally as a first step of invasome formation.

3.5.2 Materials and Methods

Cell culture and bacterial strains

HeLa ccl2 and HUVECs were cultured in DMEM (Gibco) supplemented with 10% fetal calf serum (FCS, invitrogen).

Wild type *Bartonella henselae* (*Bh*) and the mutant of *Bh* that is depleted in its effector proteins (*Bh ΔbepA-bepG*) were grown on Colombia agar plates containing 5% defibrinated sheep blood (CBA-plates) for 2d at 35°C, 5% CO_2. *Bh ΔbepA-bepG* complemented with BepC (*Bh ΔbepA-bepG*/p*bepC*) or complemented with BepF (*Bh ΔbepA-bepG*/p*bepF*) was grown on Colombia agar plates containing 10ug/mL Gentamycin sulfate and 5% defibrinated sheep blood (Gm CBA-plates) for 2d at 35°C, 5% CO_2.

In vitro infections assays

HeLa ccl2 cells were seeded into 96 well plate with 2000 cells/well. Next day, cells were washed once with 100 µL M199 with Earls Salts (M199, Gibco) supplemented with 10% FCS and infected with *Bh wt*, *Bh ΔbepA-bepG*, *Bh ΔbepA-bepG* p*bepC* or double infected with *Bh ΔbepA-bepG*/p*bepC* and *Bh ΔbepA-bepG*/p*bepF* using a multiplicity of infection (MOI) of 100, 200 and 300 bacteria/cell in M199, 10 % FCS supplemented with 500 µM IPTG. Cells were fixated for 8 min at RT with 3.7% paraformaldehyde (PFA) after 24 h or 48 h post induction.

DNA and F-actin were immunofluorescently labeled and cells were automatically imaged in three different wavelengths (12).

Immunofluorescent labeling

Indirect immunoflurecent-labeling was performed as previously described (49). In brief, extracellular bacteria were labeled using serum 2037 (rabbit polyclonal anti-Bartonella total bacteria, 1:100) and Goat anti-rabbit IgG (H+L) Alexa Fluor 488 (Molecular Probes, 1:100) prior to permeabilization with 0.1% TritonX. F-actin was labeled with TRITC-phalloidine (Sigma, 100 µg/mL Stock solution, final concentration 1:400) and DNA was stained with DAPI (Roche, final concentration 1 µg/mL).

3.5.3 Results

BepC is increasing F-actin polymerization

In previous studies, the combination of BepC and BepF was found to induce invasome formation whereas BepC alone was not sufficient. In order to gain insights into the molecular function of BepC, we performed infection assay with *Bh* that is depleted of its endogenous effector proteins (*Bh ΔbepA-bepG*) but expresses BepC ectopically (*Bh ΔbepA-bepG*/p*bepC*). As invasome formation requires massive cytoskeleton rearrangements, infected cells were analyzed for changes in F-actin polymerization. To this end, F-actin of *Bh ΔbepA-bepG*/p*bepC* infected cells was immunofluorescently labeled and compared to cells that were infected with *Bh ΔbepA-bepG* or *Bh ΔbepA-bepG*/p*bepF*.

While bacteria of *Bh ΔbepA-bepG* and *Bh ΔbepA-bepG*/p*bepF* were spread on top of the cells, *Bh ΔbepA-bepG*/p*bepC* were partially forming round aggregates. As shown in Figure 1, infection with *Bh ΔbepA-bepG* and complementation with BepF resulted in the formation of small granola of F-actin but no loci of strong actin polymerization. However, HUVECs infected with *Bh ΔbepA-G* complemented with BepC contained strong F-actin signals that were found in the same area as bacterial aggregates. Double infections of *Bh ΔbepA-G*/p*bepC* and *Bh ΔbepA-G*/p*bepF* lead to invasome formation that is identified by circular structures of actin at bacteria-rich sites as previously described (11).

3.5.4 Conclusion and Outlook

Here, we were able to show a BepC-mediated actin polymerization within the host cell at the site of bacterial entry. As a local cytoskeleton rearrangement and an actin accumulation is also observed during invasome formation, BepC-mediated actin polymerization is potentially a critical step in bacterial uptake. Additionally, cells infected with *Bh ΔbepA-G* p*bepF* formed actin granola, a characteristic phenotype of Cdcd42 activation. Consistently, BepF was shown in previous studies to function as a GEF of Cdc42.

BepC is one of three FIC-domain containing Beps of the pathogen *Bh*. While the FIC-domain containing effector proteins IbpA and VopS were shown to AMPylate small GTPases of the Rho family, preliminary studies of BepC did not indicate a similar function (43). Yet, as actin nucleation and polymerization is controlled by GTPase-signaling, BepC-mediated actin polymerization might be a first indication of an influence of BepC on GTPase signaling.

Although the target of BepC as well as its biochemical activity remains elusive at this point, the observed phenotype offers a direct read-out of BepC functionality and will be valuable in ongoing studies to identify its target protein, e.g. by siRNA screens.

Apart from the cellular effect of F-actin formation, BepC also induced the formation of bacterial aggregates which are characteristic for invasome formation. The aggregate formation could either be induced by increased inter-bacterial adhesion implying a bacterial target of BepC or by an increase of attachment to the host cell. As integrin signaling, especially by integrinβ1, was shown to mediate both of the BepC-dependent phenotypes described here (cytoskeleton rearrangements and pathogen attachment), it is tempting to speculate that BepC targets proteins that directly or indirectly influence integrin signaling.
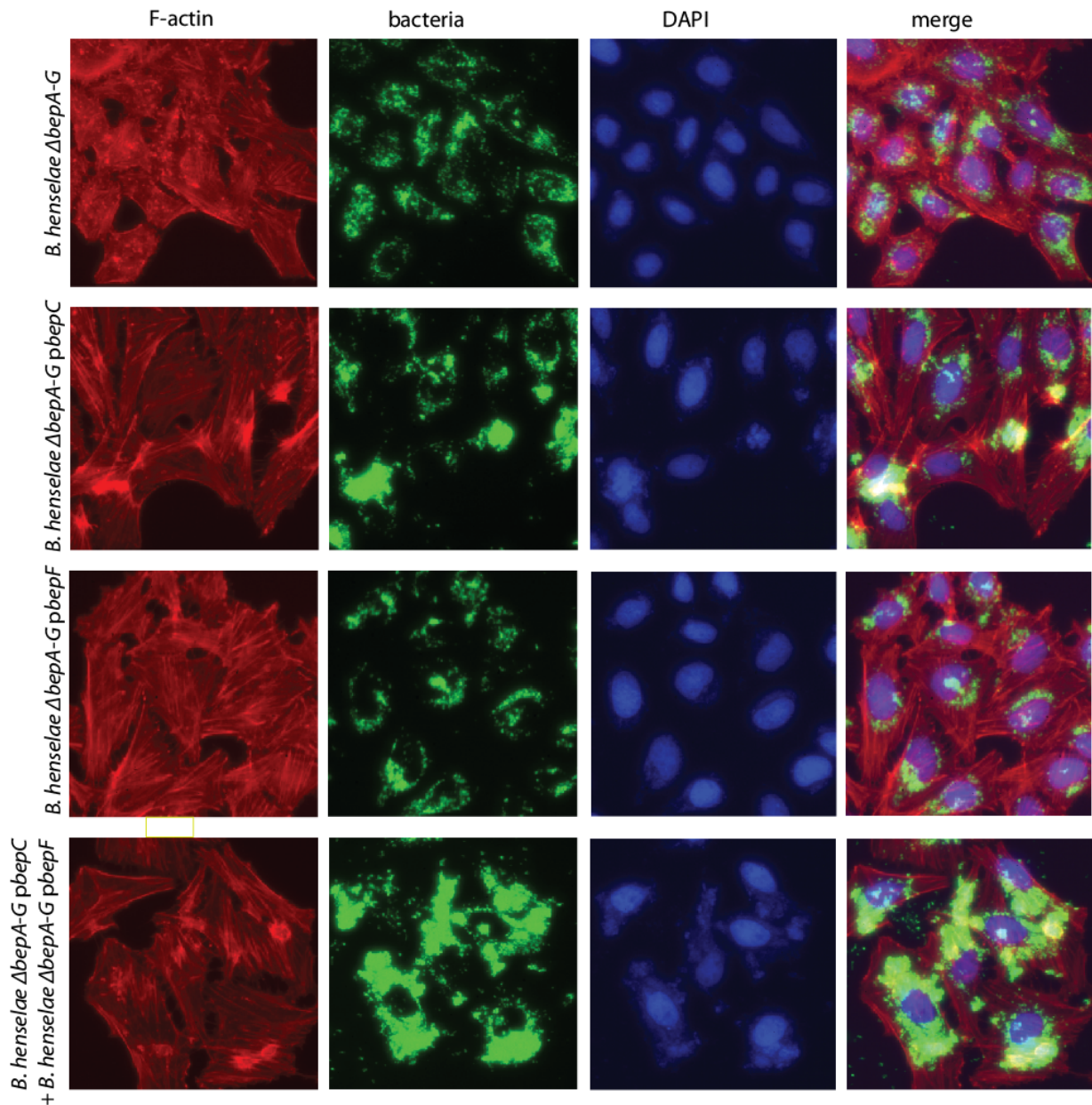
Figure 1.: BepC induces local actin polymerization in *in vitro* infection assays with HUVECS. Depicted are representative images of HUVECs that were infected with indicated *B. henselae* strains for 48 h with a MOI of 100. Cells were fixed, stained with TRITC-labelled phalloidin, DAPI and an antibody directed against *Bartonella* followed by fluorescent microscopy. Infection with *B. henselae* Δ*bepA-bepG*/p*bepC* resulted in local actin polymerization at the site bacterial aggregation on cell periphery.

4. Conclusions and Outlook

4.1 Cell type dependence of BepA homologs

Already a decade ago, *Bartonella henselae* was found to induce host cell proliferation by the inhibition of apoptosis (50). Subsequently, this phenomenon was linked to a reduction in caspase-3 activation and an increase in transcription of caspase IAPs (inhibitors of activation) (51). Furthermore, the type IV secretion effector BepA was found to be a key factor in the inhibition of host cell apoptosis (15). In 2006, domain analysis revealed that the C-terminal BID-domain is sufficient to elevate cAMP-levels and subsequently inhibit caspase-3 activity (15). While the BID-domains were shown to be required for effector translocation, the BID-domain of BepA is hence the first identified BID-domain with a second distinct cellular function.

In this study, we could show that BepA elevates AC-activity synergistically with $G\alpha_s$ and demonstrate a direct interaction between AC and BepA (see *Reasearch Article I*) (10). Furthermore, our data on biomolecular fluorescence cytometry indicate that BepA and $G\alpha_s$ are in close proximity during cellular elevation of cAMP-levels. Yet, *in vitro* assays with the plant diterpene Forskolin revealed that BepA-function is independent of $G\alpha_s$, but requires an initial coordination of the cytosolic AC-domains. Forskolin and $G\alpha_s$ synergistically increase AC-activity (52) by coordination of the cytosolic AC-domains into an active conformation with the active pocket at their interface (53). It is thus envisioned that BepA interacts with one or even both cytosolic AC-domains and captures them in an optimal coordination thereby increasing the efficiency of cAMP-production. Hence, studying the mechanism of BepA-mediated increase of AC-activity would also further the understanding of AC-dynamics which is highly interesting for the design of innovative therapeutics (54).

In addition to the BID-domain of BepA of *B. henselae* (BIDA-*Bh*), also the BID-domain of the closely related BepA ortholog of *B. quintana* (BIDA-*Bq*) was identified to inhibit apoptosis of human endothelial cells. Yet, neither the BID-domain of BepA of *B. tribocorum* (BIDA-*Bt*) -nor the paralogs BepB-*Bh* and BepC-*Bh* showed a similar activity (15). The BID-domain of BepA-*Bh* shares a sequence identity of about 40%, 50% and 57% with the BID-domain of its paralogs BepB-*Bh* (BIDB-*Bh*), BepC-*Bh* (BIDC-*Bh*) and with the orthologous BIDA-*Bt*, respectively. However, the BepA ortholog in *Bartonella quintana* (BepA-*Bq*) shows a higher sequence identity with BepA-*Bh* of approximately 64%. While the residues that are conserved only in BepA-*Bh*

and BepA-*Bq* could be essential for functionality, they are scattered over the entire sequence of the BID-domain (see appendix, Figure A1). This indicates that either only few residues at distinct protein sites mediate functionality or that, rather than the single residue identity, the overall surface properties of the BID-domain is required for the BepA-AC interaction that leads to increased AC-activity. One of these properties could be hydrophobicity and, in fact, comparison of hydrophobicity distribution reveals a high similarity between BIDA-*Bh* and BIDA-*Bq* and even BIDA-*Bt* but a low similarity for BIDB-*Bh* and BIDC-*Bh*, which are thus excluded by this criterion. Such exclusion does not apply for BidA-*Bt*, which shows a similar hydrophobicity pattern to BepA-*Bh* and BepA-*Bq* (see appendix, Figure A2-A5).

However, BepA-AC interaction is also dependent on the AC surface. While the sequence in orthologs of distinct AC isoform can be highly conserved within mammals (AC isoform 2 proteins in rat and human share a sequence identity of 98% in their cytosolic domains), conservation between different isoforms is much lower (55, 56). Accordingly, BepA-mediated activation of ACs could be isoform-dependent and preliminary assays indicated that BepA$_{Bh}$ cannot increase the activity of AC isoform 5 (data not shown). AC isoforms are tissue-specific and, in fact, endothelial cells express only a subset of them. The differential expression of AC isoforms might explain a potential cell type specificity of BepA. In fact, endothelial cells only express a subset of AC isoforms which is also tissue dependent (57). In consequence, it is not contradictory that BIDA-*Bt* does not lead to cAMP-elevation in HUVECs but at the same time potentially increases intracellular cAMP-production in other cell types.

The conservation of BepA within lineage 4 *Bartonellae* indicates that BepA orthologs still harbor an activity that contributes to pathogenicity. Potentially, this involves cAMP elevation in other cell types like macrophages or dendritic cells.

4.2 cAMP in pathogenicity

In creased intracellular cAMP production leads to caspase-3 inhibition and thus to prevention of apoptosis. Enhanced survival of vascular endothelial cells as the replicative niche of *B. henselae* sustains and promotes the persistence and replication of the intracellular pathogen. It may also explain the vasoproliferative effect observed with B. henseale infections. Howerver, cellular

responses to cAMP-signaling are cell-type dependent (15, 47). In fact, BepA-*Bh*-mediated cAMP elevation and influence on apoptosis is cell type dependent; While BepA inhibits apoptosis in HUVECs, it triggers apoptosis in Ea.hy926 cells (A. Pulliainen, data unpublished). Moreover, cAMP-signaling is not confined to apoptosis regulation but influences a plethora of cellular functions. It remains unclear if BepA-mediated cAMP elevation also benefits *Bartonella* pathogenicity at earlier stages of infection, e.g. by controlling inflammatory response. *Bartonella* spp. are mostly transmitted by either arthropods or by direct contacts with wounds (e.g. cat scratch in the case of *B. henselae*) and both ways of transmission induce a local inflammation of the host organism (58, 59). At this stage of infection, the pathogen is confronted with different immune cells and a potential control of apoptosis of professional phagocytes might ensure pathogen survival as described for *Shigella* and *Salmonella* (60, 61).

In addition, *Bartonella* spp. is proposed to travel to the lymph node via migratory cells, e.g. dendritic cells (59, 62). While antigen recognition by dendritic cells is known to increase their lifetime, it also leads to production of inflammatory markers and cytokines to activate T-cells and to induce inflammation. Two of these cytokines are MIP-1α and MIP-1β (also referred to as CCL3 and CCL4) that play key roles in inflammation signaling (63). Interestingly, cAMP-elevation inhibits the release of both markers from dendritic cells via an Epac1-dependent pathways (64). Therefore, the BepA-mediated increase in cAMP-levels could also directly interfere with inflammatory responses and simplify pathogen transport to the still elusive primary niche.

As cAMP regulates a vast number of signaling events, controlling its cellular levels allows a multifaceted manipulation of the host by a single bacterial effector although to be beneficial for pathogen persistence, this manipulation requires a high level of regulation. Apart from instability of the protein, BepA-function could possibly be controlled by additional domains or by other effectors of *Bartonella* as recently shown for BepE that decreases cytotoxic side effects of BepC (62). Interestingly, most BepA orthologs harbor an additional N-terminal FIC-domain that AMPylates unidentified targets that may further contribute to cellular effects of BepA as discussed in the following sections.

4.3 Fic proteins subvert host cell function by introducing post translational modification

A FIC-domain which was previously shown on the example of BepA-*Bh* to AMPylate unidentified host cell targets is present in most BepA-orthologs (38). As the BID-domain is sufficient to locate the whole protein at the plasma membrane and, in extension, interacts with the AC (10), the FIC-domain is possibly targeting a protein that is also located at the membrane and potentially plays a role in AC activation. Consistently with this hypothesis, the size of FIC_{BepA} targets is approximately 45 kDA as estimated by radioactive AMPylation assays which is in the range of Gα-subunits. In ongoing studies, we aim to identify the target of the FIC-domain of $BepA_{Bh}$ and its role in infection.

To this end, we established a strategy for target identification in complex samples like crude cell lysates that does not rely on stable interactions or chemically modified substrates which might impair enzyme activity (see *Reasearch Article II*) (65, 66). We used stable isotope-labeled ATP leading to distinct reporter ion-clusters in LC-MS analysis by which modified peptides can be identified. In addition to target identification, the established strategy also allows activity comparisons between mutants. In order to establish the procedure, we used the effector protein Bep2 of *B. rochalimae* ($Bep2_{Br}$) as its *in vitro* AMPylation activity was stronger than BepA-*Bh* under the used conditions and indicated a target of approximately 50 kDa (38, 43). Using the here established mass spectrometry-based strategy, we identified tubulin and vimentin as targets of Bep2 AMPylation-activity. While these proteins are highly abundant in any cell type, the level of modified peptides might be lower for different targets of other Fic proteins (e.g. BepA-*Bh*). This would impair identification of modified peptides due to undersampling effects. Hence, we are currently integrating additional fractionating steps and automated spectral analysis that is based on peak patterns to reduce sample complexity and make the consequentially challenging analysis easier.

While the Fic-domain containing effector proteins IbpA, VopS and AnkX were reported to only target small GTPases, we identified tubulin and vimentin as AMPylation targets of Bep2. Both target proteins are structurally unrelated to small GTPases and are thus representing new classes of Fic targets.

AMPylation targets are not only found on the mammalian host side, but also in bacteria. VbhT, a FIC-domain containing effector protein of *B. schoenbuchensis*, was described to AMPylate a bacterial target protein of higher molecular weight (5). Recent advances allowed the identification of topo-IV-isomerase as targets of VbhT-mediated AMPylation that causes severe growth defects in bacteria (A. Harms, unpublished data).

Interestingly, BepA$_{Bh}$, Bep2$_{Br}$ and VbhT target proteins outside of the class of small GTPases and all three show structural differences to other Fic proteins (5, 38). VopS and IbpA share similarities in their arm-domain that mediates contact to a highly conserved α-helix of Rho GTPase. The high sequence identity of 94% between Rac1, Cdc42 and RhoA in this α-helix (see appendix Figure A…) most likely causes the promiscuous AMPylation of all Rho GTPases by IbpA and VopS (28). In contrast, AnkX does not harbor a similar arm-domain but an additional β-hairpin loop that is positioned in an insert domain on top of the active groove (67). Consistently, AnkX is not targeting Rho GTPases but specifically modifies Rab1 and Rab35 (68). Apart from the lack of an arm domain, the insert domain also blocks sterically the interaction of the β-hairpin loop with target proteins indicating a completely different molecular basis for target recognition (67). AnkX further harbors a CMP-binding domain that coordinates the substrate and several ankyrine repeats that interact with the FIC-domain and are proposed to function as a scaffolding domain (67).

BepA$_{Bh}$ and VbhT structurally differ from the other described Fic proteins and neither harbor an arm-domain like IbpA nor an insert domain like AnkX (5, 38). Instead, all crystal structures of Beps revealed an N-terminal loop at the interface between FIC-domain and target (Figure 4.3.1, also see appendix Figure A6). Due to the position of this mainly unstructured loop, it could potentially be involved in target recognition or activity regulation. Accordingly, this loop might adopt a more structured conformation upon target recognition and thereby stabilize the complex. Alternatively, it could serve as a flexible shield that, when moved out, leaves the active site exposed and possibly move out leaving the active site exposed. A potential trigger for the required movement of the loop could be auto-AMPylation by the Fic protein. Interestingly, VbhT was found to self-modify a tyrosine within this N-terminal loop (Y6, unpublished data of P. Engel).

Beps also differ from other Fic proteins, by the OB-fold and the C-terminal BID-domain that is required for effector translocation into the eukaryotic host cell via the type IV secretion system

(T4SS) (13). The BID-domains of some Beps have acquired additional functions and/or are directing the effector to cellular compartments upon translocation as shown for BID-*Bh* (10, 48). Yet, a role of the BID-domains in Fic protein regulation remains unknown. Interestingly, one effector of *B. henselae*, BepC, seems to require both domains for its functionality (69). In previous studies, BepC was described to act synergistically with BepF or BepG in the uptake of bacterial aggregates via invasome formation (11). While ectopically expressed BepC was active and allowed invasome formation in infection studies, truncated constructs that were depleted of the FIC- or the BID-domain were not sufficient to enable this type of bacterial uptake (69). To investigate if the BID-domain is required for FIC-activity, we aim to identify targets of BepC.
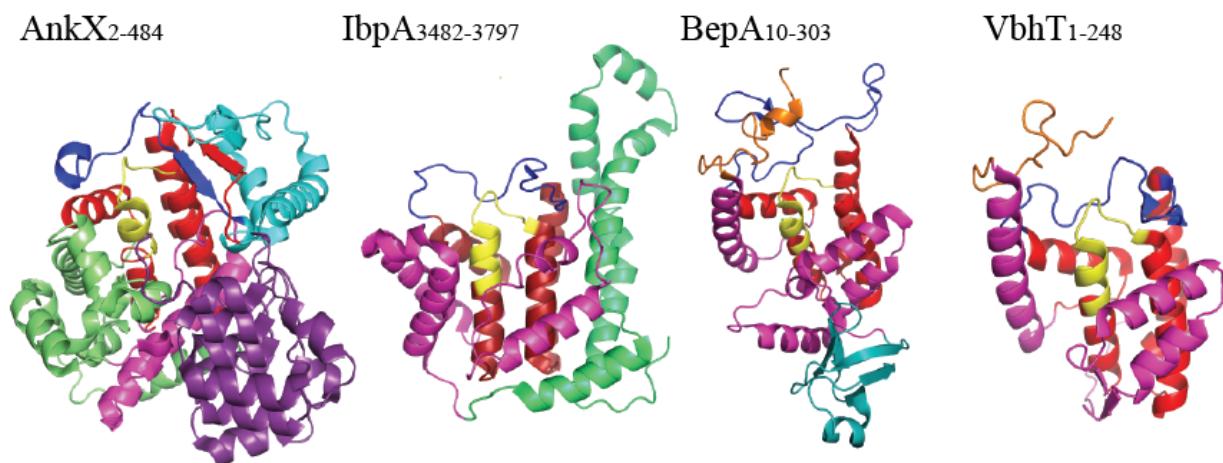
Figure 4.3.1: Target recognition motifs of different Fic proteins. Crystal structures of AnkX of *L. pneumophila*, IbpA of *H. somni*, BepA of *B. henselae* and VbhT of *B. schoenbuchensis* are shown in ribbon style. Each FIC-domain is colored in magenta with the FIC-core in red and the corresponding signature motif in yellow. The CMP-binding domain of AnkX is colored in green, ankyrin repeats in purple and insert domain in cyan. The arm domain of IbpA is colored in limegreen, the N-terminal loops of BepA and VbhT are colored in orange. The β-hairpin loops that were associated with target recognition by main chain-main chain interactions are colored in dark blue for all four structures.

4.4 Diversification of target recognition by Fic proteins

Of note, *in vitro* infections with *Vibrio parahaemolyticus* are cytotoxic, an effect that could be linked to the AMPylation activity of VopS (2). In contrast, infections with *Legionella pneumophila*, that secrete the Fic protein AnkX, are less toxic to the cell presumably due to the

high level of effector regulation (70). Several activities of *Legionella* effector proteins were shown to be subjected to spatiotemporal regulation by other secreted effectors, e.g., the phosphocholinating enzyme AnkX that is counteracted by the de-phosphocholinating enzyme Lem3 (71).

Although lineage 4 *Bartonella* secrete up to three Fic proteins, most *in vitro* infections of cell cultures with *Bartonella* are not toxic but rather inhibit host cell apoptosis. Yet, *in silico* analysis did not identify homologs of Lem3 that could reverse Bep-mediated covalent modifications. It is thus tempting to speculate that either a higher specificity of Bep-mediated AMPylation or a switch in target recognition reduces cytotoxic side effects to the benefit of the stealthy and persistent life style of intracellular *Bartonella* (8, 43). One example of an increase in target specificity is Bep1 of *B. rochalimae* that was found to AMPylate Rac1 but not Cdc42 or RhoA (41, 43). In contrast, Bep2 of *B. rochalimae* shows lower specificity and a switch of targets as it modifies both tubulin and vimentin that are not structurally related.

While a decrease in target specificity allows one effector to manipulate multiple cellular processes, it might also lead to deleterious side effects if also bacterial proteins may be targeted prior to secretion. Yet, AMPylation can be inhibited by an additional helix that either either encoded within the Fic protein or within small proteins called antitoxins that bind Fic proteins and interfere with substrate coordination (5, 27). We reported here on the example of a homolog of *B. rochalimae* that antitoxins are not specific for one Fic protein but are potently binding and inhibiting several of them. Our studies on an antitoxin homolog from *B. henselae* further indicate that the antitoxin is not essential for effector expression and translocation. It is thus envisioned that the antitoxin prohibits bactericidal side effects of Fic proteins, but is supposedly released from the effector during the process of translocation and thereby allows injection of a competent effector into the host cell.

4.5 AMPylation may regulate vimentin filaments

In contrast to small GTPases, vimentin does not bind any nucleotide and is therefore refuting the common hypothesis that Fic protein-mediated AMPylation is confined to NTPases. Identification of vimentin as an AMPylation target of Bep2 thus opened a completely new class of targets. Yet,

it remains elusive if vimentin-AMPylation has the same implication as GTPase-AMPylation, i.e., interruption of protein-protein interactions. In fact, other PTMs and in particular serine-phosphorylation were previously reported to interfere with vimentin polymerization, possibly by charge repulsions within the polymer leading to depolymerization of filaments (72, 73). Interestingly, the serine sites that are most prominent in polymerization control are located within the head domain in close proximity of the identified AMPylation residue (72, 74). AMPylation might thus potentially contribute to filament depolymerization. Apart from the contribution to cell shape as a component of the cytoskeleton, vimentin dynamics are associated with a variety of cellular responses ranging from inflammation control by NF-κB to autophagy or microbicidal activity of macrophages (75-77). In addition to vimentin, we also found Bep2 to modify tubulin which potentially indicates that Bep2 targets both proteins by interfering in cellular mechanism that involve both vimentin and tubulin. One process is the NF-κB induction by IbeA+ of *E. coli* K1 for which it was recently shown that the head domain of vimentin as well as microtubules (MTs) are essential (75). Yet, the molecular details of this induction remain elusive.

Vimentin is a global protein that regulates a variety of adaptor proteins but also protein degradation by ubiquitination (78). Best understood is its role in the recruitment of β-integrins to focal adhesion sites. It reaches focal adhesion sites via the microtubule (MT) network by hijacking plus end driven motor proteins like kinesis (79). Once extended to the focal adhesion sites, vimentin indirectly interacts with β-integrins, especially with β3-integrin, by complex formation with plectin and leads to an increase of cell attachment (79). Though no molecular studies have so far been conducted on the molecular mechanisms of *B. rochalimae* infection, integrin β-signaling was shown to play a role in the uptake of other *Bartonella* species such as *B. henselae* (12) or *B. bacilliformis* (80) that both lack orthologs of Bep2. Our ongoing studies thus aim to uncover the function of Bep2-mediated AMPylation during *B. rochalimae* infections and how it may be related to shared strategies of host cell manipulation by pathogens of the genus *Bartonella*.

4.6 The impact of tubulin AMPylation

In addition to vimentin, we also identified tubulin as an AMPylation target of Bep2 of *B. rochalimae*. TOG-domain containing proteins belong to the XMAP215/Dis1 and CLASP family and are involved in the control of MT dynamics by binding to and dissociating from tubulin in a highly controlled manner (26, 81). While dissociation is required for tubulin polymerization at the growing end of MTs to allow straightening of the αβ-tubulin subunit upon polymerization (19), a stabilized TOG-tubulin complex would increase CLASPs` potential to stabilize existing structures (20). In contrast to AMPylation on small GTPases that disrupts protein-protein interactions, we propose here that AMPylation on tubulin actually strengthens the interaction of MTs to TOG-domain containing proteins based on our pull down experiments and structural model of the complex (see Chapter 3.3).

While the role of microtubules in *Bartonella* pathogenicity remains unclear, it is better understood in bacterial infections with uropathogenic *E. coli* (UPEC), *Clostridium difficile* and *Chlamydia trachomatis*. UPECs indirectly destabilize MTs by their deacetylation leading to a dysfunction of the motor protein kinesin and resulting in increased bacterial entry (37). Kinesin is implicated in the relaxation and disassembly of focal adhesion sites by delivering key signaling factors to the cell membrane. In fact, kinesin is interacting with the actin nucleator WAVE (82) that is also involved in *Bartonella* entry by invasomes (11). Interestingly, UPEC as well as *B. henselae* enter the cell by integrin signaling (12). It is thus tempting to speculate that certain *Bartonella* species, similarly to UPECs, engage MT dynamics to increase pathogen entry.

In contrast, *C. difficile* toxin ADP-ribosylates actin which leads to actin rearrangements but also to microtubule protrusions that exert from the cell, bind the pathogen and increase bacterial entry (83). Further analysis revealed that formation of MT protrusions is independent of Rho GTPase signaling but is caused by a redistribution of capture proteins that direct the MTs to the cell cortex including EB1, CLIP-170 and ACF7 that functionally links MTs and actin (83).

Apart from pathogen entry, MTs also play a key role in cellular trafficking, e.g., endosomal maturation and bacterial redistribution as shown for *C. trachomatis* and *C. pneumonia*. Extracellular *Chlamydiae* are contained in lementary bodies (EB) that enter host cells by parasite-specific phagocytosis (84). Upon entry, EBs become localized with the host cell cytoplasm at membrane bound endosomes that mature to reticulate bodies (RBs) that are metabolically active.

After a growth period, RBs redistribute to the perinuclear region and mature to EBs that are released by bursting of the host cell. Clausen *et al.* could show that both *Chlamydia* species use the microtubule network and the minus end directed motor protein dynein (85) to reach the perinuclear region (86).

Currently, we aim to further the understanding of MT dynamics in *Bartonella* pathogenicity by performance of induced MT catastrophe and rescue assays in dependence of the tubulin-AMPylating Fic protein Bep2 of *B. rochalimae*.

4.7 Fic protein activity is limited to AMPylation

The recently described structural aspects of AnkX and IbpA allowed detailed insight into the mechanism of Fic-mediated post translational modifications (PTMs). While the orientation of the respective nucleotide is inverted between both structures, the mechanism of molecular transfer is conserved with an in-line attack on a phosphate. To this end, IbpA coordinates adenine by F3675, E3671 and Q3757 which results in an in-line attack on the α-phosphate that destabilizes the bond between α-phosphate and the bridging oxygen towards β-phosphate. AnkX coordinates cytidine by the CMP-coordinating domain via Y41 and R44. An in-line attack on the β-phosphate destabilizes the bond of β-phosphate to the bridging oxygen to α-phosphate and results in the transfer of phosphocholine. The switch from AMPylation to phosphocholination thus requires a change in substrate coordination and manifests in mutations of coordinating residues. Consistently, AnkX harbors mutations in the glycine and the second arginine that was shown to coordinate γ-phosphate in AMPylating Fic proteins.

Interestingly, several Beps of lineage 4 *Bartonellae* harbor mutations within the signature motif. Hence, we hypothesize that these Beps might not be AMPylating anymore but perform another PTM on target proteins. In fact, we could already identify phosphorylation as an artificial activity of the AMPylating effector VbhT. Structural analysis of VbhT of *B. schoenbuchensis* further revealed an alternative coordination of ATP that favors phosphorylation instead of AMPylation (A. Goepfert, unpublished data).

AMPylation is mostly associated with either prohibiting protein-protein interaction as shown for Rho GTPases upon AMPylation by VopS and IbpA or with the inhibition of nucleotide exchange

as shown for glutamine synthetase. In contrast, other PTMs like phosphorylation activate proteins or induce a switch of interaction partners and can therefore stimulate signaling cascades. Exerting different modifications depending on the substrate would allow a more differential influence on host cell signaling.

In ongoing studies, we are therefore addressing the identification of PTMs performed by different Beps and of the residues that dictate substrate specificity. This would greatly help to understand the role of Fic proteins in pathogenesis and would also allow the design and development of new tools for cell biology and innovative therapeutics.

4.8 Fic proteins are highly versatile modulators

The only published targets of Fic-mediated AMPylation are small GTPases of the Ras superfamily (2, 6, 87). GTPases cycle between an active GTP-bound state and an inactive GDP-bound form in their tightly controlled and complex regulatory networks (88, 89), where Fic proteins were described to interfere (6). IbpA and VopS are both targeting the inactive GDP-bound as well as the active GTP-bound form of Rho GTPases on their switch I region and thereby block the interaction with downstream signaling partners and also with regulators like GAPs and GEFs (6, 90). In addition, Rho GTPases are extracted from the membrane by GDIs that bind the GTP-bound form and inhibit GTP hydrolysis or exchange for GDP (91). Indeed, IbpA was shown to AMPylate Rho GTPases that are complexed with GDIs and it locks Cdc42 by AMPylation in a conformation similar to the GDI-bound form (6).

In contrast, preliminary assays with Bep1 of *B. rochalimae* indicate that this protein is not only specific for Rac1 but rather for its inactive GDP-bound form as Rac1Q61L, that is locked in its active state, was not modified (41, 43). Although further validation is required, the specificity towards one form of a target would allow an additional level of complexity in Fic protein-mediated regulation which could further increase the specificity of the effector.

Although Fic proteins were long thought of to only target small GTPases or at least NTPases, we were able to show here on the example of FIC-domain containing Beps, that Fic proteins are targeting a plethora of proteins like tubulin and vimentin. As vimentin is structurally unrelated to GTPases and is not even an NTPase, the impact of AMPylation is not restricted to nucleotide

exchange. Instead, tubulin and vimentin are cycling between a free, heterodimeric or monomeric form and a polymerized (92) form where AMPylation might influence the kinetics of these cycles.

All in all, we could show that members of the genus *Bartonellae*, like many other pathogens, manipulate a plethora of host cell pathways to the benefit of pathogenicity and further the understanding of the underlying molecular mechanisms.

We were able to identify new targets of *Bartonella* effector proteins ranging from adenylyl cyclases to components of the host cell cytoskeleton. The high diversity of effector targets indicates the global influence of the pathogen on host cellular functions and signaling events.

On the mechanistic level, we could show that *Bartonella* effector proteins employ versatile strategies ranging from stable interactions with to post translational modifications of target host proteins. We presented BepA as the first bacterial effector protein that directly targets adenylyl cyclases. The subsequent inhibition of apoptosis is proposed to protect the replicative niche of the pathogen thus indicating that the effector proteins contribute to the pathogens persistence. Furthermore, we developed a strategy to identify targets of post translational modifications which is a breakthrough for an extensive study on the role of Fic proteins in health and disease. Applying this approach, we could identify vimentin and tubulin as AMPylation targets which opened completely novel classes of Fic protein targets.

Unraveling the molecular details of BepA-activity and the comprehensive understanding of the FIC-domain will be useful in the development of cell biology tools or innovative therapeutics.

5. References

References

1. Pulliainen AT & Dehio C (2012) Persistence of Bartonella spp. stealth pathogens: from subclinical infections to vasoproliferative tumor formation. *FEMS Microbiol Rev* 36(3):563-599.
2. Yarbrough ML*, et al.* (2009) AMPylation of Rho GTPases by Vibrio VopS disrupts effector binding and downstream signaling. *Science* 323(5911):269-272.
3. Brown MS, Segal A, & Stadtman ER (1971) Modulation of Glutamine Synthetase Adenylylation and Deadenylylation Is Mediated by Metabolic Transformation of Pii-Regulatory Protein. *Proc Natl Acad Sci U S A* 68(12):2949-&.
4. Xu Y, Carr PD, Vasudevan SG, & Ollis DL (2010) Structure of the adenylylation domain of E. coli glutamine synthetase adenylyl transferase: evidence for gene duplication and evolution of a new active site. *J Mol Biol* 396(3):773-784.
5. Engel P*, et al.* (2012) Adenylylation control by intra- or intermolecular active-site obstruction in Fic proteins. *Nature* 482(7383):107-110.
6. Mattoo S*, et al.* (2011) Comparative analysis of Histophilus somni immunoglobulin-binding protein A (IbpA) with other fic domain-containing enzymes reveals differences in substrate and nucleotide specificities. *J Biol Chem* 286(37):32834-32842.
7. Worby CA*, et al.* (2009) The fic domain: regulation of cell signaling by adenylylation. *Mol Cell* 34(1):93-103.
8. Harms A & Dehio C (2012) Intruders below the radar: molecular pathogenesis of Bartonella spp. *Clin Microbiol Rev* 25(1):42-78.
9. Schulein R & Dehio C (2002) The VirB/VirD4 type IV secretion system of Bartonella is essential for establishing intraerythrocytic infection. *Mol Microbiol* 46(4):1053-1067.
10. Pulliainen AT*, et al.* (2012) Bacterial effector binds host cell adenylyl cyclase to potentiate Galphas-dependent cAMP production. *Proc Natl Acad Sci U S A* 109(24):9581-9586.
11. Truttmann MC, Rhomberg TA, & Dehio C (2011) Combined action of the type IV secretion effector proteins BepC and BepF promotes invasome formation of Bartonella henselae on endothelial and epithelial cells. *Cell Microbiol* 13(2):284-299.
12. Truttmann MC*, et al.* (2011) Bartonella henselae engages inside-out and outside-in signaling by integrin beta1 and talin1 during invasome-mediated bacterial uptake. *J Cell Sci* 124(Pt 21):3591-3602.
13. Schulein R*, et al.* (2005) A bipartite signal mediates the transfer of type IV secretion substrates of Bartonella henselae into human cells. *Proc Natl Acad Sci U S A* 102(3):856-861.
14. Engel P*, et al.* (2011) Parallel evolution of a type IV secretion system in radiating lineages of the host-restricted bacterial pathogen Bartonella. *PLoS Genet* 7(2):e1001296.
15. Schmid MC*, et al.* (2006) A translocated bacterial protein protects vascular endothelial cells from apoptosis. *PLoS Pathog* 2(11):e115.
16. Slep KC & Vale RD (2007) Structural basis of microtubule plus end tracking by XMAP215, CLIP-170, and EB1. *Mol Cell* 27(6):976-991.
17. Al-Bassam J, Larsen NA, Hyman AA, & Harrison SC (2007) Crystal structure of a TOG domain: conserved features of XMAP215/Dis1-family TOG domains and implications for tubulin binding. *Structure* 15(3):355-362.

18. Brouhard GJ, *et al.* (2008) XMAP215 is a processive microtubule polymerase. *Cell* 132(1):79-88.

19. Ayaz P, Ye X, Huddleston P, Brautigam CA, & Rice LM (2012) A TOG:alphabeta-tubulin complex structure reveals conformation-based mechanisms for a microtubule polymerase. *Science* 337(6096):857-860.

20. Al-Bassam J, *et al.* (2010) CLASP Promotes Microtubule Rescue by Recruiting Tubulin Dimers to the Microtubule. *Dev Cell* 19(2):245-258.

21. Widlund PO, *et al.* (2011) XMAP215 polymerase activity is built by combining multiple tubulin-binding TOG domains and a basic lattice-binding region. *Proc Natl Acad Sci U S A* 108(7):2741-2746.

22. Haren L, *et al.* (2006) NEDD1-dependent recruitment of the gamma-tubulin ring complex to the centrosome is necessary for centriole duplication and spindle assembly. *J Cell Biol* 172(4):505-515.

23. Guex N & Peitsch MC (1997) SWISS-MODEL and the Swiss-PdbViewer: an environment for comparative protein modeling. *Electrophoresis* 18(15):2714-2723.

24. Arnold K, Bordoli L, Kopp J, & Schwede T (2006) The SWISS-MODEL workspace: a web-based environment for protein structure homology modelling. *Bioinformatics* 22(2):195-201.

25. Kiefer F, Arnold K, Kunzli M, Bordoli L, & Schwede T (2009) The SWISS-MODEL Repository and associated resources. *Nucleic Acids Res* 37(Database issue):D387-392.

26. Al-Bassam J, van Breugel M, Harrison SC, & Hyman A (2006) Stu2p binds tubulin and undergoes an open-to-closed conformational change. *Journal of Cell Biology* 172(7):1009-1022.

27. Goepfert A, Stanger FV, Dehio C, & Schirmer T (2013) Conserved inhibitory mechanism and competent ATP binding mode for adenylyltransferases with fic fold. *PLoS One* 8(5):e64901.

28. Xiao J, Worby CA, Mattoo S, Sankaran B, & Dixon JE (2010) Structural basis of Fic-mediated adenylylation. *Nat Struct Mol Biol* 17(8):1004-1010.

29. Busson S, Dujardin D, Moreau A, Dompierre J, & De Mey JR (1998) Dynein and dynactin are localized to astral microtubules and at cortical sites in mitotic epithelial cells. *Current Biology* 8(9):541-544.

30. Peris L, *et al.* (2006) Tubulin tyrosination is a major factor affecting the recruitment of CAP-Gly proteins at microtubule plus ends. *Journal of Cell Biology* 174(6):839-849.

31. Honnappa S, John CM, Kostrewa D, Winkler FK, & Steinmetz MO (2005) Structural insights into the EB1-APC interaction (vol 24, pg 261, 2005). *Embo Journal* 24(4):872-872.

32. Fourest-Lieuvin A, *et al.* (2006) Microtubule regulation in mitosis: Tubulin phosphorylation by the cyclin-dependent kinase Cdk1. *Mol Biol Cell* 17(3):1041-1050.

33. Laurent CE, Delfino FJ, Cheng HY, & Smithgall TE (2004) The human c-Fes tyrosine kinase binds tubulin and microtubules through separate domains and promotes microtubule assembly. *Mol Cell Biol* 24(21):9351-9358.

34. Matsuyama A, *et al.* (2002) In vivo destabilization of dynamic microtubules by HDAC6-mediated deacetylation. *Embo J* 21(24):6820-6831.

35. Reed NA, *et al.* (2006) Microtubule acetylation promotes kinesin-1 binding and transport. *Current Biology* 16(21):2166-2172.

36. Hammond JW, Cai DW, & Verhey KJ (2008) Tubulin modifications and their cellular functions. *Curr Opin Cell Biol* 20(1):71-76.

37. Dhakal BK & Mulvey MA (2009) Uropathogenic Escherichia coli Invades Host Cells via an HDAC6-modulated Microtubule-dependent Pathway. *Journal of Biological Chemistry* 284(1):446-454.

38. Palanivelu DV*, et al.* (2011) Fic domain-catalyzed adenylylation: insight provided by the structural analysis of the type IV secretion system effector BepA. *Protein Sci* 20(3):492-499.

39. Kinch LN, Yarbrough ML, Orth K, & Grishin NV (2009) Fido, a novel AMPylation domain common to fic, doc, and AvrB. *PLoS One* 4(6):e5818.

40. Punta M*, et al.* (2012) The Pfam protein families database. *Nucleic Acids Res* 40(Database issue):D290-301.

41. Goepfert A (2012) Fic-Mediated Adenylylation: Catalysis and Regulation. *Ph.D. thesis* (Biozentrum Basel, Basel).

42. Lu YY*, et al.* (2013) Bartonella henselae trimeric autotransporter adhesin BadA expression interferes with effector translocation by the VirB/D4 type IV secretion system. *Cell Microbiol* 15(5):759-778.

43. Harms A (2010) FIC domains of Bartonella effector proteins - AMPylation and beyond. *Master thesis* (Biozentrum Basel, Basel).

44. Darwin KH & Miller VL (2000) The putative invasion protein chaperone SicA acts together with InvF to activate the expression of Salmonella typhimurium virulence genes. *Mol Microbiol* 35(4):949-959.

45. Darwin KH & Miller VL (2001) Type III secretion chaperone-dependent regulation: activation of virulence genes by SicA and InvF in Salmonella typhimurium. *Embo Journal* 20(8):1850-1862.

46. Schmid MC*, et al.* (2004) The VirB type IV secretion system of Bartonella henselae mediates invasion, proinflammatory activation and antiapoptotic protection of endothelial cells. *Mol Microbiol* 52(1):81-92.

47. Scheidegger F*, et al.* (2009) Distinct activities of Bartonella henselae type IV secretion effector proteins modulate capillary-like sprout formation. *Cell Microbiol* 11(7):1088-1101.

48. Truttmann MC, Guye P, & Dehio C (2011) BID-F1 and BID-F2 domains of Bartonella henselae effector protein BepF trigger together with BepC the formation of invasome structures. *PLoS One* 6(10):e25106.

49. Dehio C, Meyer M, Berger J, Schwarz H, & Lanz C (1997) Interaction of Bartonella henselae with endothelial cells results in bacterial aggregation on the cell surface and the subsequent engulfment and internalisation of the bacterial aggregate by a unique structure, the invasome. *J Cell Sci* 110:2141-2154.

50. Kirby JE & Nekorchuk DM (2002) Bartonella-associated endothelial proliferation depends on inhibition of apoptosis. *Proc Natl Acad Sci U S A* 99(7):4656-4661.

51. Kempf VAJ*, et al.* (2005) Bartonella henselae inhibits apoptosis in Mono Mac 6 cells. *Cell Microbiol* 7(1):91-104.

52. Tang WJ & Gilman AG (1995) Construction of a soluble adenylyl cyclase activated by Gs alpha and forskolin. *Science* 268(5218):1769-1772.

53. Tesmer JJG, Sunahara RK, Gilman AG, & Sprang SR (1997) Crystal structure of the catalytic domains of adenylyl cyclase in a complex with G(s alpha).GTP gamma S. *Science* 278(5345):1907-1916.

54. Feldman AM (2002) Adenylyl cyclase: a new target for heart failure therapeutics. *Circulation* 105(16):1876-1878.

55. Sunahara RK & Taussig R (2002) Isoforms of mammalian adenylyl cyclase: multiplicities of signaling. *Mol Interv* 2(3):168-184.

56. Sunahara RK, Dessauer CW, & Gilman AG (1996) Complexity and diversity of mammalian adenylyl cyclases. *Annu Rev Pharmacol Toxicol* 36:461-480.

57. Defer N, Best-Belpomme M, & Hanoune J (2000) Tissue specificity and physiological relevance of various isoforms of adenylyl cyclase. *Am J Physiol Renal Physiol* 279(3):F400-416.

58. Schweyer S & Fayyazi A (2002) Activation and apoptosis of macrophages in cat scratch disease. *J Pathol* 198(4):534-540.

59. Vermi W*, et al.* (2006) Role of dendritic cell-derived CXCL13 in the pathogenesis of Bartonella henselae B-rich granuloma. *Blood* 107(2):454-462.

60. Chen Y, Smith MR, Thirumalai K, & Zychlinsky A (1996) A bacterial invasin induces macrophage apoptosis by binding directly to ICE. *Embo J* 15(15):3853-3860.

61. Lindgren SW, Stojiljkovic I, & Heffron F (1996) Macrophage killing is an essential virulence mechanism of Salmonella typhimurium. *Proc Natl Acad Sci U S A* 93(9):4197-4201.

62. Okujava RG, P.; Lu, Y.Y.; Mistl, C.; Polus, F.; Vayssier-Taussat, M.; Halin, C.; Rolink, A.; Dehio, C. (2013) A translocated effector BepE of *Bartonella* is required for bacterial dissemination from derma to blood and safeguards migratory host cells from injury by co-translocated effectors. in *in preparation* (Biozentrum Basel).

63. Aronoff DM, Carstens JK, Chen GH, Toews GB, & Peters-Golden M (2006) Short communication: differences between macrophages and dendritic cells in the cyclic AMP-dependent regulation of lipopolysaccharide-induced cytokine and chemokine synthesis. *J Interferon Cytokine Res* 26(11):827-833.

64. Jing H, Yen JH, & Ganea D (2004) A novel signaling pathway mediates the inhibition of CCL3/4 expression by prostaglandin E2. *J Biol Chem* 279(53):55176-55186.

65. Broncel M, Serwa RA, & Tate EW (2012) A New Chemical Handle for Protein AMPylation at the Host-Pathogen Interface. *Chembiochem* 13(2):183-185.

66. Grammel M, Luong P, Orth K, & Hang HC (2011) A chemical reporter for protein AMPylation. *J Am Chem Soc* 133(43):17103-17105.

67. Campanacci V, Mukherjee S, Roy CR, & Cherfils J (2013) Structure of the Legionella effector AnkX reveals the mechanism of phosphocholine transfer by the FIC domain. *Embo J* 32(10):1469-1477.

68. Mukherjee S*, et al.* (2011) Modulation of Rab GTPase function by a protein phosphocholine transferase. *Nature* 477(7362):103-106.

69. Hauert B (2009) Identification of Cellular Protein Targets for *Bartonella* Effector Proteins. *Master thesis* (Biozentrum Basel, Basel).

70. Goody PR*, et al.* (2012) Reversible phosphocholination of Rab proteins by Legionella pneumophila effector proteins. *Embo J* 31(7):1774-1784.

71. Tan Y, Arnold RJ, & Luo ZQ (2011) Legionella pneumophila regulates the small GTPase Rab1 activity by reversible phosphorylcholination. *Proc Natl Acad Sci U S A* 108(52):21212-21217.

72. Eriksson JE*, et al.* (2004) Specific in vivo phosphorylation sites determine the assembly dynamics of vimentin intermediate filaments. *J Cell Sci* 117(Pt 6):919-932.

73. Sihag RK, Inagaki M, Yamaguchi T, Shea TB, & Pant HC (2007) Role of phosphorylation on the structural dynamics and function of types III and IV intermediate filaments. *Exp Cell Res* 313(10):2098-2109.

74. Chou YH, Bischoff JR, Beach D, & Goldman RD (1990) Intermediate Filament Reorganization during Mitosis Is Mediated by P34cdc2 Phosphorylation of Vimentin. *Cell* 62(6):1063-1071.

75. Chi F, Bo T, Wu CH, Jong A, & Huang SH (2012) Vimentin and PSF act in concert to regulate IbeA+ E. coli K1 induced activation and nuclear translocation of NF-kappaB in human brain endothelial cells. *PLoS One* 7(4):e35862.

76. Wang RC*, et al.* (2012) Akt-mediated regulation of autophagy and tumorigenesis through Beclin 1 phosphorylation. *Science* 338(6109):956-959.

77. Mor-Vaknin N, Punturieri A, Sitwala K, & Markovitz DM (2003) Vimentin is secreted by activated macrophages. *Nat Cell Biol* 5(1):59-63.

78. Phua DC, Humbert PO, & Hunziker W (2009) Vimentin regulates scribble activity by protecting it from proteasomal degradation. *Mol Biol Cell* 20(12):2841-2855.

79. Bhattacharya R*, et al.* (2009) Recruitment of vimentin to the cell surface by beta3 integrin and plectin mediates adhesion strength. *J Cell Sci* 122(Pt 9):1390-1400.

80. Williams-Bouyer NM & Hill EM (1999) Involvement of host cell tyrosine phosphorylation in the invasion of HEp-2 cells by Bartonella bacilliformis. *FEMS Microbiol Lett* 171(2):191-201.

81. Al-Bassam J & Chang F (2011) Regulation of microtubule dynamics by TOG-domain proteins XMAP215/Dis1 and CLASP. *Trends Cell Biol* 21(10):604-614.

82. Kawano Y*, et al.* (2005) CRMP-2 is involved in kinesin-1-dependent transport of the Sra-1/WAVE1 complex and axon formation. *Mol Cell Biol* 25(22):9920-9935.

83. Schwan C*, et al.* (2011) Cholesterol- and sphingolipid-rich microdomains are essential for microtubule-based membrane protrusions induced by Clostridium difficile transferase (CDT). *J Biol Chem* 286(33):29356-29365.

84. Byrne GI & Moulder JW (1978) Parasite-specified phagocytosis of Chlamydia psittaci and Chlamydia trachomatis by L and HeLa cells. *Infect Immun* 19(2):598-606.

85. Schroer TA, Steuer ER, & Sheetz MP (1989) Cytoplasmic dynein is a minus end-directed motor for membranous organelles. *Cell* 56(6):937-946.

86. Clausen JD, Christiansen G, Holst HU, & Birkelund S (1997) Chlamydia trachomatis utilizes the host cell microtubule network during early events of infection. *Mol Microbiol* 25(3):441-449.

87. Roy CR & Mukherjee S (2009) Bacterial FIC Proteins AMP Up Infection. *Sci Signal* 2(62):pe14.

88. Vetter IR & Wittinghofer A (2001) Signal transduction - The guanine nucleotide-binding switch in three dimensions. *Science* 294(5545):1299-1304.

89. Bos JL, Rehmann H, & Wittinghofer A (2007) GEFs and GAPs: Critical elements in the control of small G proteins (vol 129, pg 865, 2007). *Cell* 130(2):385-385.

90.   Luong P, *et al.* (2010) Kinetic and structural insights into the mechanism of AMPylation by VopS Fic domain. *J Biol Chem* 285(26):20155-20163.

91.   Olofsson B (1999) Rho guanine dissociation inhibitors: Pivotal molecules in cellular signalling. *Cell Signal* 11(8):545-554.

92.   Nogales E & Wang HW (2006) Structural intermediates in microtubule assembly and disassembly: how and why? *Curr Opin Cell Biol* 18(2):179-184.

6. Acknowledgments

Acknowledgments

This work was performed in the group of Prof. Christoph Dehio in the Focal area Infection Biology at the Biozentrum belonging to the University of Basel, Switzland.

First and foremost, I would like to thank my supervisor Prof. Christoph Dehio for giving me the opportunity to conduct my PhD in his lab and the open discussion we had in this time. I especially appreciate his believe in me to manage the switch from chemistry to infection biology.

Next, I would like to acknowledge Prof. Sebastian Hiller and Prof. Tilman Schirmer for the fruitful discussions in my committee meetings and their support in the last four years.

I would also like to thank Prof. Carmen W. Dessauer (University of Texas, USA) who offered me the opportunity to visit her lab and for her help in the BepA-AC project as well as Maurine Linder (Cornell University, USA) who sponsored me on the Conference of Experimental Biology.

I am very grateful to Timo Glatter for helping me set up the mass spectrometry strategies and for his patience in analyzing the endless numbers of samples even though we didn`t work with one easy to handle peptide. I am also grateful to Arto T. Pulliainen for the discussions we had on the BepA-project and the grate time we used to have. I am thankful to Larisa Kapinos-Schneider and Conrad-Eberhard von Schubert for helping me set up SPR and Live cell imaging experiments.

I would like to acknowledge the constant support by the many people of the technical and administrative staff of the 4th floors. Thank you very much for constant help and support in the back of the everyday business of science.

I am very grateful to all members of the Dehio group. The great atmosphere in our lab is what kept me going when nothing else seemed to work: Maxime Quebatte, Arto Pulliainen, Raquel Conde, Alexander Harms, Alain Casanova, Shyan Huey Low, Yun-Yueh Lu, Arnaud Goepfert, Mathias Dick, Houchaima Ben Tekaya, Simone Eicher, Rusudan Okujava, Pauli Rämö, Claudia

Mistl, Simone Muntwiler, Sarah Stiegeler, Matthias Truttmann, Marco Faustmann, Sabrina Siamer, Jonas Körner, Sayantan Saha, Dominik Buser, Damian Murezzan, Frédéric Stanger, Philipp Engel and Mario Emmenlauer.

I am very thankful to Simone C. Eicher and Maxime Quebatte for the critical feedback on my thesis.

Special thanks go to Claudia Mistl, Matthias C. Truttmann, Shyan H. Low, Lucie Hosch, Samuel Steiner, Simone C. Eicher, Matthias Kaiser and Sarah M. Stiegeler. I don`t know what I would have done without you!

Ich möchte mich besonders bei meiner Familie und bei Matthias dafür bedanken, dass sie mich bedingungslos unterstützen und sich nie über meine ständig ändernden Reiseplanungen beklagen. Nichts hilft so sehr, wie das Wissen, dass man immer zurück ins sichere Heim kann!

7. Curriculum Vitae

Curriculum Vitae

Kathrin Pieles

Date/place of birth	15/08/1985 in Oldenburg, Germany
Nationality	German

Office Address	**Private Address**
Klingelbergstrasse 50-70	Wattstrasse 16
CH-4056 Basel, Switzerland	CH-4056 Basel, Switzerland
+41 61 2672139	+41 797364872
kathrin.pieles@unibas.ch	

Academical path

11/2009-present	PhD student at Biozentrum Basel, Department: Molecular Microbiology, Focal Area: Infection Biology
11/2009	Graduation in Chemistry with Diploma
1/2009	Beginning of diploma thesis in the group of Prof. L.O.Essen
10/2008	Examinations for the diploma
10/2004	Beginning of studies in chemistry at the Philipps University of Marburg
1997-2004	Grammar school (Gymnasium Eversten OL)

Publications

2013	K. Pieles, T. Glatter, A. Schmidt, C. Dehio. An experimental strategy for the identification of AMPylation targets from complex protein samples. Submitted to *Proteomics*
2012	A.T. Pulliainen, K. Pieles, C.S. Brand, B. Hauert, A. Böhm, M. Quebatte, A. Wepf, M. Gstaiger, R. Aebersold, C.W. Dessauer, and C. Dehio. Bacterial effecttor binds host cell adenylyl cyclase to potentiate Gαs-dependent cAMP production, *PNAS*, Jun. 2012, 109(24):9581-6

Fellowship

2009-20013   Fellow of Werner Siemens Foundation, International PhD Programm, "Fellowship for Excellence"

Teaching Experience

2012-2013   Supervision of a Master student
Focal area Infection Biology, Biozentrum, University of Basel

2013   Supervision of a Rotation student
Focal area Infection Biology, Biozentrum, University of Basel

2010-2013   Assistant and tutor for undergraduate students in practical courses, "Microbiology"
Focal area Infection Biology, Biozentrum, University of Basel

03/2009-06/2009   Supervision of undergraduate students of biology in the practical course including weekly tutorials, "Chemistry"
Faculty of Chemistry, Philipps-University Marburg, Germany

Oral and Poster presentations

2013   Poster Presentation at "ETOX", Freiburg, Germany, *Manipulation of host cell signaling by bacterial FIC proteins*

2013   Oral Presentation at Conference of "Experimental Biology", Boston, Massachusettes, USA, *Manipulation of host cell signaling by bacterial FIC proteins*

2012   Poster Presentation at "Infection Biology Symposium", Biozentrum, Switzerland, *Targeting of adenylate cyclase 7/GalphaS-complex by BepA of vasculotumorigenic Bartonella henselae inhibits apoptosis of endothelial cells*

Kathrin Pieles, Wattstrasse 16, 4056 Basel, Switzerland
Tel.: +41 61 3220321, mobile: +41 797364872, kathrin.pieles@unibas.ch

2012	Poster Presentation at "Gordon Research Conference: Phosphorylation and G-protein Mediated Signaling Networks", Biddefort, Maine, USA, *Sentenced to live: how a bacterial effector inhibits host cell apoptosis by targeting adenylyl cyclase/Gαs complex*
2012	Oral Presentation at "Biozentrums Symposium", St. Chrischona, Switzerland, *Sentenced to live: how a bacterial effector inhibits host cell apoptosis*
2011	Poster Presentation at "FEMS", Geneva, Switzerland, *Targeting of adenylate cyclase 7/GalphaS-complex by BepA of vasculotumorigenic Bartonella henselae inhibits apoptosis of endothelial cells*

Additional qualification

3/2007-8/2007	Internship in Sydney, Australia, in the group of Prof. P.Lay; project: Synthesis and Analysis of Cr(III)-peptide complexes
6/2007	X-ray absorption measurements at the Synchrotron in Tsukuba, Japan
3/2008-4/2008	Student assistance in the group of Prof. M. Marahiel; project: Cloning, Expression and Purification of Patellamid *Pat*E

References

Prof. C.Dehio	Prof. L.O.Essen
Biozentrum Basel	FB Chemie
Klinglbergstr. 50-70	Hans-Meerwein-Str.
University of Basel	Philipps Universität Marburg
CH-4056 Basel, Switzerland	35032 Marburg, Germany

8. Appendix
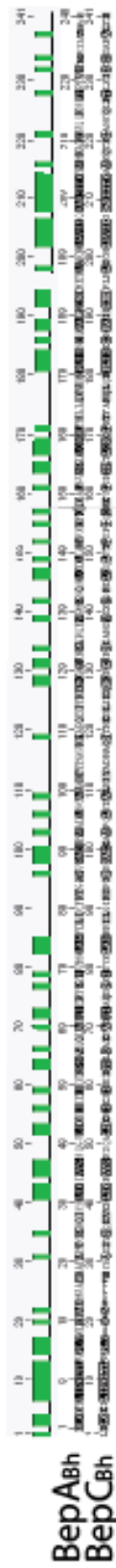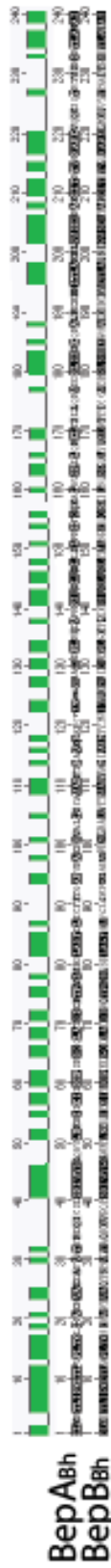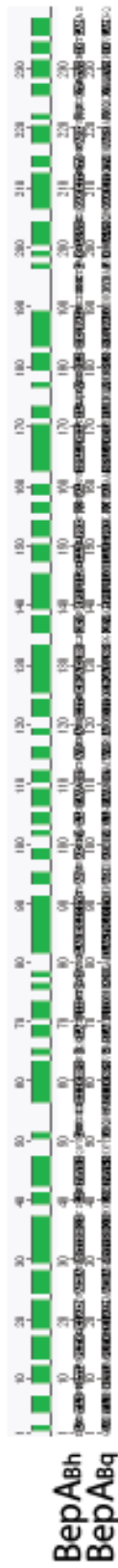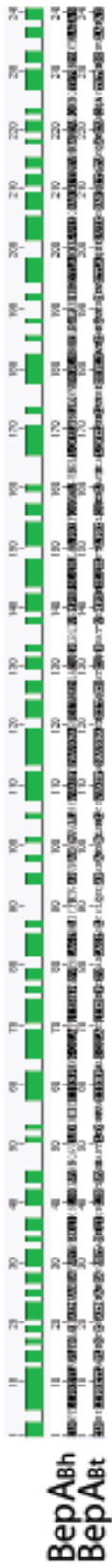
Figure A1: Sequence alignment. Alignment of BID-domain sequences of BepA from *B. henselae* with BepA of *B. tribocorum* (sequence identity of 57%), *B. quintana* (sequence identity of 64%), BepB of *B. henselae* (sequence identity of 50%) and BepC of *B. henselae* (sequence identity of 40%).
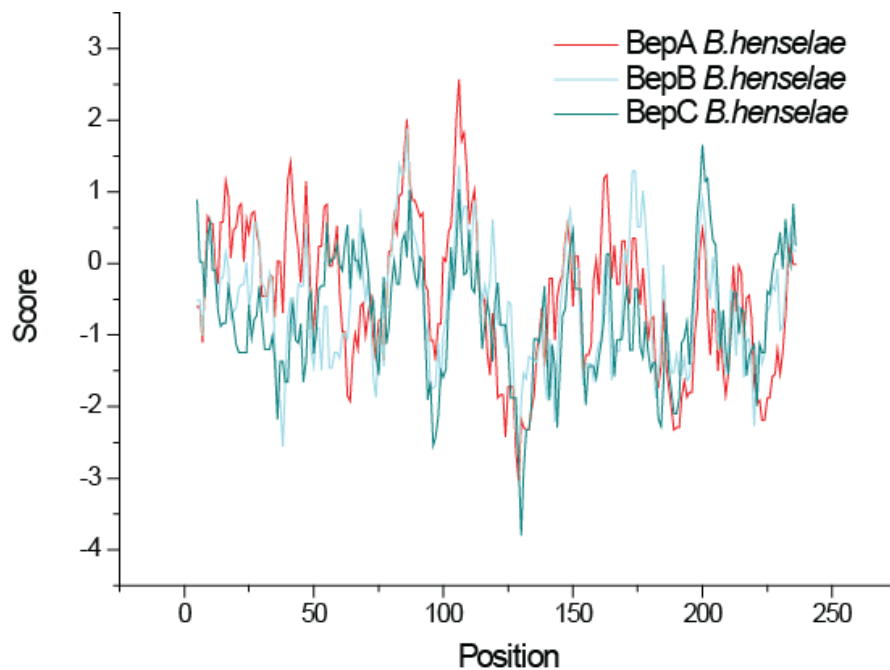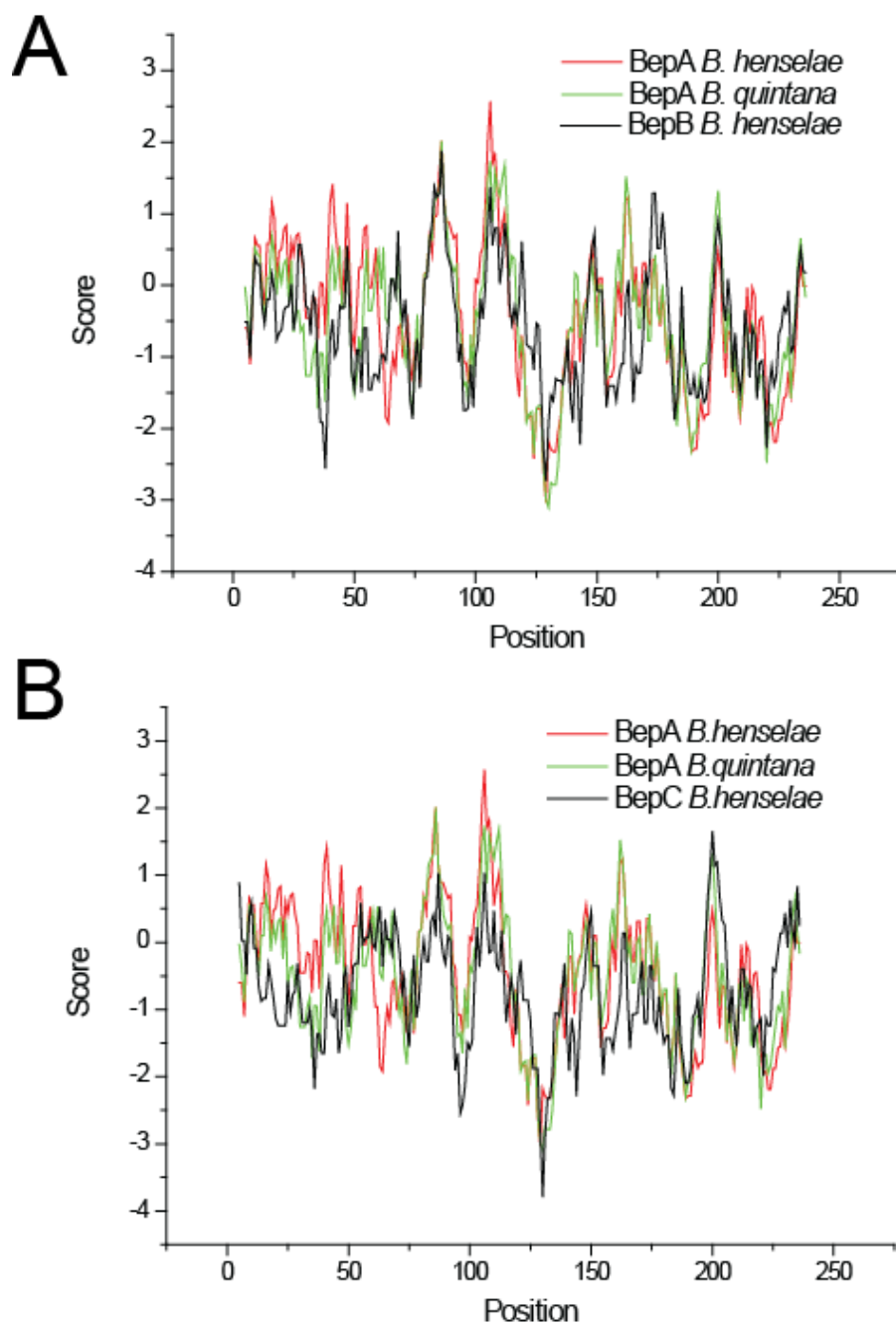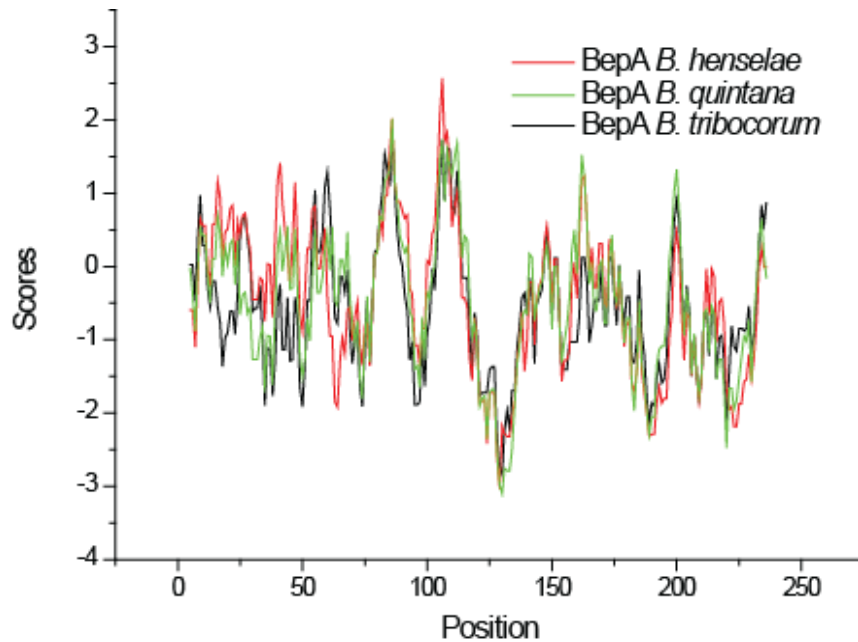

Figure A2: Hydrophibicity profiles of paralogous BID domains. Kyte&Doolittle hydropathy plots were calculated based on the primary amino acid sequence utilizing ProtScale (Expasy) (1). BepA$_{305-544}$ plot is colored in red, BepB$_{303-542}$ plot in cyan and BepC$_{292-532}$ plot in dark green.

Figure A3: Hydrophibicity profiles of homologous BID-domains. Kyte&Doolittle hydropathy plots were calculated based on the primary amino acid sequence utilizing ProtScale (Expasy) (1). A) Hydropathy of BepA$_{305-544}$ of *B. henselae* is plotted in red, BepB$_{303-542}$ of *B. henselae* is plotted in black and BepA$_{40-252}$ of *B. quintana* is plotted in green. B) Hydropathy of BepA$_{305-544}$ of *B. henselae* is plotted in red, BepC$_{292-532}$ of *B. henselae* is plotted in black and BepA$_{40-252}$ of *B. quintana* is plotted in green.

Figure A4: Hydrophibicity profiles of the orthologous BID-domains. Kyte&Doolittle hydropathy plots were calculated based on the primary amino acid sequence utilizing ProtScale (Expasy) (1). Hydropathy of BepA$_{305-54}$ of *B. henselae* is plotted in red, BepA$_{40-252}$ of *B. quintana* is plotted in green and BepA$_{305-533}$ of *B. tribocorum* is plotted in black.

Figure A5: Structure of BepC$_{1-219}$ from *B. quintana*. Crystal structure of the FIC-domain of BepC from *B. quintana* is depicted in ribbon style (left). The Fic core helices are colored in red with the signature motif in yellow and the surrounding helices in magenta. The β-hairpin loop is colored in dark blue and the N-terminal loop on top of the active site is shown in orange (data acquired and kindly provided by Isabelle Phan). View from top onto the active site is shown on the right.
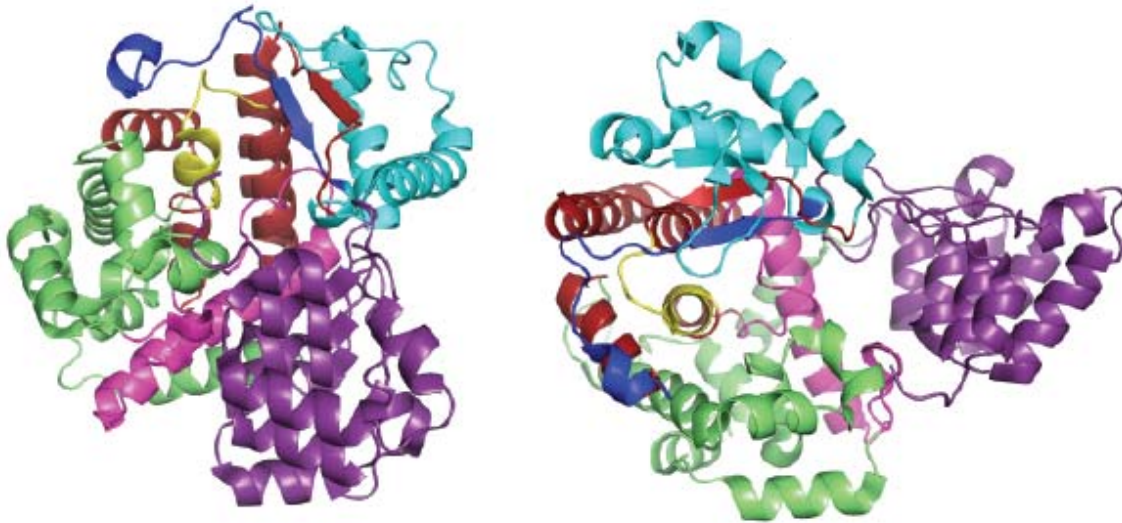
Figure A6: Structure of AnkX from *L. pneumophila*. Crystal structure of the AnkX from *L. pneumophila* is depicted in ribbon style (left). The Fic core helices are colored in red with the signature motif shown in yellow and the surrounding helices are presented in magenta. The β-hairpin loop is colored in dark blue, the insert domain is shown in cyan and the CMP-coordinating domain is colored in limegreen. The ankyrin repeats are presented in purple. View from top onto the active site is shown on the right. PDB code: 4BER.
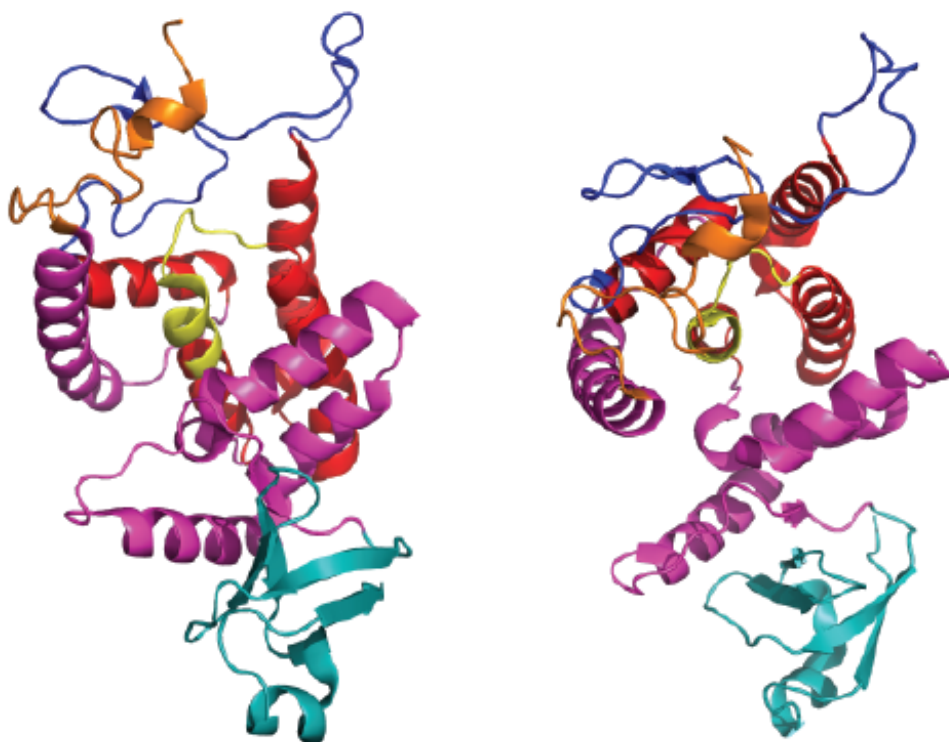
Figure A7: Structure of BepA from *B. henselae*. Crystal structure of the FIC-domain with the adjacent OB-fold of BepA from B. henselae is depicted in ribbon style (left). The Fic core helices are colored in red with the signature motif in yellow and the surrounding helices in magenta. The Bep-element with the β-hairpin loop is colored in dark blue, the N-terminal loop is colored in orange and the OB-fold in cyan. View from top onto the active site is shown on the right. PDB code: 2VZA.
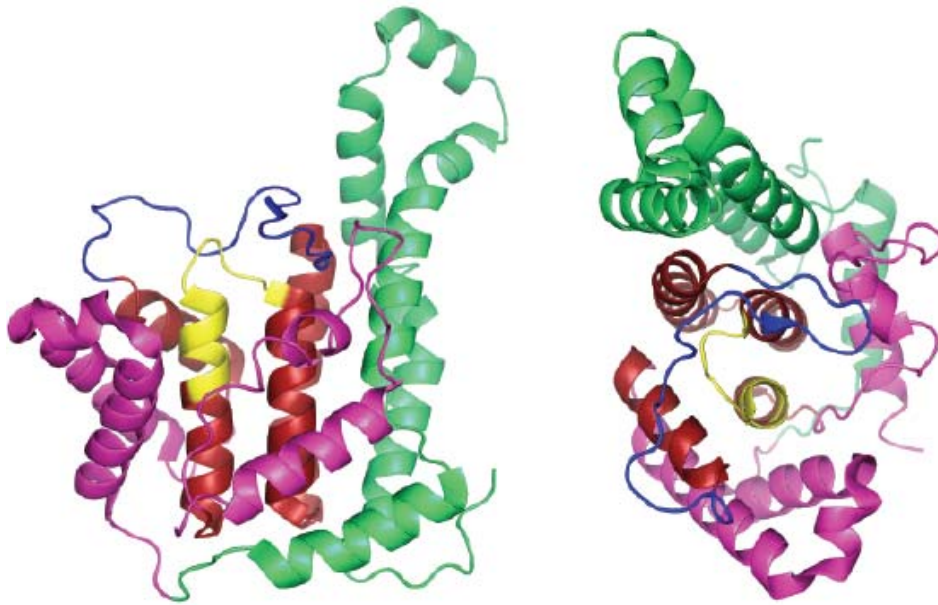
Figure A8: Structure of IbpA from *H. somni*. Crystal structure of the FIC2IbpA$_{3482\text{-}3797}$ (H3717A) of *H. somni* is depicted in ribbon style (left). The Fic core helices are colored in red with the signature motif in yellow and the surrounding helices in magenta. The β-hairpin loop involved in target binding is colored in dark blue and arm domain that mediates target recognition is colored in green. View from top onto the active site is shown on the right. PDB code: 4ITR.
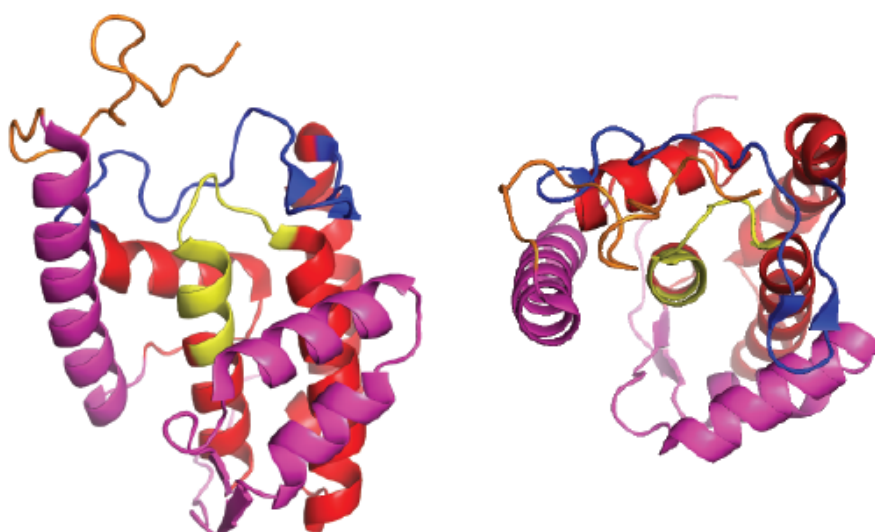
Figure A8: Structure of VbhT from *B. schoenbuchensis*. Crystal structure of the FIC-domain of VbhT from *B. schoenbuchensis* is depicted in ribbon style (left). The Fic core helices are colored in red with the signature motif colored in yellow and the surrounding helices in magenta. The β-hairpin loop is colored in dark blue and N-terminal unorganized loop in orange. View from top onto the active site is shown on the right. PDB code: 3SHG.

Figure A8: Structural model of Bep2 from *B. rochalimae*. The structure of the FIC-domain with the OB-fold of Bep2 (Bep2$_{15-305}$) from *B. schoenbuchensis* is presented in ribbon style (left). The Fic core helices are depicted in red with the signature motif in yellow and the surrounding helices in magenta. The β-hairpin loop is colored in dark blue, the N-terminal loop in orange and the OB-fold in cyan. View from top onto the active site is shown on the right. Model is based on the Structure of BepA (PDB code 2VZA) using SWISS Model (2, 3).

1. Walker JM ed (2005) *The Proteomics Protocols Handbook* (Humana Press), pp 571-607.
2. Arnold K, Bordoli L, Kopp J, & Schwede T (2006) The SWISS-MODEL workspace: a web-based environment for protein structure homology modelling. *Bioinformatics* 22(2):195-201.
3. Kiefer F, Arnold K, Kunzli M, Bordoli L, & Schwede T (2009) The SWISS-MODEL Repository and associated resources. *Nucleic Acids Res* 37(Database issue):D387-392.